Pocket Tens: Going All In on Modularity and Innovation

Team 112 Project Technical Report to the 2025 IREC

First T. Rhoads[1], Second K. Jones[2], Third J. McCarty[3], Fourth K. Hughes [4], Fifth C. Johnson[5], Sixth A. Scribner[6], Seventh E. Anderson[7], Eighth T. Miller[8], Ninth S. Beerer[9], Tenth S. Pupke[10], Eleventh H. Crawford[11], Twelfth A. Doan[11], Thirteenth N. Junkins[11], Fourteenth H. Matarwala[11], Fifteenth N. Patel[11], Sixteenth K. Karamched[11], Seventeenth M. Sullivan[11], Eighteenth J. Franke[11], Nineteenth E. Baldwin[6], Twentieth A. Gregory[5], Twenty-First D. Lundberg[11]
Twenty-Second M. Medina[11], and Twenty-Third G. Pataky[12]
Clemson University, Clemson, South Carolina, 29634, United States of America

This abstract presents an overview of our project, Pocket Tens, for the International Rocket Engineering Competition 2025, wherein our team competes in the 10k COTS category with a launch vehicle designed for advanced statistical analysis of commercial off-the-shelf altimeters. The defining characteristics of our launch vehicle include the Miniaturized Avionics for Rapid Testing, Handling, and Assessment (MARTHA) system, which supports low-cost deployment and reliable data acquisition crucial for ongoing advancements in flight computer technology. The vehicle construction features student-researched and developed (SRAD) body tubes, couplers, and structural reinforcements using carbon fiber plating. Additionally, the aero-structure incorporates a dual-camera system to capture comprehensive visual data during flight, serving a secondary mission of enhancing visual documentation. This report details the robust iterative design of our aero-structures subsystems as well as the effective and novel student research and designed (SRAD) avionics system.

[1] President, Mechanical Engineering, 216 S Palmetto Blvd, Clemson, SC 29634. Email: jtrhoad@clemson.edu.
[2] Chief Engineer, Computer Engineering, 216 S Palmetto Blvd, Clemson, SC 29634. Email: kcj4@clemson.edu.
[3] Vice President, Mechanical Engineering, 216 S Palmetto Blvd, Clemson, SC 29634. Email: jmcca22@clemson.edu.
[4] Simulations Lead, Mechanical Engineering, 216 S Palmetto Blvd, Clemson, SC 29634. Email: khughe3@clemson.edu.
[5] Recovery Lead, Electrical Engineering, 216 S Palmetto Blvd, Clemson, SC 29634. Email: crjhnsn@clemson.edu.
[6] Structures Lead, Mechanical Engineering, 216 S Palmetto Blvd, Clemson, SC 29634. Email: ascribn@clemson.edu.
[7] Software Development Lead, Computer Science, 216 S Palmetto Blvd, Clemson, SC 29634. Email: ema8@clemson.edu.
[8] Hardware Development Lead, Electrical Engineering, 216 S Palmetto Blvd, Clemson, SC 29634. Email: trm2@clemson.edu.
[9] Onboarding Coordinator, Mechanical Engineering, 216 S Palmetto Blvd, Clemson, SC 29634. Email: sbeerer@clemson.edu.
[10] Active Aero, Computer Science, 216 S Palmetto Blvd, Clemson, SC 29634. Email: spupke@clemson.edu.
[11] General Member, Mechanical Engineering, 216 S Palmetto Blvd, Clemson, SC 29634.
[12] Faculty Advisor, Mechanical Engineering, 216 S Palmetto Blvd, Clemson, SC 29634. Email: gpataky@clemson.edu.

Table of Contents

I. Nomenclature

C_p	=	Pressure coefficient
Cx	=	Force coefficient in the *x* direction
Cy	=	Force coefficient in the *y* direction
c	=	Chord
kg	=	Kilogram
Fx	=	*X* component of the resultant pressure force acting on the vehicle
Fy	=	*Y* component of the resultant pressure force acting on the vehicle
h	=	Height
m	=	Meter
mm	=	Millimeter
j	=	Waypoint index
K	=	trailing-edge (TE) nondimensional angular deflection rate
G	=	Gauss
GB	=	Gibibyte
°	=	Degree
dps	=	Degrees per second
°C	=	Degrees Celsius
°F	=	Degrees Fahrenheit
g	=	Gravitational acceleration/grams
ft	=	Feet
in	=	Inch
s	=	Second
lbm	=	Pound-Mass
lbf	=	Pound-Force
N	=	Newton
oz	=	Ounce
V	=	Volts
A	=	Amps
Ns	=	Newton-Seconds
cal	=	Caliber
mAh	=	Milli-Amp Hour
mph	=	Miles per hour
MPa	=	Megapascal
hPa	=	Hectopascal
psi	=	Pounds per Square Inch
hz	=	Hertz
MHz	=	Megahertz
KB	=	Kibibyte
MB	=	Mebibyte
*k*Ω	=	Kilo-ohm
uF	=	Microfarad
nF	=	Nanofarad

II.Introduction

A. Clemson University

Clemson University is a public land grant research institution in Upstate South Carolina, centered between Charlotte, NC and Atlanta, GA. With a student population of over 28,000 undergraduate and graduate students, Clemson hosts a diverse set of academic colleges, including the College of Engineering, Computing and Applied Sciences (CECAS); College of Science (COS); Wilbur O. and Ann Powers College of Business (COB); and more. “Clemson combines the benefits of a major research university with a strong commitment to undergraduate teaching and individual student success. Students, both undergraduate and graduate, have opportunities for unique educational experiences throughout South Carolina, as well as in other countries. Experiential learning is a valued component of the Clemson experience, and students are encouraged through Creative Inquiry, internships, and study abroad to apply their learning beyond the classroom. Electronic delivery of courses and degree programs also provide a variety of learning opportunities. Clemson’s extended campus includes teaching sites in Greenville, Greenwood, Anderson and Charleston, eight research campuses and extension centers in every county of South Carolina, as well as four international sites. The University is committed to exemplary teaching, research, and public service in the context of general education, student engagement and development, and continuing education. In all areas, the goal is to develop students’ communication and critical-thinking skills, ethical judgment, global awareness, and scientific and technological knowledge” [5].

B. Clemson University Rocket Engineering

The Clemson University Rocket Engineering team, also known as CURE, is the primary source of aerospace involvement and education at Clemson University, as there is no formal discipline within aerospace. The CURE mission is to introduce the aerospace industry to Clemson University for all demographics, develop future leaders worldwide, and research cutting-edge technology. CURE is a delegated student organization (DSO) of Clemson University's CECAS, meaning we are direct representatives of CECAS and the University. To provide the outlet for Aerospace Engineering to the Clemson Student body, CURE participates in the annual International Rocket Engineering Competition by designing, manufacturing, and launching a large team vehicle fit for the 10k Commercial-Off-The-Shelf (COTS) Mission. Additionally, the CURE team incentivizes all members' personal certifications by hosting Level 1 (L1) and Level 2 (L2) high-power certification rocket build days and launches. Furthermore, members enhance their hand machining capabilities with hand tools, lathes, and mills.

Our team is divided into the Administrative, Engineering, and Financial divisions. The delegation of these three divisions allows each team to focus directly on their role, leading to more efficient and productive work. The Administrative Division, led by the Vice President, oversees onboarding, outreach, certifications, and all safety precautions. The Engineering Division oversees all design, simulation, and manufacturing of the vehicle and all electrical components. The Chief Engineers of Mechanical and Electrical Systems oversee the Engineering Division. Lastly, the Financial Division oversees all budgeting, sponsorships, social media, and procurement for the team and is led by the Director of Finance. The President oversees the upper leadership team and the organization as a whole. The full, descriptive breakdown of the organization can be seen in Figure 1 below.

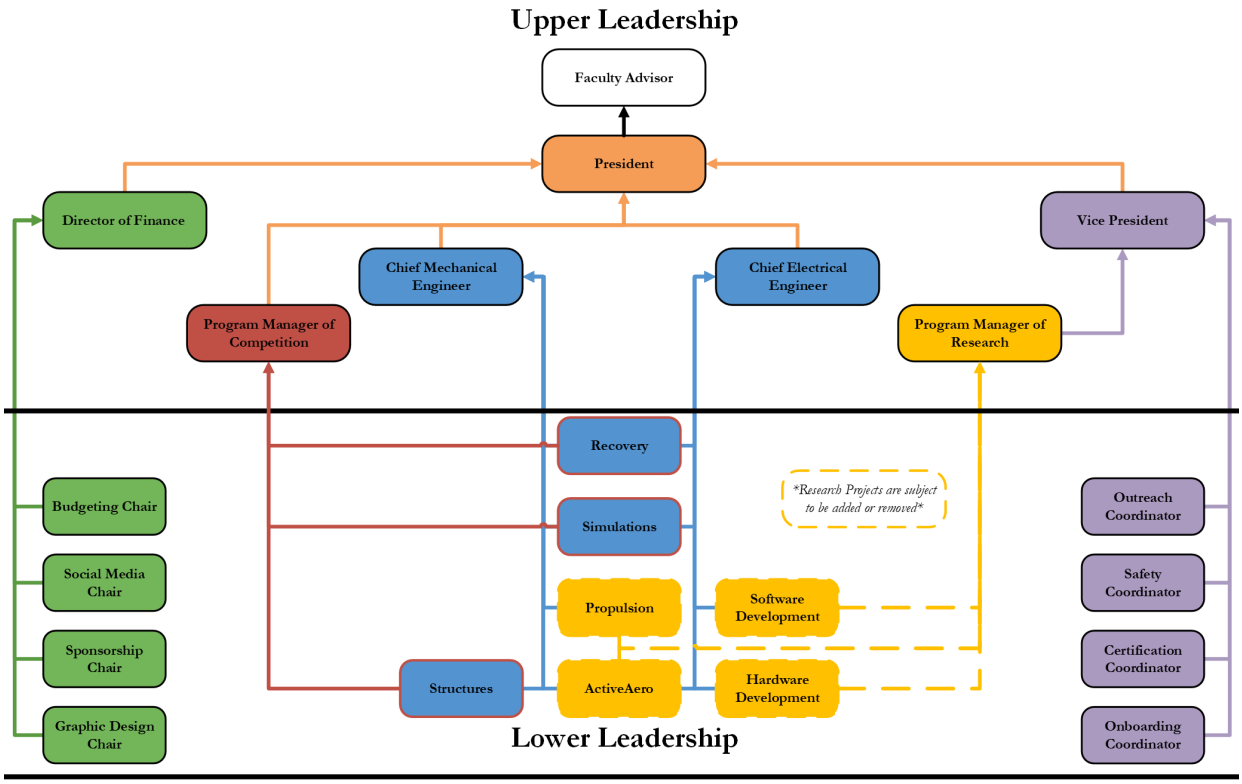

Figure 1 Clemson University Rocket Engineering organization chart for 2024-2025.

1. *Administrative Division*

The Administrative Division oversees the organization's internal affairs and processes, looking for avenues to drive greater recruitment, retainment, and member value. Additionally, the Administrative Division seeks to further the Organization's involvement and engagement across the student body, university system, and local population. This includes, but is not limited to, participating in outreach and volunteering events, scheduling tech talks with various speakers/companies, and collaborating with Science, Technology, Engineering, and Math (STEM) events and organizations at the K-12 level. In addition, the Administrative Division oversees the safety and compliance of all organization engineering projects within not only local, state, and federal law, but Tripoli Rocket Association (TRA), National Association of Rocketry (NAR) policies and university guidelines. This division is highlighted in purple above in Figure 1, and is led by the Vice President. Lower Leadership members of the Administrative Division are identified by the moniker/suffix of "Coordinator" in their title.

There are three primary objectives of the Administrative Division: ensure compliance and safety of all engineering projects, develop and cultivate valuable member experiences, and provide onboarding counsel for new members of all skills and backgrounds. The first of these three objectives is handled primarily by the Safety Coordinator. Each Subteam must notify the Safety Coordinator and receive written approval for all tests involving energetics of any form, as well as allowing enough time for possible filing of authorization documentation from university officials for specific tests. Additionally, the Safety Coordinator must be present, or designate a qualified substitute in their absence, for all official organization launches, including research or competition vehicle flights, to ensure compliance with TRA/NAR practices on range and safe precautions during flight operations.

The second objective of the Administrative Division is handled by the Outreach Coordinator. The organization schedules a variety of events throughout the academic year for its members on and around campus. These can range from tech talks with speakers from the university or companies/government agencies to social events for members in the local area. The third objective of the Administrative Division is provided by the Certification and Onboarding Coordinators. The organization has implemented a formal onboarding program that aims to more effectively recruit

and retain new members, subsequentially integrating them across the organization in each division. The program permits any new member to launch a TRA Level 1 certification rocket through the team after paying semester dues, with the option to continue onto a Level 2 certification, if desired. Simultaneously, new members are introduced to the different areas of rocketry and opportunities provided by the organization, while also being encouraged to explore the diverse set of technical focuses fundamental to the organization's mission. This creates a customized learning path for each new member that will foster organization-wide engagement and retention.

2. *Recovery – Competition Team*

The Recovery Subteam is responsible for the mechanical design and fabrication of the recovery bay, as well as parachute sizing, and the electrical design and fabrication of the recovery harness. The Subteam oversees designing the wiring diagram for the recovery bay as well as the actual wiring of the bay. This Subteam is also in charge of all ejection tests for the vehicle to determine the proper amount of black powder for each charge and to ensure successful parachute deployment. The Subteam is also the primary party responsible for coordinating the recovery of the vehicle after launches. This Subteam had previously been a part of our "Avionics" Subteam, which included what is now the Hardware and Software Subteams, in addition to Recovery. This Subteam has six active members.

This year, one area of focus for the Subteam was creating a bay that improves the redundancy of the recovery harness. The Subteam accomplished this goal by introducing a third altimeter to the bay and adding a redundant wiring setup that connects across separate bulkhead connections. This ensures that even in the event of an entire connector failure the vehicle's recovery bay loses no functionality.

Another goal this Subteam had was to minimize the time and complexity of assembling the bay and integration into the rest of the vehicle. This was accomplished by adding electrical connectors to any point of disassembly. Furthermore, the Subteam utilized cable flags on all the cable/wires and all connectors to minimize any confusion when assembling the vehicle. The team implemented a modular backplane design as well, where each module can be independently installed onto any part of a central backplane. This allows for easier experimentation of different bay configurations. The limited use of soldering of the bay throughout allows for not only reduced manufacturing times, but greater observability as solder joints are not able to be observed for joint quality.

3. *Simulations – Competition Team*

The Simulations Subteam is responsible for ensuring that the vehicle's design is stable and safe to fly, designing components that interact directly with airflow, and predicting flight parameters before launch. The Subteam oversees the length, weight, and center of gravity of both individual portions of the vehicle and the vehicle as a whole. Additionally, the Subteam designs the fins of the vehicle based on how it changes the stability of the vehicle and the fin shear velocity. The Subteam determines what nose cone shape and size will be used on the vehicle. The Simulations Subteam decides on what motor is used at the competition; this decision was based on simulating how the vehicle will perform with different M and N class motors. The Simulations Subteam primarily uses OpenRocket as its flight simulation method to determine flight parameters, with RASAero to further confirm our simulations [10, 14]. The Subteam has 12 active members.

The Simulations Subteam is responsible for predicting the performance of the launch vehicle. For predicting the apogee of the vehicle, the Subteam uses OpenRocket to create a model of the vehicle in the program. Openrocket then enables the Subteam to simulate how the vehicle would perform with different motors, at different locations, and with different weather conditions [10]. We also ensure that when the weights and sizes of components are changed, that it would not interfere with the vehicle's ability to fly.

The Subteam is also responsible for computer verification of designs. The primary way that the Subteam does this is through Finite Element Analysis (FEA) on both internal and external components to verify the robustness of the design. The Subteam uses a mixture of ANSYS Mechanical and SolidWorks to complete this analysis [15, 20]. Regarding components that interact with the airflow while the vehicle is in flight, the Subteam uses computer simulations and numerical methods to help prove that the design is safe. For the fins of the vehicle specifically, the Subteam is responsible for calculating the shear velocity of the design through a series of equations and modeling the vehicle in OpenRocket to choose a design that leads to an acceptable stability [10].

4. *Structures – Competition Team*

The Structures Subteam is responsible for designing, analyzing, and fabricating the rocket's primary structural components, ensuring the vehicle maintains integrity under all mechanical and aerodynamic loads throughout launch, ascent, deployment, and descent. These components include the airframe, fins, recovery housing, camera and SRAD electronic mountings, motor tube, and internal supports that interface with other subsystems.

For the 2024–2025 competition cycle, the Subteam prioritized using carbon fiber and fiberglass composites due to their high strength-to-weight ratio and proven performance under dynamic loading. Fiberglass composites were selected for the majority of airframes to ensure higher RF telemetry efficiency than carbon fiber counterparts. Members utilized in-house layup techniques to fabricate the airframe and fins, minimize air pockets, and ensure uniform epoxy distribution to prevent delamination and structural failure.

The team has approximately sixteen active members with varying manufacturing certifications through Clemson's Cook Engineering Laboratory. These certifications allow the safe and effective use of manual lathes, mills, waterjets, and laser cutters. Structures members used this equipment to produce bulkheads, fin slots, internal mounting structures, and motor tube supports. Layup molds were redesigned to ensure more consistent part quality and allow for mold replacement in the event of fabrication errors—improving overall process repeatability and robustness.

Structures also supports the Hardware Subteam by designing and fabricating components that house or interface with avionics and recovery systems. Computer Aided Design (CAD) software such as SolidWorks and OnShape were used extensively to model these structures and simulate their integration with other subsystems. The organization's expanding 3D printing capabilities allowed for rapid prototyping of avionics housings and pull pin switches, accelerating design iteration and fit testing.

In collaboration with the Simulations Subteam, Structures contributed to defining body tube length and fin sizing to meet aerodynamic stability requirements. Communication with the Hardware Subteam was critical during the final phases of integration, and early coordination helped prevent redesigns late in the build schedule.

5. *Active Aero – Research Team*

Active Aero is a research team within the Organization dedicated to designing and creating an active control system to hit a target apogee. The system combines custom mechanical engineering and electrical engineering design as well as active control software. Working with the Software Development Subteam, the device dynamically changes the drag on the vehicle. If the software predicts that the vehicle will overshoot the target apogee in flight, it will deploy a set of flaps acting as brakes to add drag and slow down the vehicle to reach the target apogee. The inspiration of this project revolves around maximizing the flight performance score as well as the Barrowman Award, meaning if the team can purposefully overshoot the vehicle for a target apogee and use airbrakes to slow the vehicle on ascent, we can more reliably and accurately hit a target apogee. This Subteam features eight active members.

6. *Hardware Development – Research Team*

The Hardware Development Team is primarily responsible for designing and building data collection hardware for the flight vehicle, as well as other research and certification vehicles the Organization develops. The team works closely with the Software Development Team on integrated projects and collaborates with other Subteams on custom electrical systems. The Hardware team is responsible for the development of the MARTHA avionics platform that enables in-flight data collection for the flight vehicle. Additionally, the team is furthering Printed Circuit Board (PCB) design within the team with the Just an Expanded MARTHA (JEM) project that seeks to provide a more comprehensive flight platform. Lastly, the Hardware team oversees the manufacturing of 2-series 2-parallel (2S2P) and 4-series (4S) Lithium-Ion (Li-Ion) 18650 cell battery packs to power avionics platforms and onboard camera systems. This Subteam includes 10 active members.

The Hardware team developed the Statistical Analysis of Variance of Altimeters (SAVA) payload for this year's flight vehicle to better understand the differences between altitude measurements and readings across different altimeter chips and altitude calculation methods.

7. *Propulsion – Research Team*

Following a hiatus on the team, Propulsion is a renewed Subteam that is responsible for the design, development, and testing of hybrid rocket motors for research and future competition use. Currently, the team's experience with hybrid motors includes flying commercial motors. More specifically, the team has used three 38 mm Contrail H-class motors used for certification flights as well as one 98 mm Contrail L-class used for as one of the team's research vehicles. For the upcoming year, the goals for the Subteam are as follows: design and manufacture a 54 mm custom hybrid motor to gain practical experience with hybrid motor development and design and manufacture a test stand to record and measure data on impulse, temperature, and pressure to classify the motor. This smaller scale motor serves as an intermediate step before scaling to a larger competition grade system. Design objectives for the motor include safe integration of the oxidizer flow, injector configuration, nozzle geometry, and iterative refinement through static fire testing. In parallel, the Subteam will work with organizational leadership to identify a test site for static fire testing.

These efforts are to proceed alongside the motor development timeline, to ultimately conclude before the first static fire test is required.

The team also has experience with wired ground station equipment, which involves systems for oxidizer fill, purge, and motor ignition from a safe distance. Current hardware replicates a provided wired system borrowed from the team's mentor, Peter Tarlé, enabling early validation and operational testing alongside a working example. Future development on ground station equipment will transition toward a fully wireless control system to support increased pad distances, enhance robustness, introduce fault tolerance, and ensure reliable telemetry and control under remote operation conditions as expected for competition conditions.

8. *Software Development – Research Team*

The mission of the Software Development Research Team is to design, test, and integrate reliable software solutions that support all SRAD flight computer and ground station systems. The team supports the Hardware Development and Active Aero Subteams along with payload efforts, all of which feature custom electronics built around programmable microcontrollers, including the MARTHA device. Responsibilities include developing and maintaining the firmware for these systems, as well as creating custom software for ground station systems including data extraction and dashboard monitoring. Current device firmware encompasses sensor drivers, data saving formats, state detection algorithms, state machines, and apogee prediction models. The team also maintains the organization's GitHub repository for robust version control across the multiple concurrent software projects [3]. This Subteam includes twelve active members.

C. Budget Analysis

This section provides a thorough analysis of the budget for the CURE organization, detailing the financial allocation and management strategies employed throughout the Pocket Tens' project lifecycle. It outlines the total funds available, sources of funding, and a breakdown of expenditures across various categories such as materials, labor, testing, and administrative costs. This analysis aims to ensure transparency in financial operations and demonstrate how strategic budget allocation supports the project's goals and enhances our capability to deliver a successful vehicle design. Furthermore, the discussion includes a review of financial efficiencies and areas where cost savings were realized without compromising the quality or safety of the vehicle. This budget analysis reflects the current financial status and serves as a foundational tool for future fiscal planning and resource allocation within the team.

1. *Sources of Funding*

The CURE organization's financial resources are derived from various sources that support different facets of our project, Pocket Tens, ensuring comprehensive coverage of all necessary expenses. As a DSO, most of our funding comes from Clemson University's Student Funding Board (SFB), which annually supports our rocket engineering activities' operational and material costs. This funding is crucial for maintaining the continuity of our projects each academic year. The CECAS also plays a significant role in our financial ecosystem. The CECAS partially sponsors our travel to competitions and testing locations and funds the certification rocket initiative.

Our partnership with Science Applications International Corporation (SAIC) further enriches our funding landscape. SAIC sponsors our Active Aero Subteam, which focuses on developing an active control system for aero braking. This system is designed to enhance the precision and effectiveness of our launch vehicles, representing a critical component of our research and development efforts.

In addition to financial contributions, our project benefits significantly from in-kind support. OnShape and Ansys provide free access to advanced engineering software, indispensable for our design and simulation tasks. To assist with administrative and financial tasks, AirTable is an extremely important asset in organizational management. The communication platform Slack also offers an educational discount, allowing the organization to maintain a professional communication database. Moreover, Chomarat supplies us with high-quality carbon fiber materials for constructing robust and efficient aerostructures. This combination of monetary support and material sponsorship enables our team to push the boundaries of academic and practical achievements in rocket engineering.

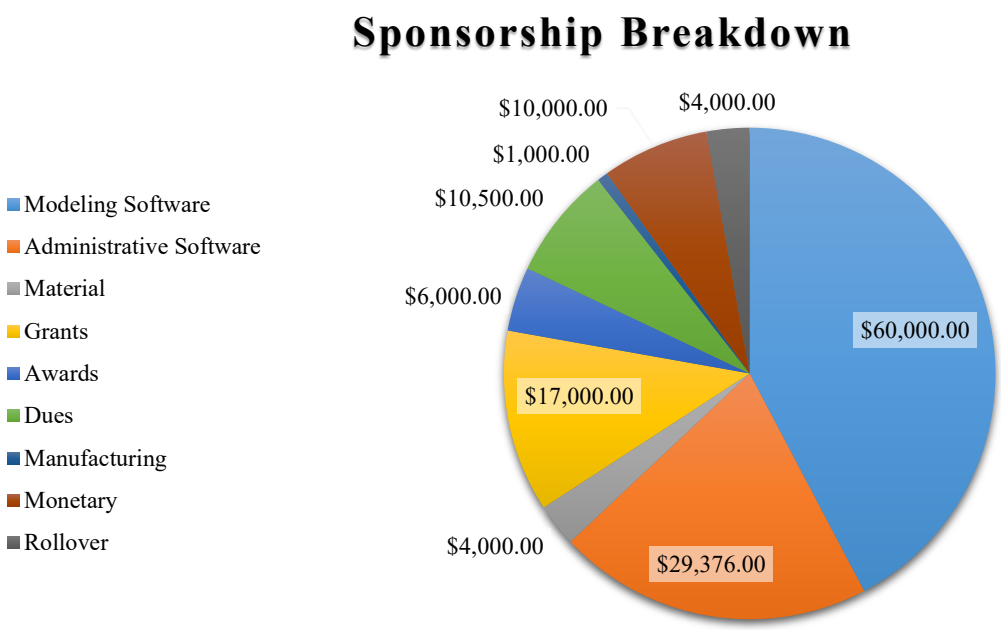

Figure 2 Sponsorship funding breakdown for CURE 2024-2025.

2. *Organization Budget*

The CURE team operates with an annual budget of $35,000.00, sourced primarily from the SFB ($19,312) and additional funding from rollover budget from previous years (~$4000) and monetary funding from sponsors and alumni (~$10,000). This funding supports the diverse needs of our organization, ensuring each project phase is adequately financed while promoting an efficient and strategic allocation of resources.

The organization's budget is intricately structured to cover specific needs across multiple Subteams, each responsible for the vehicle's development. These categories include Hardware Development, Structures, Simulations, and more. Notably, the Travel category, which amounts to approximately $5000 to $10,000 in total cost, is fully sponsored by the CECAS, thus relieving the budget of significant travel expenses and allowing for more focused spending on technological and structural advancements. However, $5000 has been budgeted for emergency expenses while traveling. A detailed budget summary can be seen in Figure 3 below.

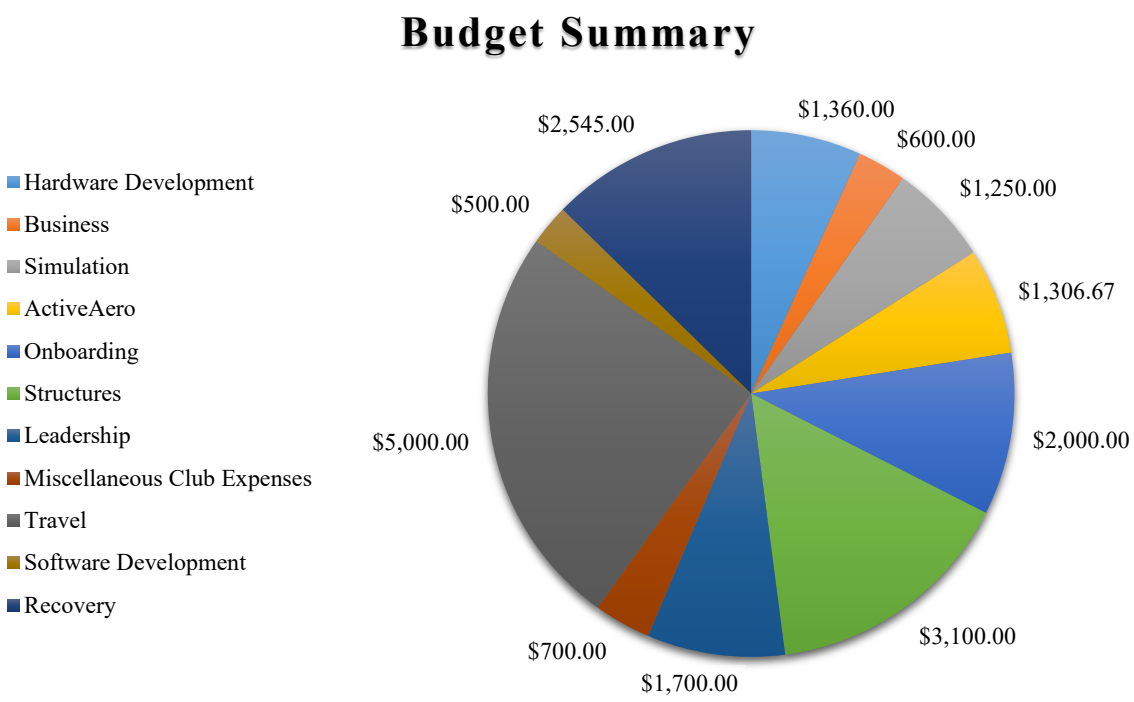

Figure 3 Budget breakdown of the CURE organization for 2024-2025.

Before funds are distributed, each Subteam undergoes a rigorous budget request process, which includes a comprehensive project review and timeline, an itemized list of necessary materials, and a detailed rationale behind the requested budget and specific items. This process ensures that every dollar allocated aligns with our strategic goals and maximizes the potential for successful project outcomes.

3. *Procurement Analysis*

The CURE organization has utilized a sophisticated procurement system using AirTable, enhancing our ability to track and manage expenditures with greater accuracy and transparency [2]. This system has allowed us to streamline our procurement processes, ensuring that all purchases are aligned with our project's needs and budget constraints. Our procurement strategy is divided into several major categories, as illustrated in the accompanying Figure 4. These categories represent the various areas where funds are allocated, each supporting a specific aspect of the rocket engineering project, called buckets.

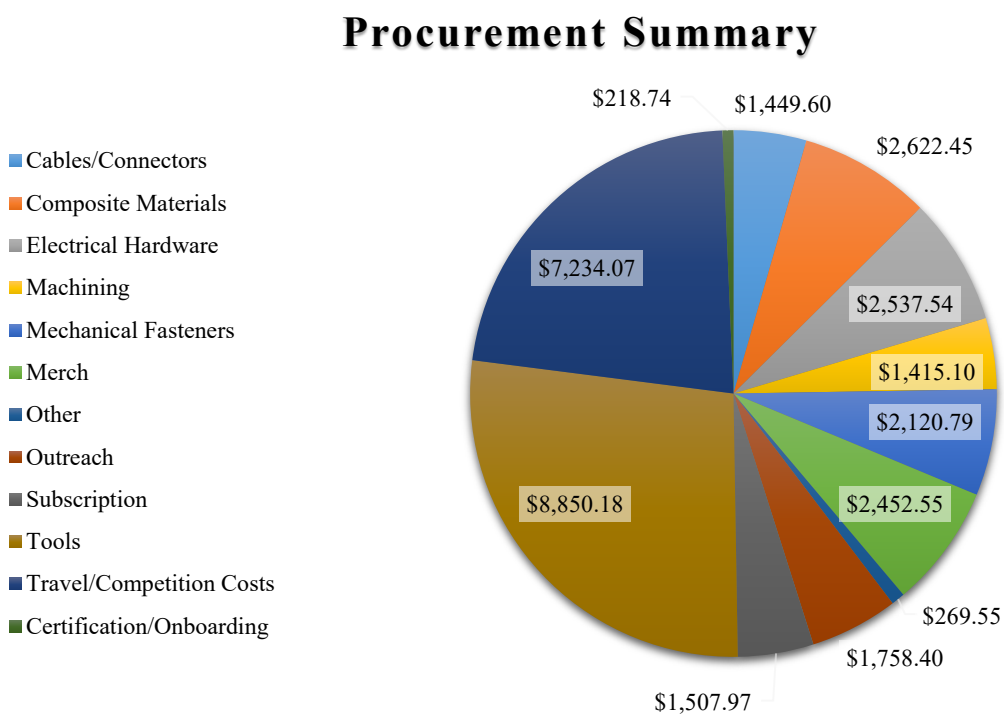

Figure 4 Procurement totals by item bucket for 2024-2025.

The introduction of AirTable has facilitated a more nuanced approach to financial management, allowing us to monitor spending in real time and adjust procurement strategies swiftly [2]. This agility has been instrumental in identifying areas where cost savings can be realized without compromising the quality or safety of our launch vehicles. For instance, bulk purchases of composite materials, hardware, and rocket motors have enabled negotiating discounts. Figure 4 details the breakdown of expenditures across all procurement categories. This visual representation helps quickly assess which areas consume the most resources and where adjustments may be needed. For example, the significant investment in tooling and mechanical fasteners are justified by the need to manufacture a launch vehicle by hand physically. Meanwhile, the lower spending on merchandise and orientation materials reflects a balanced approach to non-essential expenditures.

Through this detailed procurement analysis, the CURE team ensures that every dollar spent is meticulously accounted for and strategically utilized, reinforcing our commitment to excellence and fiscal responsibility in all rocketry endeavors.

III.System Architecture Overview

The Clemson University Rocket Engineering organization's launch vehicle, "Pocket Tens," is one of the most novel designs for the University to date. While being one of the team's most technically advanced launch vehicles, "Pocket Tens " is also foundational for the organization's future. One of the primary goals of this vehicle was to create a simple, modular design that can be improved upon each year with a focus on the ease of assembly. A CAD render of "Pocket Tens" can be seen in Figure 5 below.

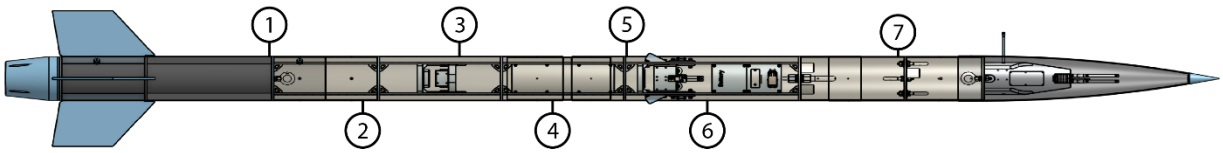

Figure 5 CAD assembly of fully integrated launch vehicle.

The vehicle entered the 10k COTS competition with an AeroTech M2500T motor consisting of, from left to right of Figure 5, a motor section (1), ballast section (2), SRAD avionics section (3), 3U CubeSat payload section (4), camera (5) and recovery electronics section (6), and nose cone section (7). All structural components of the launch vehicle are constructed of SRAD components. These include composite body tube layups, cut composite bulkheads, and in-house machined and carbon-reinforced nylon 3D printed payload components. This design is not flight-proven but is an iteration of the largely successful design of the previous year's vehicle. Integral components of the vehicle have been tested and proven in ground tests and all electronic systems have been thoroughly tested for circuit continuity, short circuits, and functionality while fully integrated. These tests include ejection testing, fin load testing, structural rigidity testing, and flight state recognition for SRAD systems.

A. Propulsion Subsystems

Motor selection is critical to determining how much a launch vehicle can weigh, how stable it will be during flight, and what apogee it can reach. Because the vehicle is competing in the 10k COTS competition, Clemson Rocket Engineering's vehicle would need to lift approximately 50 *lbm* to an apogee of 10,000 *ft* for the competition. This mass was based on the model of the vehicle in OpenRocket, with the mass of individual components being based on the previous years design. After analyzing thrust curve data for each of AeroTech's class N and M rocket motors, it was decided that a M2500T AeroTech motor should be used [25]. Additionally, the team flew with the M2500T in both the 2023 and 2024 IREC launches on launch vehicles of similar geometry and weight as this year's design. With this year's design of the vehicle, the motor would be required to lift 41.3 *lb*m while achieving 10,000 *ft.* Though simulations, the team has determined that it can do with this motor.

Furthermore, the thrust curve of the M2500T allows the vehicle to achieve an off-the-rod velocity of 106 *fts,* which is a crucial value for making sure that the vehicle is stable mid-launch. This value is greater than the minimum value of 98 *ft/s*, showing that the vehicle would have a safe liftoff. The motor also provides a near constant thrust of 2,700 *N* for the first three seconds of its burn time, minimizing irregular stresses that a more variable rocket motor thrust curve might cause. The team's familiarity with the selected motor, as well as the stability and stress benefits, play a large role in increasing the team's confidence in the launch vehicle's success at IREC.

B. Aero-structures Subsystems

The design of this year's vehicle is an iteration of last year's design, with improvements made in the construction techniques and quality control of SRAD components. The vehicle has been validated through ejection testing and simulations. The airframe consists of a nosecone, recovery parachute tube, COTS electronics tube, SRAD electronics tube, and motor tube.

1. Nose Cone

The nose cone is a COTS Wildman 31 *in* 5:1 Tangent Ogive, with an integrated fiber glass coupler extending into the payload tube one body caliber. The nose cone also includes a COTS machined aluminum tip with a shoulder extending into the nose cone and is secured with a threaded fastener and washer. For the design of the launch vehicle, the team initially decided on a 24 *in* 4:1 Tangent Ogive nose cone, but as the design was finalized the apogee was predicted to be higher than desired. This led to the team selecting the current nose cone, as it will experience more drag mid-flight, bringing the apogee of the launch vehicle closer to 10,000 *ft*.

2. Body Tube Airframes

The upper and lower main airframes are constructed using SRAD hand-layup fiberglass, with West Systems 105 Epoxy Resin and 209 Extra Slow Hardener. Fiberglass is the material of choice due to its RF transparency, ensuring proper signal transmission for GPS tracking and future telemetry projects. The manufacturing process, which involves wrapping a rigid tube mandrel with mylar, woven peel ply, and fiberglass layers, has been developed over the past four years. The process begins with positioning the body tube mandrel on two wooden stands with a trough that can hold them as seen in Figure 6.

Figure 6 Composite sheet being wrapped and coated with an epoxy and hardener mixture.

The wooden stands are gripped with metal C-clamps on a tabletop, two per stand. The mylar film is layered on the mandrel and then is coated with a layer of epoxy resin, with a pre-measured ratio of three parts resin to one part 209 extra slow hardener. Once the film is coated, a wrap of peel ply fabric is added. The coating process is repeated for the single peel ply wrap. A single fiberglass woven sheet, 76 inches long, is then wrapped around the mandrel to complete four total layers of fiberglass. A final layer of woven peel ply is wrapped around the outside to improve the consistency of the outer surface finish and lock the epoxy resin in place.

Figure 7 Composite tube curing in vertical position for twenty four hours.

Figure 8 Composite tube being sanded using a rotary hand Dremel.

As seen in Figure 7, the mandrel is left standing on a well-positioned wooden stand on the ground floor, so it can go through the curing process, for at least 24 hours. After 24 hours, the body tube is ready to be extracted from the mandrel and is ready to be post processed as seen in Figure 8. The result is an extremely strong tube for the airframe, capable of withstanding over 600 *lbf* of compressive longitudinal force. The total length of the launch vehicle is 11 *ft* 11-11/16 *in*. The nosecone, parachute airframe, upper main airframe, lower main airframe, and motor section are the following lengths, respectively: $8-\frac{15}{16}$", $14-\frac{15}{16}$", $33-\frac{9}{16}$", $27-\frac{7}{16}$".

2. Couplers

The couplers are manufactured using a similar process to the body tubes, utilizing a 3D-printed mandrel, to ensure proper sizing of a 5.80" outer diameter. Three mated mandrels were used to create the coupler. Each mandrel is designed in such a way that they can be epoxied together to create a larger mandrel which the coupler can be created from. Similar to the body tubes, couplers are made of a plain loose fiberglass weave to ensure RF transparency. The mylar film is used to create a boundary between the mandrel and coupler, allowing for a smooth extraction from the mandrel once cured. The use of peel ply on the outer edge remains the same, allowing for smoother surface finish. The curing process takes 36 hours until work hardened, in which post processing can occur. Once cured, the couplers are measured to a desired length before sanding down excess material. The result of these dimensioned couplers will bind the main bodies of the launch vehicle airframe to the nosecone and motor tube. The holes for the couplers for the nosecone and motor tube are drilled for ¼ - 20 fasteners while the main body will have 4-40 fasteners.

3. Bulkheads

Bulkheads are composed of a circular carbon fiber plate. The 6" in diameter bulkheads are cut from 0.25" thick COTS Dragon Plate[8]. The bulkheads are water jetted out of the sheet and post-processed using drill presses and sandpaper to prepare the surface. They serve as additional supports to the vehicle's tubes and act as fastening points for the spars. The bulkheads and spars are joined with 1" x 1" aluminum gussets[25] fastened with ¼" - 20 x 1 *in* thin head bolts[26]. The launch vehicle consists of ten bulkheads: one ring bulkhead, two centering ring bulkheads, one upper motor bulkhead, three main section bulkheads, and three recovery bulkheads.

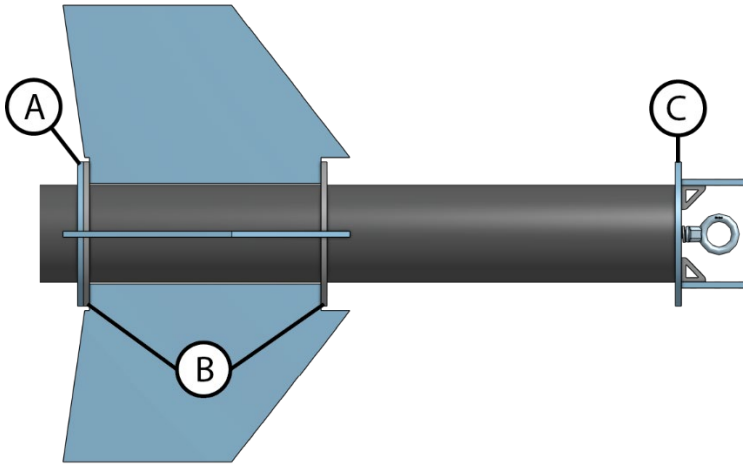

Figure 9 Cutaway view of motor section to view section bulkheads.

The ring bulkhead, Figure 9A, is in the bottom motor section and is cut with a waterjet and is used to attached the boattail to the motor tube. The holes jetted in the ring bulkhead are further post processed with a 7/15" drill bit. Composite inserts were inserted into the holes in the ring bulkhead following post processing such that the boat tail can be fastened to the motor section. Two centering rings center the inner motor assembly and allow the fins to be indexed radially, Figure 9B. The upper motor bulkhead, Figure 9C, sits at the bottom of the main section spars, with an eye bolt securing the main section to the motor section. The upper motor bulkhead is joined to the inner motor tube with a carbon fiber composite layup and epoxy fillet to create a solid body.

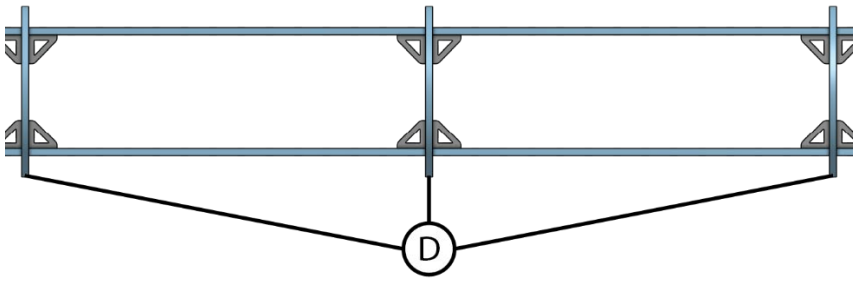

Figure 10 Cutaway view of main section to view section bulkheads.

Three identical main section bulkheads Figure 10D connect and separate the SRAD, Payload, and COTS sections. Carbon fiber composite spars run through each of these sections. The spars are capped with the lower recovery

bulkhead Figure 11E which is fastened to the spars and sits directly above the recovery electronics. The middle recovery bulkhead Figure 11F is epoxied into the airframe with a silica thickened epoxy fillet. The upper recovery bulkhead Figure 11G is epoxied to an aluminum machined adapter which is radially bolted with ¼" - 20 set screws in the nosecone shoulder.

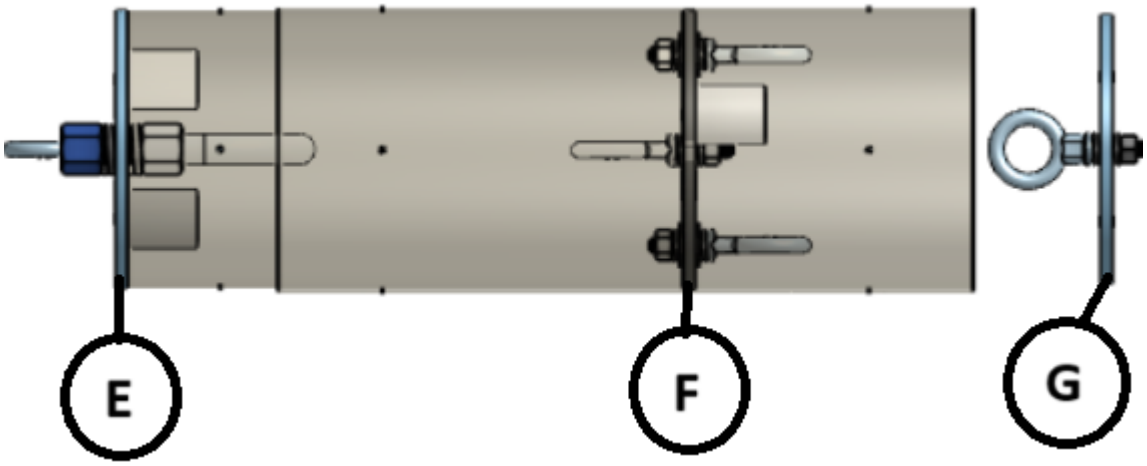

Figure 11 Cutaway view of recovery section to view section bulkheads.

4. Motor Tube

The inner and outer motor tube were made through a similar process to that of the body tubes. Carbon fiber weave was used instead of fiberglass weave. Carbon fiber has a higher strength-to-weight ratio than fiberglass and supports higher pressure loads that are expected on the tubes due to the motor burn. Additionally, the factor of RF transparency is much less of a concern due to the location of the motor tube relative to dipole antennas present on the vehicle and their toroidal propagation pattern. The process of manufacturing involves wrapping a rigid tube mandrel with one wrap of mylar, a layer of woven peel ply, four wraps of a single 45-45 carbon fiber plain woven sheet, and then another layer of woven peel ply. In between each layer, a 3:1 ratio of West Systems 105 epoxy resin and 209 extra slow hardener is used following manufacturing specifications and guidelines.

The fins are made of ¼ *in* thick G10 fiberglass. This is a change compared to last year's launch vehicle where a carbon fiber plate was used. This design change is because the G10 saves weight and cost, while meeting the required factor of safety for fin flutter. The G10 fins are assembled to the motor section utilizing a through-wall construction. They are inserted into 1/4 *in* wide, 10-inch-long slits sanded and cut into the outer motor tube.

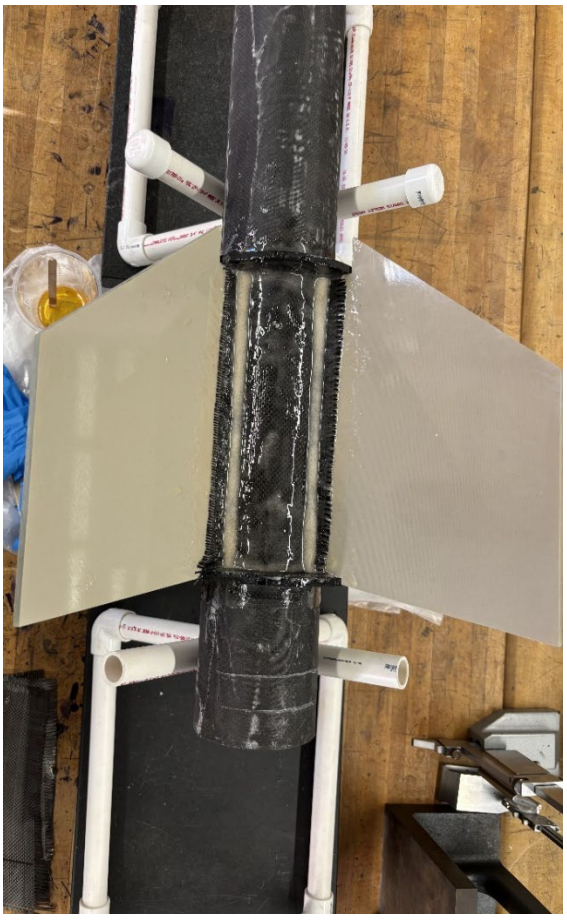

Figure 12 Internal assembly of motor tube.

Figure 13 Internal tip-to-tip carbon fiber layup and epoxy fillet of internal motor assembly.

The fins are rigidly mounted by epoxying them to the inner motor tube with an epoxied layer of carbon fiber in-between structural fillets and epoxied to the epoxied centering rings attached to the inner motor tube, as seen in Figure 12 and Figure 13. The fins also are filleted to the inner motor tube with a carbon fiber layup going from fillet to fillet to add extra strength as well as improve the evenness of the fillet and thus the weight distribution. Finally, the fins are epoxied to the outer body tube with additional fillets, as seen in Figure 14, to ensure structural integrity and load transfer during flight. The fins were designed to be able to achieve high-speed flight without tearing off due to shear force. A more detailed justification of the fin design is located in Appendix A-A and the factor of safety of the fins was calculated to be 3.4 in Appendix A-C.

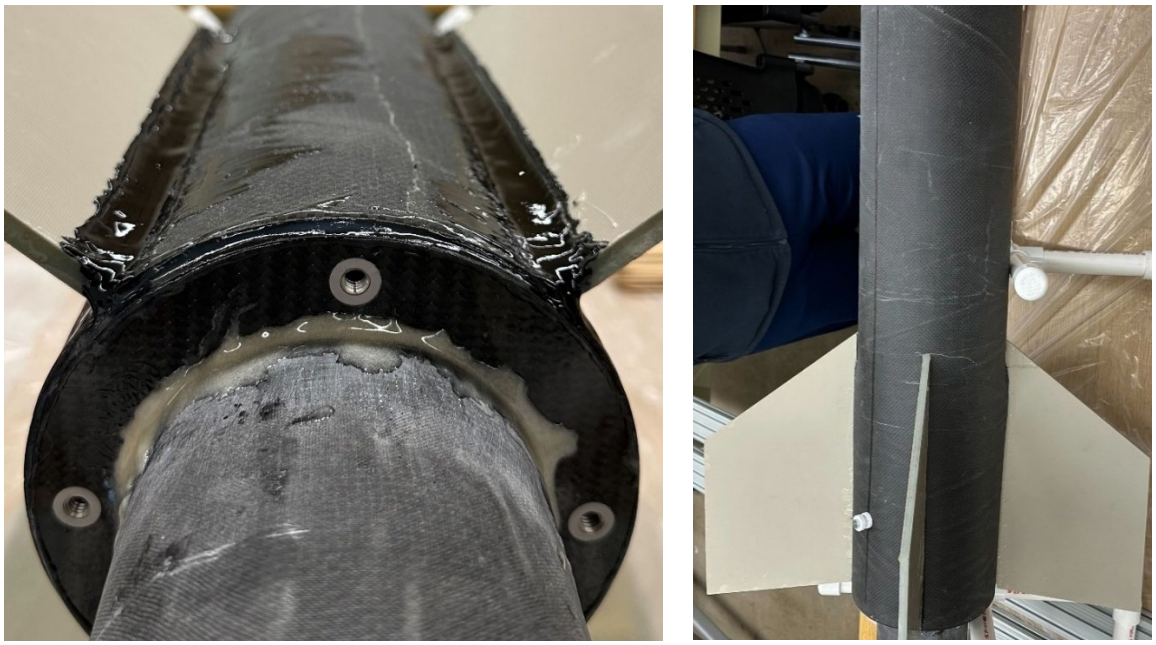

Figure 14 Exterior carbon fiber motor tube is attached to the interior motor tube through epoxy fillets.

The fins include a single layer tip-to-tip-to-tip-to-tip hand layup of plain woven carbon fiber sheet. The carbon fiber spans the length across all fins and over the exterior motor tube to mate the motor section as one, solid body. Each fin is further wrapped with another carbon fiber layup to provide rigidity to the fin edges and tips, as seen in Figure 15. This decision was made to ensure the fins withstand the excessive landing forces that may damage fins without a hand layup reinforcement. Also, this hand layup reinforcement improves the airflow along the surface around the fins by making a more consistent transition from the fins to the body tube around the fin fillet, as seen in Figure 15.

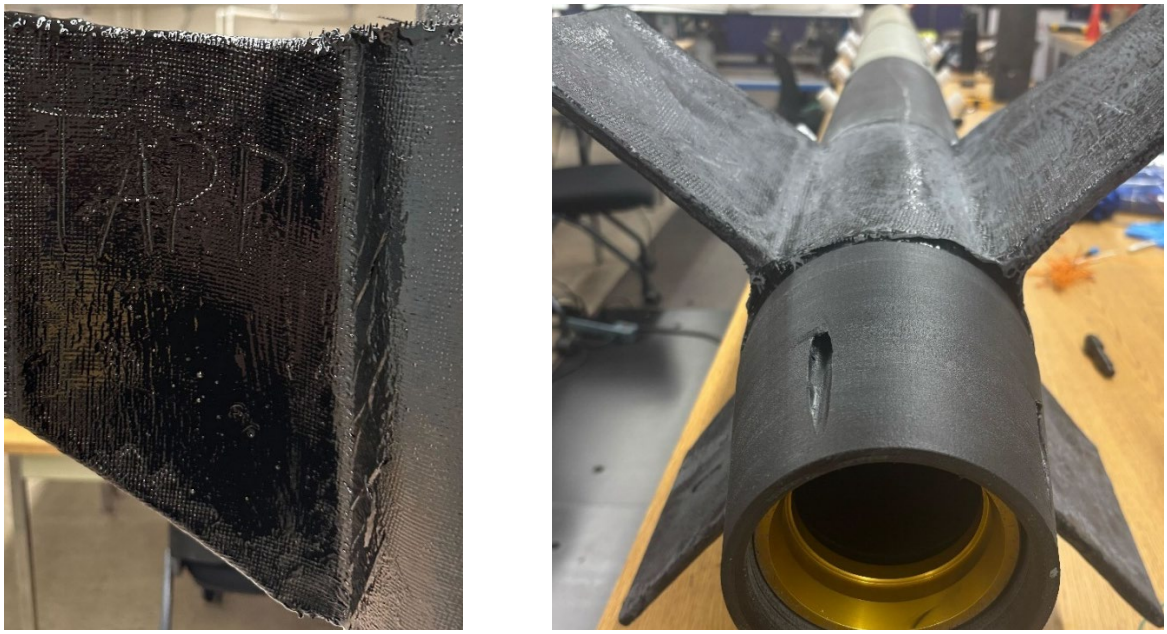

Figure 15 Tip-to-tip-to-tip-to-tip carbon fiber layup followed up with an orthogonal carbon fiber weave along the tin perimeter.

The aft motor retention uses the machined shoulder threaded into the motor case, which fits tightly against the inner motor tube. The forward motor retention is a carbon fiber bulkhead epoxied to both the body tube and inner

motor tube acting as a thrust plate, with a forged eyebolt[10] rated to 1300 *lbf* threaded tightly into the forward threaded hole on the motor case. The 6.00” long boat tail is 3D printed from carbon fiber reinforced nylon and is screwed into threaded inserts embedded into the rear centering ring. The boat tail is for aerodynamic purposes only, and not for motor retention.

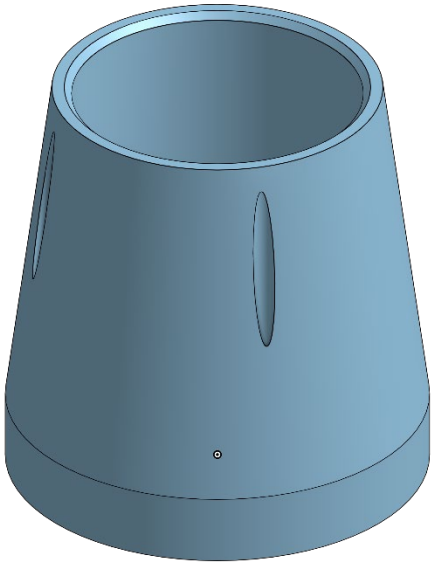

Figure 16 Rendering of boat tail with reliefs for fasteners.

5. Spars

Spars were utilized in conjunction with the bulkheads to compose the internal structure of the launch vehicle. Similarly to the bulkheads, spars were constructed using the same 0.25” thick COTS Dragon Plate carbon fiber of 0-90 orientation. The purpose of the spar design is to make assembly simple. Since all the internals are connected, they can be assembled separately from the airframe of the launch vehicle and then be inserted into the correct location within the vehicle. The design of the spars also allows for modularity over the year and upcoming years due to the holes within the spars. Each spar has centered ¼-20 holes 1 *in* apart from each other allowing for iterations to be made to the internal systems without having to change the design of the spars or manufacture new ones.

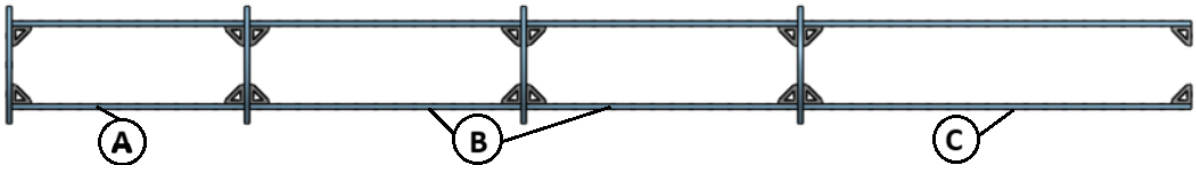

Figure 17 Rendering of main section to view spars.

From left to right, two 12” spars, shown in Figure 17A, were used as the internal structure for the ballast section, connecting the upper motor bulkhead to the lowest main section bulkhead. Next, two 14” spars, seen in Figure 17B, were used as the internal structure for the SRAD section, connecting the lowest main section bulkhead to the second. For the payload internal section, two 14” spars shown in Figure 17B connect the middle main section bulkhead to the highest main section bulkhead. The COTS section includes two 20” spars, seen in Figure 17C, connecting the upper main section bulkhead to the lower recovery bulkhead. All spars are equipped with one vertical line of ¼-20 holes centered along the spar and with center distances of 1” from each other. The spars are connected to each bulkhead through 1”x1” L-shaped aluminum gussets, with ¼-20 screws connecting the spar and bulkhead to either hole in the gusset. ¼-20 lock nuts are pre fastened to the side of the gusset using a silica thickened epoxy-hardener mixture in which the bulkhead is attached, a change made for ease of assembly.

C. Recovery Subsystems

1. Design Philosophy

The recovery subsystem for this year's flight vehicle is built on the team's experiences at IREC and independent research vehicles launched over the last four years. The recovery system in the vehicle utilizes a dual deployment system with a dual bay drogue and main parachute architecture, where the drogue is deployed at/just after apogee, and the main parachute is deployed at 1000 *ft*. The dual bay architecture refers to the placement of parachute bay(s) within the vehicle, where in a dual bay architecture, the drogue and main parachute bays are separated by a bulkhead but are side by side and in a continuous section. Whereas, in a dual split bay architecture, the parachute bays would be separated by one or more sections of the vehicle, and a single bay architecture would store the drogue and main parachutes in the same bay. No SRAD electronics are used in any way for recovery purposes. In addition to this, the vehicle's recovery subsystem utilizes recommended parts and practices from the IREC Design Test & Evaluation Guide's (DTEG) Appendix B: Safety Critical Wiring Guidelines [18]. With this, there were three main areas of improvement of the recovery subsystem for this year's flight vehicle: Increased redundancy, reduced manufacturing times, and improved assurance. Changes that highlight these goals can be found in Table 1 Primary recovery revisions and goals for IREC 2025. **Error! Reference source not found.** below shows the CAD representation of the recovery subsystem electronics, while Figure 19 shows the produced and installed module into the spars section.

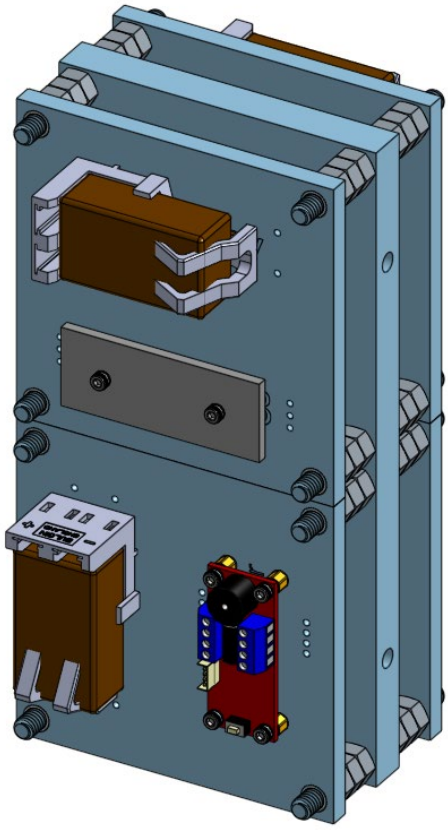

Figure 18 CAD Render of recovery electronics.

Figure 19 Production version of recovery electronics

2. Subsystem Overview

The recovery subsystem can be functionally broken down into two primary components: Parachute deployment and GPS tracking. The GPS tracking component uses two Featherweight GPS trackers and associated ground stations to maintain a connection with the vehicle before, during, and after flight. GPS tracking is covered in more detail independently at the end of this section, while the remaining portions cover the electrical and mechanical elements of the parachute deployment component. The main section of the recovery bay, shown in Figure 20 and Figure 21, utilizes

a modular backplane-based design and holds the batteries and arming switches for all three altimeters, as well as the altimeters themselves.

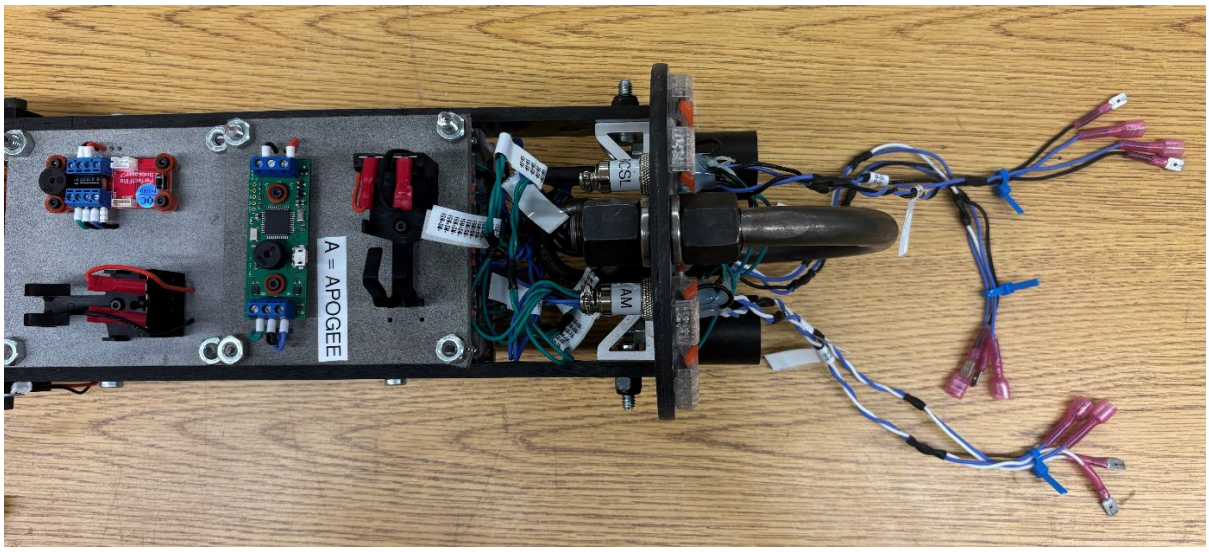

Figure 20 Fully installed recovery bay showing StratoLogger and AIM USB altimeters

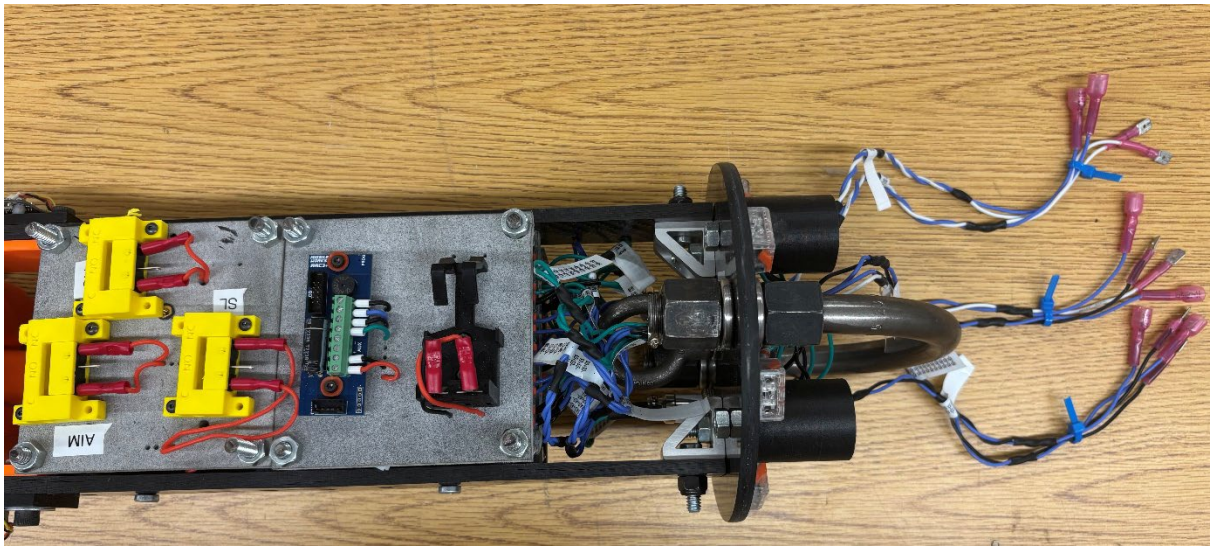

Figure 21 Fully installed recovery bay showing switch module and RRC3+ altimeter

Additionally, in-line 1-to-2 Wago Lever Connectors (WLCs) were installed at the forward end of the bay to enable redundant wiring across three detachable eight-pin aviation connectors that screw into the main parachute bulkhead. Cabling for the drogue deployment is routed through the main parachute bay where it is protected by expandable webbing. Deployment cabling for the main parachute is broken out on the bulkhead into individual WLCs where signals can be rejoined and charges can be clipped into each WLC and inserted into the charge wells. Each connector is potted with hot glue for electrical and mechanical reliability. Spade connectors on the drogue deployment cabling within the main parachute bay provide a designed failure point to enable vehicle separation upon main deployment. The drogue deployment cabling then connects to two detachable eight-pin aviation connectors, where it follows the same process of breaking out to WLCs, clipping in, and potting as the main deployment cabling.

The parachute deployment component of the recovery subsystem utilizes a tri-altimeter setup with primary and secondary drogue and main charges, for a total of four charges across two different deployment bays. A symbolic representation of this configuration can be found in Figure 22. The primary altimeter, an AIM USB 3.0, is wired to both the primary drogue and main charges with a main deployment altitude of 1000 *ft*. The secondary altimeter, the StratoLogger CF, is wired to both the secondary drogue and main charges with a two second apogee delay and main

deployment altitude of 950 *ft,* which would be 1.25 *s* after a primary main deployment. The tertiary altimeter, an RRC3+, is wired to both the primary and secondary drogue and main deployment charges. The RRC3+ uses a three second apogee delay with a main deployment altitude of 900 *ft*, which would be a 2.25 *s* delay upon a failed primary and secondary deployment.

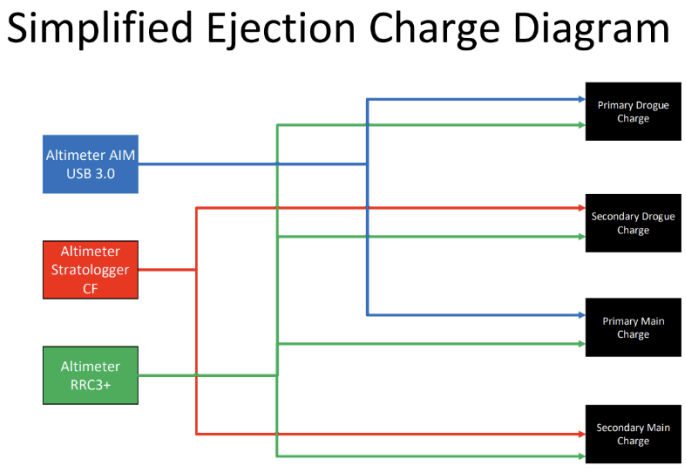

Figure 22 Symbolic wiring diagram of for deployment charges.

To achieve each area of improvement with this year's recovery subsystem, a set of changes from the previous subsystem were introduced, focused primarily on the electronic element of the system. These changes were meant to balance each one of the improvements listed prior, without impinging on another area. The changes can be found in Table 1 and are detailed further in the section.

Table 1 Primary recovery revisions and goals for IREC 2025.

Change	Goal	Description:
Addition of RRC3+	Increased redundancy	Addition of RRC3+ provides another layer of redundancy in the recovery subsystem
Use of 22 AWG wire	Improved assurance	Standardization of 22 AWG wire across the recovery subsystem creates more uniform wiring
Use of Ferrules	Improved assurance	Ferrules provide better and more reliable connection to screw terminals than bare wire
Greater use of Wagos	Ease of manufacturing	Use of Wago Lever Connectors as signal splitters/joiners eliminates soldering
Use of spade connectors	Ease of manufacturing	Use of spade crimp connectors further eliminates soldering and provides a removable connection
Cable flags	Improved assurance	Use of cable flags marks every cable with a unique identifier to maintain organization
Backplane based design	Ease of manufacturing	A modular backplane centered design allows for greater flexibility in component placement
Connector wiring	Increased redundancy	Redundancy in wiring across connectors increases reliability in the event of a failure
Expandable sleeving	Improved assurance	Use of expandable sleeving protects wiring exposed to ejection charges to preserve for future flights
U-Bolt retention	Improved assurance	Eliminates the possibility of spinout failures during parachute deployment

3. Mechanical Structure

For the main mechanical structure of the recovery bay, a modular backplane design was selected. This design was chosen for the ability to freely configure and reconfigure the recovery bay throughout the development process, giving greater flexibility and adaptability to emerging challenges throughout the design process compared to previous designs. The backplane system houses each of the three altimeters, 9*V* batteries, and arming switches for each altimeter. The backplane is mounted with two ¼-20 bolts into the main spar section at 1.5 *in* from the forward and aft ends of the plane. This gives 5 *in* of distance between two sets of bolts on the backplane for a total length of 8 *in* for the backplane. Within the backplane, there are eight 0.2 *in* height slots to provide routing paths for wires that transition from one side of the plane to the other. The slots are bunched in groups of four with a 0.667 *in* spacing between each slot, a 0.6 *in* spacing from the forward and aft section of the backplane, and a 1.2 *in* spacing in the center of the backplane. A model of this design can be found in Figure 23, while the produced design is shown in Figure 24. The backplane is 3D printed out of PA12 nylon on an HP Multi Jet Fusion 3D printer. PA12 was chosen as the material due to its mechanical and thermal properties [26]. PA12 features favorable tensile strength at 47, and a melting point of ~180 °C [27]. Additionally, PA12 features a heat deflection temperature of ~87°C, meaning that even in the rugged and hot climate of IREC, the bay will not experience deformation due to temperature before or during flight [28].

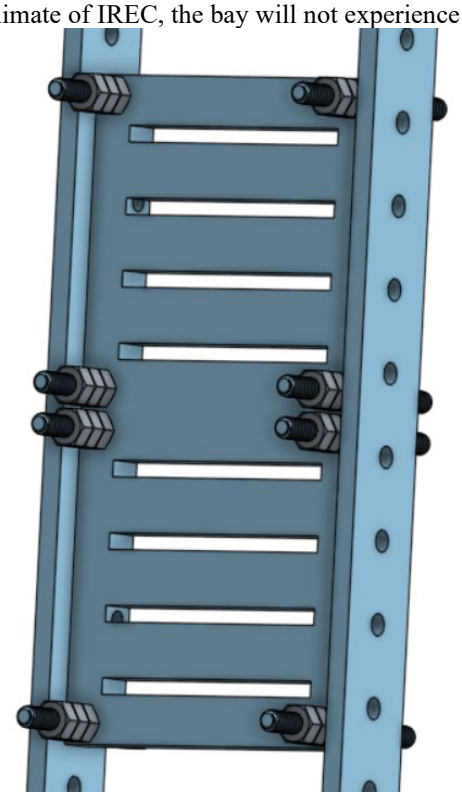

Figure 23 Final CAD model of recovery back plane.

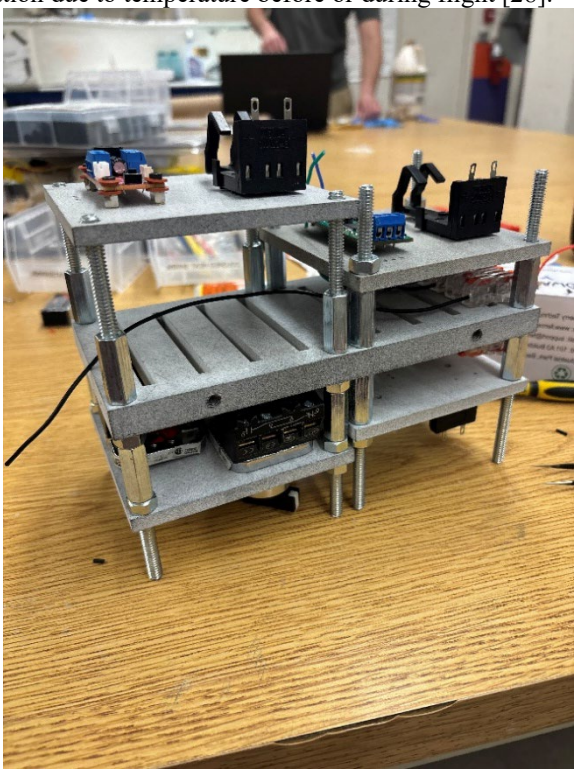

Figure 24 Initial installation of recovery backplane.

Each 8 *in* backplane segment is then broken down into four 4 *in* x 4 *in* modules, with two modules on each side of the plane. Each module is then mounted to the backplane with a set of four ¼-20 threaded rods[27] that run through the backplane, supplying a mount for modules on both sides of the plane. Each module uses ¼-20 coupling[28] and hex nuts[29] as spacers to provide clearance between the backplane and the module, inserting the rods through the holes in the module's corners. This spacing can be adjusted by adding/subtracting nuts from the threaded rod stack up, as well as adjusting the overall placement of the nuts along the threaded rod. After each module is placed on the threaded rod, a ¼-20 lock nut[30] is installed on each corner to lock the module in place. Like the backplane, each module is printed out of PA12 nylon, which was chosen for its mechanical and thermal properties discussed prior. Each module features 4-40 heat inserts[31] for mounting components. Additionally, each module is specifically designed for the altimeter/components present on the module and features custom 22 AWG sized holes for each signal to allow a friction fit connection through the hole but maintain strain relief on the entire harness, as seen in Figure 27. This creates a cleaner interface for each altimeter and isolates cable organization to the internals of the bay, and not near any altimeter, where it could cause issues such as shorts or depression of a debug button.

When a component, such as an altimeter, is mounted to the module, a 4-40 x 1/4 *in* tall aluminum standoff[32] is mounted into the threaded insert. To provide electrical isolation between the standoff and the component, a rubber washer is inserted between the standoff and the underside of the component, where a 4-40 nylon screw[33] is then used to mount the component in place. For symmetry and assurance, and additional rubber washer is placed between the nylon screw and the top of the component. This configuration decreases the effect of vibrations on each component, reducing the likelihood of a mounted component becoming unscrewed during flight, as well as a screw terminal on a component from backing out.

There are two primary types of backplane modules within the recovery bay. These are the altimeter and switch modules. The switch module holds the arming switches for all three altimeters, while the altimeter module holds both the altimeter and the power supply (9*V* battery) for the altimeter. Each altimeter is armed through a custom designed locking pull pin switch that utilizes a keying mechanism to prevent accidental arming. This mechanism is further discussed in *Altimeter Selection and Configuration*.

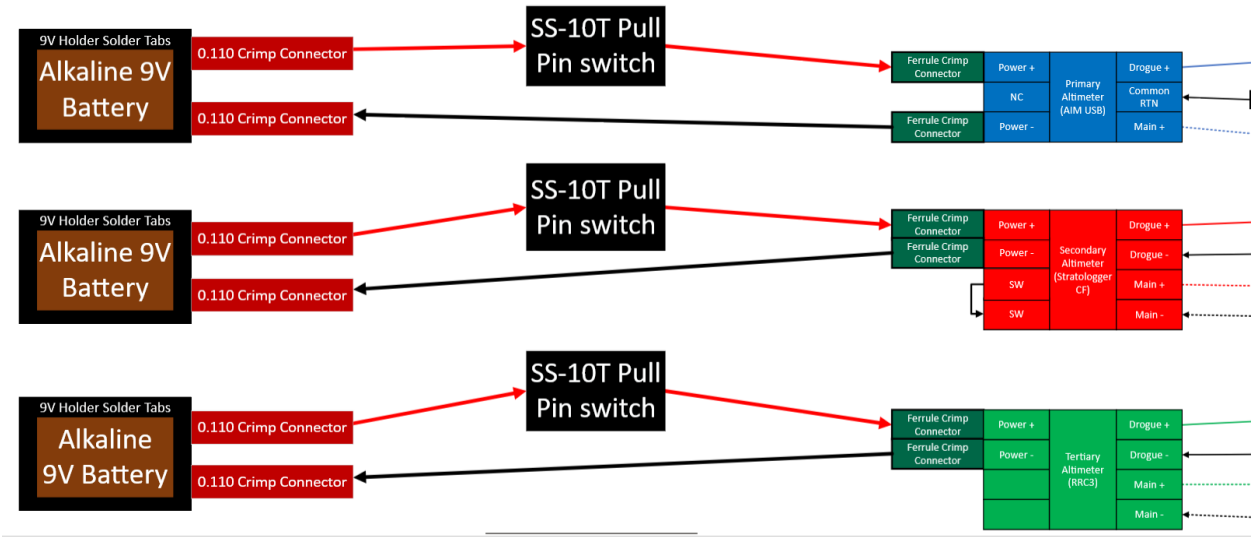

Figure 25 Redundant power configuration of recovery altimetry.

One side of the backplane features the AIM USB 3.0 and StratoLogger altimeters, while the opposite side holds the RRC3+ altimeter and the switch module. The switch module is located on the aft module mount of its side of the backplane, as this is to help reduce the total height needed to reach each switch, although use of a ladder at the pad is expected still.

At the forward edge of the backplane, twelve in-line 1-to-2 Wago Lever Connectors (WLCs) are adhered using Gorilla Glue[39] into two banks of six. These connectors provide a central hub for all routing to ejection charges, which is discussed further in *Wiring Architecture*.

The recovery system uses an AIM USB 3.0 as its primary altimeter, while a StratoLogger CF is used as the redundant secondary altimeter. A tertiary altimeter is implemented as well with an RRC3+. Each altimeter is independently powered and wired across each e-match, The AIM USB is connected to each of the primary drogue and main charges, while the StratoLogger is connected to the secondary drogue and main charges, for a total of four deployment charges within the vehicle. The AIM deploys the drogue chute at apogee, 10,178.9 *ft*, and the main chute at 1000 *ft* while the StratoLogger has a two second apogee delay and deploys the main chute at 950 *ft*. The RRC3+ is independently wired to both the primary and secondary drogue and main parachute charges. The RRC3+ uses a three second apogee delay and main deployment altitude of 900 *ft*.

Each of the four charges use 4F black powder[34] as the explosive to provide the deployment force. The primary drogue charge uses 1.75 *grams*, while the secondary charge uses 3.25 *grams* of black powder. The primary main charge uses 2.5 *grams.* and the secondary charge uses 5.0 *grams* of black powder. A more detailed analysis and discussion of the calculations and methodology to determine these values can be found in *Deployment System*32.

In total, there are five retention mechanisms within the vehicle: shock cords, swivels, quick links, eye-bolts, and a U-bolt. These five mechanisms of retention secure the three segments of the vehicle during and after deployment of all parachutes. The forward drogue parachute retention consists of two 1300 *lb* rated forged eye-bolts (Figure 54D). A 42 *ft* shock cord will span through each eye-bolt connected to the upper recover bulkhead (Figure 54C), leading to

the parachute lagging the rest of the vehicle by approximately 21 *ft*. The eyelets of the shock cord are connected to a 3000 *lb* rated quick link (Figure 54B) followed by a 3000 *lb* rated swivel (Figure 54E). This connects to the drogue parachute, which is a Fruity Chutes 48 *in* Iris Ultra (Figure 54A), through another quick-link and swivel that slows the vehicle to a descent rate of 40.9 *ft/s*. A separate swivel and quick-link is used to connect the nosecone through another 42 *ft* shock cord (Figure 54F)

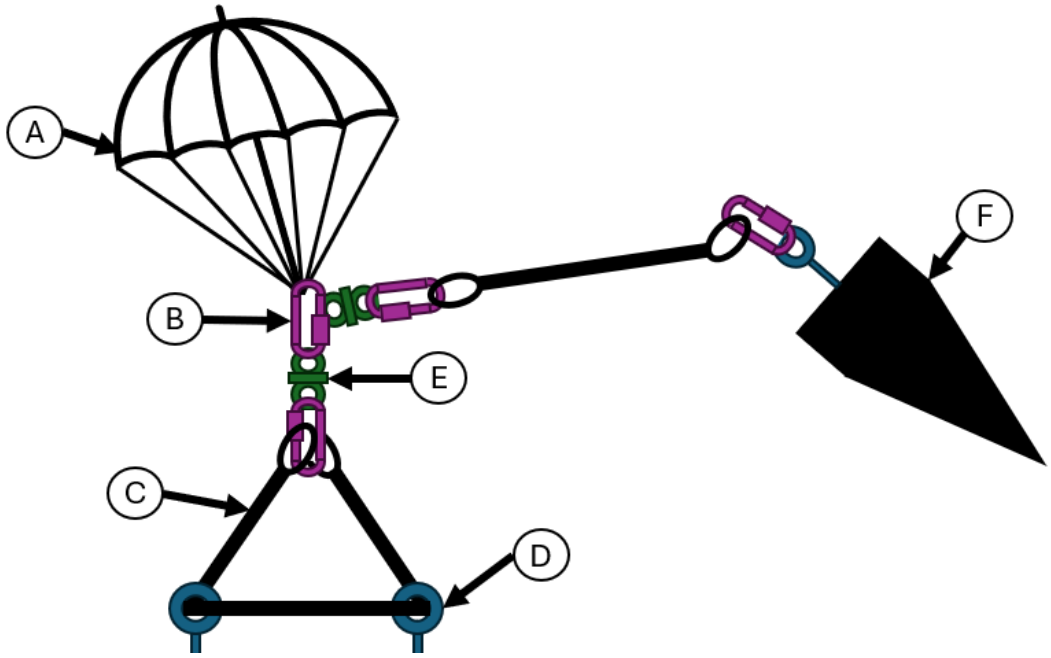

Figure 26 Plan for drogue deployment system.

The main parachute harness consists of a U-bolt rated at 5300 *lb* on the aft bulkhead which is connected with a quick-link rated at 3000 *lb.* 42 *ft* of nylon webbing shock cord rated at 3000 *lb* connects the U-bolt to the main parachute, a Fruity Chutes Iris Ultra 120 *in* parachute, through a 3000 *lb* swivel. The forward bulkhead is connected to the rest of the body through another quick link that connects to a 1300 *lb* rated eye-bolt. Under the main parachute, the vertical velocity will be reduced to 13.7 *ft/s*.

4. Altimeter Selection and Configuration

Previous recovery subsystems implemented an altimeter system with two altimeters. In the past, these were a StratoLogger CF[35] from PerfectFlite and an AIM USB[36] from Entacore [22, 24]. While this proved to be an effective setup, we found the AIM USB to not be as easy to work with as other altimeters, an example of this being altitude reported as meters. In lieu of this, we chose to add the RRC3+[37] from Missile Works as a tertiary altimeter on this year's vehicle [23]. This was due to the RRC3+'s reputation within the rocketry community, large feature suite for future projects, and stable development/availability. However, due to our lack of experience in using the RRC3+, we did not feel comfortable in placing it immediately as our primary or secondary flight computer. Our organization has done three flights with the RRC3+ as a secondary altimeter, but none to the scale of the IREC competition vehicle. We will be using this IREC as confirmation of the RRC3+ as a reliable altimeter platform. In addition to this, in anticipation of the 2026 IREC requiring the Featherweight Blue Raven altimeter on all flights, per the IREC DTEG, we plan to transition the RRC3+ to take the place of the AIM USB, and fill with RRC3+'s current place with the Blue Raven.

We chose the AIM USB for the vehicle's primary altimeter due to the continued reputation of Entacore's products within the rocketry community, the relative cost compared to other altimeters, and the ease of configuration. We chose the StratoLogger CF for the vehicle's secondary altimeter due to the small total size of the altimeter as well as the well known reputation of the altimeter.

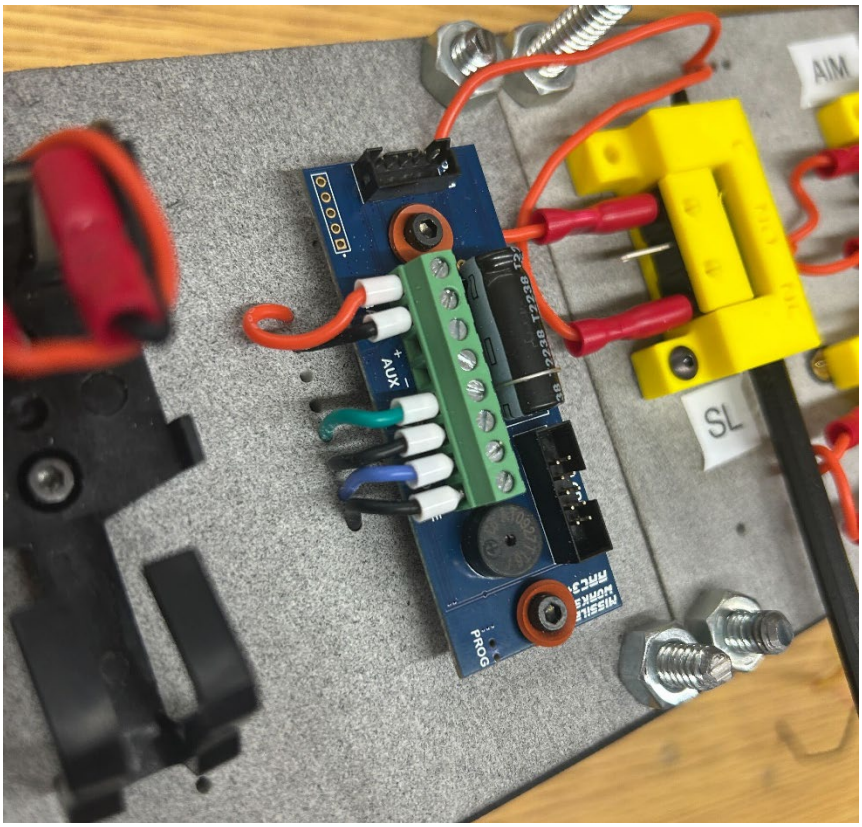

Figure 27 RRC3+ altimeter installed with power and ejection lines wired.

Each altimeter in the parachute deployment component of the recovery subsystem acts as an independent and redundant unit in regard to the other altimeters. Each altimeter is powered by a different alkaline $9V$ battery and is switched on independently through an Omron Electronics SS-10T[38] SPDT switch. Each switch has a custom build housing around it that allows for a pin to be inserted, depressing the button of the switch and preventing the flow of electricity to the altimeter. When the pin is removed, the button is released and power flows to the altimeter. To remove the pin from the switch/vehicle, one must first pull the pin as far out as they can. Then one must rotate the pin 90° clockwise and then pull out further, before rotating back 90° counterclockwise and removing the pin from the vehicle. This system effectively locks the pin in place when it is inserted into the vehicle, decreasing the likelihood of accidental arming of an altimeter throughout the flight preparation process. The SS-10T switch was selected not just for its ability to act as a pull pin switch, but it's heavy mechanical shock resistance. The resistance to mechanical malfunction, where malfunction is defined as a closed or open circuit of the contact at a max of 0.001 *s*, is 300 *m/(s^2)*, or approximately 30 *g*.

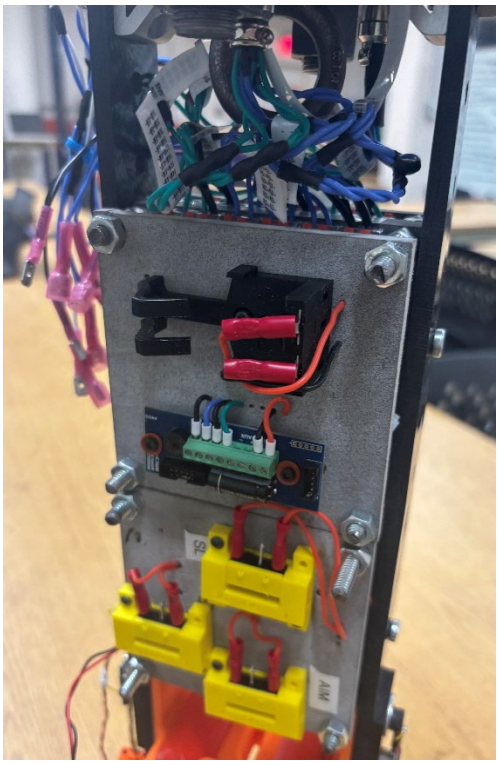

Figure 28 Switch and RRC3+ modules for recovery bay.

Each $9V$ battery is held secure through a Bulgin BX0033[40] $9V$ battery holder that has tabs for 0.110 *in* crimp connectors to attach. This was chosen since it is the same connector used on each pull pin switch, thereby creating continuity across sections of the subsystem and decreasing overall complexity. This configuration can be found in Figure 25, while the produced version of this can be found in Figure 28. These holders provide an easy means to install and uninstall batteries while also providing a secure mount and resistance to high *g* and vibrational loads.

5. *Wiring Architecture*

This section will focus on the architecture of parachute deployment lines for the flight vehicle. Throughout the document, the referenced wiring diagram will maintain the following color coding: Blue refers to the AIM USB, red refers to the StratoLogger CF, and green to the RRC3+, while a solid line indicates that the deployment line is for the drogue parachute, and a dashed line for the main parachute. The architecture of the wiring and charge deployment for the flight vehicle is a step up in complexity, compared to previous designs. However, it is also a step up in the reliability and redundancy of the system overall, especially in the case of failure of wired connections within the subsystem. In past designs, each of the two altimeters' charge lines were wired through an 8-pin aviation connector where one altimeter's drogue and the other altimeter's main charge lines were paired with each other, and vice versa. Although this proved effective, and only required 8 total wires, this implementation does not protect against more complex failures and does not provide adequate horizontal redundancy throughout the ejection charge line system. This represented room for significant improvement in redundancy and assurance but would have to balance with increasing the complexity of manufacturing and use of the recovery system.

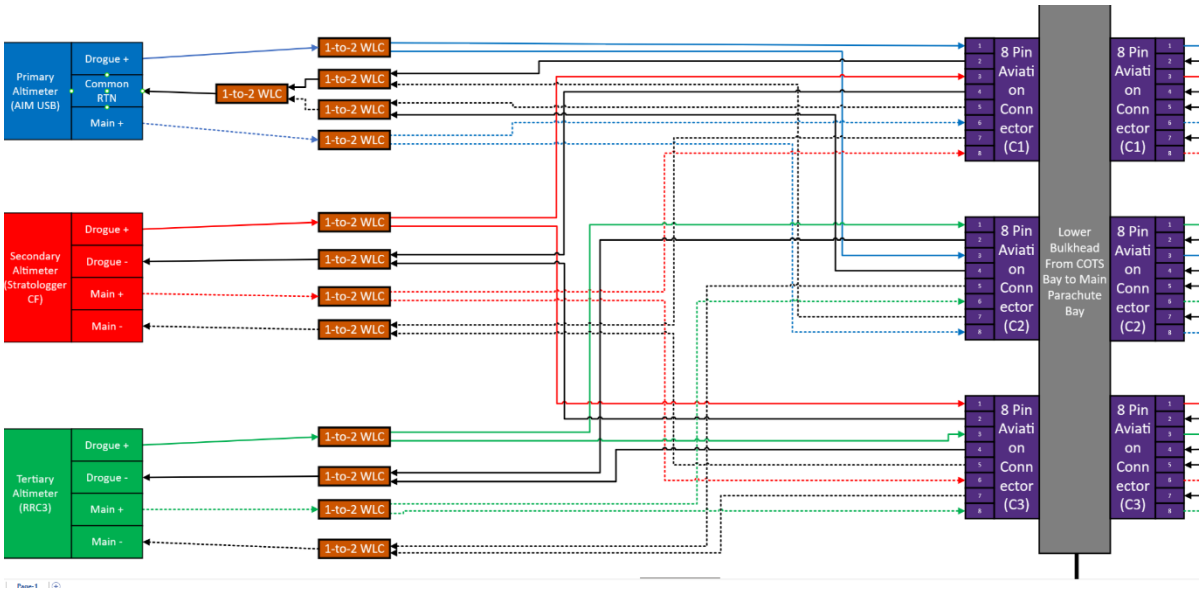

Figure 29 Wiring diagram of recovery systems, focusing on splitter connections.

The architecture of the ejection wiring for the flight vehicle can be broken into three sections: The Splitter section, Transition section, and Joining section. The Splitter section, Figure 29, splits each ejection signal into two parallel paths using in-line 1-to-2 Wago Lever Connectors. An additional WLC is used to split the AIM USB common return line for deployment charges to individual paths that can then be split again. Each WLC is labeled to indicate which set of signals from each cable should be inserted. These paths are then wired as positive and negative pairs to two different 8-pin aviation connectors, ensuring redundancy in case of a connector failure. Each connector is pinned out such that no two connectors feature either the same allocation of signals or any of the same pair twice, as shown in Table 2. This creates an interface where each connector contains a unique combination of altimeters and deployment signals from altimeters. The WLCs are configured into two banks of six connectors that sit at the forward point of the recovery backplane underneath each module.

Table 2 Altimeter Allocation for Splitting Section Connectors

Connector	Altimeter 1	Altimeter 2
1	AIM USB	StratoLogger CF
2	RRC3+	AIM USB
3	StratoLogger CF	RRC3+

This design distributes and lessens the impact of individual failures across all three connectors by providing alternative paths for deployment signals. Additionally, it means that no one failure of a connector or altimeter can eliminate the dual redundancy, both vertically and horizontally, of the system. Secondly, even in the case of dual connector failure at the lower bulkhead, dual vertical redundancy of deployment charges can be maintained, while dual horizontal redundancy can be maintained, even with dual altimetry failures during flight.

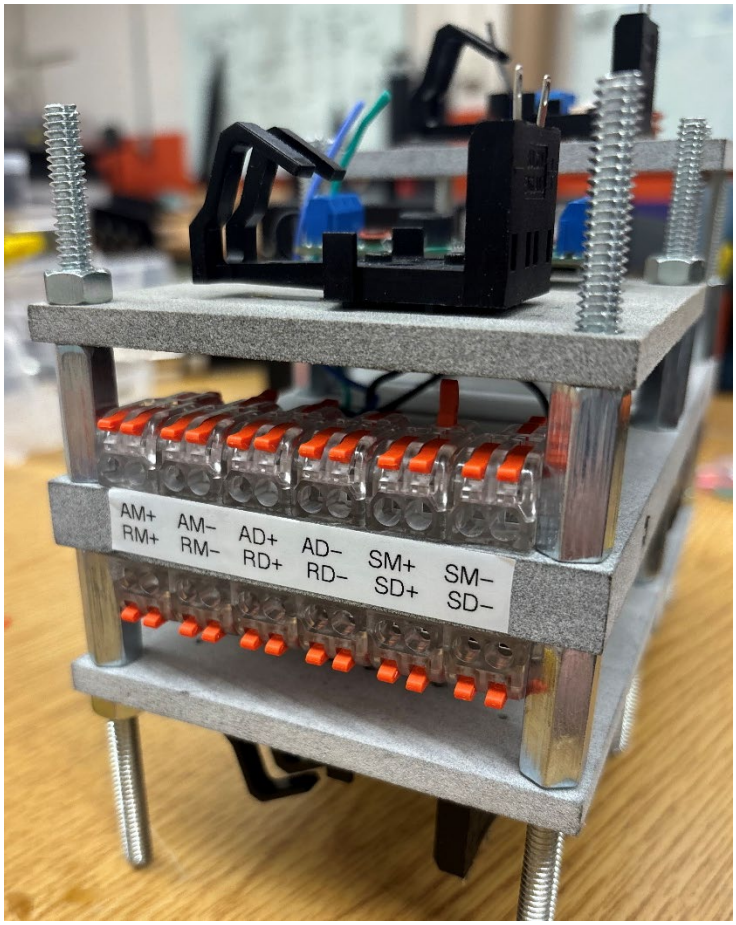

Figure 30 In-line WLC installation for splitter section of the recovery system.

The Transition section of the wiring of the recovery section, found in Figure 31, is represented by cabling of all of the drogue deployment lines through the main parachute bay. There are twelve signals in total, one half of the total signals delivered by the Splitter section. These signals travel through the main parachute bay, where they then connect to two 8-pin aviation connectors. Each connector utilizes the first six pins of the connector, leaving two free pins on each connector. The remaining pins of the connectors were not used to maintain the consistency of the pinouts of each connector throughout the entire recovery system. In the future, this could be used to provide a third deployment line for two altimeters, but this was deemed unnecessary for the project/scope. The Transition section also uses spade crimp connectors[42] to create a detachment join inside of the main parachute bay. This creates a designated point of failure for the design upon the deployment of the main parachute. Further discussion on this is continued in *Termination Styles*.

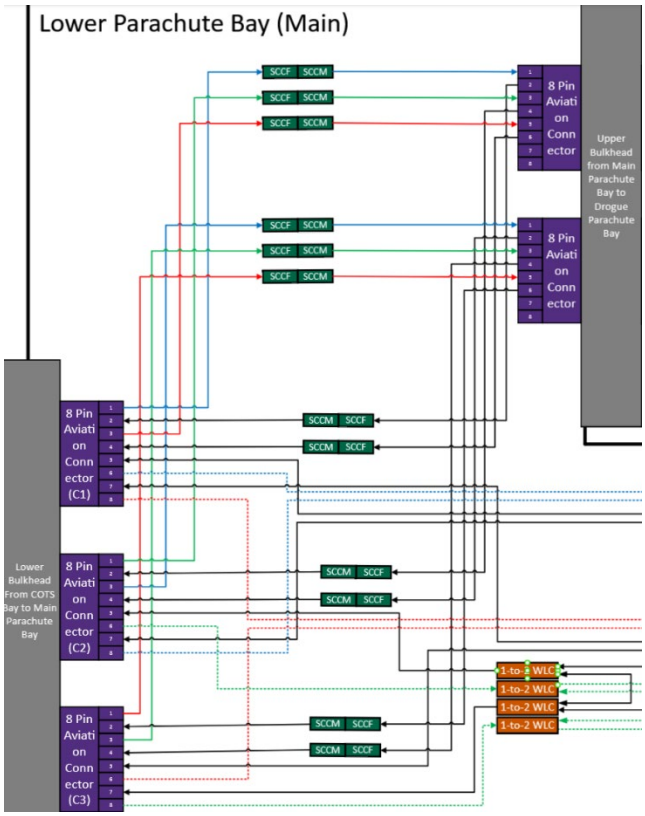

Figure 31 Transition section diagram of recovery system wiring.

The Joining section of the recovery system wiring refers to the rejoining of signals that were split during the Splitter section of the recovery system. The Joining section is present within the main or drogue parachute recovery bay but each section follows the same architecture/approach. Due to this, we will use the drogue bay, seen in Figure 32 as an example of the Joining section. A comprehensive view of the system's wiring can be found in Appendix G: Engineering Drawings. The Joining section uses 1-to-2 Wago splitters in a reverse configuration to take two signals and converge them into one. These signals are then connected to the leads of each e-match, which are packed with the primary or secondary charge. A manufactured example of the Joining section can be found in Figure.

The primary difference of the Joining section to the Splitter section is the configuration of the RRC3+ deployment lines. Since the RRC3+ connects to both the primary and secondary charges for both the drogue and the main, taking the two input lines and reducing them to one would only result in needing to re-split the lines and a single point of failure, while not joining the lines would mean that a failure of one positive line and one negative could result in the inability of the altimeter to fire the charge. The configuration should allow for either positive or negative line to fail and still be able to fire either the primary or secondary charge.

The solution to this problem is to split the incoming deployment lines into four lines, but then to short the two splitters together with two of the output signals. The other two signals then run to each deployment charge. This is done for each of the negatives as well and can be found in Figure below. This creates a path for current to flow to either the primary or secondary charge, no matter if or which positive and/or negative wire may fail during flight.

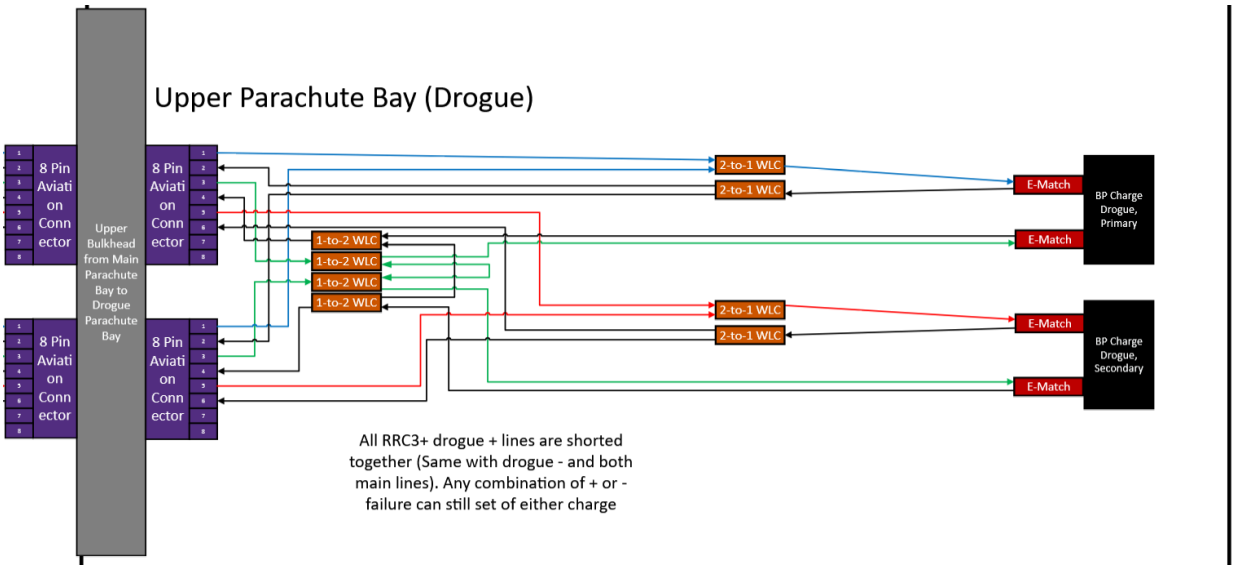

Figure 32 Joining section of drogue parachute deployment bay.

6. *Wiring Standards*

Standards for wiring and naming were implemented across the recovery subsystem of the vehicle for standardization of best practices and organization. Due to the relative complexity of the recovery subsystem's wiring, compared to previous iterations, well found and reliable standards were critical to ensuring usability and coherence throughout the subsystem. A number of these practices were adopted from the IREC DTEG Appendix B: Safety Critical Wiring Guidelines, while others are known to be best practices.

All wires are run as cables, where a cable is defined as two or more wires that share a common purpose. Through this, all cables are wrapped as twisted pairs, to reduce the effects of electromagnetic interference (EMI) noise on the signals on each wire. Additionally, each wire is stranded core 22 American Wire Gauge (AWG) throughout the entire recovery subsystem. Stranded core wire was chosen over solid core wire for the flexibility and commercial availability, without significant compromise on current carrying capabilities for ejection charge lines. Regarding wire colors, red was reserved for positive supply voltage by each battery, while black and white were reserved for negative/return paths, or ground. Blue was reserved for the positive line of all drogue ejection charge lines, while green was reserved for main ejection charge lines.

After fitting each cable to the length of its run, providing enough slack for strain relief during flight, each cable was twisted by inserting the ends of each wire into the drill bit hole of a cordless drill, and then twisted to produce the twisted pair. This was chosen over twisting each cable by hand as hand twisting does not allow for full radial wrapping of each wire around each other, thereby not minimizing the effects of noise on the wires in the cable. Once the cable was twisted, a 0.5 *in* piece of watertight heat shrink[46] was placed every 2.5 *in* of cable to ensure that the cable maintained its shape. From this point, the ends of each wire on the cable were stripped back to allow for attachment to either WLC's or screw terminals. Per the recommendation from Wago, WLC connections were stripped back 11 *mm,* or approximately 0.44 *in*, while screw terminal connections were stripped back 0.2 *in*. If a wire was to connect to a spade crimp connector, then the wire was stripped back 0.5 *in* to provide a solid crimp and electrical connection.

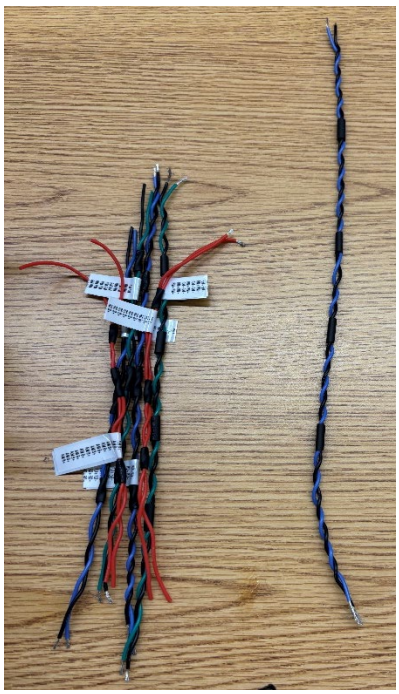

Figure 33 Set of completed twisted pair cables to reduce EMI interference.

The cable was then formally installed into the recovery subsystem. If the cable attached to screw terminals, the cable was fed through the subsystem to the terminal, where then a ferrule[44] was crimped onto the stripped back wire. This provides a sturdy and solid connection between the screw terminal and the wire while the ferrule, and hot glue potting, provides protection against exterior shorts at the connection point. After final installation, the cable was named and labeled using a label maker[45] to make the cable's purpose and the wires within the cable. A standard naming convention for altimeters and drogue/main parachutes was used across the entire bay, which can be found below. The suffixes 1 or 2 and/or +/- were added to the end of each cable wrap to delineate between redundant cabling and the signals contained within the cable. This system ensures that anyone can understand and track the cables installed and their purpose.

Table 3 Naming conventions of recovery cable flags and labels.

Name	Purpose
A/AM	AIM USB Altimeter
S/SL	StratoLogger CF Altimeter
R/RC	RRC3+ Altimeter
M/MN	Main Parachute
D/DG	Drogue Parachute

7. Deployment System

Deployment of the drogue parachute requires 1.56g in the primary charge and 3.125g in the secondary charge of 4F black powder. Deployment of the main parachute requires 2.5g in the primary charge and 5.0g in the secondary charge of 4F black power. All the black powder charges are tightly packed in rubber gloves with 2 e-matches per charge with each e-match going to its own altimeter. The redundancy of charges with an increase in the amount of black powder ensures the greatest chance of ejection even in the event of an altimeter or charge failure. Due to the use of black powder and flammable materials in the bay, the shock cords and parachutes are used with flame retardant parachute bags, dog barf, and a fire blanket. 3D printed carbon fiber nylon charge wells are used to house each of the black powder charges in their respective bays. These charge wells are screwed in place through holes in each one of the bulkheads.

8. *Termination Styles*

Previous recovery systems were too vehicle specific and tedious to manufacture and assemble for the flight vehicle. This included large amounts of soldering, which was tedious and could not be observed for joint quality by competition officials. Limiting soldering to defined and necessary locations within the bay, not only improves assurance and decreases manufacturing strain, but provides a more observable product. To substitute soldering, crimped connections were introduced throughout the subsystem, through ferrules, 0.110 *in* quick connectors, and spade crimp connectors. Additionally, the use of Wago lever connectors for splitting and joining signals together was expanded upon, compared to previous designs. An example of splitting signals using WLCs is shown in Figure 34. Wago lever connectors have been utilized by our team in previous IREC competitions and provide a secure and easily detachable connection between two or more wires. These two changes greatly reduced the total number of soldered connections within the subsystem.

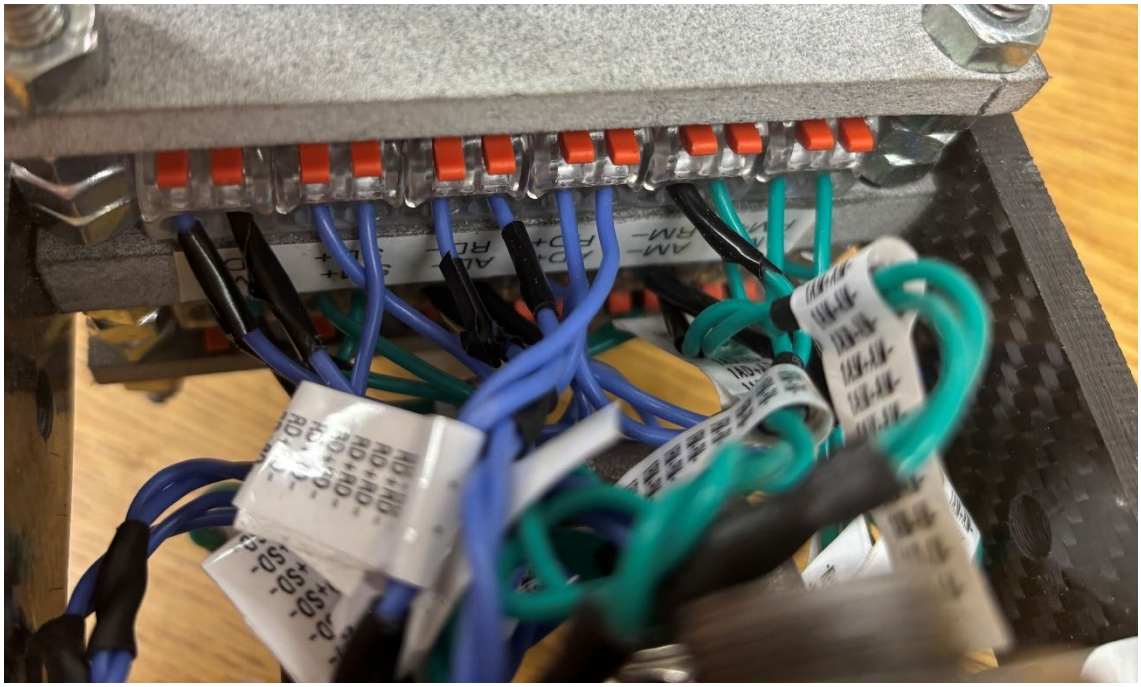

Figure 34 Installation of splitter section with aviation connectors.

Where soldering was deemed necessary was the connections between bulkheads for ejection charge lines on each 8-pin aviation connector. All connections were double insulated with watertight heat shrink to protect external and internal shorts of the signals of the connector. In addition to this, to further assure electrical isolation and mechanical stability, each connector was potted with hot glue, as seen in Figure 35 Main parachute bulkhead with potted aviation connectors. If soldering was needed to extend a wire from a potted connection, then a clear solder seal connector was used to join the two new wires. Solder seal connectors[43] utilize clear heat shrink and solder embedded within the connector to provide a secure, watertight, and observable connection.

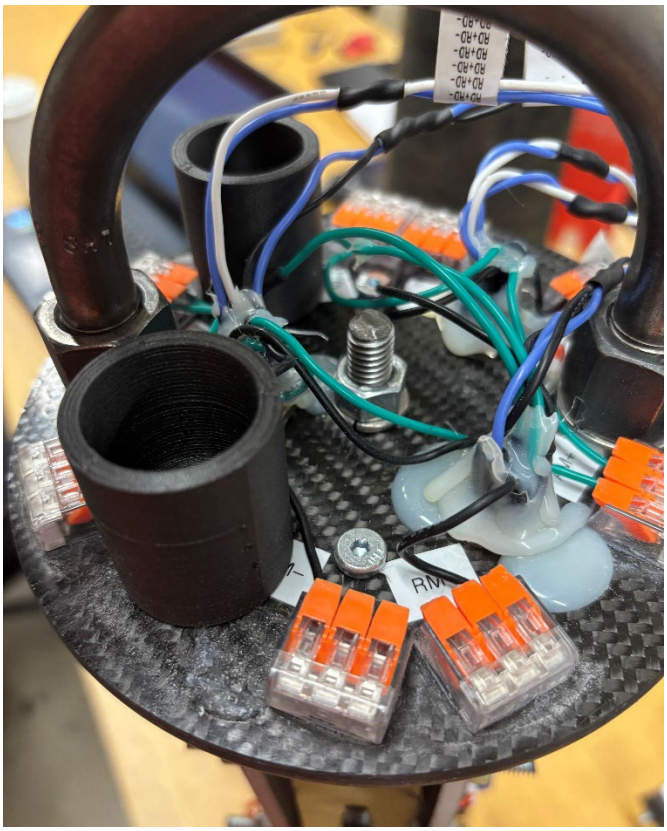

Figure 35 Main parachute bulkhead with potted aviation connectors.

The connection from the main parachute bay to the drogue parachute bay, made by spade crimp connectors, was cited as a point of concern, the connection could prove to be too strong of a connection. This would prevent separation and thereby the deployment of the main parachute. However, to counteract this, each spade crimp connector was manually loosened to still provide a reliable connection but reduce the total pull-out force of the connectors. Before making modifications to the connectors, the total pull out force was measured with a force gauge to be 19.8 *lbf*, which exceeds the 28.1 *lbf* produced by the primary main black powder charge, but only by a factor of safety of 1.5. After loosening each connector, the total pull out force was measured to be 4.4 *lbf*, which exceeds the 28.1 *lbf* produced by the primary main black powder charge by a factor of safety of 6.4. Additionally, the cabling for the connection between the main and drogue parachute bays provides minimal strain relief to allow for the near maximum force of the charge to disconnect the cabling properly. Due to the exposed nature of the cabling in this section of the subsystem, the entire set is wrapped in nylon webbing, or "snakeskin" allowing for further electrical isolation and protection against the black powder ejection charge.

9. GPS Tracking

We use a pair of Featherweight GPS trackers[12] paired with two Featherweight ground stations[11], each connected to its own iPhone, to allow for accurate, real-time tracking of our vehicle. Each tracker utilizes the default 900 *MHz* quarter wave dipole antenna. This was chosen due to the toroidal propagation patten that delivers high signal strength in many directions. We chose a single cell 18650 cylindrical Li-Ion with a metal shell rated at 2.6 *Ah* to provide power for each tracker. Each tracker is switched on from outside of the vehicle via the onboard switch for the tracker. This can be actuated through the use of a pick, or dental tool, through a hole in the airframe. The Featherweight GPS tracker datasheet lists the battery life for the provided 400 *mAh* 1S Lithium Polymer (LiPo) battery as 4.5 *hr* [6]. Extrapolating this out, and through our own observations, 2.6 *Ah*, would result in an estimated 29 *hr* battery life. This allows for reliable GPS location transmission in many conditions, including a delayed or scrubbed launch. A CAD model of the section can be seen in Figure 36.

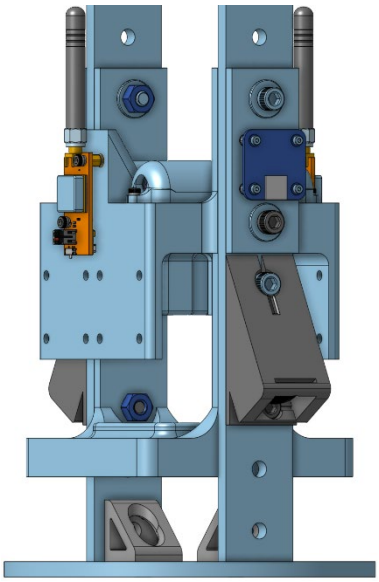

Figure 36 CAD render of camera section and GPS trackers

D. Payload

The payload system for this year's launch vehicle aims to solve a critical problem when designing SRAD flight computers. There are many altimeters that are simultaneously small, cost effective, and easy to acquire, making it challenging to choose the best one, especially for a component that is critical for accurate state detection. In the past, our organization relied on the MPL3115A2 and BMP3xx series of altimeters, with mixed reliability from both, especially when mounted on a MARTHA PCB. To test these altimeters head-to-head, the payload system includes three altimeters, all connected to the same flight computer, being polled at the same rate. The data from each sensor, and from other altimetry on board, will be compared post-flight to determine the best performing altimeter or gain additional insights into such a critical component.

The exact hardware configuration of the payload system includes a single flight computer connected to the three altimeter developer boards using a protoboard. The flight computer is a FeatherS3[34], which offers a low cost, high performance, and standalone setup which fits the needs of a project of this nature. Additionally, the organization has experience with these development boards from previous flight computer projects. The altimeters include a BMP388 representing the BMP3xx series, a BMP180 representing the BMP1xx series, and an MPL3115A2. It will be powered by a single 18650 battery cell and mounted in the launch vehicle in the main section of the vehicle. Data will be saved to a 16 *GB* micro-SD card.

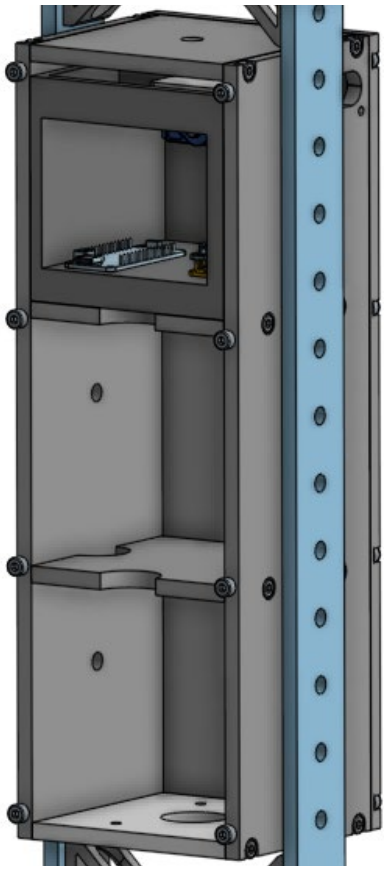

Figure 37 CAD render of payload section

This vehicle's payload frame, Figure 37, was chosen due to a variety of factors. Firstly, this payload frame was constructed entirely out of 1/4 *in* 6061-T6 aluminum plate and was flight-proven, having flown in the 2022 and 2024 Spaceport America Cup. The thick aluminum frame allows the payload to be able to withstand the high accelerations of both launch and parachute deployment. Additionally, it enables significant customizability. Components such as the sensor bay or ducts can be directly mounted to the frame at any arbitrary point by simply drilling and tapping holes in the plate.

A major criterion for the payload was ease of assembly. As previous payloads have had issues with being quickly assembled immediately before launch, the speed of assembly of this year's payload subsystem was a top priority. To achieve this, several features were built into the design of the payload. Firstly, previous payloads were often made in multiple parts that each needed to be installed into the vehicle separately, leading to long and complicated assembly procedures. To aid in this area, this payload was designed to fit into one single superstructure with the 3U CubeSat bolting directly to the structural camera section frame, greatly reducing lead time prior to launch. From dry runs performed in house and right before the test launch, the entire installation process from installing the batteries to securing the superstructure into the airframe took less than 4 minutes. Another benefit of this design paradigm was that the payload subassembly could be assembled off site prior to launch, further reducing assembly time and risks of broken or missing parts.

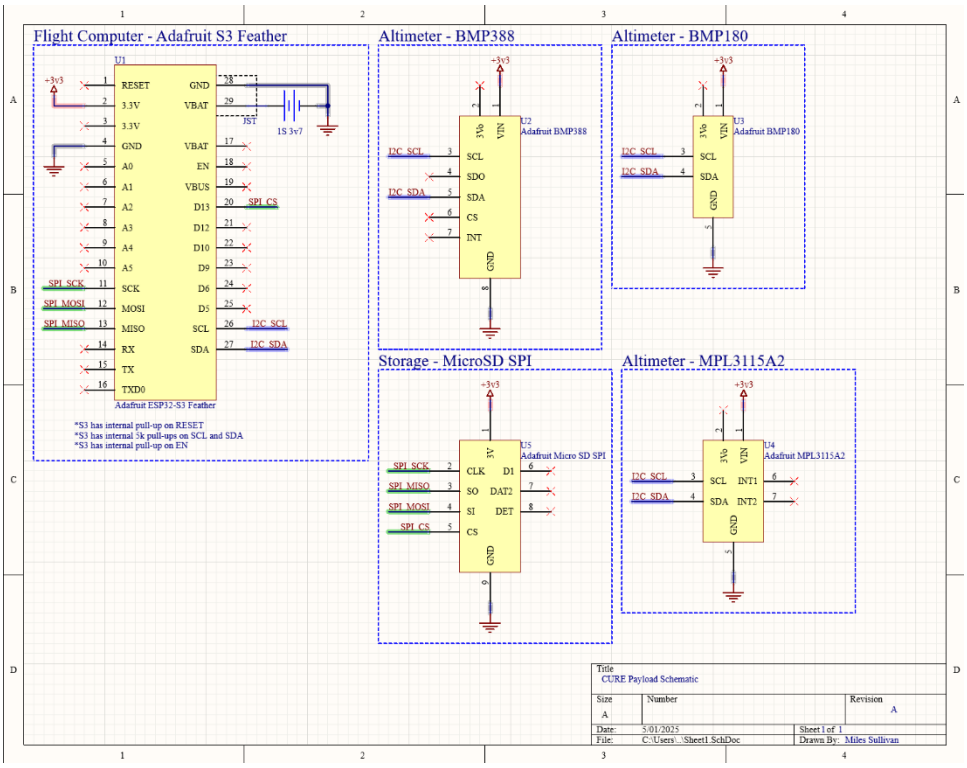

Figure 38 Schematic of payload system.

The software for the flight computer will be relatively simple, since the computer is merely recording data, instead of making inferences on said data. It will poll each sensor via I2C and then save each value to a micro-SD card. Because the micro-SD card is 16 *GB* and each poll of the three sensors will use 16 bytes of storage (4-byte timestamp + 3 * 4-byte altitude values), we'll be able to perform one billion polls before running out of storage. At 100 *hz*, it will last over 2500 *hr*.

After recovery, data from all three sensors will be extracted from the micro-SD card and analyzed. This analysis will include direct comparisons of raw values to evaluate agreement between sensors, as well as frequency analysis using Fourier transforms to identify potential noise patterns introduced during flight. Additional methods may include calculating rates of change and observing response delays during key flight events. The goal of this analysis is to determine which altimeter offers the most consistent and reliable performance in a launch environment, helping guide future SRAD flight computer designs.

E. SRAD Hardware Design

In previous years, our team has used Raspberry Pi-based designs for SRAD avionics systems. These designs proved to be both cost-inefficient and bulky. Additionally, such designs were fragile and only supported limited features. Last year we decided to expand into creating our own custom avionics platforms. This created a new area for the team, which last worked with printed circuit boards (PCB) before the COVID-19 pandemic. Our design, beginning last year, is the Miniaturized Avionics for Rapid Testing, Handling, and Assessment (MARTHA) board, which records gyroscope data, acceleration, orientation, pressure, temperature and altimetry data on our flight. The team is building from the MARTHA design with the team's new newest prototype, "Just an Expanded MARTHA" (JEM), which achieves the same goals but with more precision and storage.

1. Design Philosophy and Requirements

As a developing and maturing aspect of our team, communicating and understanding the design philosophy is crucial to providing context for current and future projects. We are confident that this area of our team will grow and develop to tackle novel challenges and enhance our understanding of rocketry. However, progress must be incremental, and attempts to complete large, complex projects without the requisite technical and financial capital will only result in cyclic failure. Starting small, using publicly accessible designs, and creating a platform for others to build from is crucial to long-term success. Secondly, as a smaller team, minimizing cost inefficiencies is essential to

ensuring that the project is financially viable. Lastly, providing features that benefit and develop other aspects of the team gives enhanced purpose and meaning to the project.

Our design specifications and requirements have been undefined in recent years. This has led to designs that were subpar and contained easily catchable mistakes. This year, one goal of the Hardware Subteam has been creating a "PCB and Electrical Design Standards" document for current and future use in the organization. This document is meant to standardize the electrical design process in general as the organization moves into more complex electrical design. This includes documentation and standardizing key technical aspects of a design such as component selection and schematics. This way, we can prevent future mistakes by thorough documentation of previous successes and failures. This can also improve the efficacy of future generations, allowing them to make more educated design choices.

The inspiration for MARTHA emerged from a need for flight data to qualify and quantify changes to flight computer software. Additionally, through efforts within our team, we can launch over two dozen L1 and L2 certification flights each semester using certification kits. This represents a prime opportunity to collect subscale flight data. By designing a system small enough to fit within one of the standardized electronic sleds of these kits, we can enhance the development of future projects and build a comprehensive set of flight data for future testing. This reduction in scale makes designing, assembling, and integrating flight computers through this practice much easier and more economical than before. Through implementing systems for data collection and filtering with state detection, we can provide a foundation from which others can build. This design philosophy will allow us to build better SRAD avionics affordably and incrementally with an emphasis on frequent flight testing and verification of systems.

2. Hardware Development

The development cycle for the MARTHA v1.3 prototype spanned five months and was grounded in design principles established by previous iterations. Enhancements were introduced to improve overall performance and reliability. All schematic and PCB design work was conducted using Altium Designer [XX], selected for its widespread industry adoption, robust cloud-based collaboration tools, and extensive documentation and training resources.

MARTHA v1.3 retains most of the core data acquisition components from earlier versions. The extended design timeline was primarily due to a complete PCB layout redesign and the integration of additional power management and data collection modules. 3D renders of the v1.3 assembly are shown in Figure 39and Figure 40 below. Note that some component models were unavailable and are not shown in the renders.

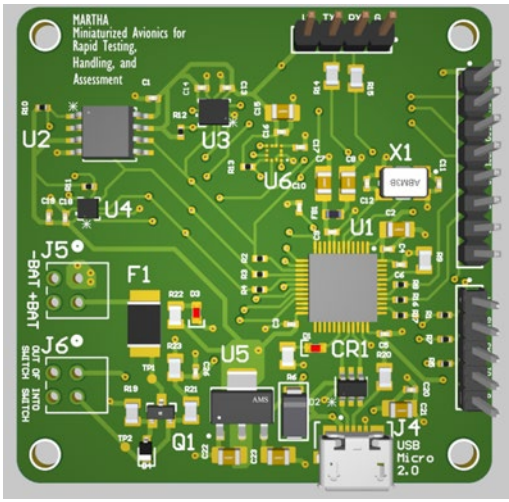

Figure 39 Render of student developed MARTHA board (FRONT).

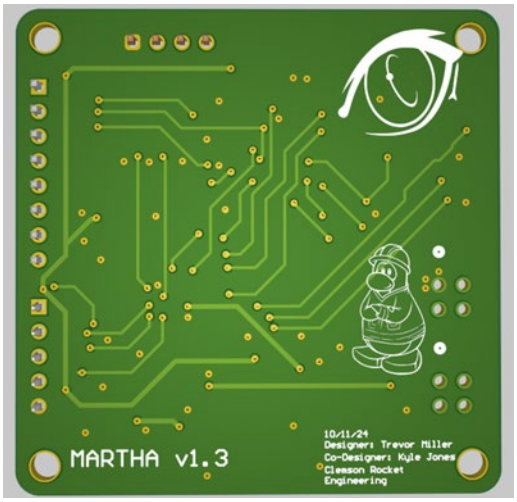

Figure 40 Render of student developed MARTHA board (BACK).

This iteration of the design draws heavily from prior MARTHA architectures, with a series of targeted improvements to enhance performance, reliability, and manufacturability. The system is built around an STM32F103CBT6 (U1) [XX] microcontroller unit (MCU), selected for its 128 *KB* flash memory. This change doubles the flash memory capacity compared to the previously used STM32F103C8T6, providing the microcontroller with increased storage for firmware and giving the Software Subteam greater flexibility for implementing more advanced features.

Power regulation is provided by an AMS1117-3.3 (U5) low dropout regulator (LDO), with power and data interfacing supported via a Universal Serial Bus (USB) connection. Additional headers are included for Universal Asynchronous Receiver-Transmitter (UART) communication and Serial Wire Debug (SWD) programming.

Key enhancements in version 1.3 include the transition from Inter-Integrated Circuit (I^2C) to Serial Peripheral Interface (SPI) communication, significantly increasing data throughput and system responsiveness. The altimeter subsystem was upgraded from the MPL3115A2 to the BMP390 (U4) [XX], offering improved accuracy and environmental resilience. Onboard storage was transitioned from a microSD card interface to a W25Q128JVSIQ (U2) [XX] SPI flash memory module, improving robustness and simplifying PCB layout.

Electrical protection measures were also introduced, such as electrostatic discharge (ESD) and reverse polarity protection. A P-channel metal-oxide-semiconductor field-effect transistor (MOSFET) was implemented for reverse polarity protection in conjunction with a diode on the battery input, and a dedicated fuse was included in the battery power path to mitigate overcurrent scenarios.

The sensor suite includes a full nine degrees of freedom (9-DoF) inertial measurement unit (IMU), composed of an LSM6DSOX [XX] accelerometer/gyroscope and an LIS3MDL [XX] magnetometer, in addition to the BMP390 altimeter. This provides a significant advantage over alternate configurations, which use a 6-DoF IMU and/or an altimeter. While the enhanced sensor package increases per-unit cost, it enables advanced capabilities such as reliable state detection—an essential function for future avionics platforms. The capabilities of the MARTHA sensor suite are listed in Table 4.Table 4 MARTHA sensors specifications.

Capturing high-resolution, multi-axis sensor data during early development is critical for validating and qualifying future systems with expanded features. Without this baseline, retroactive data analysis would be unreliable or infeasible. Thus, this design reflects a deliberate balance between long-term capability and financial feasibility. The selected sensors meet the required performance specifications while remaining cost effective.

Table 4 MARTHA sensors specifications.

Parameter	Sensor	Resolution	Minimum Value	Maximum Value
Acceleration	LSM6DSOX (U3) [XX]	4.9 x 10-6 *g*	-16.0 *g*	16.0 *g*
Rotation	LSM6DSOX (U3) [XX]	0.061 *dps*	-2000.0 *dps*	2000.0 *dps*

Magnetic Field	LIS3MDL (U5) [XX]	4.9 x 10-6 G	-16.0 G	16.0 G
Altitude	BMP390 (U4) [XX]	0.82 *ft*	-7368 *ft*	37369 *ft*
Temperature	BMP390 (U4) [XX]	0.5 *°C*	-40 *°C*	85 *°C*
Pressure	BMP390 (U4) [XX]	0.03 hPa	300 hPa	1250 hPa

The sensor subsystem schematic is presented below in Figure and in greater detail in **Appendix G: Engineering Drawings**. Each sensor is configured for standard SPI communication, with all available interrupt lines routed to the microcontroller to support low-latency, interrupt-driven drivers. Standard-value decoupling capacitors (100 *nF* and 1 *μF*) are strategically placed on power pins to ensure signal integrity and reduce power supply noise, contributing to overall system stability and robustness.

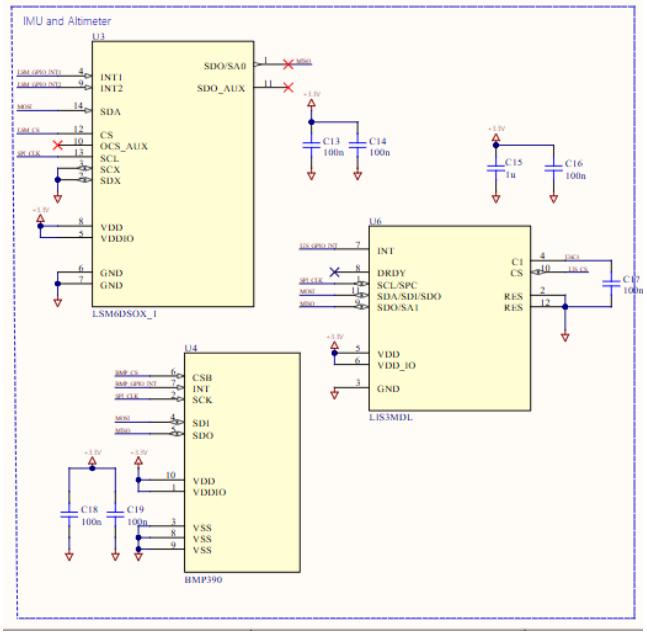

Figure 41 Schematic for MARTHA sensors, further expanded upon in Appendix G: Engineering Drawings.

A secondary design consideration for MARTHA is the method of onboard data storage, with two primary options evaluated: SPI-based flash memory and microSD cards. Earlier MARTHA revisions employed microSD cards to accommodate pre-flight data logging in the absence of onboard state detection. However, with the recent integration of reliable state detection algorithms developed by the Software Subteam, flash memory has become the preferred solution. Flash chips offer advantages in cost, physical footprint, and mechanical robustness compared to microSD interfaces.

State detection enables the system to programmatically identify launch events, allowing pre-flight data to be discarded in real time and maximizing the utility of limited storage capacity. Although the reduced storage space imposes constraints on data retention and requires more efficient memory management strategies by the Software team, it ensures that only flight-relevant telemetry is captured, significantly streamlining the data pipeline. **Error! Reference source not found. Error! Reference source not found.** Figure 42 below.

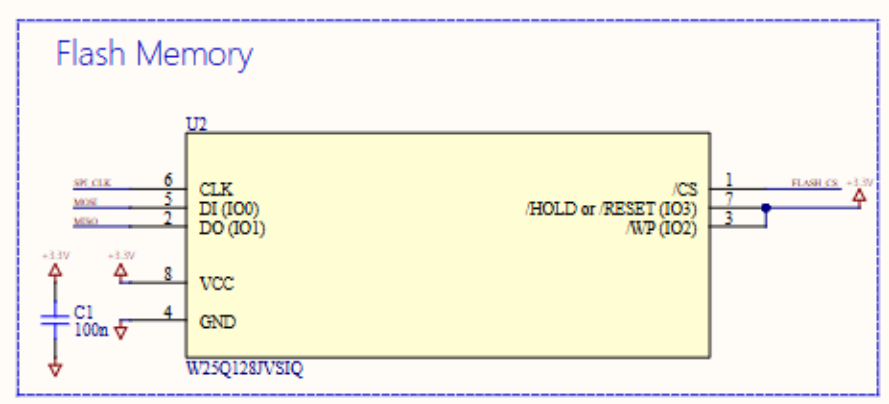

Figure 42 MARTHA schematic of flash memory as seen in Appendix G: Engineering Drawings.

The final key design decision involved defining the board's power distribution and voltage regulation strategy. All onboard components operate at 3.3 *V,* necessitating a reliable and consistent power supply. Although less efficient than a buck converter, an LDO – AMS1117-3.3 (U5) – was selected due to its lower cost, reduced complexity, and proven reliability under the board's low current draw conditions. The simplicity of LDO integration made it the optimal choice for this application.

As outlined earlier, when powered via the battery input, the supply passes through a fuse (F1) for overcurrent protection and a P-channel MOSFET (Q1) to guard against reverse polarity. When powered via the USB interface (J4), the input path includes a Schottky diode (D2) for reverse polarity protection and a USBLC6-2SC6 (CR1) transient voltage suppression array for electrostatic discharge (ESD) protection. In both cases, the regulated 3.3V output is provided by the LDO (U5). The complete power architecture is illustrated in the schematic shown in Figure 44.

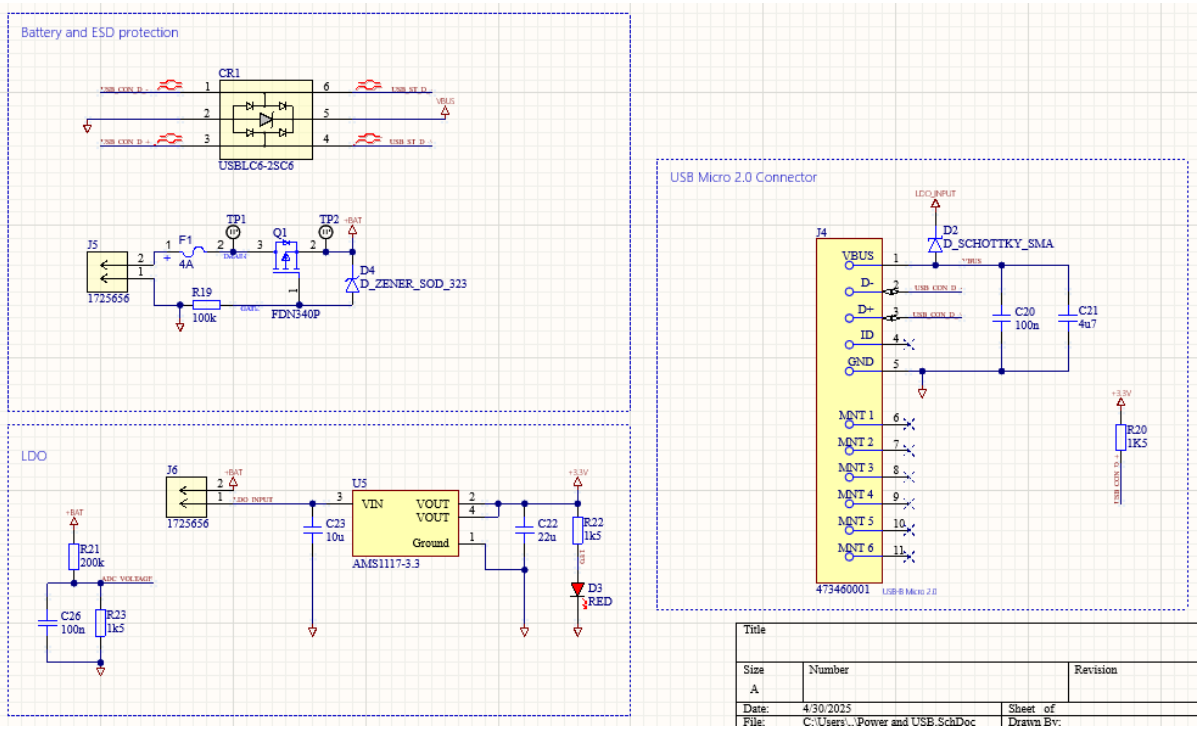

Figure 43 MARTHA power and voltage regulation schematic as seen in Appendix G: Engineering Drawings.

As seen in Figure 43, the microcontroller interfaces with all onboard peripherals—including sensors and the flash memory chip—via a shared SPI bus. Each SPI device is assigned an individual chip select (CS) line, which is pulled high using 10 $k\Omega$ resistors and routed directly to dedicated GPIO pins on the MCU for independent device addressing.

Interrupt lines from the sensors are also connected to configurable GPIO pins on the MCU, enabling event-driven data handling and precise timing control. For firmware development and debugging, the board includes breakout headers for SWD, providing seamless integration with the Software Subteam's toolchain.

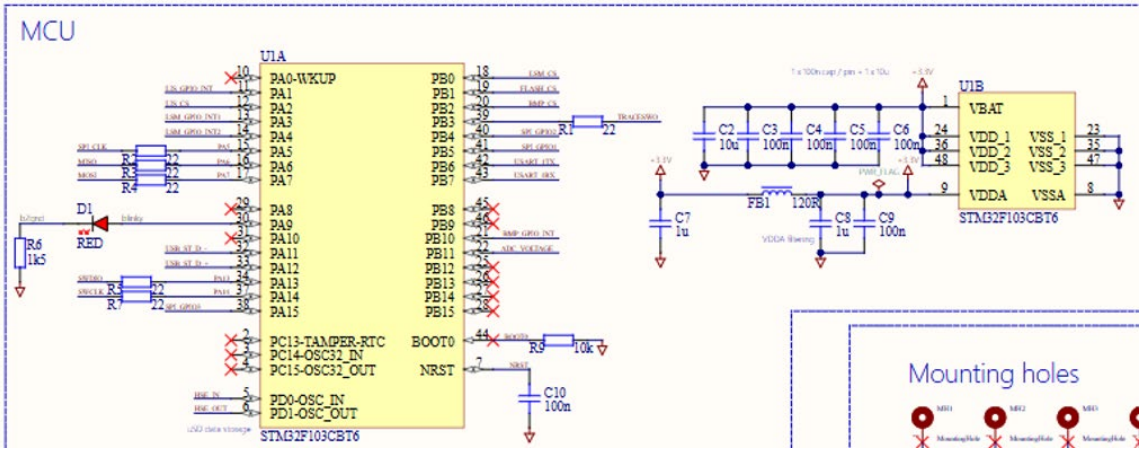

Figure 44 MARTHA MCU schematic as seen in Appendix G: Engineering Drawings.

During the layout phase, it was immediately clear that component density would present a significant challenge, as the design required a large number of components to be placed on one side of a compact PCB. As such, careful attention was given to minimizing noise, crosstalk, and electromagnetic coupling within the constrained layout area. MARTHA v1.3 adopts a four-layer stack-up with the following configuration: signal / ground / ground / signal. The use of dual internal ground planes facilitates low-impedance return paths across the board, simplifying layout constraints and providing inherent noise isolation between the top and bottom signal layers. There has been discussion in the team about changing the lower ground plane to a power plane in the future to reduce impedance on the power plane and make power layout much simpler.

Component placement was strategically divided by function: digital and sensor components were located on the opposite side of the board from analog and power circuitry to minimize interference and coupling between power and data signal paths. The microcontroller was positioned slightly off-center to optimize routing accessibility to both domains. This layout strategy is illustrated in Figure 45. To further reduce signal integrity issues, the layout adhered to the 3W rule, traces should be three times their width away from any other traces, where feasible, ensuring adequate spacing between high-speed or sensitive signal traces to mitigate mutual inductive and capacitive coupling.

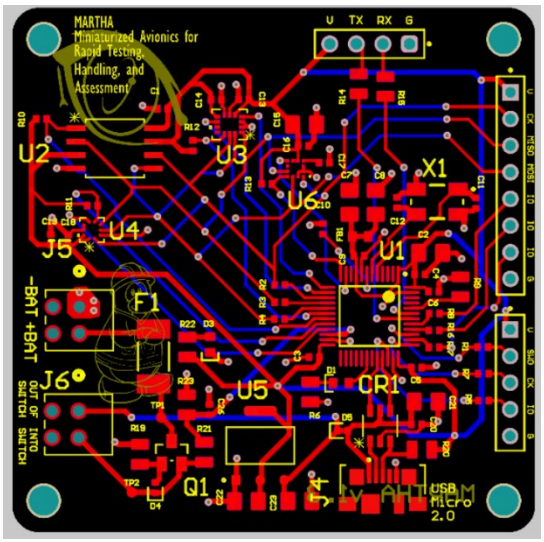

Figure 45 The layout for MARTHA v1.3.

As MARTHA represents the club's first fully integrated custom PCB flight computer, encountering design and implementation challenges was expected. By the fourth iteration (v1.3), the goal was to achieve a stable, production-ready design—though several issues still emerged. Notably, inconsistencies were identified in the implementation of the reverse polarity and ESD protection circuits. Additionally, three out of the five assembled boards experienced issues where the software was unable to establish serial communication with the altimeter at startup. These failures are likely attributable to a combination of factors, including potential manufacturing variability, handling inconsistencies during assembly, and possibly suboptimal SPI trace routing introducing signal integrity problems.

Ultimately, only two boards exhibited fully functional sensor suites. These outcomes underscore the importance of establishing a more standardized and robust design and assembly workflow. They also highlight the need to prioritize design for manufacturability (DFM) in future iterations to improve consistency and overall system reliability.

F. Software Development

The flight computer firmware developed by our organization is designed around three core principles: portability, performance, and reliability. By adhering to these principles, we ensure our software can be easily reused across multiple systems, meet the demands of an unpredictable launch environment, and continue running smoothly when it matters the most.

The first principle is portability. Our organization uses a large variety of flight computers and microcontrollers including ESP32 and STM32-based systems. As a result, it's essential that core code can be reused across all these systems to avoid wasting time reinventing the wheel. For example, sensor data collection, data logging, and state estimation are universally needed across our systems, so we created the "Avionics" repository within our GitHub Organization [39]. It includes all the algorithms mentioned above written in a generic and modular manner. Each of our flight computers utilizes the "Avionics" repository as a sub repository and then configures the modules using constructors. To support portability, we chose PlatformIO as our primary development environment [13]. PlatformIO is built on an open-source ecosystem with extensive library management tools. It's entirely cross-platform and cross-architecture, making it accessible to all of our team members and able to build for all of our boards. By only changing a few configurations, we are able to flash the same firmware on both ESP32 and STM32-based systems, from a Windows, Linux or Mac host computer.

Performance is the next of our main concerns when writing flight computer firmware. We measure performance in two ways: amount of useful data saved and accuracy of state detection. Data logging is important for post-flight analysis, and simulation testing. Accurate state detection, such as detecting launch, burnout, apogee, drogue deployment, main deployment, and landing are important for activating other processes at the right time such as high-speed data logging or payloads.

To start with our first performance metric, the amount of useful data saved is measured in bytes. However, it is difficult to determine what is "useful." For example, the temperature of the vehicle does not change rapidly, and there are very few post-flight analyses that depend on frequent temperature measurements. As such, we only log temperature at 1 *hz* while acceleration and altitude data are logged at 100 *hz*, saving space. For example, MARTHA only has 16 *MB* of storage. If we were to save all 15 data streams shown in Table 5 at 100 *hz*, MARTHA would run out of space after only 44 minutes, however, when we reduce some of those streams to 10 *hz* or even only 1 *hz*, MARTHA can record data for 81 minutes. Once we start saving data at different rates, the order of the data is no longer guaranteed. To address this, labels must be added for each 4-byte value, this is seen in our novel data format Byte5 shown in Figure 46.

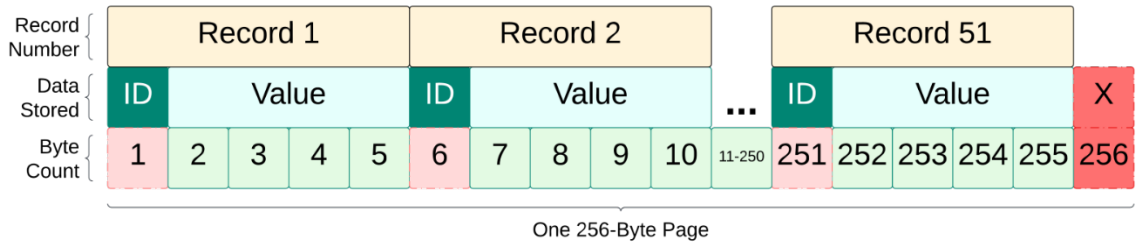

Figure 46 Byte5 data format diagram. Shows each data record using 5 bytes (1 byte for the ID and 4 for the corresponding value). In a 256-byte page, one byte is wasted as padding and 51 are used for IDs, leaving 204 bytes of true data or 79.69%.

In Byte5, every record consists of a 1-byte ID followed by a 4-byte value (typically a float or integer). These 5-byte records are not a power of two, so they fail to fit cleanly into a 256-byte page without wasting 1 byte for padding. You could also consider the 1-byte IDs of each record wasted space as a consequence of using such a flexible format. All-in-all 52 bytes are not used for pure data on each page (20.3%). When compared to a system that uses 64-byte chunks, avoiding the non-power-of-two problem and the need for labels, since each chunk has a consistent internal order, we find it impossible to save 64 bytes of meaningful data at 100 *hz*, there simply isn't enough data worth saving, yet some metrics need the full 100 *hz*. Factoring that in, it leads to an average waste of 37.5%, since most of the chunk is full of non-useful data, which is much worse than Byte5.

Our other metric of performance, state detection accuracy, becomes critical since with Byte5, MARTHA only gets 65 minutes of data saving time. MARTHA saves data to the flash chip in a circular fashion, wrapping back to the front after reaching the end. Once launch is detected, all the data from one minute prior to launch to everything written afterwards is marked as "sacred" and can never be overwritten. After about 64 minutes, MARTHA will wrap back to where the data was first marked "sacred" and then stop saving. This prevents the data recorded while waiting for recovery from overwriting the far more interesting launch data. In essence, MARTHA will always have the one hour of data immediately following launch. Overall, Byte5, coupled with launch detection, gives us the best data saving performance by capturing the most useful data.

Table 5 Variable data logging rates per data stream with Byte5 labels.

Data Stream Name	Bytes per save	Saves per second (*hz*)	Total Bytes per second
Altitude	5	100	500
Acceleration (x, y, z)	5*3 = 15	100	1500
Gyroscope (x, y, z)	5*3 = 15	100	1500
Temperature	5	1	5
Magnetometer (x, y, z)	5*3 = 15	1	15
Flight Status	5	10	50
Timestamps	5	100	500
Super Loop Rate	5	1	5
Flight ID	5	1	5
TOTALS	5*15 = 75		**4080**

We measure state detection accuracy in seconds. That is, how many seconds delayed was the state detected by the flight computer. The two most important states are launch and apogee, so we'll focus on those two. Launch detection is carried out using a rolling median filter applied to the magnitude of acceleration. The filter is a half second wide and contains 20 samples each separated by 25 *ms*. Several checks are used to ensure the window width and intervals between samples are within predefined tolerances during runtime. Apogee detection utilizes a vertical velocity estimation module which uses a 1D Kalman filter that fuses both altimeter data and acceleration data to estimate velocity [37]. When that velocity is negative, and our current altitude measure is more than 2 meters less than the peak altitude, we register apogee. Figure 47 shows the performance of our most recent MARTHA systems. With launch

there is a quarter second delay (due to the half second filter) and with apogee detection we are about a three quarter second delay (due to requiring a 2-meter altitude drop).

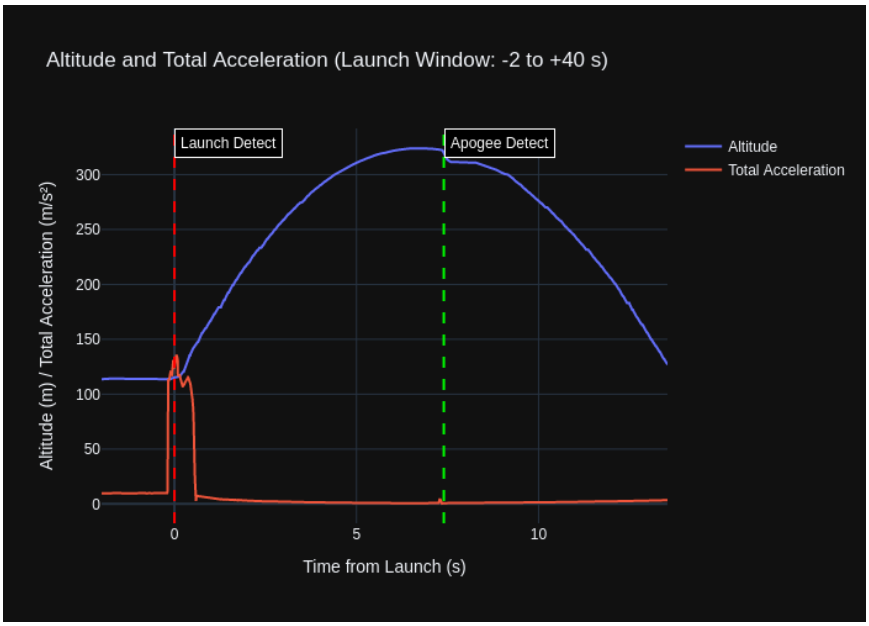

Figure 47 Launch and apogee detection from MARTHA on a level 1 certification launch. Launch was detected .21 seconds late and apogee was detected .73 seconds late.

The final core principle after portability and performance is reliability. Reliability has become a much stronger focus in the past year due to the growing complexity of our systems. We tackle reliability in two main ways: Keeping things easy to use and testing relentlessly. For ease-of-use, all software is designed with the knowledge that launch environments are tough and hectic. If a system is too complicated, it'll be used incorrectly. This is reflected in MARTHA with its orientation-independent state detection systems. The vertical velocity estimator determines the vertical axis at launch by sampling the highest acceleration, so it can be mounted in any orientation. On power-up MARTHA will blink slowly (1 *hz*) to indicate that all system is initialized and that it is ready to fly. Anything else indicates a problem, which can be addressed through a MARTHA flowchart seen in Figure 48. Once MARTHA detects launch, it automatically safeguards the important data until a special command from the ground station resets it. In essence, MARTHA's software helps it remain easy-to-use and consistent.

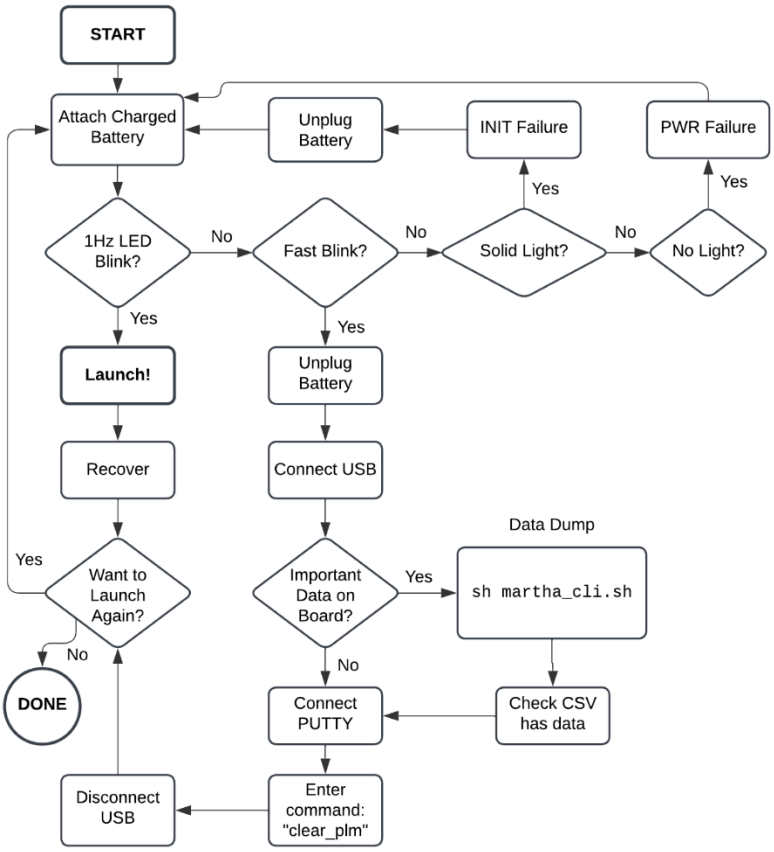

Figure 48 MARTHA operational flowchart.

The other side of reliability is our relentless testing. We do not trust any software that hasn't been thoroughly validated. We use a combination of unit tests, on-board tests, and full data injection tests. Unit tests are handled by our Native repository [36]. It allows us to compile and run flight firmware on our laptops as if it's running on real embedded hardware. This is done through a hardware abstraction layer (HAL) between our firmware and Arduino Core, allowing us to substitute functionality with native equivalents.

For our on-board tests, we flash the actual hardware with a suite of unit tests. After execution, the flight computer streams the results back to the host over serial. This is orchestrated using PlatformIO and the general flow is shown in Figure 49.

Our most powerful testing method is full data injection. In these tests, we stream previous flight data over serial to the flight computer, which then uses the streamed data in place of real-time collected sensor data. We built a simulation version of each sensor's drivers to pull from a centralized sensor stream handler and delivers that data to other system through the same interface used by the real hardware drivers. This gives a perfect emulation for testing the entire program rather than pieces of it.

When we ran full data injection tests on MARTHA, the state detection delays and data logging rates closely mirrored those observed during actual flights. Since introducing these robust testing practices, all five of our most recent flights involving custom software have performed flawlessly, without any significant faults or deviations.

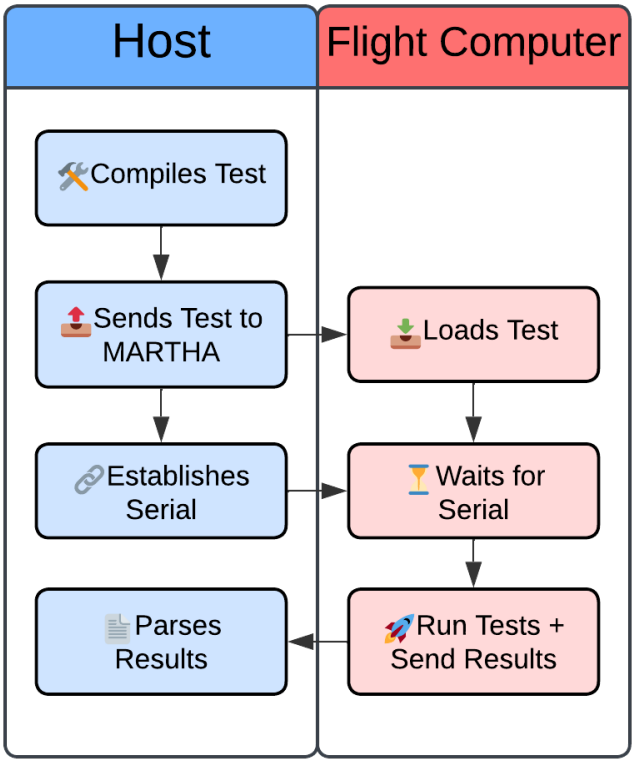

Figure 49 On-board MARTHA testing flow.

To reiterate, our flight computer software is built on three core principles: portability, performance, and reliability. By leveraging PlatformIO and a shared core Avionics repository, we write modular, cross-platform code that can be deployed across many systems. Performance is achieved through efficient data logging with our custom Byte5 format and precise state detection using real time Kalman filtering and sensor fusion. Reliability is ensured through our simplified user experience and robust testing practices, including full data injection simulations.

IV.Mission Concept of Operations Overview

The CONOPS Overview is a comprehensive section detailing the sequence of phases that the CURE team's mission will undergo, from pre-assembly to landing. The overview of the CONOPS phases is described in **Error! Reference source not found.** 17 below.

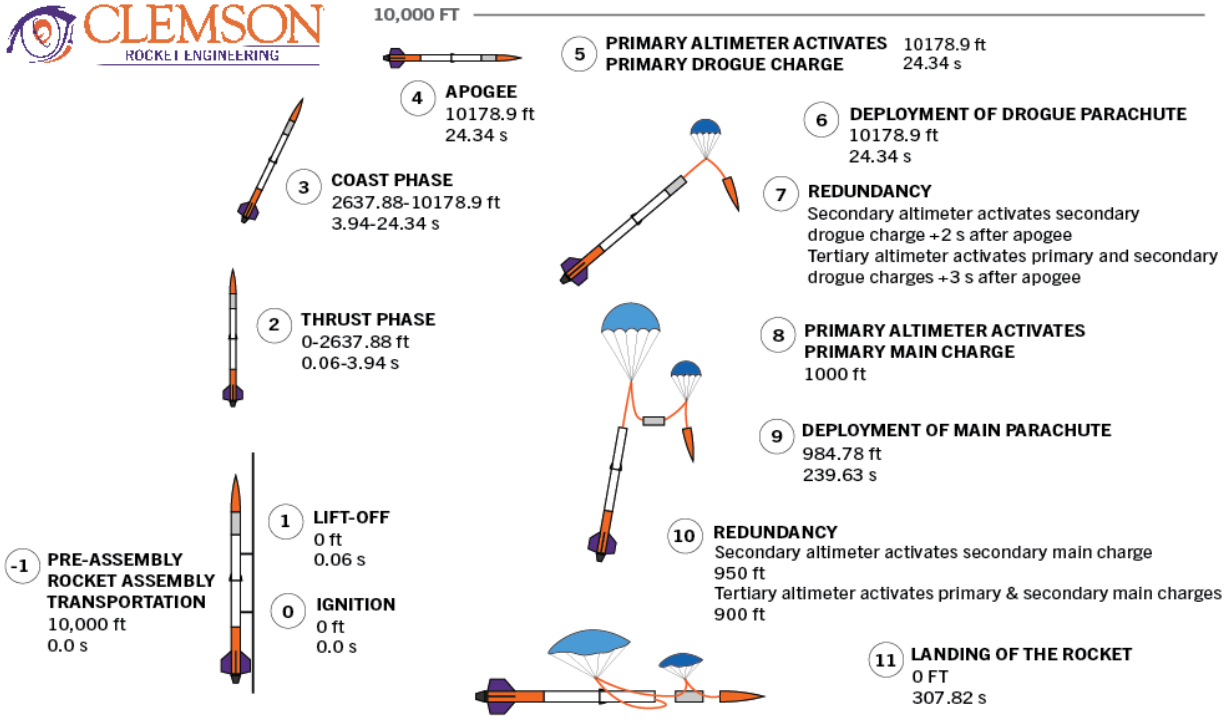

Figure 50 CONOPS overview of nominal flight for Pocket Tens.

The CONOPS Overview illustrates these phases, outlining the nominal operations and interactions of all subsystems during each stage, beginning with Phase -1: Pre-Assembly, Vehicle Assembly, and Transportation. Here, the team assembles and prepares the vehicle for launch. Then, the mission progresses through ignition, lift-off, thrust, coast, apogee, parachute deployment, and landing. Each phase is described, highlighting the role of various subsystems such as avionics, propulsion, and recovery systems and defining the critical events that signify transitions between phases. These transitions are triggered by specific mission events such as the ignition signal, motor burnout, reaching apogee, and altitude milestones for parachute deployment, all culminating in the safe recovery of the vehicle post-mission. This structured approach ensures clarity in mission planning and execution, allowing for precise coordination and monitoring of each phase in relation to the mission's overarching goals and objectives.

A. Phase –1 Pre-Assembly, Rocket Assembly, Transportation

During the pre-assembly phase, all members of the team will work to assemble the payload and avionics bays. Once both the avionics and payload system are assembled and the electronics for payload is turned on, both bays will be secured into the vehicle body. Once the bays are secured in their respective body tubes, each body tube will be secured together, and the launch vehicle will be carried and loaded on the pad.

B. Phase 0 Ignition

Once the vehicle is loaded onto the pad, cameras will be turned on, the payload will be turned on, the recovery bay will be armed and tracking verified, and the e-matches will be loaded into the motor. After a confirmed avionics signal from the spectator area, Spaceport officials will ignite the e-matches, beginning motor burn, and the vehicle will begin accelerating off the launch rail.

C. Phase 1 Lift-Off

After the motor ignition, the motor will burn for 3.88 seconds. According to motor information, the vehicle should leave the 17 *ft* launch rail at a velocity of 106 *ft*/s. Lift-off occurs at T+0.06 seconds at an altitude of 0 *ft*. Each SRAD flight computer detects the launch at this point, affirming departure.

D. Phase 2 Thrust Phase

According to simulations, the M2500T motor will provide an average thrust of 2,500 N. Since each COTS altimeter is altitude based, launch is detected at this point. The thrust phase of the flight will take place between T+0.06 and T+3.94 seconds, propelling the vehicle from 0 ft to approximately 2,637.88 *ft*.

E. Phase 3 Coast Phase

Following motor burnout at T+3.88 seconds, the vehicle will coast until apogee. This phase will occur between T+3.94 and T+24.34 seconds from 2,637.88 *ft* to 10,178.9 *ft*.

F. Phase 4 Apogee

According to OpenRocket simulations, the predicted apogee is 10,178.9 *ft*. Apogee will be reached at T+24.34 seconds. This altitude and timing will be confirmed post-flight by altimeters in the payload and SRAD avionics bays.

G. Phase 5 Deployment of Drogue Parachute

At apogee, the AIM USB will attempt to ignite the primary drogue charge to deploy the drogue parachute from the drogue parachute bay. The StratoLogger CF, the secondary flight computer, will ignite the secondary drogue charge to attempt to deploy the drogue parachute two seconds after apogee has been reached. Finally, the RRC3+, the tertiary flight computer, will attempt to deploy both the primary and secondary drogue parachute charges three seconds after apogee. The primary recovery event occurs at T+24.34 seconds where the secondary event occurs at T+26.34 and the tertiary event at T+27.34. Drogue will inflate and decrease vertical velocity to 40.7 *ft/s*.

H. Phase 6 Deployment of Main Parachute

At 1000 *ft*, the AIM USB will fire the primary main deployment charge, ideally deploying the main parachute. The StratoLogger CF, the secondary flight computer, will then fire the secondary main deployment charge at 950 ft, or approximately 1.25 *s* after a failed main deployment attempt. At 900 *ft* AGL, the RRC3+ will attempt to deploy both the primary and secondary main deployment charges. This occurs approximately 1.25 *s* after a failed main deployment attempt of the StratoLogger, assuming a failed main deployment attempt by the AIM USB as well. The nominal deployment is predicted to occur at T+239.63 seconds, while a secondary and tertiary deployment would occur at T+240.88 seconds and T+242.13 seconds respectively. Main will inflate and decrease vertical velocity to 13.7 *ft*/*s*.

I. Phase 7 Landing of the Rocket

After the vehicle has landed at between T+307.82 and T+310.64 seconds, the recovery team will travel to and recover the launch vehicle. To accomplish this, the recovery team will use the onboard Featherweight GPS trackers and in-hand ground station to track the vehicle’s location.

V.Conclusion and Lessons Learned

J. Conclusion

Throughout the year, CURE has worked to develop our launch vehicle, "Pocket Tens," and its incorporated subsystems. Following last year's launch vehicle, we have grown and further developed systems within the vehicle's flight programs to ensure a successful flight. Through SRAD Avionics systems with the MARTHA boards, the further development and testing of the team's Active Aero system, and the statistical analysis of COTS altimeters onboard the Payload, the CURE team has established projects that can be continued and improved for years. The mechanical foundation can be iterated upon and improved, but it is secure enough such that major design revisions will not be required. With this foundation and revived motivation, CURE has made it a mission to have a flight ready vehicle for IREC 2026 by November 2025.

K. Lessons Learned

1. Organizational Management

Over the past year, it has become evident that our organizational structure and management needed substantial revision to encourage growth and continued success. Our organization has had to adapt as the technical demands of creating a launch vehicle have evolved from primarily mechanical to heavily incorporating electrical and software systems. The Clemson University Rocket Engineering organization underwent a comprehensive restructuring in response to these evolving technical challenges. The restructuring included a complete overhaul of the leadership framework, as depicted in Figure 1 Clemson University Rocket Engineering organization chart for 2024-2025.

One of the significant changes in this restructuring was the division of the chief engineer role into two distinct positions: one focusing on mechanical integration and the other electrical integration. Previously, the chief engineer role was more hands-on, directly involved in designing every launch vehicle subsystem. We have transitioned this position to a high-level systems engineer role to oversee the integration of diverse technical aspects better. Additionally, we introduced the role of Software Development Lead, tasked with overseeing the design and integration of all software subsystems.

As part of this organizational shift, we also revised our constitution to detail the organization's mission, clarify who and what we represent, and define the role of every person and leadership position within CURE. The organization has grown by 20% and with this momentum, we are setting ambitious goals to design and launch a vehicle by the end of November 2025. This trajectory reflects our capability to achieve greater technical heights and highlights our commitment to continual improvement and innovation within our team.

2. *Administra*tive Division

The Administrative Division underwent a substantial refurbishment this year, with the introduction of an integrated onboarding program for new members, enhanced focus on member engagement within the team, and active collaboration with the university and outside entities. Starting in Fall 2024, new members attended multiple onboarding sessions with each placing emphasis on the daily operations and technical focuses of a specific Subteam. The Subteam leads guided new members through a group activity during these sessions that highlighted a concept crucial to their overall contribution in the organization. While this iteration of the program saw an uptake in new member interest towards the beginning of the semester, it was evident that those in the onboarding process were not retaining the skills, nor the information provided by these sessions as much as hoped. The learning curve for new members during the sessions proved to be too intimidating, hindering new members instead of encouraging them.

Following this test run, the focus of the program shifted in the Spring semester towards having new members build their own HPR certification rockets during the onboarding sessions. In each of these sessions, a Subteam lead would give a brief presentation on the operations of their Subteam, how the cert each new member built pertains to the goals of that Subteam, and what skills new members could obtain by being active participants in the Subteam's weekly meetings. By having new members build their own cert rockets, there were hopes that they would be more active participants in their education within the organization and would take investment towards their personal projects as motivation to explore and develop their skills in a Subteam. The latter version of the program proved to be more beneficial as new member retention increased as a whole and resulted in multiple new members obtaining TRA Level 1 certification. The largest takeaway from the program is that in the following academic year, it would be prudent to address certification supply issues before they occur, and the program would benefit from more thorough representation of the projects pursued by each Subteam.

Additionally, this year the organization decided on switching from launching certification vehicles on solid motors to a hybrid majority. While this is a more sustainable choice in the long run than launching certifications exclusively on solid motors, it comes with its own challenges that might be best avoided. Newer members attempting certifications were not familiar with the setup process for hybrid motors, resulting in slowdowns during launch days that prevented an optimal number of certification rockets from being launched. The additional complexity of hybrid motors only further complicated the certification process, confused members, and prevented the team from reaching its desired amount of certified members.

Furthermore, in the past year the organization has seen growth in nearly all aspects of outreach. There have been bi-weekly social events, multiple tech talks with industry specialists, and active participation in a series of university sponsored tabling events. As the organization has become more present within the community and outside of it to various companies/agencies, it has been granted more opportunity for collaboration in the future and facilitated the procurement of new members as well as the enhancement of the member experience. While the improvement in organizational outreach is notable, it could be even better with more consistent communication to the entities the organization has previously worked with to maintain connections and renewed efforts to build relationships with companies/agencies from varying fields.

3. Recovery – Competition Team

Although this was the first year of a formal Recovery Subteam, there were a few team members with extensive experience in designing, manufacturing, and testing recovery bays in the past four years. Still, the year provided many lessons learned to the team, as a focus solely on recovery allowed the Subteam members to dive deeper into possible ways to improve the system.

With the desire to move away from the AIM USB altimeter, the addition of the RRC3+ proved to be a lesson in incorporation of new untested commercial components. The tertiary role of the RRC3+ in this year's system allows for full operation and exploration of the system without compromising the system integrity as a whole. We believe that the process of integrating new commercial elements into the system will pay dividends when the Subteam adopts the Blue Raven altimeter for the 2026 IREC as well.

Additionally, since the Subteam was new for this year, there were many junior and first year members who joined. This required significant training and upskilling in nomenclature, design, best practices, resources, manufacturing, and testing. Lessons covered everything from proper parachute packing techniques and practice, to altimeter beep readings, and understandings of vertical and horizontal redundancy techniques, among others. Understanding development of learning roadmaps and how best to teach/upskill new members proved to be a valuable lesson.

Unfortunately, since the Subteam was new, the team did not handle much of our own CAD work. This led to inconsistencies with CAD that forced redesigns later in the design cycle than they should have been. Owning and actively managing your own CAD work was a major lesson learned for the Subteam for future years.

Lastly, there were a series of design flaws understood with this recovery system design that can be refined and reviewed for the coming year to further improve our core design elements of improving redundancy, increasing assurance, and reducing manufacturing times.

The first of these was the dual bay architecture for our parachutes. While this design allowed for a recovery bay to be lower within the airframe than a dual split bay design, as well as one contiguous main section, it introduced more design problems than it solved. Two large points of concern were the protection of drogue parachute cabling in the main bay, as well as the assured separation of the drogue cabling upon main deployment. Although these two issues were eventually understood/mitigated, a dual split bay would not have encountered these issues in the first place. Secondly, a dual split bay architecture would have allowed for one less 8-pin aviation connector in total throughout the vehicle, which would have saved space on bulkheads already filled with retention devices, charge wells, and other screws/bolts.

The second of these was the use of fully pinned out 8-pin aviation connectors. The same style connector was used in the previous year's bay design, however, only four out of the eight pins were used. When fully pinning out a connector, we found that reassembling the connector housing to be especially challenging. The wires on their own would fit, but the addition of heat shrink around each wire as well as a layer around the entire cable proved to be a limiting point for the cover of the connector. To supplement this, we put extra emphasis on potting each aviation connector. In addition to these issues, manufacturing of these connectors requires soldering techniques, and not at the beginner skill level. This means that only members who are skilled/trained enough to do this soldering can assist with this element of the production of the bay. This element was easily the largest commitment in labor and time across the entire bay. Therefore, elimination of the aviation connectors entirely, while still allowing for detaching and secure installation into bulkheads, would benefit all three design principles. Our idea is to transition to using cat5 ethernet cables for a variety of reasons [8]. The cabling is relatively inexpensive, widely commercially available, standardized, comes pre-twisted/packaged, solid core, 24 AWG (close to 22 AWG), and contains 8 conductors. Solid core wire is able to carry greater currents than stranded core and could be directly clipped into a WLC. The availability of 8 conductors means that no overall architecture changes to the wiring would need to be done, but for connections between bulkheads, RJ45 ethernet couplers could be installed into the bulkheads themselves. This would reduce all the time and effort of the production of our current connectors to splicing a cable and then attaching a connector to a port. Design iterations like this were one of the greatest lessons learned this year.

4. Simulations – Competition Team

The Simulations Subteam was created this competition year in order to expand upon and become more specialized in the tasks that the previous Flight Dynamics Subteam was responsible for. The most impactful changes between the tasks of the Flight Dynamics and Simulations Subteams were the discontinuation of the creation of in-house nosecones and the introduction of FEA as a method of verification of the launch vehicle's design.

With the expansion of the Subteam's responsibilities, it soon became clear that we needed to start smaller and gradually increase our work instead of doing so all at once. We had initially tried to break the Subteam's members into different projects, but because many of the members had less experience with computer modeling software, this

idea became less feasible. In future years, it would be best to teach new members how to set up and run models first before splitting people up to work individually on different parts of the vehicle.

In addition, one task that was given to the Simulations Subteam was the design of the camera shrouds in the vehicle. Because this component was important for being able to capture video of the vehicle's launch, the Simulations Subteam had prioritized this task over other tasks. However, the steps needed to design the camera shrouds were not something that members of the Simulations Subteam had much experience in. The people within this Subteam did not have experience in the CAD program that the team used to design components, and the design would need to be changed when ever the design of the vehicle changed. This led to this project dragging on and taking up time that needed to be spent on modeling the launch vehicle. The camera shroud project was shifted to other members of the team for the Subteam to be able to focus on tasks that better align with the vision of the Subteam.

5. Structures – Competition Team

The Structures Subteam, coming off last year's failed recovery at the 2024 IREC due to the loss of the motor tube in flight, was tasked with designing and creating a more feasible internal system. The biggest changes the team would make to the launch vehicle were the use of a spar system to hold all the internal components, the use of U-bolts for recovery processes, and better acknowledgement of our assembly process. As described in full detail in Aero-structures Subsystems, the concatenation of the spar and bulkhead system increased the ease of assembly for this iteration of the launch vehicle's internal structures. For improving the knowledge around the assembly process, exact step by step instructions were scribed as assembly occurred. Furthermore, timing for each step was recorded, such that iterative progress could be achieved.

Throughout the year the team was challenged with the new design of its internals in the spar system. After the design and FEA of the spars, the team needed to water jet the spars out of a carbon fiber plate. In past years we have used Clemson University's water jet; however, it was, and still is, broken. The task of finding a company that would water jet both our small holes used in the spars as well as the highly delaminate G10 fiberglass plate was deemed to be significantly easier than in reality. This year, the team established a working relationship with the center for composite manufacturing at the Clemson University International Center for Automotive Research (CU-ICAR). In future years, the process for finding companies to water jet our parts will be expedited. The team hopes to continue fostering the relationship with CU-ICAR for the foreseeable future, barring the completion of our university's own waterjet machine. We will also be less worried of price as we have found that there is no right answer when it comes to which company is best, but rather there are many answers, some better than others.

The team opted this year to implement 3D printed mandrels for coupler and inner motor tube creation. The discretization of points in a circle that a 3D printer implements through its gcode initially failed to capture the desired cylindrical form of mandrel required for our manufacturing standards. Furthermore, due to the relatively high filament expenditure and print time, layer shift resulted in several print failures. The changes the team would make in the future are to require an enclosed printing environment and finer resolution of print. The enclosed printing preventing layer shift failure, and the high print resolution increasing the number of straight-line intervals that approximate the cylindrical mandrel.

In constructing the SRAD assembly for this year's launch vehicle, members of structures were tasked with developing housing to accommodate MARTHA flight computers. With a Subteam composed entirely of mechanical engineers, many members found themselves without extensive knowledge of the electrical components being integrated into the assembly. To encourage collaboration between members, and to ensure a design that followed technical standards of both Subteams, the Hardware and Structures teams began limited joint meetings with design engineers of both disciplines. The team will continue this practice in later iterations of the launch vehicle and hopes to formalize these meetings such that electrical integration is not an issue during the assembly process.

6. Active Aero – Research Team

Coming into the Fall 2024 semester, Active Aero had a partly functional test vehicle and no working brakes. The first month was spent repairing the test vehicle and getting it ready to fly again for a test flight using brakes. The rest of the semester was used to design the entire braking system as a joint effort between mechanical and electrical engineers. In previous years, Active Aero had somewhat functional designs but had failed to come to fruition. This was due to a lack of consideration taken into account for both sides of mechanical and electrical design. The first design several years ago was designed around the electrical system but made the system too heavy and too large to easily incorporate into a vehicle. The second design was much lighter and smoother mechanically but failed to take into account the design requirements the electrical side would need with an overpowered and inaccurate motor to drive the flaps. Neither of these designs flew.

The third design from this year had both electrical and mechanical engineering students come together to design a system that would work for both parties in the test vehicle. The design was light, using aluminum and 3D printed parts

where applicable. The design became a reality during the Spring 2025 semester, as it went into a testing phase to verify the entire assembly worked as expected and could be seamlessly integrated into an existing vehicle.

Up until this point, Active Aero had been using breadboards and breakout boards for the controls electronics for the brakes. But after a partially successful launch in April 2024 where the vehicle was recovered but the flight computer failed to record data due to the flaws of breadboards, it was time to move away from a breadboard. A custom PCB was designed and manufactured electrically identical to the breadboards so that all of the breakout electronics could be soldered to the PCB with no changes required to existing code or hardware. Software was hard at work as well during this time, getting the Active Aero codebase up to par with the rest of the team's existing software. Once the two were ready independently, the PCB and software also underwent rigorous testing to ensure proper integration and that the brakes would deploy safely in flight.

In February 2025, there was an attempted launch day for Active Aero, but the vehicle never made it off the pad. This was due to several flaws and mistakes made leading up to the launch day that weren't made evident until the team was on the field. These flaws and mistakes include, but are not limited to, insufficient nosecone volume for new parachutes to be packed inside, finnicky upper motor retention that took over 30 minutes and a hole in the side of the airframe to mount the motor, faulty ground station equipment for a hybrid fill/purge sequence, and finally a low member retention rate for the day that slowed down progress drastically throughout the day.

In April 2025, the Active Aero team made its way back out to the launch field, fixing every mistake made in February. The goal for that day was to fly the vehicle with brakes deployed during the coast phase. The simulated apogee without brakes was 4500 feet, which meant the vehicle was looking for at least 400 feet of apogee removed due to brake deployment. After a few minor hiccups throughout the day, the vehicle made its way to the pad and flew a total of approximately 3900 feet, meaning that the project was a success. Unfortunately, the vehicle itself had a recovery issue where the main parachute did not fully unfold and hit the ground with only the drogue fully inflated leaving excessive damage to the vehicle's structure. All electronics and the motor were recovered intact, leaving the team in a good place to redesign and rebuild a better test vehicle in the future.

7. Hardware Development – Research Team

The Hardware Subteam had a lot of success and some opportunities to learn from failures this academic year. The primary lesson taken away from this year is the need for a commitment to electrical design standards and documentation, especially when it comes to PCB design specifically. The team is currently undertaking development of an "Electrical and PCB Design Standards" document to provide a generalized design flow of PCB design projects, as well as an archive of best practices, common conventions, industry practices, and implementation guidelines. This document is important to lay the foundation for future development. The Subteam effectively paused all active PCB development as a recognition of the document's importance. Upon completion of this document, members of the team will take the knowledge gained by this process to better understand and guide development of future PCB projects.

Another primary lesson we learned was how to recognize proper goals for projects and setting steppingstones between large design goals. Throughout the year, the Hardware Subteam worked to develop our own in-house Ground Station Equipment (GSE) system. Originally, this system would operate over wireless communication, instead of a wired connection with extension cords. However, an in-house GSE system, much less a wireless one, had never been developed prior to this. Throughout the year, the Subteam realized this and reoriented itself to recreating an exact copy of the GSE system that had been loaned from our mentor. This was a critical lesson as it took one half the time to produce and manufacture the copy of the GSE than the time it had taken to get to the current point of producing our own system from scratch. We were able to test this GSE system multiple times this spring at our local range launching hybrid Level 1 certification rockets.

Finally, the Hardware team learned that creating a standardized product instead of a minimally viable one is critical for success. When hand-making 2s and 4s battery packs, the battery packs were inconsistently shaped. This led to the integration of the batteries into the avionics and camera bays being unnecessarily difficult. In the future the team will need a more standardized process when manufacturing things by hand and establish specific design parameters to meet.

8. Propulsion – Research Team

Propulsion is a revived Subteam this year, as it was shut down a few years prior. This means the current students do not have first-hand experience to learn from. This does not mean there is nothing to learn from. The Subteam was initially shut down a few years ago due to safety concerns. Clemson staff saw that the students at the time were cutting corners and not taking the utmost care for safety that was expected from such a Subteam that should realistically require the most care for safety. The lessons to be learned from this history of the Subteam are that absolutely no corners will be cut, every point of concern will be addressed, and every safety precaution taken to ensure student and property well-being. In the coming years, the Propulsion Subteam will do everything in its power to address safety concerns and do everything correctly to maintain an active and successful team.

9. Software Development – Research Team

The Software Development Subteam explored several new systems and ideas this year, gaining insights that have already improved our capabilities as a team. One major area of growth was learning to interface directly with flash memory, moving away from typical file system abstractions. This approach gave us much finer control over performance and reliability, but required the development of custom tools and binary data formats. The first semester was largely dedicated to this effort, which ultimately elevated the team's embedded systems experience and laid the foundation for more advanced architectures moving forward.

Another big takeaway of the year was the importance of rigorous testing. In both industry and rocketry teams, the best software stands out because of rigorous testing. With that in mind, we introduced unit testing via our custom Native environment, onboard hardware test suites, and full flight data injection. These new practices enabled us to validate performance on real flight data and contributed directly to the number of successful flights we had.

A third lesson we learned was the criticality of maintaining organization-wide software alignment. When looking at the Active Aero software, we discovered it to be using a version of our Avionics repository that was over 200 commits behind. Updating it and fixing compatibility problems took substantial effort and coordination but led to the first well-timed brake deployment in an Active Aero flight. In the future, we plan to ensure the Software Development teams play a closer role in the software of the Active Aero team, ensuring we both benefit from new discoveries and updates. To do this, we'll utilize members who are in both the Software Development and Active Aero teams as communication points to ensure consistency.

Appendix A: System Weights, Measures, and Performance Data

A. Rocket Information

The launch vehicle is 143.6875 *in* with one stage. The vehicle has an external diameter of 6.227 *in*. There are four fins which have a semi-span of 6.25 *in*, a tip chord of 7 *in*, a root chord of 11 *in*, and a thickness of 0.3 *in*. The dimensions of the fins were selected based on initial designs of the rocket. Tapered swept fins were chosen as the type of fins due to this fin type being able to achieve high speeds. One downside to this design is that it has the potential to be susceptible to fin flutter. To ensure that the windspeed is able to withstand the design, the fin flutter velocity was calculated to be 3493.22 *ft/s*. Because the maximum velocity of the vehicle in flight is expected to be 1026 *ft/s*, this leads to a factor of safety for the fins to be 3.4.

The total vehicle weight is 59.1 *lbm*, the propellant weight is 4.409 *lbm*, and the empty motor case is 7.49 *lbm*. The payload weight is 2.45 *lbm*. The vehicle weighs 59.1 *lbm* at liftoff with a center of pressure at 107 *in* from the nose, and a center of gravity 89.527 *in* from the nose.

B. Propulsion Information

The motor chosen was a COTS solid Aerotech M2500T[15]. This is an M Class motor with an average thrust of 2,500 *N*, a total impulse of 9,671 *Ns*, and a motor burn time of 3.9 *s.* Using this motor, the launch vehicle would be able to reach the target apogee of 10,000 *ft* with an off-rod velocity of at least 100 *ft*/s, providing for a stable launch. Based on the team's simulations in OpenRocket, the vehicle will have an off-rod velocity of 106 *ft*/s and predicted apogee of 10,178.9 *ft*. Shown below in Fig. 18 is the thrust curve for the M2500T motor [10].

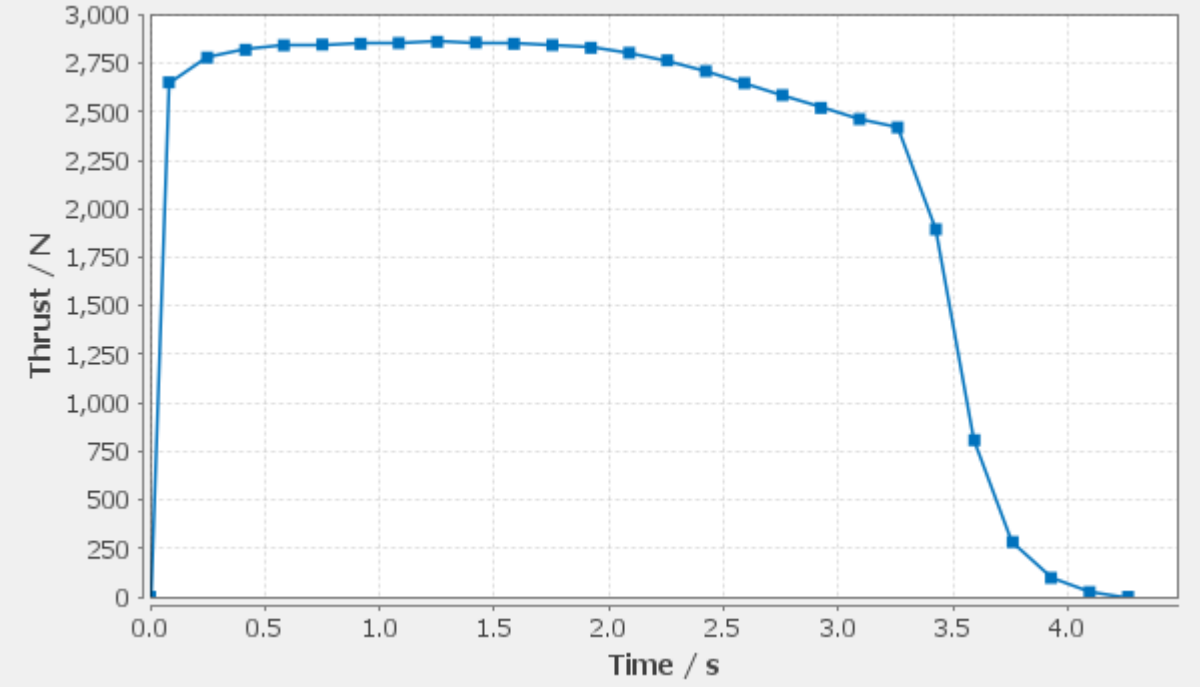

Figure 51 Thrust curve of a M2500 rocket motor.

C. Predicted Flight Data

Predicted flight data including launch rail length, liftoff thrust-weight ratio (X:1), rail departure velocity, minimum static margin, maximum acceleration (G), maximum velocity, fin flutter velocity, target, and predicted apogee.

For the rocket launch at IREC, the OpenRocket simulation with a M2500T motor had a predicted apogee of 10,178.9 *ft*, an off-rod velocity of 106 *ft/s*, and a stability of 2.85 *cal* [10]. These values, alongside other predicted flight data, are shown below.

To determine whether the fins would exceed flutter, the fin flutter velocity was calculated. This process begins with calculating the wing area, S. The equation for calculating this value is shown in Eq. 1.

$$S = \left(\frac{cr + ct}{2}\right) \cdot b \tag{1}$$

where cr refers to the root chord, ct refers to the tip chord, and b refers to the semi-span of the fins. After calculating the wing area, this can be used to calculate the aspect ratio, AR, using Eq. 2.

$$AR = \frac{b^2}{S} \tag{2}$$

Additionally, the taper ratio (λ) was calculated with Eq. 3.

$$\lambda = \frac{ct}{cr} \tag{3}$$

The temperature (T) and pressure (P) at the altitude of maximum loaded can be calculated with Eq. 4-5. The altitude (h_g) used is the same as the ground level for the launch field, or 2,945 *ft*. The altitude of maximum loading (h) was determined to be the same as the altitude for the ground level. The temperature at the ground level (T_g) was estimated to be 100 *F*.

$$T = T_g - 0.00356 \cdot (h - h_g) \tag{4}$$

$$P = \left(\frac{2116}{144}\right) \cdot \left(\frac{T + 459.7}{456.7 + T_g}\right)^{5.256} \tag{5}$$

These three equations are used to calculate the geometric values that are needed to find the fin flutter velocity. The next equations are based off the location of the flight. The speed of sound, a, at IREC is calculated using Eq. 6.

$$a = \sqrt{1.4 \cdot 1716.59 \cdot (T + 4600)} \tag{6}$$

From these values, the fin flutter velocity can then be calculated using Eq. 7-8.

$$G_{b,ff} = \frac{1.337 \cdot AR^3 \cdot P \cdot (\lambda + 1)}{2 \cdot (AR + 2) \cdot \left(\frac{t}{cr}\right)^3} \tag{7}$$

$$V_{ff} = a \cdot \sqrt{\frac{G}{G_{b,ff}}} \tag{8}$$

where G refers to the shear modulus of elasticity and t refers to the thickness of the fins. Overall, the factor of safety for the fins was calculated to be 3.4.

Table 6 Predicted flight data for IREC launch.

Specification	Value	Units
Launch Rail Length	17	ft
Liftoff Thrust-Weight ratio	9.36	X:1
Velocity off Rail Rod	106	ft/s
Maximum Acceleration	332	ft/s^2
Maximum Velocity	1,026	ft/s
Fin Flutter Velocity	3493.22	ft/s
Predicted Apogee	10,178.9	ft
Stability Margin	2.85	cal
Average Thrust	2,461	N
Total Impulse	9,573	Ns
Burn Time	3.88	s

D. Simulated Flight Profile

The flight graph below is used to predict the flight of the team's launch vehicle at the International Rocket Engineering Competition. The apogee is predicted to be 10,178.9 *ft*. For this simulation, an average windspeed of 15 mph was used with a standard deviation of 4 mph and a turbulence intensity of 10%. The direction of wind was 90 degrees from north and the simulation used international standard atmospheric conditions. These conditions were 9.17 °C and 910.18 *mbar*. The launch site information was based on where the vehicle would be launching at IREC, with a latitude of 31.1 degrees North, a longitude of 104 degrees west, and an altitude of 2945 *ft*. The length of the launch rod was set to 17 *ft*, and the launch direction was directly upwind.

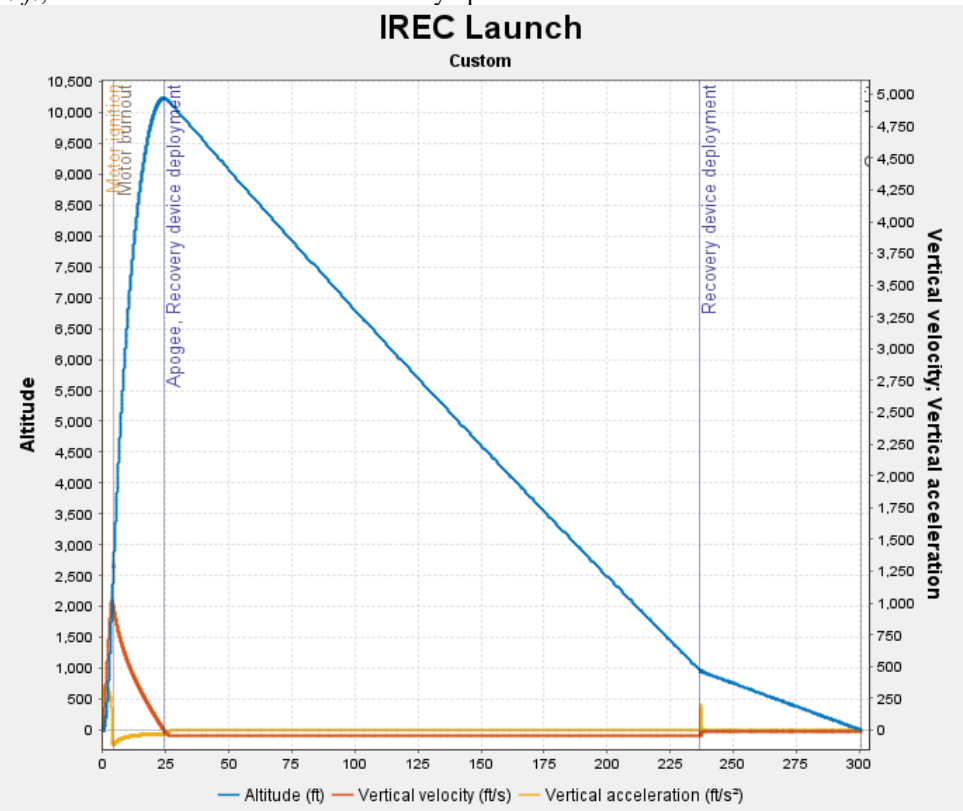

Figure 52 OpenRocket flight simulation of Pocket Tens at IREC launch.

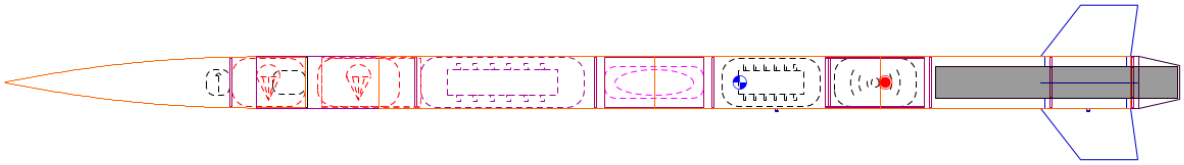

Figure 53 OpenRocket model of Pocket Tens, International Rocket Engineering Competition vehicle.

E. Recovery Information

Recovery information, including the COTS and redundant altimeters used, drogue primary and backup deployment charges, drogue deployment altitude, drogue descent rate, main primary and backup deployment charges, main deployment altitude, main descent rate, shock cords and mechanical links.

The recovery system uses an AIM USB 3.0 as its primary altimeter, while a StratoLogger CF is used as the redundant secondary altimeter. A tertiary altimeter is implemented as well with an RRC3+. Each altimeter is independently powered and wired across each e-match, The AIM USB is connected to each of the primary drogue and main charges, while the StratoLogger is connected to the secondary drogue and main charges, for a total of four

deployment charges within the vehicle. The AIM deploys the drogue chute at apogee, 10,178.9 *ft*, and the main chute at 1000 *ft* while the StratoLogger has a two second apogee delay and deploys the main chute at 950 *ft*. The RRC3+ is independently wired to both the primary and secondary drogue and main parachute charges. The RRC3+ uses a three second apogee delay and main deployment altitude of 900 *ft*.

Each of the four charges use 4F black powder as the explosive to provide the deployment force. The primary drogue charge uses 1.75 *grams*, while the secondary charge uses 3.25 *grams* of black powder. The primary main charge uses 2.5 *grams.* and the secondary charge uses 5.0 *grams* of black powder. A more detailed analysis and discussion of the calculations and methodology to determine these values can be found in *Deployment System*, 32.

In total, there are five retention mechanisms within the vehicle: shock cords, swivels, quick links, eye-bolts, and a U-bolt. These five mechanisms of retention secure the three segments of the vehicle during and after deployment of all parachutes. The forward drogue parachute retention consists of two 1300 *lb* rated forged eye-bolts (Figure 54D). A 42 *ft* shock cord will span through each eue-bolt connected to the upper recover bulkhead (Figure 54C), leading to the parachute lagging the rest of the vehicle by approximately 21 *ft*. The eyelets of the shock cord are connected to a 3000 *lb* rated quick link (Figure 54B) followed by a 3000 *lb* rated swivel (Figure 54E). This connects to the drogue parachute, which is a Fruity Chutes 48 *in* Iris Ultra (Figure 54A), through another quick-link and swivel that slows the vehicle to a descent rate of 40.9 *ft/s*. A separate swivel and quick-link is used to connect the nosecone through another 42 *ft* shock cord (Figure 54F)

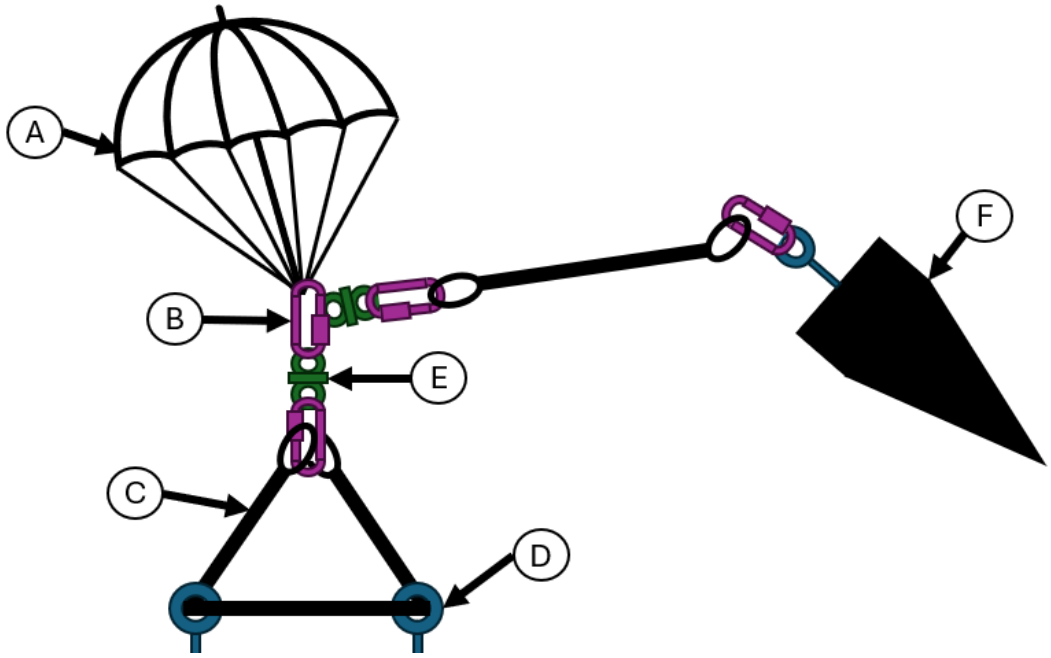

Figure 54 Plan for drogue deployment system.

The main parachute harness consists of a U-bolt rated at 5300 *lb* on the aft bulkhead which is connected with a quick-link rated at 3000 *lb.* 42 *ft* of nylon webbing shock cord rated at 3000 *lb* connects the U-bolt to the main parachute, a Fruity Chutes Iris Ultra 120 *in* parachute, through a 3000 *lb* swivel. The forward bulkhead is connected to the rest of the body through another quick link that connects to a 1300 *lb* rated eye-bolt. Under the main parachute, the vertical velocity will be reduced to 13.7 *ft/s*.

Appendix B: Project Test Reports

A. Recovery System Testing

A.1 Redundancy

1.a. AIM, StratoLogger CF, and RRC3+ altimeters all use independent batteries and arming switches

i Batteries are secured with dedicated 9*V* battery holders that clamp onto batteries.

ii Connection from battery to switch and from switch to altimeter use 0.110 *in* crimp connectors. Connectors on battery and switch are designed for this connector

iii High acceleration shock resistance, ~30*g*, of altimeter switches maintains power even during flight conditions.

1.b. All cabling is twisted pair connections to provide protection against EMI

i All cabling follows standard wire color convention to prevent accidental incorrect assembly/integration

ii All cabling follows standard cable flag naming procedures to give clear indication of cable purpose and prevent incorrect assembly/integration.

iii All cabling uses watertight heat shrink, and all soldered connections utilize two layers of heat shrink

a. All soldered connections are potted for assurance against electrical shorts and mechanical stability

iv Cabling in through deployment bays uses expandable sleeving to protect against deployment events

1.c. Three different flight computers provide dissimilarly redundant systems

i Mitigates failure modes by flight computer hardware/software

ii Maintains dual redundancy in the case of altimeter failure during flight

1.d. Redundant wiring across 8-pin aviation connectors within recovery system allows for multiple independent current paths for deployment charges in the case of a wiring failure/back out.

i Use of aviation connector for ejection charge lines ensures locking connection through vehicle bulkheads for deployment.

1.e. Both Featherweight GPS trackers use independent batteries and onboard arming switches

i 2.6 *Ah* 1S Li-Ion 18650 packaged battery provides approximately 29 *hr* of uptime for each altimeter.

a. Calculated through Featherweight GPS tracker datasheet where 400 *mAh* 1S LiPo provides 4.5 *hr* uptime to tracker.

1.f. Figure of wiring found on following pages

Full Diagram:

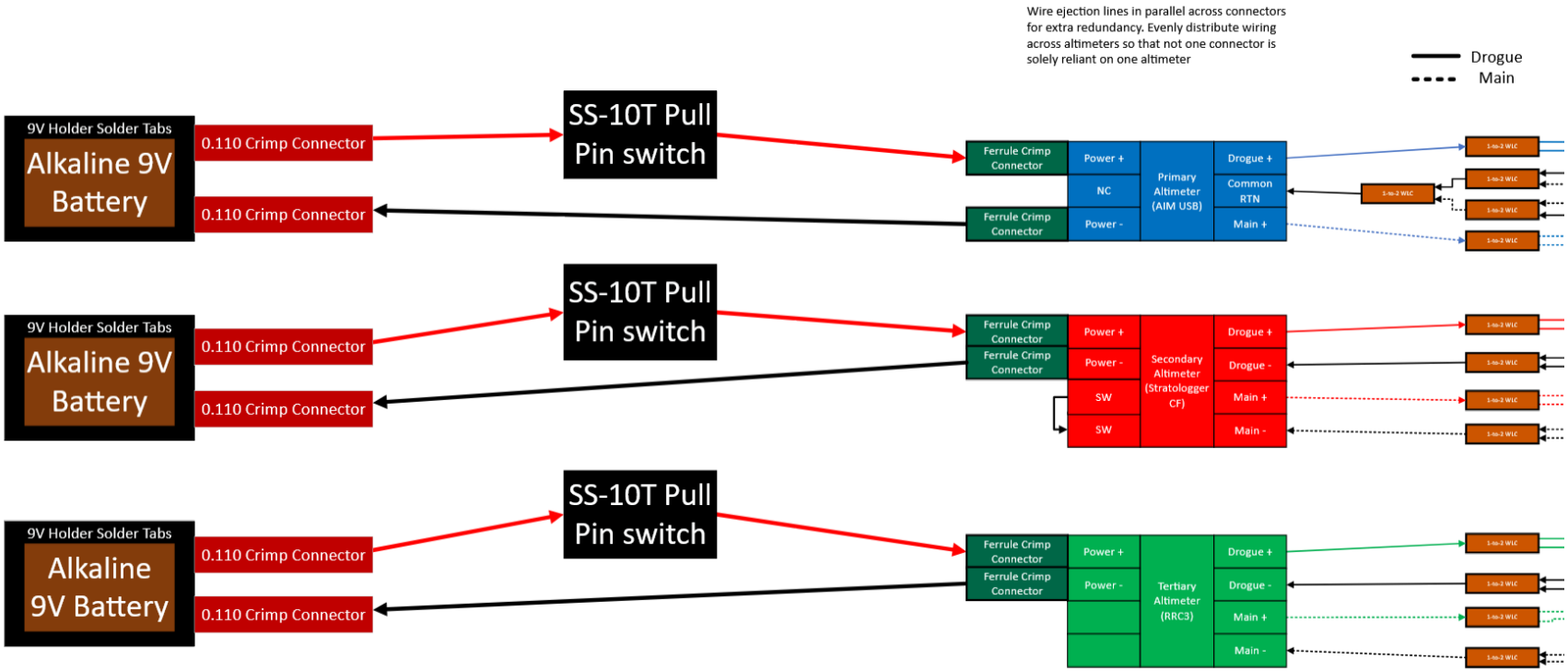

Figure 55 Recovery wiring diagram from power to altimeter out

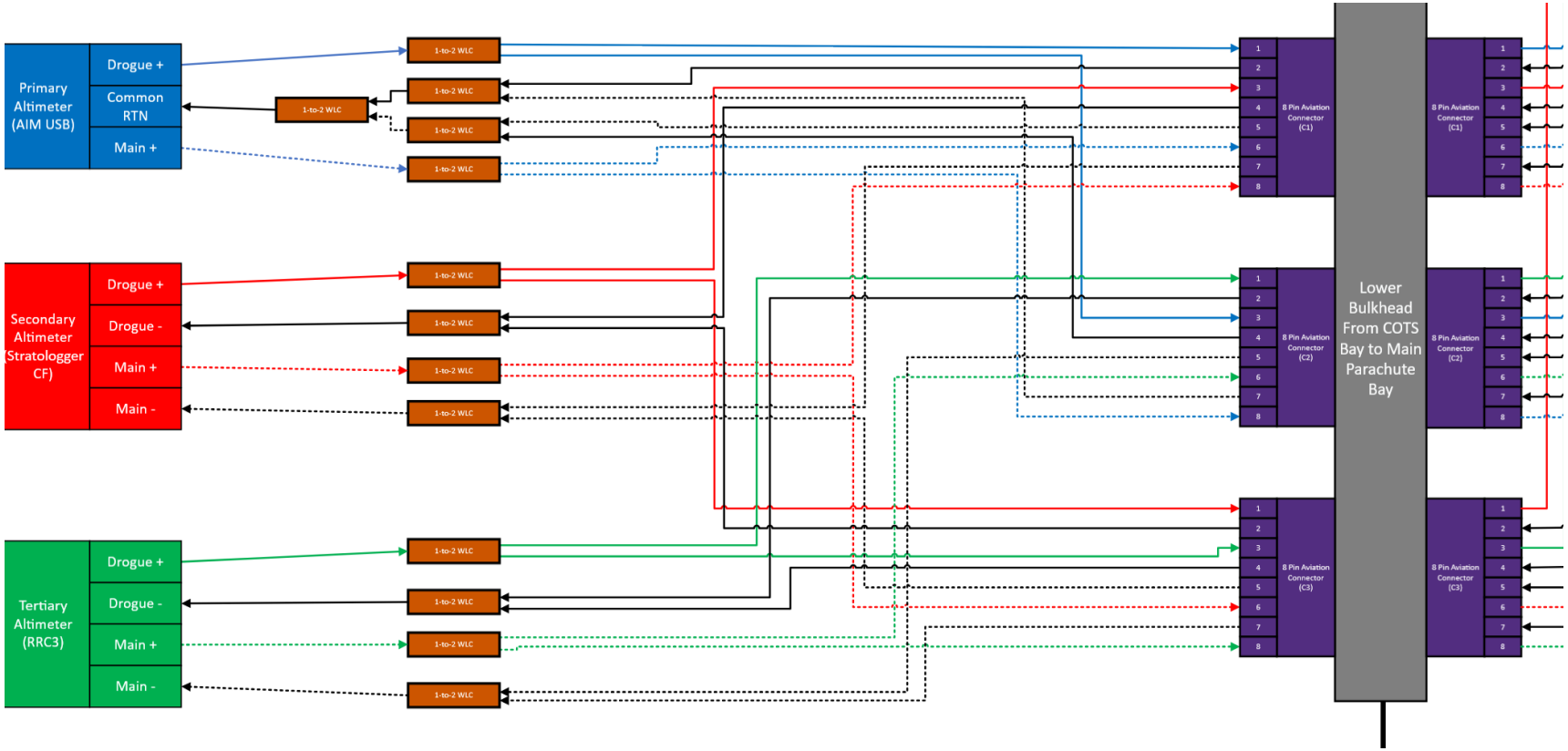

Figure 56 Recovery wiring diagram from altimeter out to aviation connectors

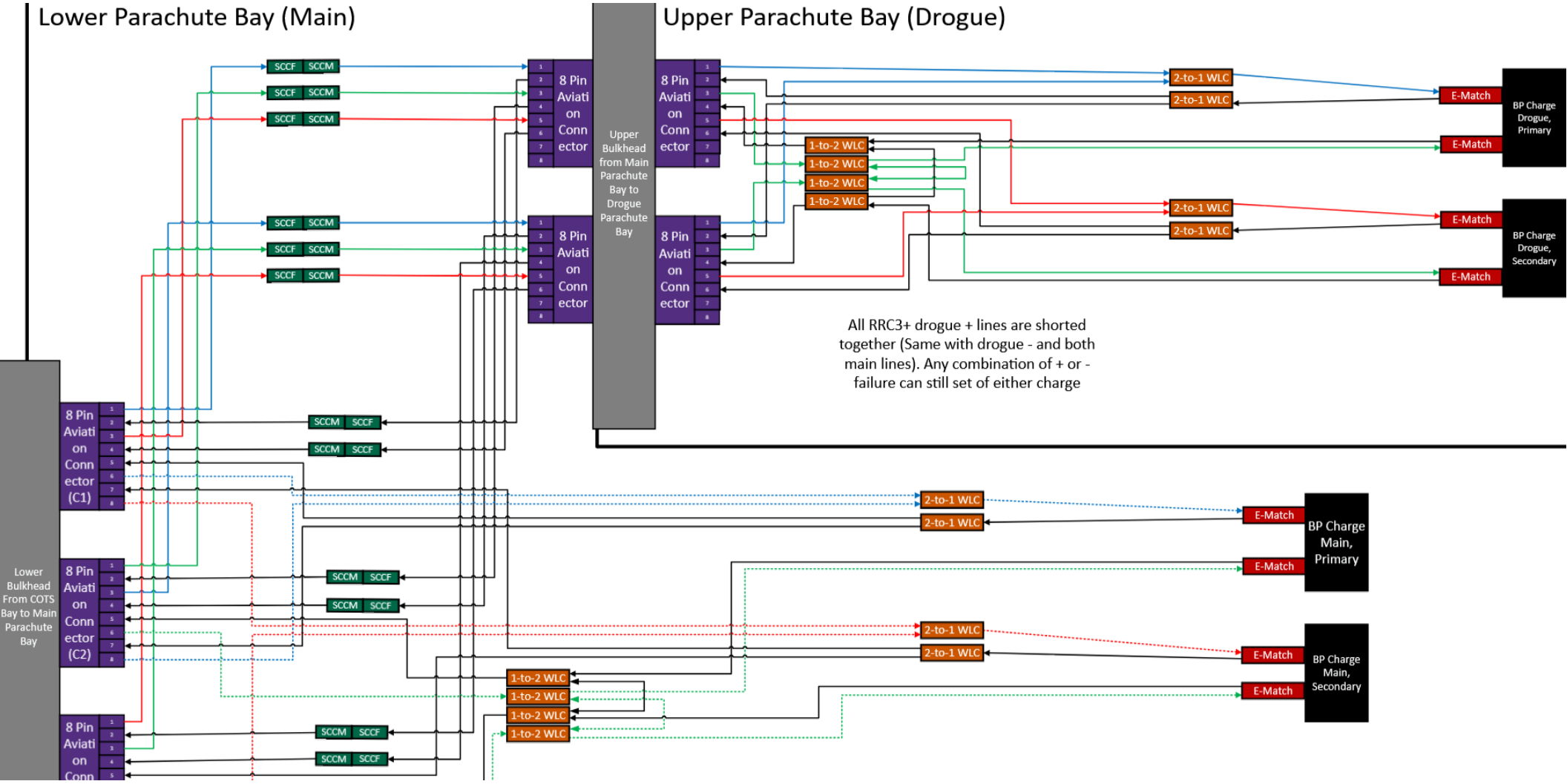

Figure 57 Recovery wiring diagram from aviation connectors to BP charges

Type Electronics Function
Date 7 Febuary 2025
Description
Power on test of flight computers while integrated into recovery bay.
Result
All three flight computers booted with no issue and entered ready to launch state.
Action items None needed.

Type Battery Drain
Date 14 February 2025
Description
Test flight computers' battery drain characteristics at flight temperatures to gauge longevity.
Result
All three flight computers sustained ready for launch state for over six hours at launch conditions (~105°*F*) with an indistinguishable decrease in battery voltage.
Action items None needed.

Type Continuity Testing on Recovery Bay
Date 5 April 2025
Description
Verification of the continuity test done on the recovery bay, this test was done on the fully finalized wiring of the recovery system which checked the continuity from the terminal on the altimeter to the bulkheads 2 to 1 clips. This was done for main and drogue, positive and negatives lines.
Result
Successful continuity was found between all connection points by use of a digital multimeter.
Action items
None needed.

Type Deployment
Date 12 April 2025
Description
Deployment testing of flight computers lighting e-matches on primary drogue and main channel. Fully integrated test confirming proper wiring, adequate charge weights, mechanical construction, integration, and proper body tube separation.
Result
One test completed on both primary drogue and main charge. Successful firing of approximately 1-gram black powder charge from StratoLogger flight computer, unsuccessful separation of body tubes from one another.
Action items Increase amount of black powder used and further sand each tube interface area

---

Type Deployment
Date 12 April 2025

Description

Second deployment test, lighting e-matches on both primary drogue and main charges. Fully integrated test confirming proper wiring, adequate charge weights, mechanical construction, integration, and proper body tube separation.

Result

Successful firing of approximately 1.5-gram black powder charge from StratoLogger flight computer, unsuccessful separation of body tubes from one another.

Action items Increase amount of black powder used and further sand each tube interface area

---

Type Deployment
Date 19 April 2025

Description

Fully integrated deployment test of primary drogue and main charges. Manual lighting of e-matches through direct wiring from battery. Confirm adequate charge weights, mechanical construction, integration, and proper body tube separation.

Result

Two successful tests of primary drogue and main charges using 1.75-grams of black powder and 2.5-grams of black powder for the drogue and main respectively. Consistent measurement of separation at approximately 20 *ft*.

Action items None needed

Type Electronics Function
Date 26 April 2025

Description

Verification of e-match lighting by primary and secondary flight computer systems while fully integrated into the vehicle. Verify proper wiring and connections through aircraft connectors within integrated vehicle. Simulated charge deployment through flight computer interface software.

Result

Successful light of all e-matches by all channels on both primary and secondary flight computers.

Action items None needed.

THIS PAGE INTENTIONALLY LEFT BLANK

THIS PAGE INTENTIONALLY LEFT BLANK

A.4 Minimum Thrust-to-Weight Ratio

The thrust-to-weight ratio can be calculated with Eq. 9,

$$T{:}W = {}^{T_{init}}/_{W_{tot}} \tag{9}$$

where T_{init} is the initial thrust of the high-powered AeroTech M2500T-P COTS motor supplied by Balsa Machining and W_{tot} is the total launch vehicle weight including all major and subsystems, the payload, and motor. The initial thrust of the M2500T-P is 2482.8 *N* and the total weight is measured to be 59.1 *lbm*. The thrust-to-weight is calculated using equation (1) as,

$$T{:}W = \frac{2482.8}{59.1}\left[\frac{N}{lbm}\right] \cdot \frac{1.000}{1.000}\left[\frac{lbm}{lbf}\right] \cdot \frac{1.000}{4.48822}\left[\frac{lbf}{N}\right] = 9.36{:}1\ [-]$$

where the thrust-to-weight ratio is 9.36. Note, on earth a *lbm* is equal to a *lbf*. The minimum thrust-to-weight ratio required is 5:1, where we have designed our vehicle to have a higher ratio by a factor of 1.872.

B. SRAD Propulsion System Testing

THIS PAGE INTENTIONALLY LEFT BLANK

C. SRAD Pressure Vessel Testing

THIS PAGE INTENTIONALLY LEFT BLANK

D. SRAD GPS Testing

THIS PAGE INTENTIONALLY LEFT BLANK

E. Payload Recovery System Testing

THIS PAGE INTENTIONALLY LEFT BLANK

Appendix C: Engineering Simulation Validation

A. Static Structural Analysis

In order to determine the robustness of the launch vehicle, the factor of safety was calculated for several different 'weak points' within Pocket Tens. These components and assemblies were selected due to expected high loading applied to the launch vehicle at these points: the bottom motor bulkhead, the motor centering rings, the telemetry bulkhead, and the upper and lower recovery bulkhead sections. To calculate the safety factor, an FEA for each component was performed with a static-structural analysis within ANSYS Mechanical.

For these simulations, the components looked at consisted of three materials: structural steel, carbon fiber plating, and carbon fiber reinforced nylon. The default structural steel material in ANSYS's Engineering Data Source was used for simulations. The material data for the carbon fiber plate was obtained from MatWeb [19]. The material data for the carbon fiber reinforced nylon was obtained from MatWeb [21]. The material properties for the three materials that were used in the static structural analysis are shown in Figure 58, Figure 59, and Figure 60.

Properties of Outline Row 3: Carbon Fiber Plate

	A	B	C	D	E
1	Property	Value	Unit		
2	Material Field Variables	Table			
3	Density	1.42	g cm^-3		
4	Isotropic Elasticity				
5	Derive from	Young's Modulus and Poisson...			
6	Young's Modulus	101	GPa		
7	Poisson's Ratio	0.286			
8	Bulk Modulus	7.866E+10	Pa		
9	Shear Modulus	3.9269E+10	Pa		
10	Tensile Yield Strength	945	MPa		
11	Compressive Yield Strength	758	MPa		
12	Tensile Ultimate Strength	1040	MPa		
13	Compressive Ultimate Strength	945	MPa		

Figure 58 Material properties of carbon fiber plate

Properties of Outline Row 4: Structural Steel

	A	B	C	D	E
1	Property	Value	Unit		
2	Material Field Variables	Table			
3	Density	7850	kg m^-3		
4	Isotropic Secant Coefficient of Thermal Expansion				
6	Isotropic Elasticity				
7	Derive from	Young's Modulus and Poisson...			
8	Young's Modulus	2E+11	Pa		
9	Poisson's Ratio	0.3			
10	Bulk Modulus	1.6667E+11	Pa		
11	Shear Modulus	7.6923E+10	Pa		
12	Strain-Life Parameters				
20	S-N Curve	Tabular			
24	Tensile Yield Strength	2.5E+08	Pa		
25	Compressive Yield Strength	2.5E+08	Pa		
26	Tensile Ultimate Strength	4.6E+08	Pa		
27	Compressive Ultimate Strength	0	Pa		

Figure 59 Material properties of structural steel

Properties of Outline Row 3: CF Reinforced Nylon

	A	B	C	D	E
1	Property	Value	Unit		
2	Material Field Variables	Table			
3	Density	1.23	g cm^-3		
4	Isotropic Elasticity				
5	Derive from	Young's Modulus and Poisso...			
6	Young's Modulus	10.2	GPa		
7	Poisson's Ratio	0.29			
8	Bulk Modulus	8.0952E+09	Pa		
9	Shear Modulus	3.9535E+09	Pa		
10	Tensile Yield Strength	148	MPa		
11	Compressive Yield Strength	148	MPa		
12	Tensile Ultimate Strength	153	MPa		
13	Compressive Ultimate Strength	153	MPa		

Figure 60 Material properties of nylon reinforced with carbon fiber.

4. *Telemetry Bulkhead Assembly*

The telemetry (TM) bulkhead is used to connect the vehicle's telemetry insert to the recovery systems and the nose cone and allows for a backup GPS tracking system to be equipped on the launch vehicle. It is responsible for keeping the nosecone section of the vehicle connected to the rest of the vehicle via a shock cord when the parachutes have deployed. In order for the team to be confident that the bulkhead would be able to withstand the impulse of the parachutes ejecting. The TM bulkhead section consists of the bulkhead itself, an eyebolt that connects to the shock cord, and the hardware needed to connect the eyebolt to the bulkhead. The bulkhead is made out of the carbon fiber plating, while the rest of the materials were assumed to have been made out of structural steel. The material assignments are shown below in Figure 61 and Figure 62.

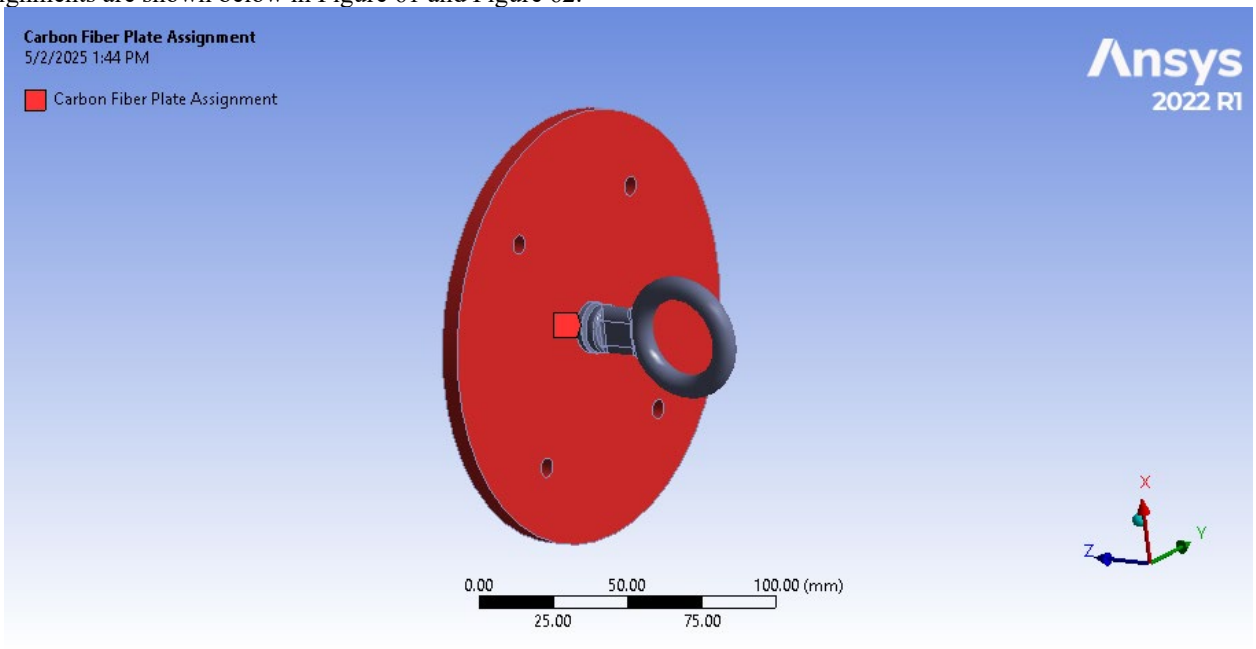

Figure 61 Carbon fiber plate material assignment for telemetry bulkhead assembly.

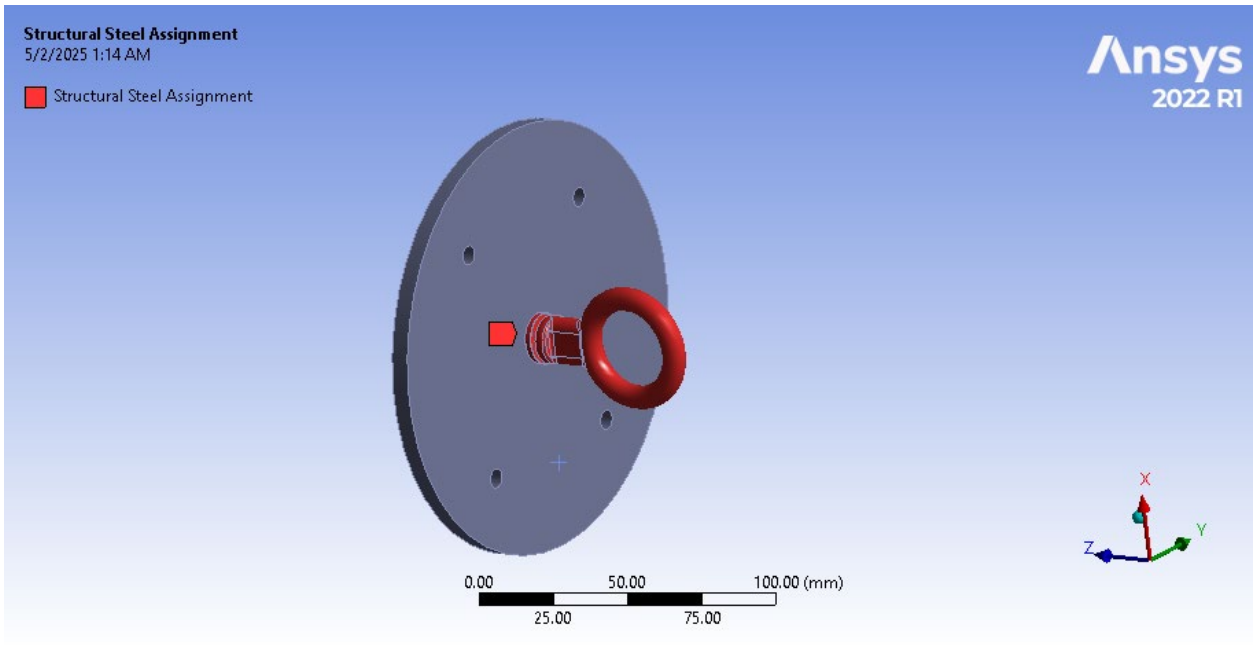

Figure 62 Structural steel material assignment for telemetry bulkhead assembly.

For the mesh of the geometry of the TM bulkhead system, two meshes were created. Because of their small size, the washers located between the eyebolt, nut, and bulkhead used a body size mesh with an element size of 1 *mm*. The other components used a body size mesh with an element size of 5 *mm*. The mesh is shown in Figure 63.

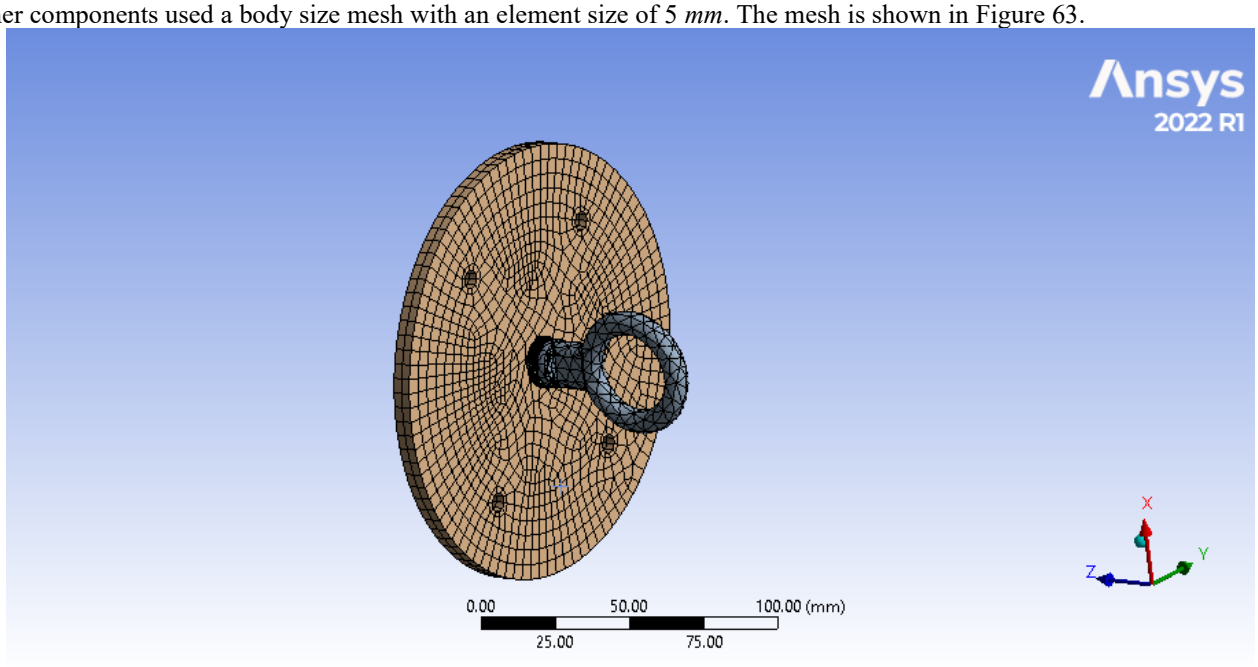

Figure 63 Finite element analysis mesh for telemetry bulkhead assembly.

The system was fixed via the outer face of the bulkhead to represent the part being attached to the nose cone at this location. The load was applied to the 'eye' of the eyebolt pointed in the direction away from the bulkhead to represent where the shock cord will apply the surge force. The surge force was estimated to be a maximum of 35 N based on the ejection charges used. The full loading of the model is shown in Figure 64.

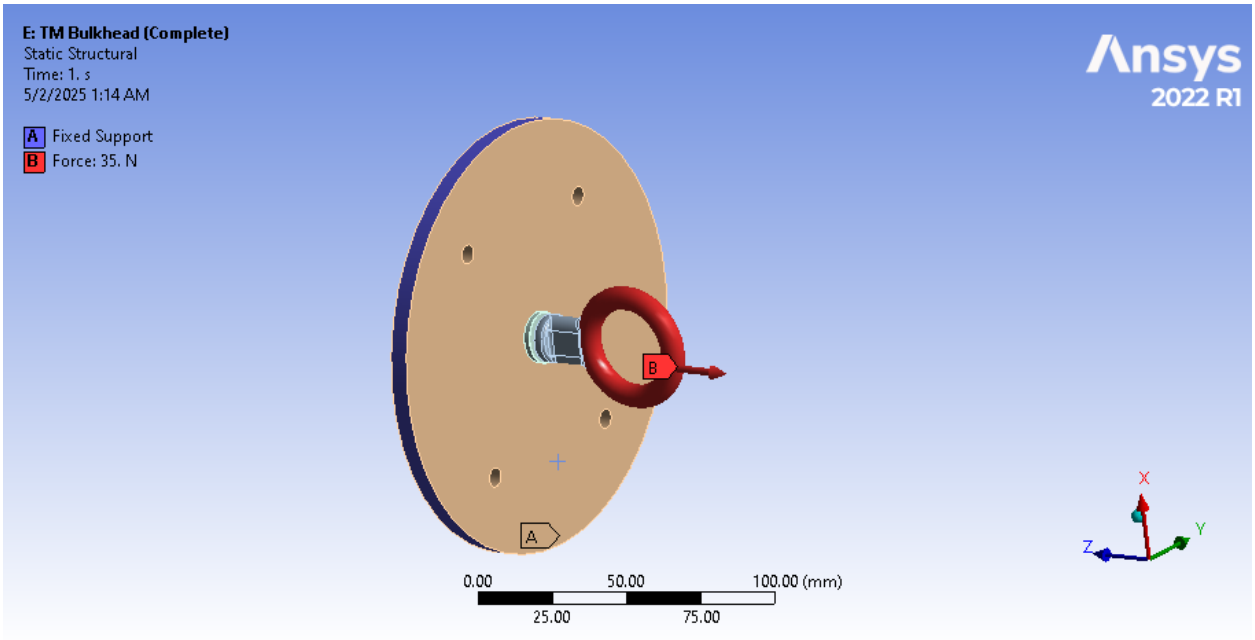

Figure 64 Full loading of telemetry bulkhead assembly.

The von Mises stresses applied to the entire system were calculated and are shown in Figure 65. As shown, the maximum stress that the TM bulkhead system is expected to undergo is 6.47 *MPa*. Based on the yield strength of structural steel being 250 *MPa* and the yield strength of the carbon fiber plating being 758 *MPa*, this leads to a factor of safety of 38.64 for the steel components and 117.15 for the carbon fiber plate components. As shown in the figure, the portion of maximum loading is not visible, which implies that it is concentrated around the threads of the eyebolt, which means that the factor of safety for the bulkhead is much higher. This simulation allows the team to feel confident in their design, so that they know that the system is robust enough to withstand the forces due to recovery systems. Additionally, the total deformation of the system was also simulated in Figure 66. With a maximum deformation of 0.00196 *mm*, the TM bulkhead system will have negligible damage and would be ready to relaunch.

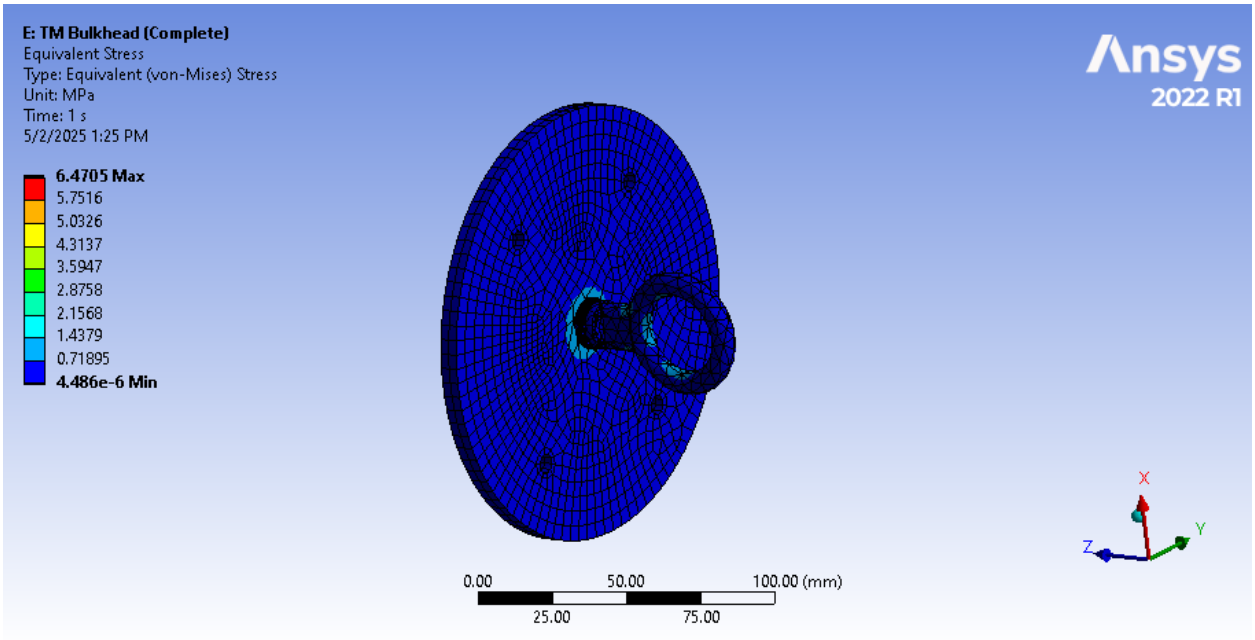

Figure 65 Von-Mises stress of telemetry bulkhead assembly under load.

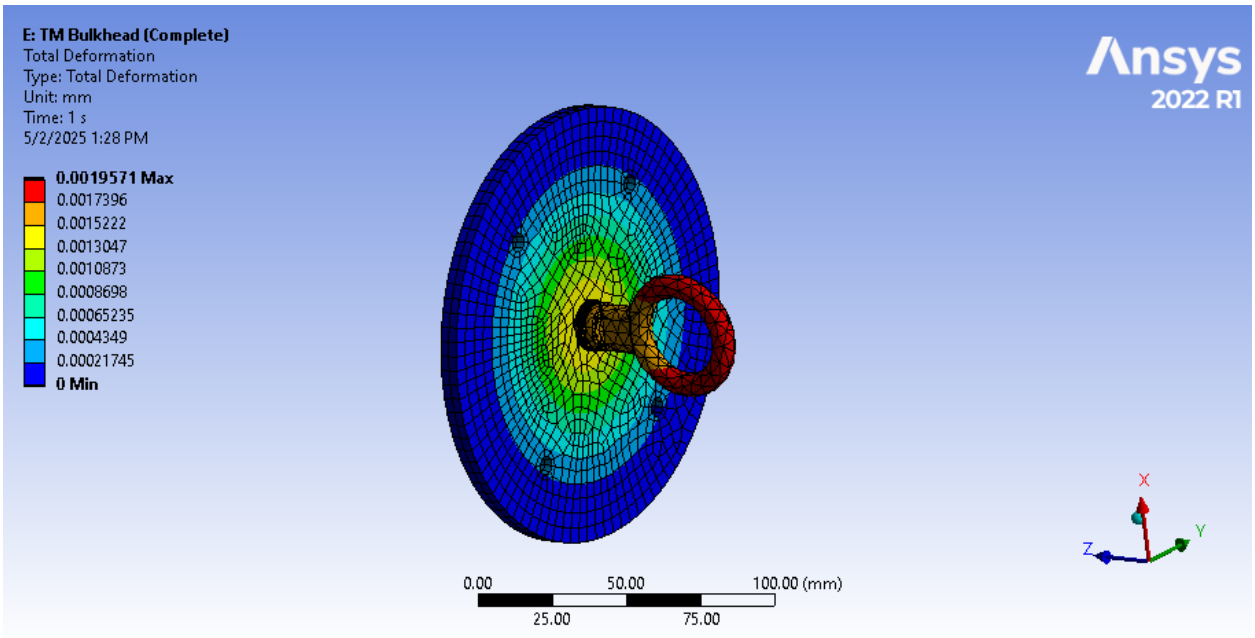

Figure 66 Total deformation of telemetry bulkhead assembly under load.

A. Upper Recovery Bulkhead Assembly

The upper recovery bulkhead assembly is responsible for connecting both the drogue and main parachutes together when ejected. This means that it is important for this portion of the vehicle to be able to withstand the ejection forces of both parachutes. The upper recovery bulkhead assembly consists of the recovery bulkhead that connects the assembly to the vehicle, three eyebolts that connect the assembly to the other portions of the vehicle via the shock cords, the ejection charge wells, and the hardware connecting the wells and eyebolts to the bulkhead. The ejection charge wells are made of carbon fiber reinforced nylon, the bulkhead is made from carbon fiber plate, and the eyebolts and hardware are assumed to be made from structural steel. The material assessments for these components are shown in Figure 67, Figure 68, Figure 69, and Figure 70.

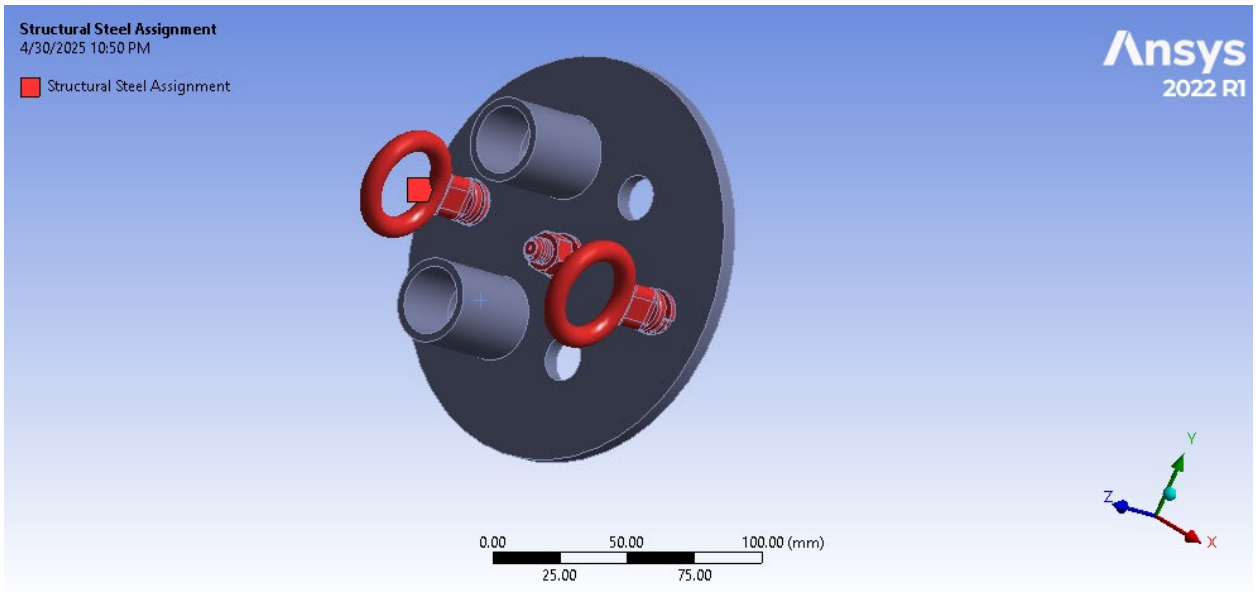

Figure 67 Structural steel material assignment of top of upper recovery bulkhead assembly.

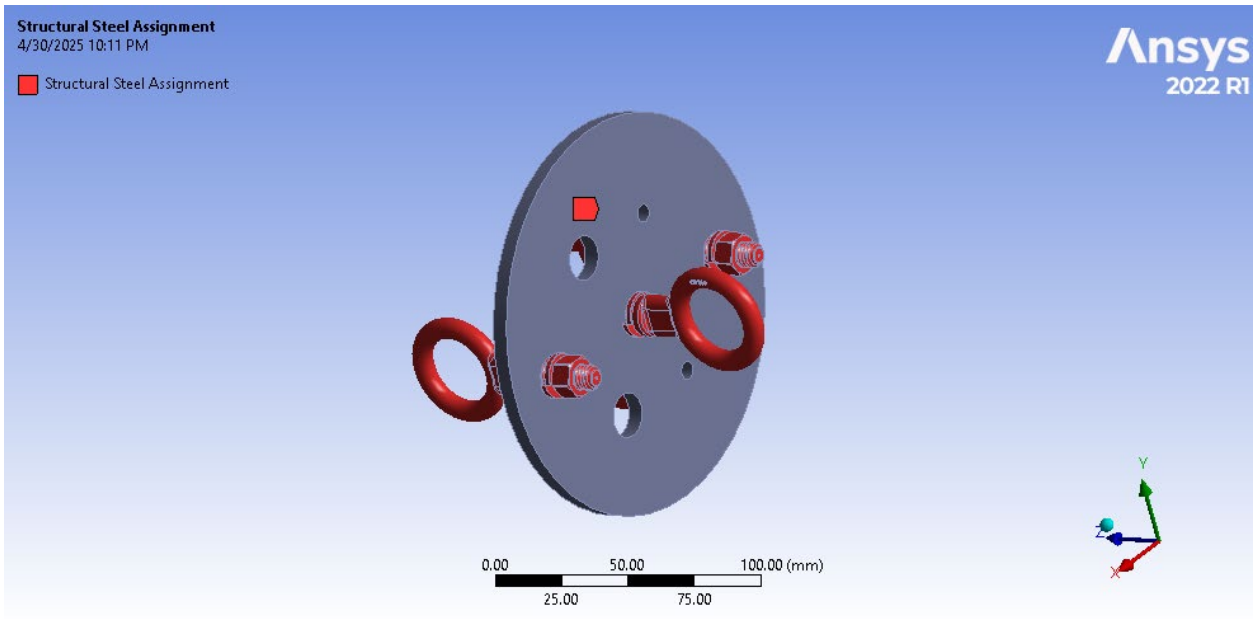

Figure 68 Structural steel material assignment of bottom of upper recovery bulkhead assembly.

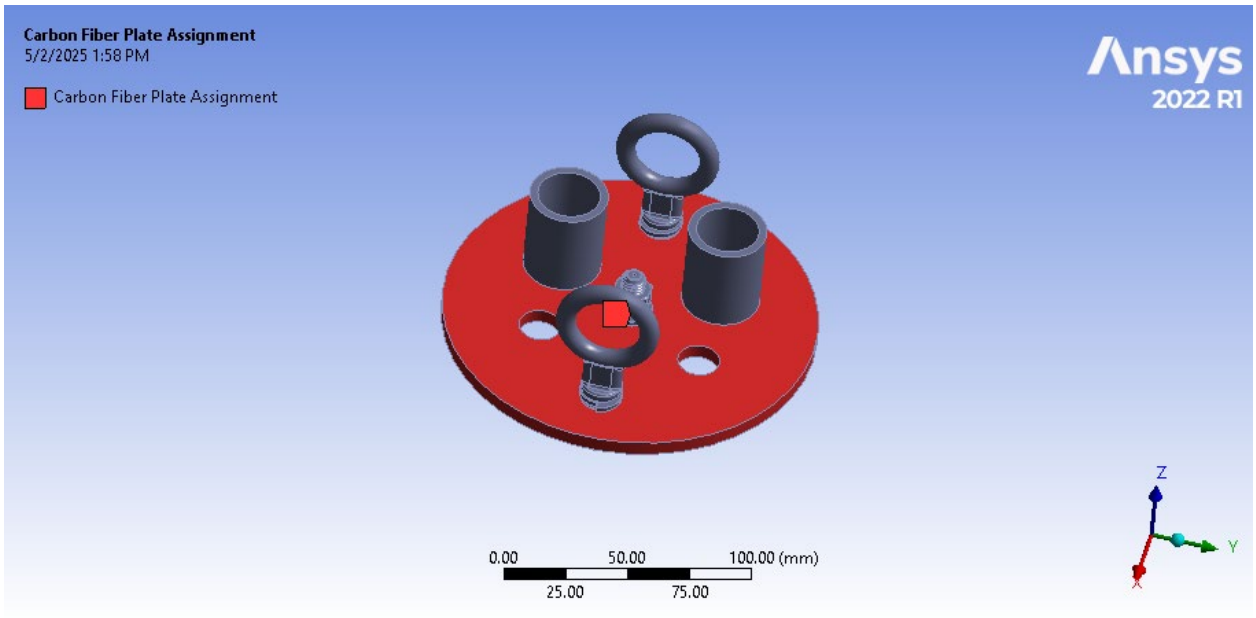

Figure 69 Carbon fiber plate material assignment of upper recovery bulkhead assembly.

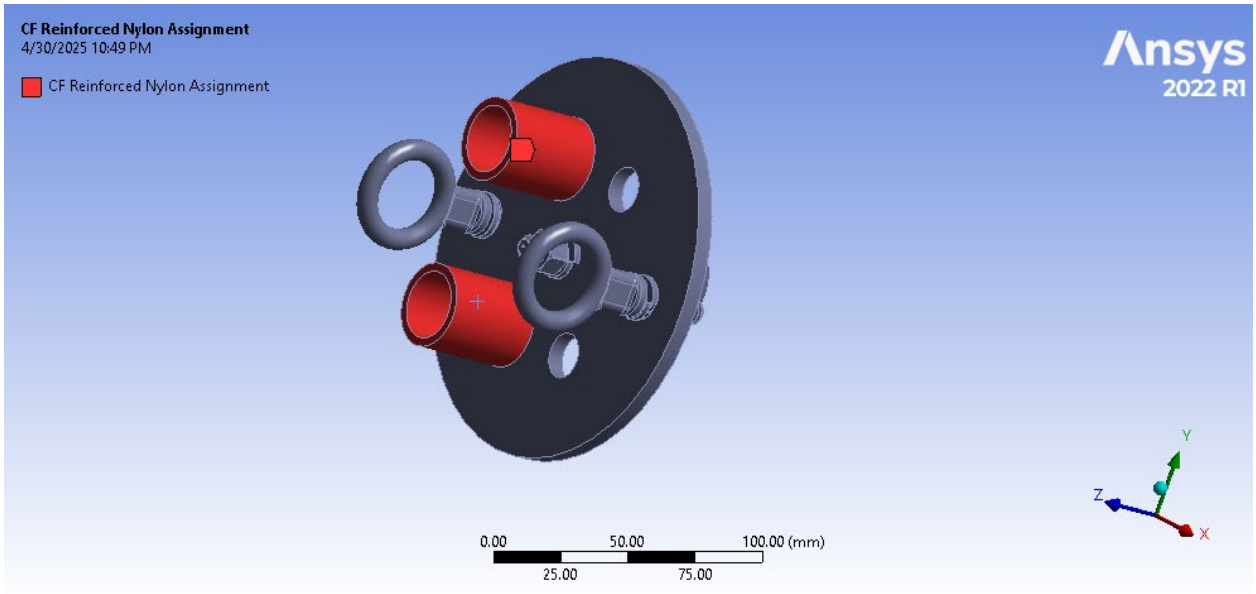

Figure 70 CF reinforced nylon material assignment of upper recovery bulkhead assembly.

For the mesh of this geometry, there were two meshes made. The washers had a body sizing mesh with an element size of 1 *mm* due to their small size, and the rest of the components used a body sizing mesh with an element size of 5 *mm.* The mesh for the geometry is shown in Mesh of upper recovery bulkhead assembly..

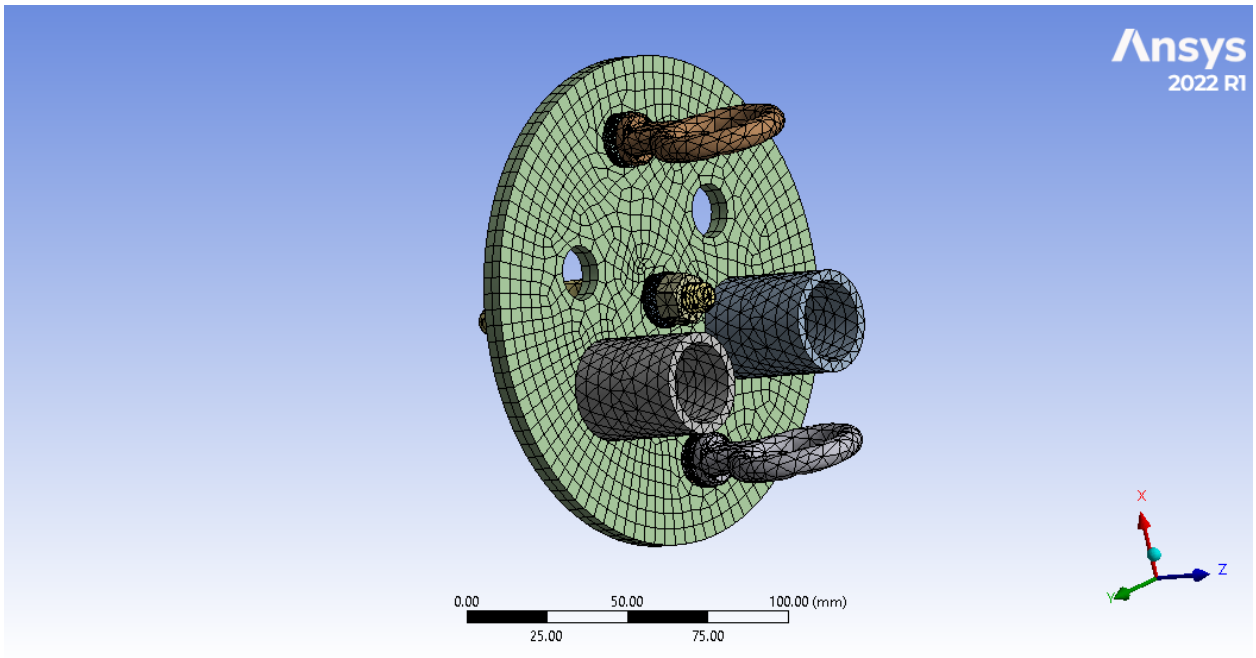

Figure 71 Mesh of upper recovery bulkhead assembly.

The outer face of the bulkhead is fixed to represent how the bulkhead is epoxied into the recovery tube. The loading is applied to each of the eyebolts to represent the surge force from ejection. The estimated surge force of 35 *N* is applied to the singular eyebolt on one side of the bulkhead. A force of 17.5 *N* is used for the eyebolts on the other side of the bulkhead because it was assumed that the surge force would be distributed equally between the two eyebolts. All forces are applied to the 'eyes' of the eyebolts and are pointed away from the bulkhead, as that is the direction that the shock cord would move and apply the surge force. This loading assumes that both parachutes would be ejected at the same time, which is not the case in practice. However, the team wanted to ensure that the upper recovery bulkhead assembly would be able to survive this hazard. The loading is shown below in Figure 72.

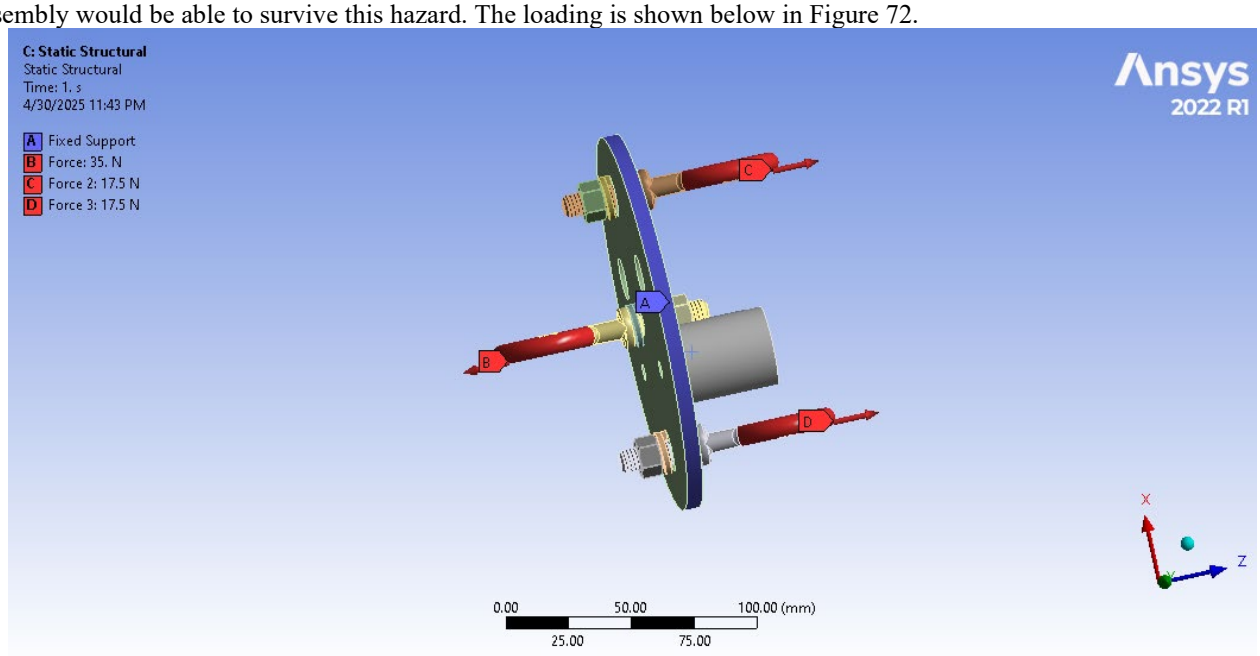

Figure 72 Loading of upper recovery bulkhead assembly

From the static structural simulation, the von Mises stresses applied to the assembly were obtained. The maximum stress was then found to be 104.19 *MPa*. While this number is high, as mentioned previously, this does not mean that the maximum stress is applied to the entirety of the assembly. As shown in Figure 73, the majority of the assembly does not experience the maximum stress, and it is concentrated around small enough areas of the assembly to where it would not have a major impact. By using the yield strengths of 250 *MPa* for structural steel, 748 *MPa* for carbon fiber plate, and 148 *MPa* for the carbon fiber reinforced nylon, the factor of safety for the structural steel components is 2.399, the factor of safety for the carbon fiber plate components is 7.28, and the factor of safety for the carbon fiber reinforced nylon components is 1.42. While these factors of safety are low, these safety factors are also for the case of extreme loading. In a launch with no hazards occurring, the parachutes will not eject at the same time and the factor of safety would be higher. Additionally, as seen in Figure 74**Error! Reference source not found.**, the maximum deformation at extreme loading is 0.042 *mm*, meaning that there would be little visible damage to the upper recovery bulkhead assembly in this case.

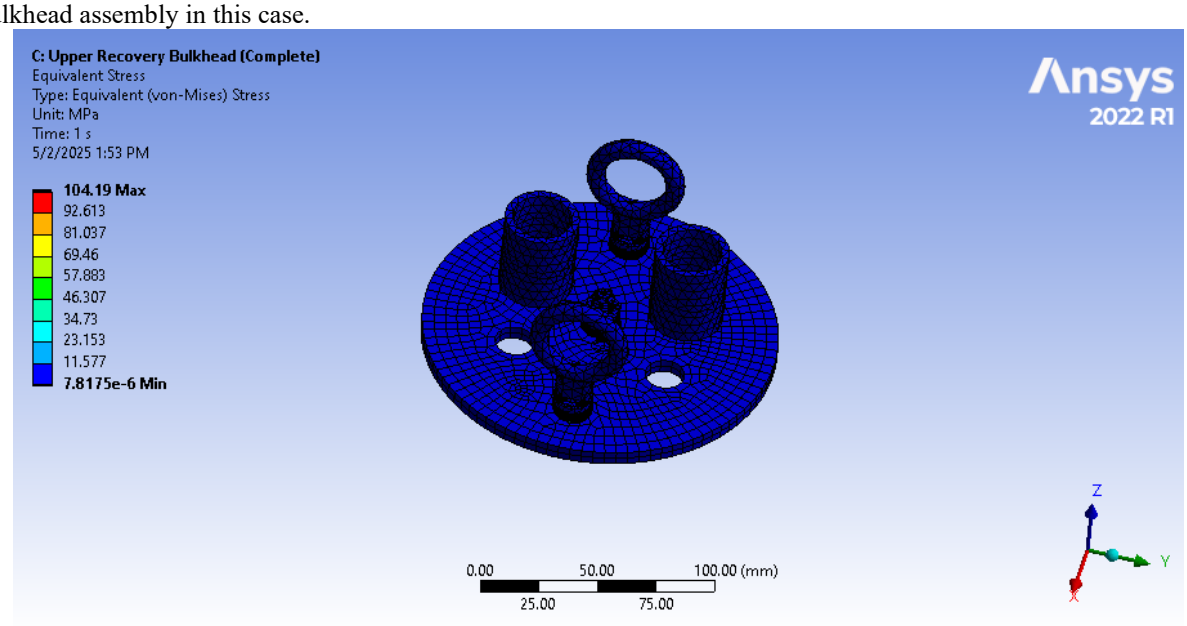

Figure 73 Von Mises stress of upper recovery bulkhead assembly under load.

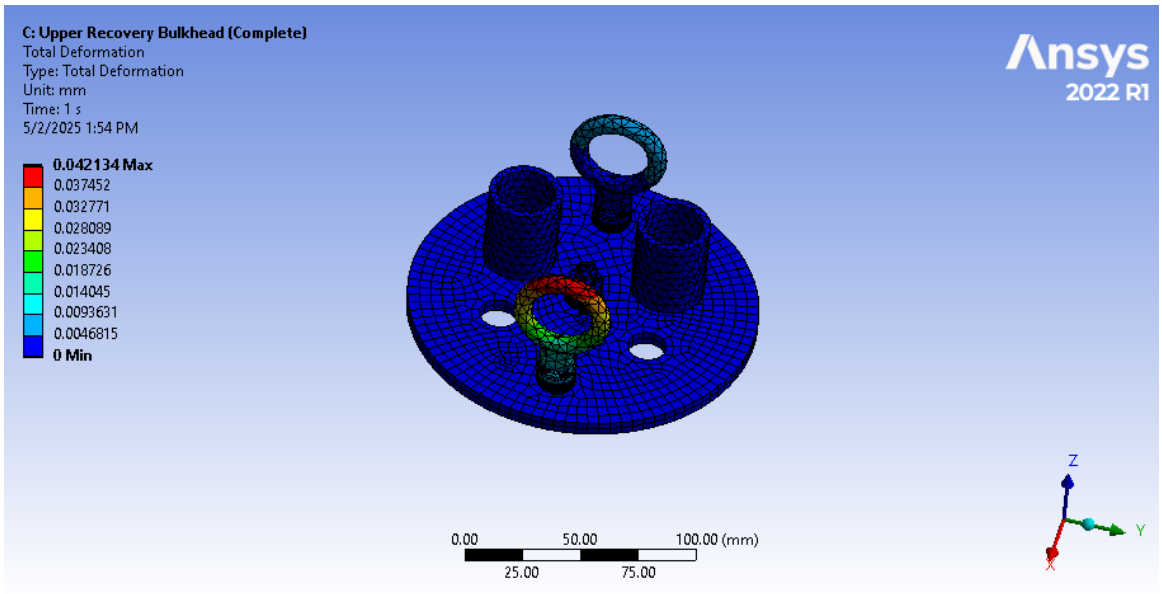

Figure 74 Deformation of upper recovery bulkhead assembly under loading.

B. *Lower Recovery Bulkhead Assembly*

The lower recovery bulkhead assembly connects the recovery systems to the lower portions of the launch vehicle and to the upper potions of the vehicle when the parachutes have been deployed via a shock cord. This assembly consists of two ejection charge wells, which are made from carbon fiber reinforced nylon, a bulkhead made from carbon fiber, and a U-bolt and its connecting hardware, which are all assumed to be made from structural steel. This assembly consists of two ejection charge wells, which are made from carbon fiber reinforced nylon, a bulkhead made from carbon fiber plate, and a U-bolt and its connecting hardware, which are all assumed to be made from structural steel. The material assessments for this simulation are shown in Figure 75, Figure 76, and Figure 77.

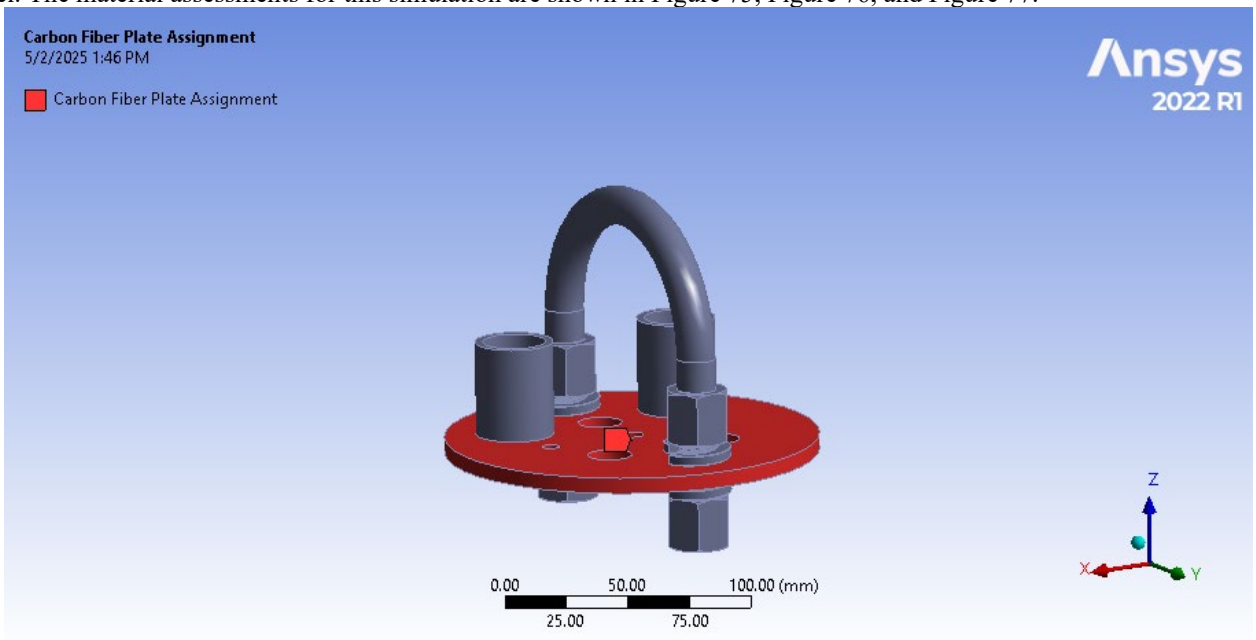

Figure 75 G10 material assignment for lower recovery bulkhead assembly.

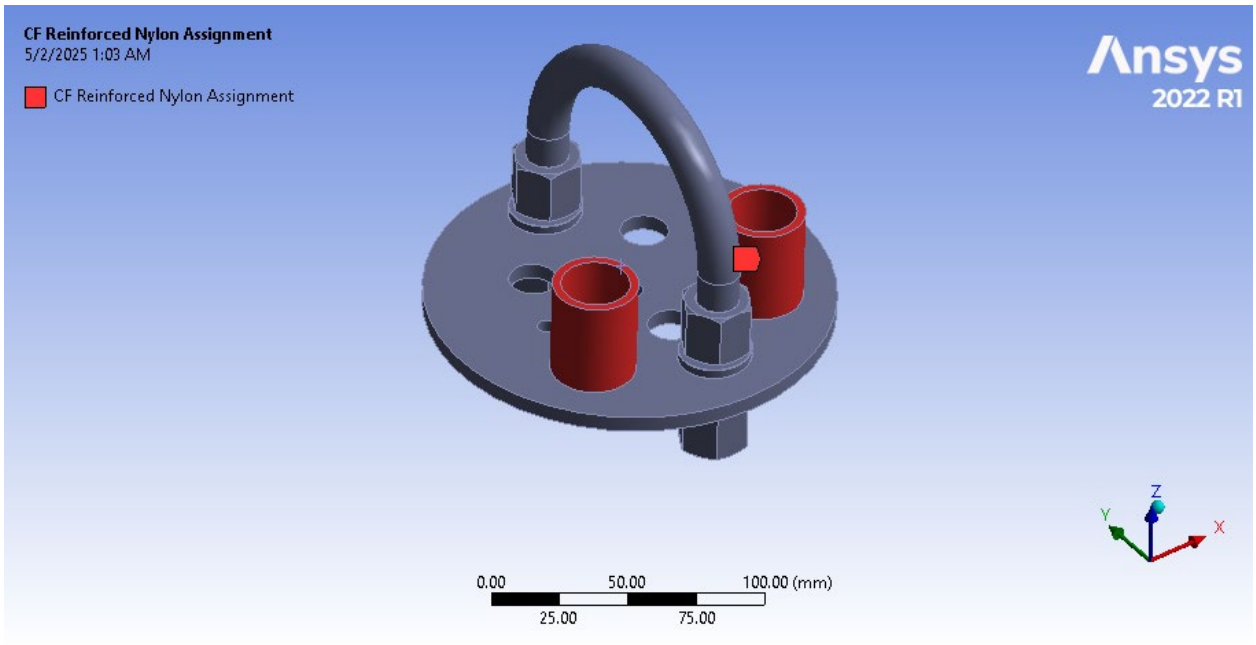

Figure 76 Carbon fiber reinforced nylon material assignment for lower recovery bulkhead assembly.

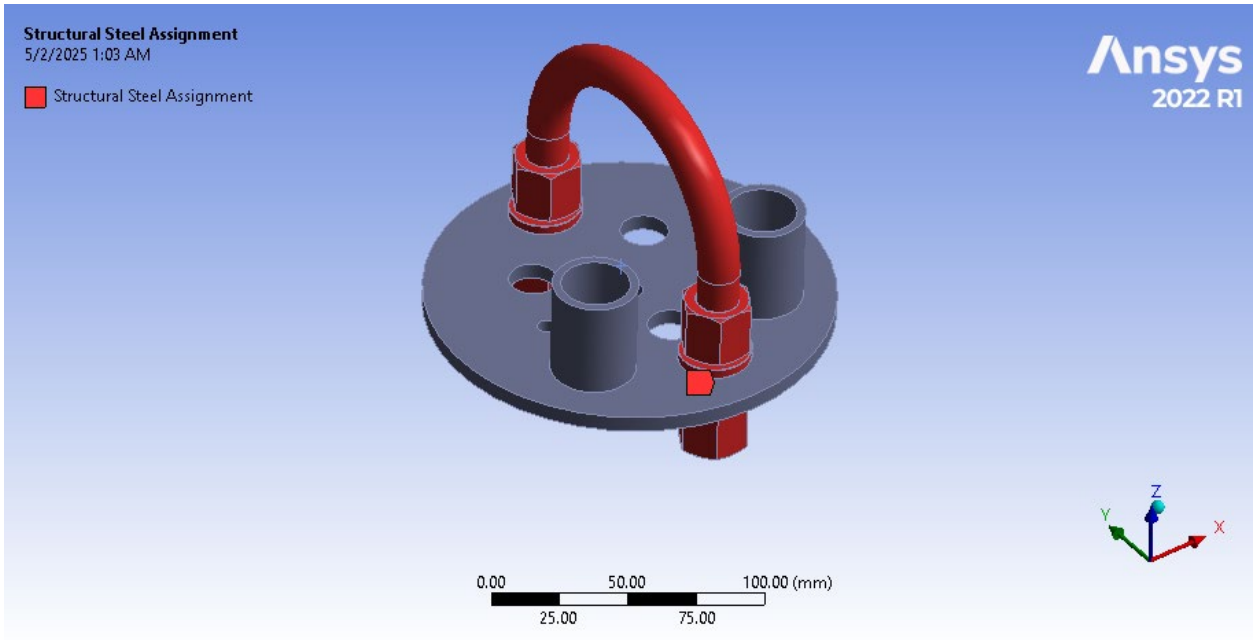

Figure 77 Structural steel material assignment for lower recovery bulkhead assembly.

For this geometry, two meshes were created. The washers required a body size mesh with an element size of 1 *mm* due to their size, while the rest of the components used a body size mesh with an element size of 5 *mm*. The mesh of the geometry is shown in Figure 78.

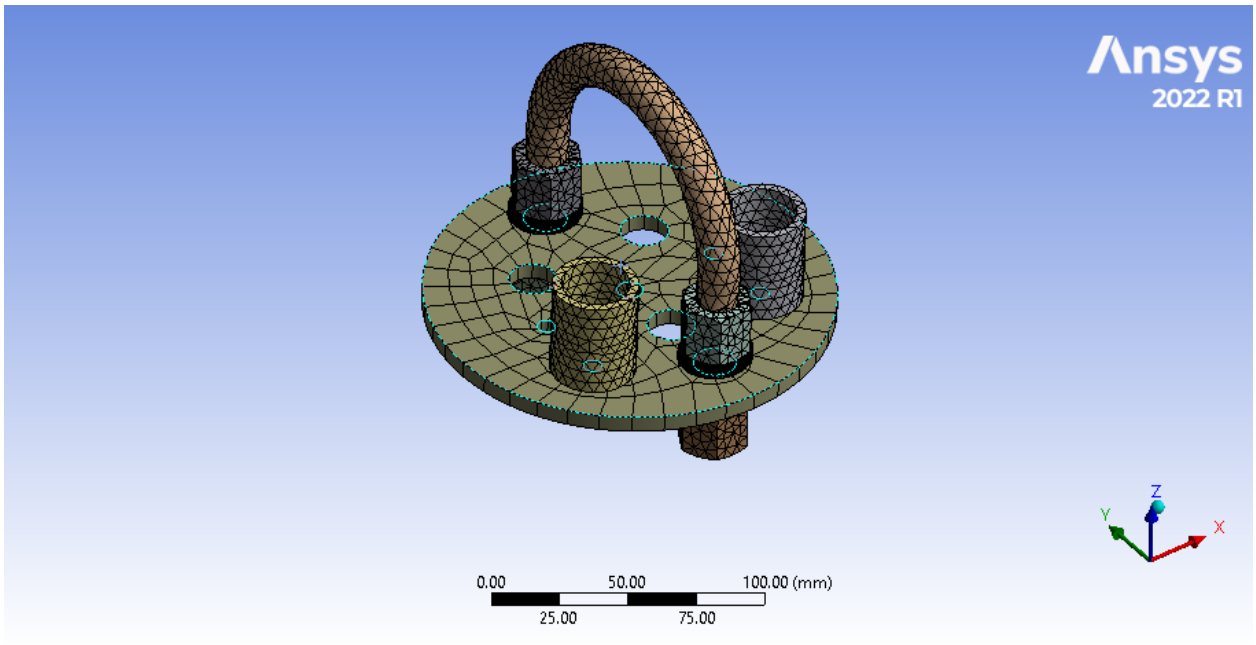

Figure 78 Finite element analysis meshing of lower recovery bulkhead.

For this assembly, the outer face of the bulkhead was fixed to represent the body tube that houses the assembly. Additionally, the inner faces of two holes in the bulkhead were fixed to represent the connection via screws to the spar system of the launch vehicle. A force of 35 *N* was applied to the U-bolt pointed away from the bulkhead to represent the surge force of the parachute. The full loading is shown in Figure 79.

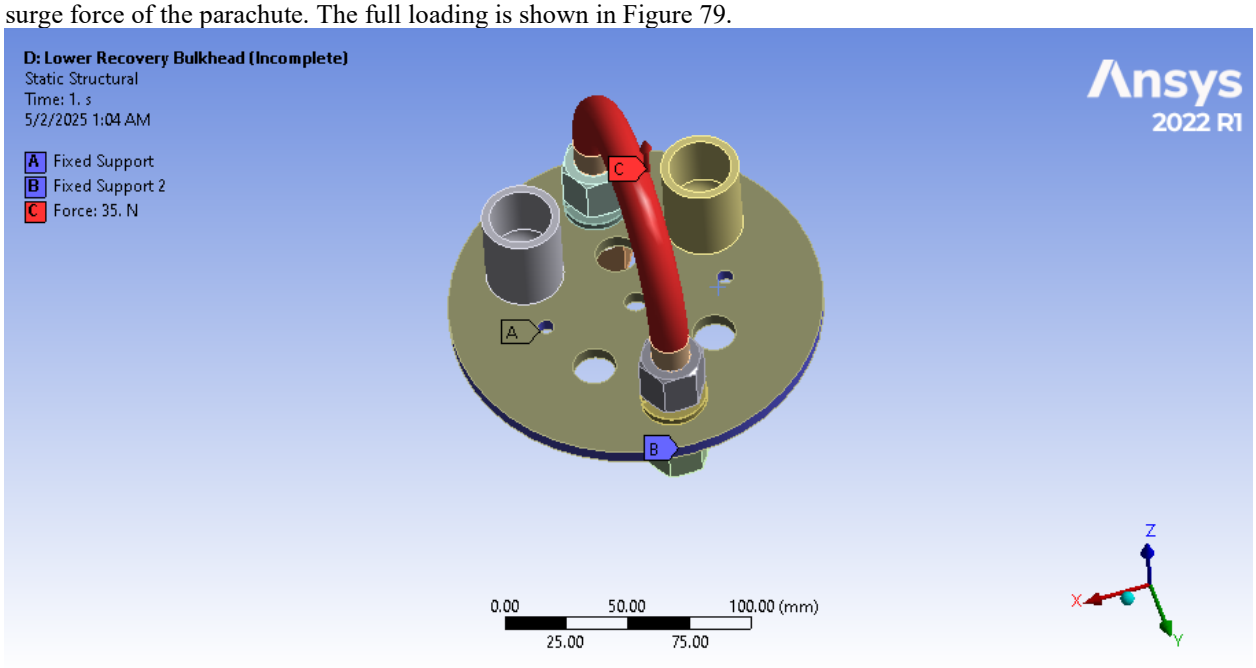

Figure 79 Applied loading of lower recovery bulkhead.

From the static structural analysis, the von Mises stress and total deformation of the system was calculated. From the von Mises stress, which is shown in Figure 80, the maximum stress that the assembly experiences is 1.703 MPa. Based on the yield strength of structural steel being 250 MPa, the yield strength of carbon fiber plate being 758 MPa, and the yield strength of carbon fiber reinforced nylon being 148 MPa, the factor of safeties for the components made

from these materials are 146.84, 445.23, and 86.93, meaning that the design of this system would be able to withstand the forces of deployment and would be able to easily relaunch after being recovered. Additionally, Figure 81 shows that the maximum deformation on this assembly is 0.00025 *mm*, which shows that there would be no noticeable damage to this assembly due to parachute deployment.

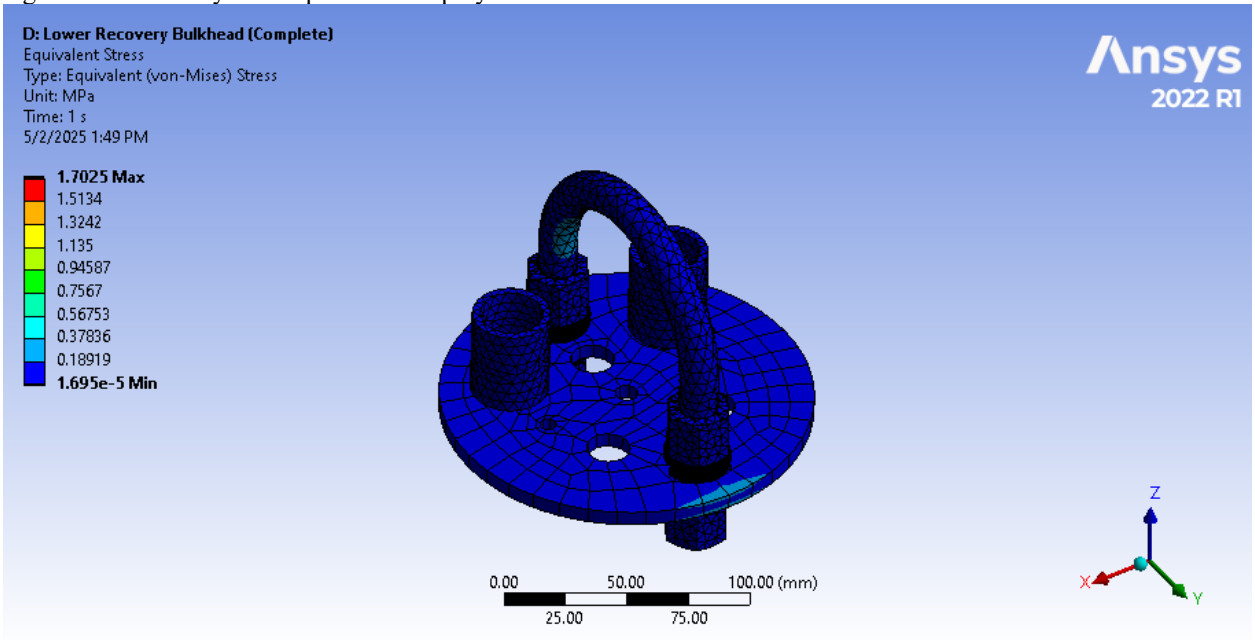

Figure 80 Von-Mises stress of lower recovery bulkhead assembly under load.

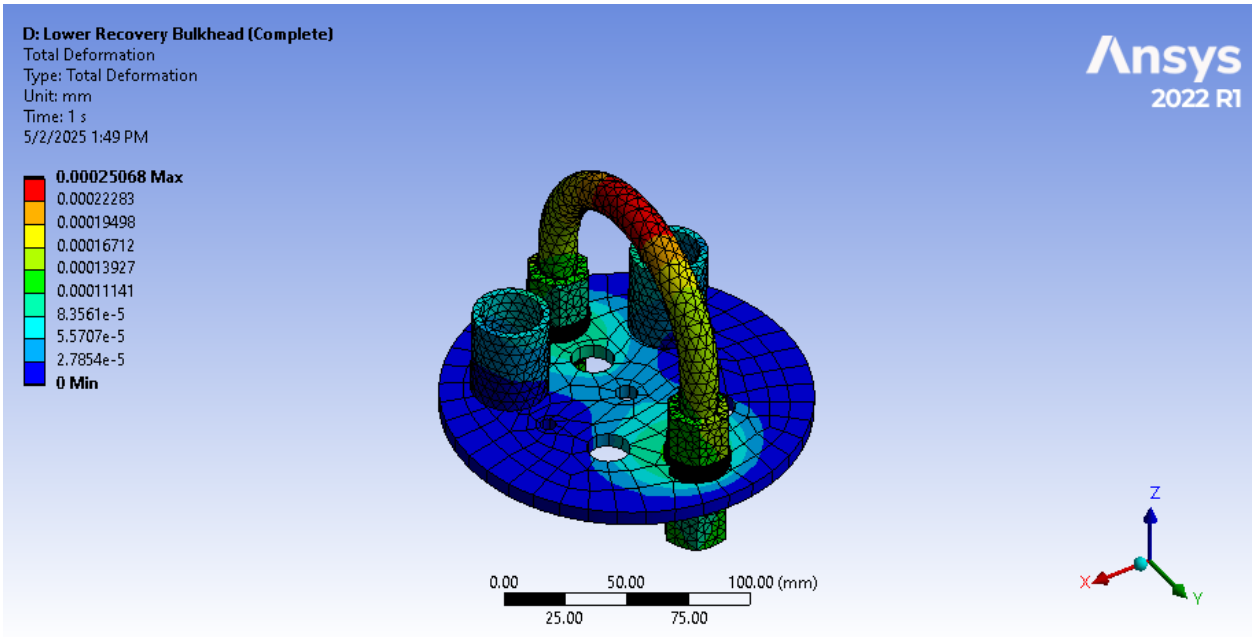

Figure 81 Deformation of lower recovery bulkhead assembly under load.

C. Bottom Motor Bulkhead

The bottom motor bulkhead is responsible for connecting the bottom of the motor tube to the boat tail of the rocket and helping to center the inner motor tube. It is made from carbon fiber plate and uses a body sizing mesh with an element size of 5 *mm*. The mesh of this component is shown below in Figure 82.

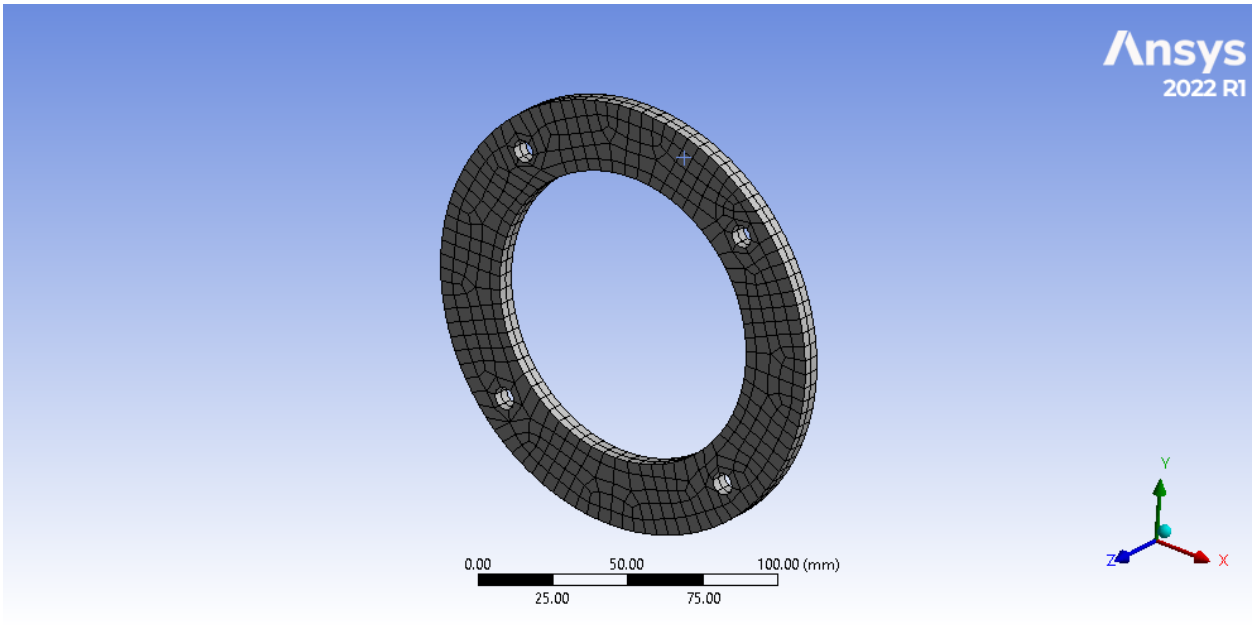

Figure 82 Finite element analysis mesh of bottom motor bulkhead.

The bulkhead was fixed on both its inner and outer faces to represent where the bulkhead is epoxied to the motor tube and inner motor tube. A force of 4293 *N* was applied to the internal face of the bulkhead pointed into the face. This number comes from the maximum thrust of the motor multiplied by a factor of 1.5. The loading of the component is shown in Figure 83.

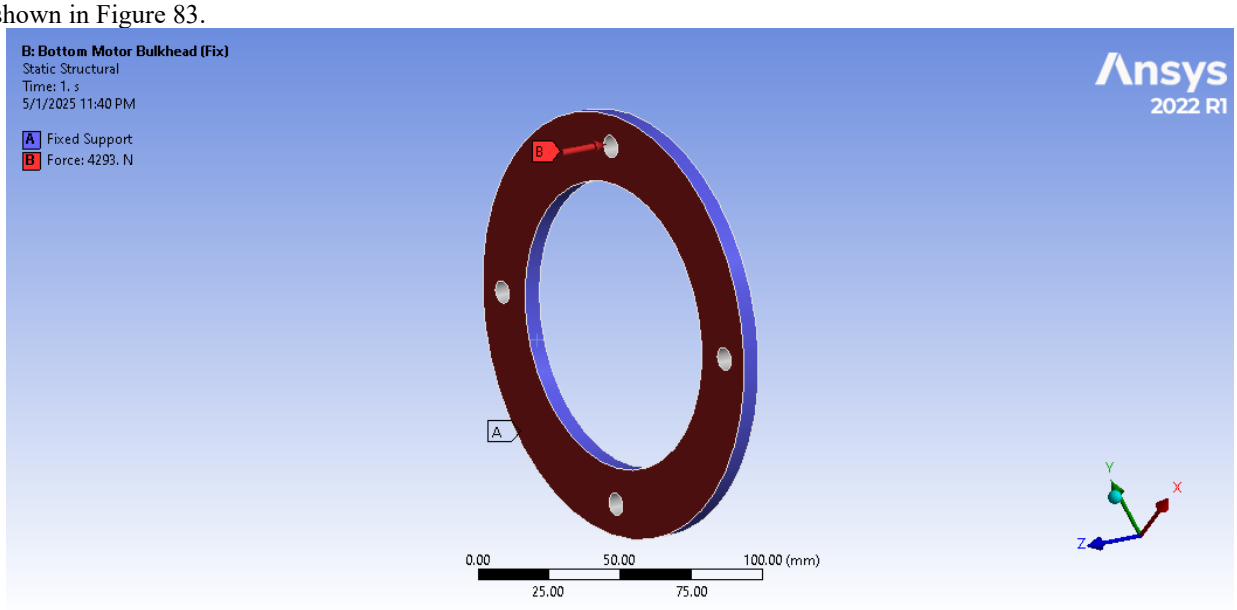

Figure 83 Applied loading parameters for bottom motor bulkhead.

Using ANSYS Mechanical, the von-Mises stress and total deformation were calculated, which are shown in Figure 84 and Figure 85, respectively. From this, it can be found that the maximum stress that would be applied to the bulkhead would be 3.35 MPa. From the yield strength of carbon fiber plate, which is 758 MPa, this leads to the component having a factor of safety of 226.42. This shows that the design of the bottom motor bulkhead is robust and would be able to withstand the launch of the vehicle easily. Additionally, the maximum deformation was found to be 0.00033 *mm*, which shows that there would be minimal damage to this component.

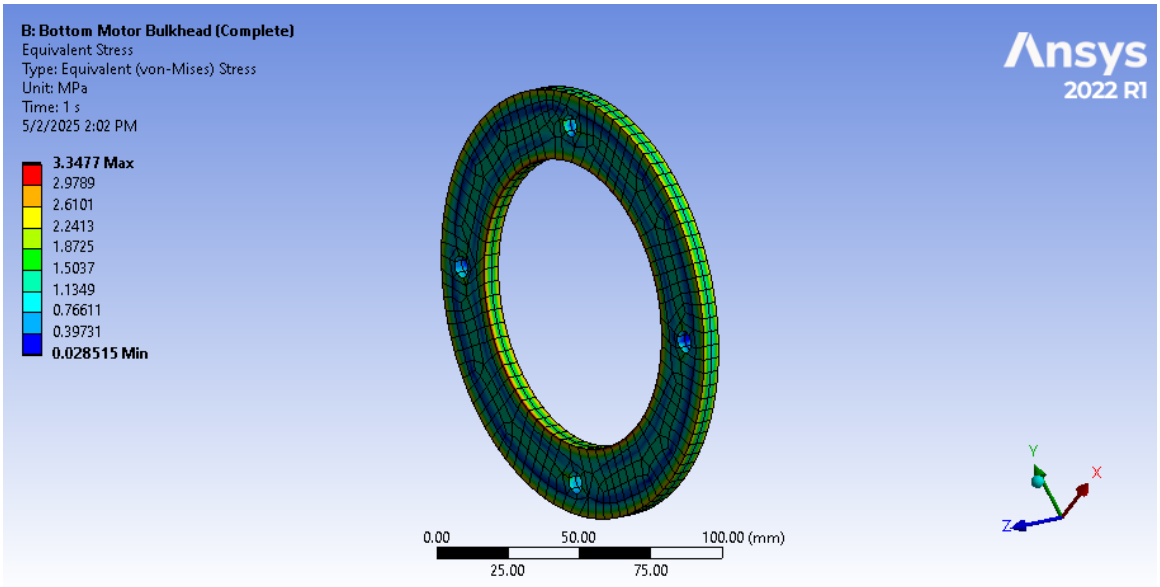

Figure 84 Von-Mises stress of bottom motor bulkhead under load.

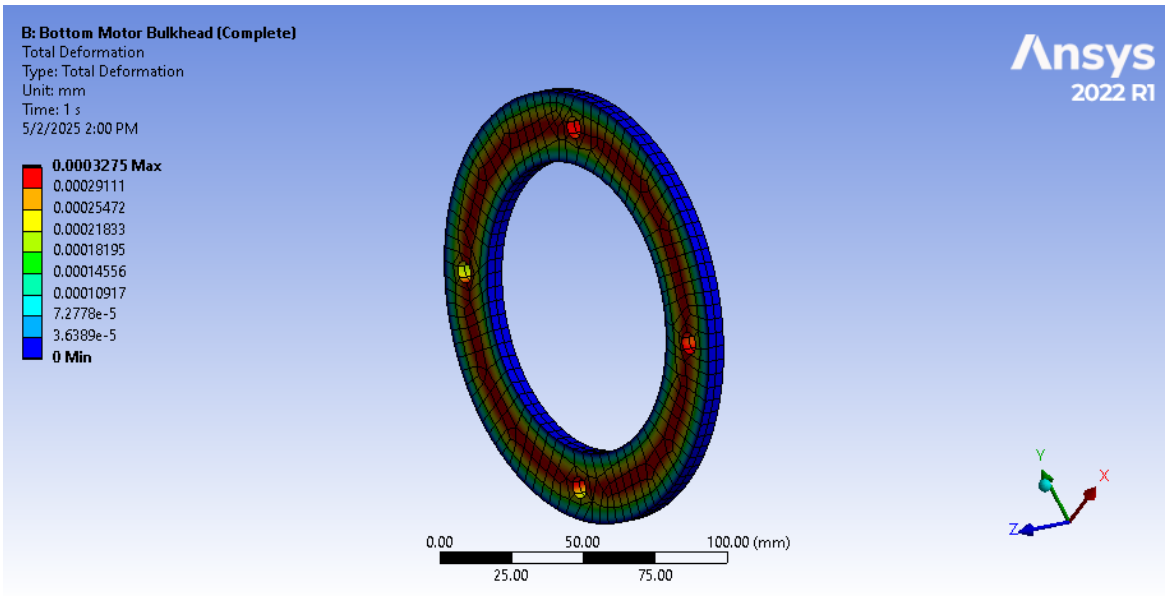

Figure 85 Deformation of bottom motor bulkhead under load.

5. *Centering Ring*

The centering rings are used to hold the fins into place and to center the motor within the motor tube. They were modeled to verify that they would withstand the force of the motor during the launch of the vehicle. Within ANSYS Mechanical, a static structural system was created with the motor fin tab ring model imported as the geometry. For this model, the only material used was carbon fiber plate. For the mesh of the geometry, a body sizing mesh with an element size of 5 *mm* was created. This mesh is shown in Figure 86 below.

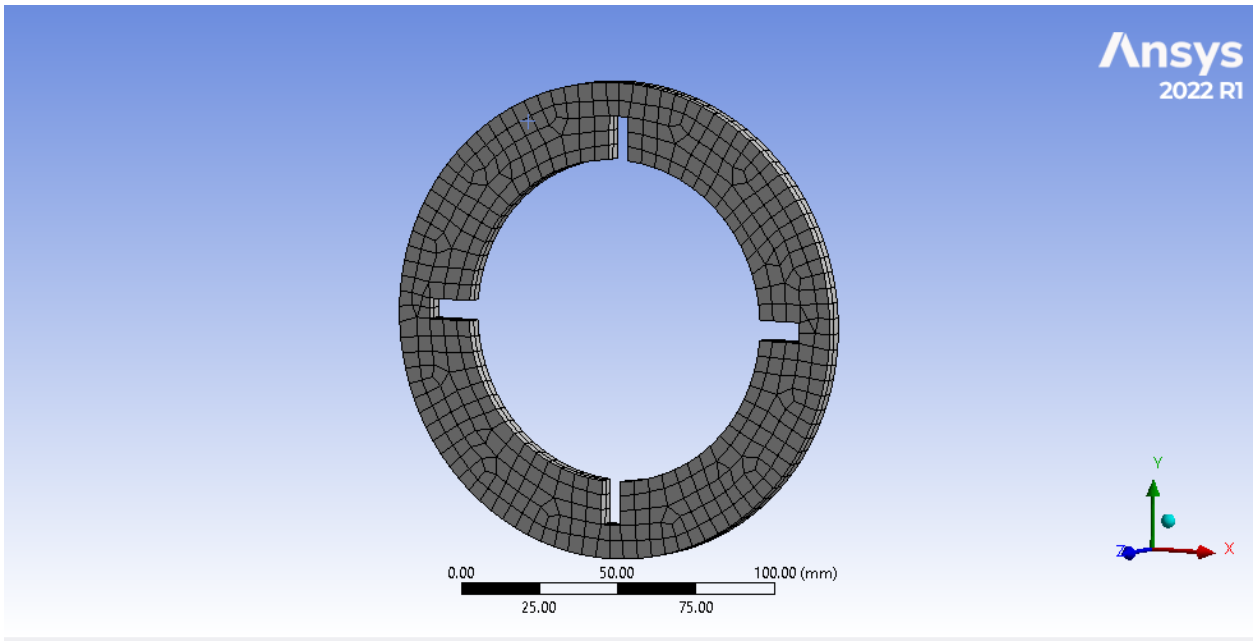

Figure 86 Finite element analysis mesh of centering ring.

The component was fixed on its outer and inner faces to represent the part being epoxied into the motor tube and onto the inner motor tube. On the internal face of each of the fin tab slots, a force of 1073.25 *N* was applied perpendicular to this face to represent the shear force due to the motor. This location was selected as this was determined to be the weakest point within the component. This force was selected based on scaling the maximum thrust of the motor by a factor of 1.5. This number was then divided by four because it was assumed that the component would divide the force equally between the four weak points. The full loading of the model is shown in Figure 87 below.

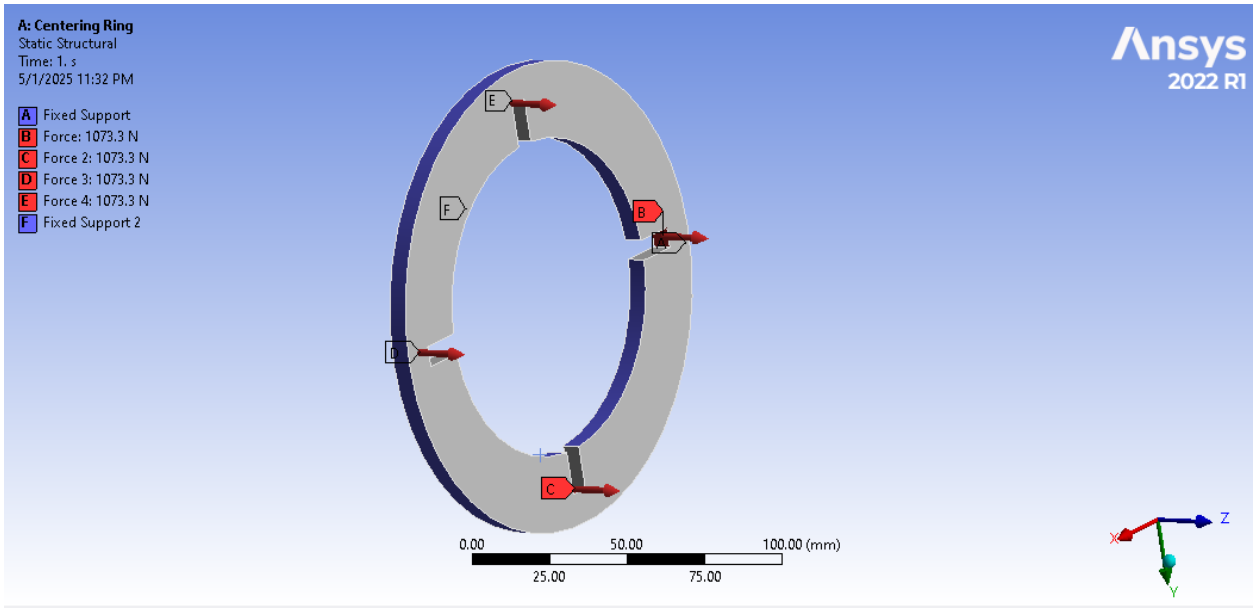

Figure 87 Applied loading parameters of centering ring.

From this study, the total deformation and von-Mises stresses were calculated in Figure 89. The maximum stress that the component will undergo was simulated to be 79.287 *MPa*. Based on the yield stress of 758 *MPa* for carbon fiber plate, this leads to a factor of safety of 9.56 for this component. This proves that the motor fin tab rings would

withstand the thrust of the motor, meaning that they are robust enough for launch. Additionally, the maximum deflection that the rings will undergo is 0.0086 *mm*, as determined in Figure 88, which is at the corners surrounding the fin tab slots. This is a non-issue and shows that the component will not undergo major damage in the launch. The deflection and Von-Mises stress of the applied loading is shown in Figure 89 with a true deformation scale.

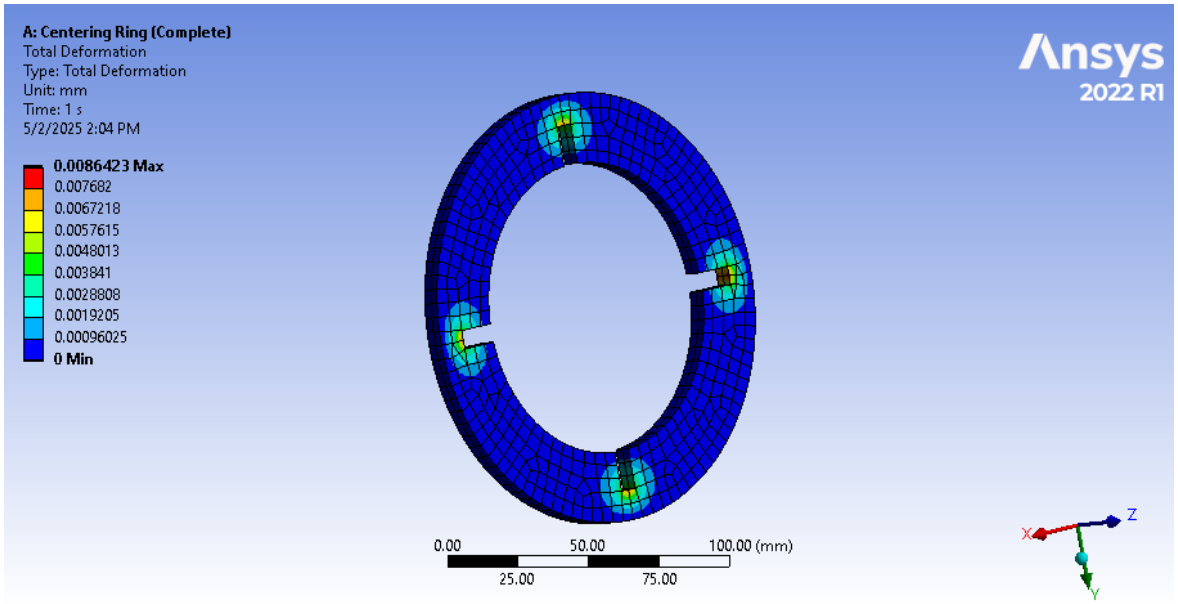

Figure 88 Deformation of centering ring under load.

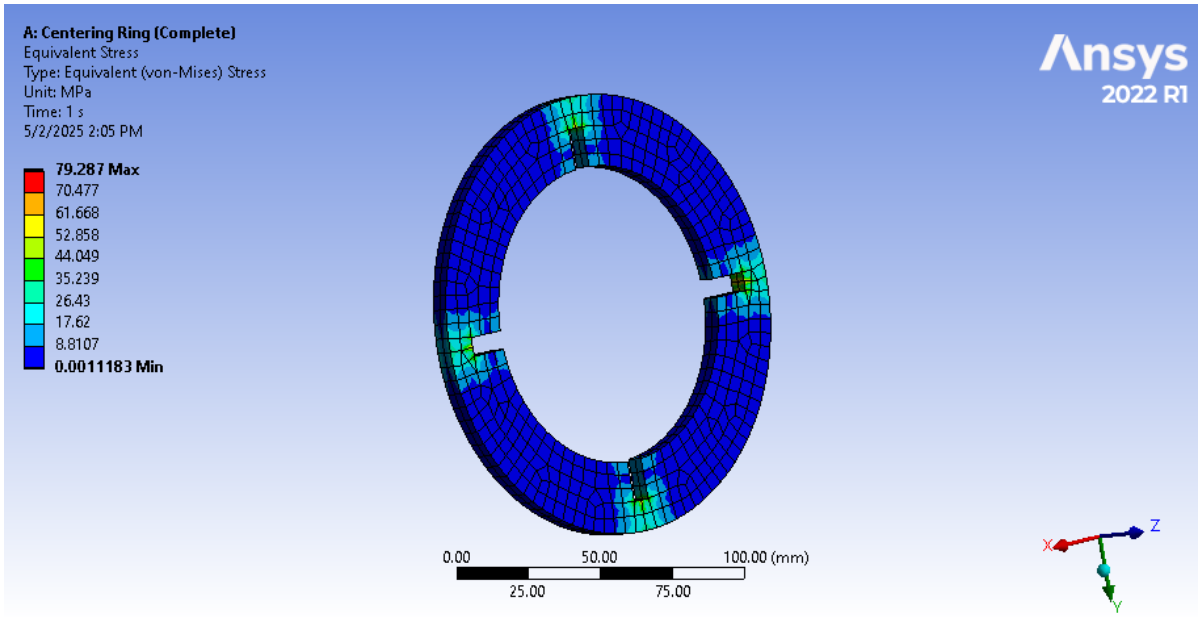

Figure 89 Von-Mises stress of centering ring under load.

Appendix D: Hazard Analysis

Appendix D: Hazard Analysis offers an in-depth examination of potential hazards associated with the project, focusing on aspects such as hazardous material handling, transportation, and storage of propellants, among other safety-critical design components. This analysis is designed to ensure the safety of all operating personnel by meticulously detailing the risks involved and presenting effective mitigation strategies for each identified hazard. By methodically addressing both procedural and design-related safety issues, this appendix aims to minimize risks and enhance overall operational safety, adhering to regulatory compliance and engineering best practices. Our hazard matrix can be seen in Table 7, below.

Table 7 Hazard analysis of project Pocket Tens.

Team 21	**We'll 'C' What Happens**			**5/10/2024**
Hazard	**Possible Causes**	**Risk of Mishap and Rationale**	**Mitigation Approach**	**Risk of Injury after Mitigation**
Epoxy lands in eyes, on skin, or is ingested during manufacturing process	Improper Eye Protection	Medium; Large amounts of epoxy are used throughout manufacturing process, so proper PPE is a must	High attention detail and strict enforcement of PPE measures while handling epoxy resin or hardener	Low.
	Improper glove and lab coat skin coverage			
	Improper face and respirator use			
Explosion of solid-propellant rocket motor during launch with blast or flying debris causing injury	Motor end closures fail to hold	Medium; Visual inspections are the most that can be done, but there may be subsurface cracking that can only be detected with ultrasound.	Inspect grains and ensure they are in proper condition.	Low.
	Motor case unable to contain normal operating pressure		Inspect motor case for damage during final assembly before launch	
	Cracks in propellant grain		Only essential personnel in launch crew will be a minimum 500 feet from rocket at launch, in abidance with TRA guidelines. However, ESRA has a system for personnel to be 2000 feet, decreasing possibility of injury by a factor of 16.	
Vehicle deviates from nominal flight path, intercepts personnel at high speed	Under stable vehicle steering into high wind as it departs from rail	Medium; Payload weighed less than expected during test launch.	Weight has been added to the payload to ensure a stable flight.	Low.
	Over stable vehicle tipping over as it departs from rail		Refrain from launching in winds exceeding 20 *mph*, but design launch vehicle to remain nominal in winds above this limit	

	Coupler failure on motor ignition		Aero-structures have been checked for any crack propagation and replaced as necessary.	
Recovery system fails to deploy, vehicle or payload comes in contact with personnel at an excessive speed	Recovery Systems overheat.	Medium; while battery drain tests have been performed high heat can cause lack of hardware and power function	Thermal protection via deployment bag.	Low.
	Power malfunction.		Ensure recovery systems are flight tested and successful.	
	Wet black powder.		Follow proper checklists, ensuring all steps are followed.	
Recovery system partially deploys, launch vehicle comes in contact with personnel	Recovery Systems overheat.	High; due to previous launches not including in-depth checklists, drogue or main non-deployment has occurred.	Thermal protection via deployment bag.	Medium.
	Power malfunction.		Ensure recovery systems are flight tested and successful.	
	Wet black powder.		Follow proper checklists, ensuring all steps are followed.	
Black powder charges prematurely ignite outside the launch vehicle.	Improper handling of black powder	Low; black powder is stored and transported in airtight, AC-controlled locations. Black powder is only handled by experienced personnel.	Ensure black powder is storage container is correctly sealed.	Low.
	Improper storage of black powder		Ensure black powder is secured during transportation.	
Black powder charges prematurely ignite inside the vehicle.	Improper handling of black powder	Medium; High heat may cause electronic failure or other hazards. Yanking of e-matches can cause premature activation.	Ensure black powder is storage container is correctly sealed.	Low.
	Improper storage of black powder		Ensure cautious handling of e-matches.	
	E-Matches prematurely go off.		Ensure following of proper checklists.	
Rocket motor does not ignite when given command, but ignites during investigation.	Delay of e-match signal.	Medium; risk of accident can always occur.	Proceed with extra caution when approaching a failed motor ignition.	Medium.
			Wait minute after attempted motor ignition, as required by TRA guidelines.	

			Encourage competition officials to maintain proper handling of their Wilson FX system which has a double relay safety mechanism.	
Recovery system deploys during assembly or prelaunch, causing injury.	Flight computers are prematurely powered and engage.	Medium; Due to the nature of black powder and energetics, danger is always there.	Ensure electronics bay does not stop beeping.	Low
	E-match prematurely activated, causing deployment.		Independent switches for flight computer power on and arming charges.	
			Provide enough slack in e-matches and do not pull on them.	

Appendix E: Risk Assessment

Appendix E: Risk Assessment provides a comprehensive overview of the risks and reliability concerns pertinent to the mission. This section meticulously catalogs all identified failure modes that could jeopardize mission success. It presents these in a structured matrix aligned with the mission phases outlined by the CONOPS. A detailed mitigation strategy is elaborated for each risk identified, addressing potential issues through specific process improvements and design modifications. This appendix aims to ensure that participants are fully informed of the potential challenges and the proactive measures to mitigate these risks, thereby enhancing the project's overall reliability and success rate. The values for likelihood are dependent on historical data of all teams flying at the SAC. The varying levels of likelihood and impact can be seen in Table 5 Risk Level Designation.

Table 5 8**Risk level designations.**

Level	Likelihood	Impact
1	Minimal Chance (1-2%)	No effect on the mission
2	Possible (2-5%)	Minor impact on technical performance
3	Probable (5-10%)	Affects mission success
4	Highly Possible (10-20%)	Significant risk to mission critical systems
5	Definite Chance (>20%)	Human Risk

Table 69able 6 presents a detailed Risk Assessment for the project. It outlines the potential failure modes of various components and systems, their effects, inherent risk levels, and the respective mitigation plans to reduce these risks. Each entry in the table identifies a specific potential failure, describes the possible consequences of such a failure, assesses the risk in terms of likelihood and impact, and details the actions taken to mitigate the risk to more manageable levels. The mitigation strategies encompass procedural adjustments, enhanced manufacturing practices, rigorous testing, and quality control measures. This structured approach ensures that risks are systematically identified, assessed, and mitigated to support the stability and safety of the project. The table also illustrates the effectiveness of the mitigation strategies by comparing initial and mitigated risk levels, thereby highlighting the tangible benefits of the risk management processes employed.

Table 69 Risk assessment table for Pocket Tens.

Potential Failure Mode	Potential Effects of Failure	Risk Levels	Mitigation Plan	Mitigated Risk
Improperly cut Body Tube	Higher Drag, non-rigid body joints	Likelihood: 2 Impact: 1	Sanding of Body Tube edges, smooth surface finish	Likelihood: 1 Impact: 1
Crack propagation from holes in airframe	Loss of rigidity in body tube, structural failure of body tube	Likelihood: 2 Impact: 2	Reinforce holes with epoxy	Likelihood: 1 Impact: 2
Improperly secured fins	Loss of fin, catastrophic loss of vehicle	Likelihood: 3 Impact: 4	High attention to detail throughout manufacturing process, through-wall and tip to tip layup	Likelihood: 2 Impact: 4
Improperly secured bulkheads	Shift of Avionics or Payload, loss of stability	Likelihood: 3 Impact: 2	High attention to detail, testing of each bulkhead	Likelihood: 1 Impact: 1
Fins bent or damaged	Erratic flight behavior	Likelihood: 4 Impact: 3	Use of fin jig and level, and careful storage during transport. Fin covers made from pool noodles to protect tips.	Likelihood: 2 Impact: 3

Centering Rings out of alignment	Erratic flight behavior	Likelihood: 3 Impact: 2	Quality control of manufactured angles during construction. Verification of proper alignment with test flight.	Likelihood: 1 Impact: 2
Improperly secured Camera Shroud	Increased Drag, loss of shroud	Likelihood: 3 Impact: 1	Ensure proper bolted connection between body surface and camera shroud	Likelihood: 2 Impact: 1
Avionics wires caught or snagged during integration	Damage to avionics systems	Likelihood: 4 Impact: 1	Use of integration lists and visual inspection throughout integration process. Ensure properly lacked wire runs and quick connectors.	Likelihood: 2 Impact: 1
Payload detaches during descent	Loss or damage to payload	Likelihood: 2 Impact: 1	Flight tested to ensure connection.	Likelihood: 1 Impact: 1
Motor retention fails	Motor falls out of vehicle after boost	Likelihood: 2 Impact: 3	Secure forward and aft retention with epoxy and screws, forward eye bolt fully screwed in	Likelihood: 1 Impact: 3
Drogue parachute becomes entangled	Higher than expected descent velocity	Likelihood: 1 Impact: 2	Careful packing of drogue parachute, deploy main parachute prior to excessive velocity and flight test the software.	Likelihood: 1 Impact: 2
Main parachute fails to fully deploy	Higher than expected descent velocity	Likelihood: 4 Impact: 3	Careful packing of main parachute using properly stored packing bag, checklist of line connections	Likelihood: 3 Impact: 2
Main parachute deploys at apogee	Excessive drift of vehicle	Likelihood: 4 Impact: 1	Careful packing of main parachute, ejection testing, testing of shear pins. Ensure properly sized ejection charges to prevent hammering. Perform realistic ground tests followed by flight tests.	Likelihood: 3 Impact: 1
Arming switch fails and a flight computer turns off.	Minor loss of data, due to two other redundant flight computers.	Likelihood: 2 Impact: 1	Ensure switches are fully armed in place and are connected to avionics bay correctly.	Likelihood: 1 Impact: 1
Recovery Systems Overheat on the Pad.	Potential loss of vehicle, no chute deployment.	Likelihood: 3 Impact: 4	Ensure recovery systems are flight tested and there is temperature mitigating finish to the vehicle. Arrive and launch early.	Likelihood: 2 Impact: 3

Loss of GPS signal from trackers within vehicle during flight.	Potential loss of vehicle.	Likelihood: 3 Impact: 3	Dual redundancy of trackers, eliminating single point of failure. Monitor battery voltage of GPS throughout preflight and launch. Use of RF transparent materials in line of the antenna's toroidal propagation pattern. Screen record phone GPS interface during flight to record path of vehicle throughout flight. Use easily distinguishable colors to increase vehicle's visual footprint on landing	Likelihood: 1 Impact: 2
No ignition from e-match charges.	No motor ignition.	Likelihood: 3 Impact: 3	Ensure e-matches are correctly attached. Follow pre-launch checklists.	Likelihood: 2 Impact: 2
Premature motor ignition.	Potential motor explosion and human injury.	Likelihood: 2 Impact: 5	Ensure e-matches are correctly attached. Follow pre-launch checklists. Coordinate with ESRA Solid PAS personnel to ensure the Wilson FX is disarmed prior to installing igniter.	Likelihood: 1 Impact: 4
Parachute deploys at motor burnout.	Destruction of vehicle.	Likelihood: 1 Impact: 4	Ensure Avionics correctly detects apogee, using applicable filters and delays Ensure barometric holes are properly sized and positioned. Ensure forward retainer on motor is secure. Avionics are flight tested.	Likelihood: 1 Impact:3
Motor fails to burn all fuel during lift-off.	Potential failure to apogee.	Likelihood: 3 Impact: 2	Ensure COTS motor is structurally sound and grain is good.	Likelihood: 2 Impact: 2
Vehicle rail guide breaks during ignition.	Potential human risk and vehicle deviation.	Likelihood: 4 Impact: 5	Ensure rail guide is properly installed and follow preflight checklists. Ensure rail and rail guide are properly aligned before launch.	Likelihood: 2 Impact: 4
Motor does not produce enough thrust for lift-off.	Potential failure to apogee or	Likelihood: 2 Impact: 3	Ensure COTS motor is structurally sound and grain is good. Ensure	Likelihood: 1 Impact: 2

	failure to launch.		motor simulations are correct. Use a trusted motor vendor and a certified M-class motor.	
Vehicle deviates from nominal flight path.	Potential human risk.	Likelihood: 4 Impact: 5	Ensure rail is properly fastened and follow preflight checklists. Angle rails away from flight line and in accordance with TRA guidelines.	Likelihood: 2 Impact: 3
Trailer involved in crash.	Potential human risk. Potential risk to launch vehicle.	Likelihood: 3 Impact: 5	Ensure to travel with a diverse Subteam pool. Follow all driving laws and regulations. Ensure trailer and towing vehicle are properly fitted for travel.	Likelihood: 2 Impact: 4
Team transportation is involved in an accident.	Potential human risk.	Likelihood: 2 Impact: 5	Ensure to travel with a diverse Subteam pool. Follow all driving laws and regulations. Ensure travel vehicle is properly fitted for travel.	Likelihood: 2 Impact: 4
Organization funds run out.	Potential risk of mission failure. Potential to have no launch vehicle.	Likelihood: 5 Impact: 4	Team properly budgets each fiscal year and adheres to a strict budget. Enough funds are in excess to allow for emergency funds as necessary.	Likelihood: 1 Impact: 1
Team runs out of time for vehicle manufacturing.	Potential risk of mission failure via nonflight.	Likelihood: 5 Impact: 4	Ensure vehicle is assembled and undergo a successful test flight with enough time for manufacturing and assembly after flight.	Likelihood: 1 Impact: 1

Appendix F: Assembly, Preflight, Launch, Recovery, and Off-Nominal Checklists

The Off Nominal checklist covers alternate process flows for dis-arming/safeing the vehicle/system based on identified failure modes. The first point of each subsection within each checklist indicates whether one of these failure modes has occurred. The failure mode can be found below the yes/no question this with the letter/number combination of the specific failure, as well as an explanation of the failure, with possible notes/other failure modes extending into the misc. notes section of the subsection. Each subsection of the Off Nominal checklist lists the identified failure modes for each of the other checklists (Assembly, Preflight, Launch, and Recovery) that require dis-arming/safeing; with the subsections of each failure mode containing the subsequent process flow within. The Off-Nominal checklist is not all encompassing, and only includes failure modes for which dis-arming/safeing of the vehicle is needed.

Precautions include the following:

The use of clear, unambiguous flight ready language. The traditional "Go No Go" terminology has significant risk associated if the "No" is not copied, resulting in a false "Go" signal. As such Green/Red terminology is used to eliminate this risk.

A. Assembly Step Procedure:

A.1 Ejection Charge Preparation

1.a. Drogue Primary

i Apply proper PPE per ESRA specifications
ii Prepare rubber glove finger, tape, two e-matches, and precision scale
iii Check continuity of each e-match, visually inspect for damage
iv Measure out 1.56 *grams* of 4F black powder, close black powder container
v Pour black powder into glove finger
vi Insert both primary drogue e-matches into powder inside the glove finger
vii Tape glove finger tightly closed and wrapped, ensuring e-matches are secured, and black powder is sealed and can hold until the BP is burnt
viii Place assembled ejection charge into charge well
ix Clearly label charge as "DROGUE PRIMARY CHARGE"

1.b. Drogue Secondary

i Apply proper PPE per ESRA specifications
ii Prepare rubber glove finger, tape, two e-matches, and precision scale
iii Check continuity of each e-match, visually inspect for damage
iv Measure out 3.125 *grams* of 4F black powder, close black powder container
v Pour black powder into glove finger
vi Insert both secondary drogue e-matches into powder inside the glove finger
vii Tape tightly closed glove finger and wrapped, ensuring e-matches are secured, and black powder is sealed and can hold until the BP is burnt
viii Place assembled ejection charge into charge well
ix Clearly label charge as "DROGUE SECONDARY CHARGE"

1.c. Main Primary

i Apply proper PPE per ESRA specifications
ii Prepare rubber glove finger, tape, two e-matches, and precision scale
iii Check continuity of both e-matches, visually inspect for damage
iv Measure out 2.5 *grams* of 4F black powder, close black powder container
v Pour black powder into glove finger
vi Insert both primary main e-matches into powder inside the glove finger.
vii Tape glove finger closed, ensuring e-matches are secured, and black powder is sealed
viii Clearly label the charge as "MAIN PRIMARY CHARGE"

1.d. Main Secondary

i Apply proper PPE per ESRA specifications

ii Prepare rubber glove finger, tape, two e-matches, and precision scale

iii Check continuity of e-matches, visually inspect for damage

iv Measure out 5.0 *grams* of 4F black powder, close black powder container

v Pour black powder into glove finger

vi Insert both secondary main e-matches into powder inside the glove finger

vii Tape glove finger closed, ensuring e-matches are secured, and black powder is sealed

viii Clearly label charge as “MAIN SECONDARY CHARGE”

A.2 Parachute Preparation

2.a. Drogue Parachute Preparation

i Visually inspect each panel of drogue parachute for rips, tears, or punctures

ii Visually inspect full length of each shroud line and shock cord for severed, frayed, torn, or brittle sections

iii Lay drogue parachute flat on a stable, clean working surface sheltered from wind and dust

iv Following manufacturer guidelines, fold drogue parachute in half such that the shroud lines align cleanly, and there are no large wrinkles in the parachute

v Fold towards the center panel by panel, such that the shroud lines remain organized, until it meets the shape of a triangle with a rounded bottom edge

vi Perform a Z-fold such that the top point of the triangle remains on top of the folded parachute

vii Perform a Z-Fold of the shroud lines, ensuring lines remain untangled

viii Wrap final length of shroud lines once, and no more, around folded drogue parachute such that the parachute exits the parachute bay prior to unfolding

ix Group drogueparachute and lines together, and set in sheltered, clean place

2.b. Main Parachute Preparation

i Visually inspect each panel of main parachute for rips, tears, or punctures

ii Visually inspect the full length of each shroud line and shock cord for severed, frayed, torn, or brittle sections

iii Lay main parachute flat on a stable, clean working surface sheltered from wind and dust

iv Following manufacturer instructions, fold main parachute

v Carefully insert main parachute into deployment bag

vi Following manufacturer instructions, organize shroud lines onto deployment bag

vii Set packed main parachute in sheltered, clean place

2.c. Shock Cord Preparation

i Create a knot 10 ft from one end of the cord

ii Insert a quick link through loops placed at the ends of the shock cord and in the knot

iii Place the swivel at both ends of the shock cords with an additional quick link to eventually attach to the eyebolts

iv Fold the shock cords in a Z fold and wrap one wrap of painter's tape around the fold to hold it in place

v Repeat again for the second shock cord

A.3 Ballast Bay Preparation

3.a. Pre-Assembly

i Gather four ¼-20 x ¼ *in* button head screws

ii Gather two ¼-20 x 3/8 *in* hex drive screws

iii Gather two ¼-20 nuts

iv Gather four ¼-20 pem nuts

v Gather five ¼-20 lock nut

vi Gather four 1 *in* x 1 *in* gussets

vii Gather one "yo-yo" rail guide

viii Gather seven thin-headed ¼-20 x 1 *in* bolt.

ix Screw ¼-20 x 1 *in* bolt into rail guide

x Gather two 12 *in* long spars for ballast

xi Align bottom faces of spars and bottom faces of gussets to be parallel to each other

xii Align spar hole with gusset mounting hole to be concentric

xiii Insert ¼-20 x 1 *in* thin-headed bolt into concentric gusset-spar hole with the bottom face of the screw head coincident to the inner gusset face.

xiv Screw lock nut over thin-headed ¼-20 x 1*in* until tightly secured

xv Repeat Steps 3.a.viii to 3.a.xi until all four gussets are attached flat faces are in opposing directions to the outside of the spars

xvi Epoxy a nut to the inside face of the remaining upper gusset hole to allow for ease of assembly

xvii Gather Loctite[47]

xviii Gather a 3/8 *in* eye-bolt

xix Gather four ¼-20 x ¾ *in* bolts

xx Gather the boat tail

xxi Gather assembled motor casing

xxii Gather motor section

xxiii Set motor section on X-stands to begin preparation of assembly

xxiv Slide boat tail onto lower motor section and align holes as externally marked

xxv Insert ¼-20 x ¾ *in* into each of the four boat tail holes

xxvi Tighten bolds until head begins to deform the boat tail

3.b. Assembly

i With spar facing outward, align lower spar gusset hole to be concentric with composite insert of upper motor bulkhead

ii Apply Loctite to ¼-20 x 3/8 *in* screw

iii Insert ¼-20 x 3/8 *in* hex drive screw through gusset hole

iv Loosely screw in bolt so spar can swivel

v With the spar facing outward, ensure the gusset's midplane is parallel to the center hole of the upper motor bulkhead

vi Tighten bolt until spar is secure and cannot rotate, and then do at minimum an additional quarter turn with the bolt

vii Repeat steps 3.b.i to 3.b.vi for the other spar

viii Insert assembled motor casing through inner motor tube

ix Apply Loctite to 3/8 *in* eye-bolt

x Screw eye-bolt through center hole of the upper motor bulkhead and into motor casing until eye-bolt shoulder is flush to bulkhead surface

xi Slide motor tube coupler over spars and align using external markings

xii Insert rail guide assembly externally through the concentric motor tube and coupler hole

xiii Screw on lock nut to rail guide assembly and tighten until rail guide material begins to compress

xiv Inserts button head screws into four remaining holes externally

xv Screw on ¼-20 pem nuts and tighten until inner coupler begins to deform

xvi Add and secure mass into ballast section as necessary

3.c. Post-Assembly Checklist

i Ensure spars are parallel and secured

ii Ensure motor eye-bolt is secured

iii Ensure coupler is secured

iv Ensure rail guide is secured and is in-line with the lower rail guide

A.4 SRAD Avionics Bay Preparation

4.a. Pre-Assembly

i Gather four ¼-20 x ¼ *in* button head screws

ii Gather four ¼-20 pem nuts

iii Gather six thin-headed ¼-20 x 1 *in* bolt.

iv Gather four ¼-20 lock nut

v Gather four 1 *in* x 1 *in* gussets

vi Gather two 14 *in* spars

vii Gather two MARTHA electronic boards

viii Gather one 2S2P lithium ion battery pack

ix Gather eight 4-40 split washers

x Gather eight 4-40 standoffs

xi Gather eight 4-40 nylon washers

xii Gather eight 4-40 x 3/8 *in* screws

xiii Gather upper SRAD housing

xiv Gather lower SRAD housing

xv Gather six ¼-20 x ¾ *in* bolts

xvi Gather six ¼-20 washers

xvii Gather one main bulkhead

xviii Align bottom faces of spars and bottom faces of gussets to be parallel to each other

xix Align spar hole with gusset mounting hole to be concentric

xx Insert ¼-20 x 1 *in* thin-headed bolt into concentric gusset-spar hole with the bottom face of the screw head coincident to the inner gusset face.

xxi Screw lock nut over thin-headed ¼-20 x 1*in* until tightly secured

xxii Repeat Steps 4.a.xviii to 4.a.xxi until all four gussets are attached flat faces are in opposing directions to the outside of the spars

xxiii Epoxy a nut to the inside face of the remaining upper gusset hole to allow for ease of assembly

xxiv Inserts ¼-20 x ¼ *in* button head screws into four coupler holes externally

xxv Screw on ¼-20 pem nuts and tighten until inner coupler begins to deform

xxvi Epoxy1/4-20 pem nut to allow for ease of assembly

4.b. Assembly

i Align holes of main bulkhead so gusset holes are concentric to bulkhead holes

ii With spar facing outward, align lower spar gusset hole to be concentric with epoxied nut of upper ballast gusset spar

iii Insert ¼-20 x 1 *in* thin-headed hex drive screw through gusset hole

iv Loosely screw in bolt so spar can swivel

v With the spar facing outward, ensure the gusset's midplane is parallel to the center hole of the upper motor bulkhead

vi Tighten bolt until spar is secure and cannot rotate, and then do at minimum an additional quarter turn with the bolt

vii Repeat steps 4.b.ii to 4.b.vi for the other spar

viii Align lower SRAD housing with the sixth spar hole from the bottom

ix Insert ¼-20 x ¾ *in* bolt into the sixth hole and tighten lower SRAD housing with a ¼-20 nut

x Place 2S2P battery inter center of lower SRAD housing

xi Slide upper SRAD housing and align upper housing hole with the fifth hole from the top

xii Insert ¼-20 x ¾ *in* bolt into the fifth hole and tighten upper SRAD housing with a ¼-20 nut

xiii Insert ¼-20 x ¾ *in* bolt into the eighth hole from the bottom and tighten SRAD housing with a ¼-20 nut

xiv Put split washer over threaded section of 4-40 standoffs

xv Repeat step 4.b.xiv until eight washer-standoff pairs are made

xvi Insert washer-standoff pair into heated insert of upper SRAD housing

xvii Repeat step 4.b.xvi until eight washer-standoff pairs are screwed in

xviii Insert 4-40 x 3/8 *in* screw into nylon washer

xix Repeat step 4.b.xviii until eight washer-screw pairs are made

xx Align both MARTHA boards until each board has its own associated four standoffs

xxi Insert washer-screw pair into MARTHA mounting hole and tighten into standoff

xxii Repeat step 4.b.xxi until all eight washer-screw pairs are tightened down
xxiii Unscrew ¼-20 x ¼ *in* button head screws from coupler
xxiv Slide lower airframe over assembly until it is flush with the exterior motor tube
xxv Insert ¼-20 x ¼ *in* button head screws externally through airframe and coupler and tighten until pem nuts begin to deform the composite tubing

4.c. Post-Assembly
i Ensure spars are parallel and secured
ii Power MARTHA boards with an XT-30 splitter

A.5 Payload Bay Preparation

5.a. Pre-Assembly
i Gather four ¼-20 x ¼ *in* button head screws
ii Gather four ¼-20 pem nuts
iii Gather six thin-headed ¼-20 x 1 *in* bolt.
iv Gather four ¼-20 lock nut
v Gather four 1 *in* x 1 *in* gussets
vi Gather two 14 *in* spars
vii Gather Payload housing
viii Gather Payload cover
ix Gather sixteen 4-40 x 3/8 *in* screws
x Gather four ¼-20 x ¾ *in* bolts
xi Gather four ¼-20 washers
xii Gather one main bulkhead
xiii Align bottom faces of spars and bottom faces of gussets to be parallel to each other
xiv Align spar hole with gusset mounting hole to be concentric
xv Insert ¼-20 x 1 *in* thin-headed bolt into concentric gusset-spar hole with the bottom face of the screw head coincident to the inner gusset face.
xvi Screw lock nut over thin-headed ¼-20 x 1*in* until tightly secured
xvii Repeat Steps 4.a.xviii to 4.a.xxi until all four gussets are attached flat faces are in opposing directions to the outside of the spars
xviii Epoxy a nut to the inside face of the remaining upper gusset hole to allow for ease of assembly
xix Inserts ¼-20 x ¼ *in* button head screws into four coupler holes externally
xx Screw on ¼-20 pem nuts and tighten until inner coupler begins to deform
xxi Epoxy1/4-20 pem nut to allow for ease of assembly

5.b. Assembly
i Align 3 of the 4 aluminum cubesat walls with each other so holes are concentric
ii Align aluminum cubesat ceiling and floor so its inserts are concentric with the walls
iii Screw in 4-40 bolts into previously aligned holes leaving one wall off for internals
iv Align electronics holes concentrically with payload housing holes
v Screw electronics into the housing using 4-40 bolts
vi Align electronic housing hole concentrically within the cubesat holes
vii Attach electronic housing to cubesat using 4 ¼-20 bolts
viii Align the final aluminum wall concentrically so the holes line up with the previously attached walls
ix Use 4-40 bolts to screw in final cubesat wall
x Align cubesat holes concentrically with holes along the payload 14” spars. Payload will fit with little to no room for error.
xi Use ¼-20 bolts to attach cubesat to the internal spar system

5.c. Post-Assembly
i Ensure Spars are parallel
ii Power on payload electronics

A.6 Camera Bay Preparation

6.a. Pre-Assembly
i Gather four 4-40 x 3/8 *in* button head screws
ii Gather four 4-40 pem nuts
iii Gather six thin-headed ¼-20 x 1 *in* bolt.
iv Gather four ¼-20 lock nut
v Gather four 1 *in* x 1 *in* gussets

vi Gather two 20 *in* spars
vii Gather two Featherweight GPS trackers
viii Gather one 4S lithium ion battery pack
ix Gather twelve 4-40 split washers
x Gather twelve 4-40 standoffs
xi Gather twelve 4-40 nylon washers
xii Gather twenty-four 4-40 x 3/8 *in* screws
xiii Gather upper camera housing
xiv Gather lower camera housing
xv Gather four switch housings
xvi Gather four switches
xvii Gather eight ¼-20 x 1 *in* bolts
xviii Gather eight ¼-20 washers
xix Gather eight ¼-20 nuts
xx Gather one main bulkhead
xxi Align bottom faces of spars and bottom faces of gussets to be parallel to each other
xxii Align spar hole with gusset mounting hole to be concentric
xxiii Insert ¼-20 x 1 *in* thin-headed bolt into concentric gusset-spar hole with the bottom face of the screw head coincident to the inner gusset face.
xxiv Screw lock nut over thin-headed ¼-20 x 1 *in* until tightly secured
xxv Repeat Steps 6.a.xxi to 6.a.xxiv until all four gussets are attached flat faces are in opposing directions to the outside of the spars
xxvi Epoxy a nut to the inside face of the remaining upper gusset hole to allow for ease of assembly

6.b. Assembly

i Align holes of main bulkhead so gusset holes are concentric to bulkhead holes
ii With spar facing outward, align lower spar gusset hole to be concentric with epoxied nut of upper payload gusset spar
iii Insert ¼-20 x 1 *in* thin-headed hex drive screw through gusset hole
iv Loosely screw in bolt so spar can swivel
v With the spar facing outward, ensure the gusset's midplane is parallel to the center hole of the upper payload bulkhead
vi Tighten bolt until spar is secure and cannot rotate, and then do at minimum an additional quarter turn with the bolt
vii Repeat steps 6.b.ii to 6.b.vi for the other spar
viii Align lower camera housing with the third spar hole from the bottom
ix Insert ¼-20 x ¾ *in* bolt into the third hole and tighten lower camera housing with a ¼-20 nut
x Place 4S battery inter center of lower camera housing
xi Slide upper camera housing and align upper housing hole with the sixth hole from the bottom
xii Insert ¼-20 x ¾ *in* bolt into the sixth hole and tighten upper camera housing with a ¼-20 nut
xiii Insert ¼-20 x ¾ *in* bolt into the eighth hole from the bottom and tighten camera housing with a ¼-20 nut
xiv Put split washer over threaded section of 4-40 standoffs
xv Repeat step 6.b.xiv until twelve washer-standoff pairs are made
xvi Insert washer-standoff pair into heated insert of upper camera housing
xvii Repeat step 6.b.xvi until twelve washer-standoff pairs are screwed in
xviii Insert 4-40 x 3/8 *in* screw into nylon washer
xix Repeat step 6.b.xviii until twelve washer-screw pairs are made
xx Align both camera boards until each board has its own associated four standoffs
xxi Insert washer-screw pair into camera mounting hole and tighten into standoff
xxii Repeat step 6.b.xxi until eight washer-screw pairs are tightened down
xxiii Align both featherweight boards to their specified location
xxiv Insert washer-screw pair into featherweight mounting hole and tighten into standoff
xxv Repeat step 6.b.xxiv until last four washer-screw pairs are tightened down

6.c. Post-Assembly

i Put in pull pins to discharge cameras
ii Ensure spars are secured

A.7 Recovery Electronics Bay Preparation

7.a. Pre-Assembly

i Gather lower recovery bulkhead
ii Gather recovery electronics bay
iii Gather four ¼-20 x ¾ *in* hex bolts
iv Gather six ¼-20 washers
v Gather three pull pins
vi Gather two charge wells
vii Gather one U-bolt
viii Gather one eye-bolt
ix Gather four 5/8 *in* split-lock washers
x Gather four 5/8 *in* nuts
xi Gather two 3/8 *in* split-lock washers
xii Gather one 3/8 *in* nut
xiii Gather Loctite
xiv Gather four thin-headed ¼-20 x 1 *in* bolt
xv Gather two ¼-20 lock nuts

7.b. Assembly

i Align recovery bay so central mounting holes are concentric with the fifth and ninth holes from the top of the spar
ii Insert four ¼-20 x ¾ *in* hex bolt into ¼-20 washer
iii Insert four washer-bolt pair into the fifth and ninth holes on both spars
iv Tighten all four washer-bolt pairs
v Completely screw two 5/8 *in* nuts onto U-bolt, one to each arm.
vi Slide 5/8 *in* split-lock washer over each arm of the U-bolt
vii Insert U-bolt into upper face of lower recover bulkhead
viii On the other side of the bulkhead slide 5/8 *in* split-lock washer onto each arm of the U-bolt
ix Screw in 5/8 *in* nut into each arm of the U-bolt until fully secured to tbe bulkhead
x Slide 3/8 *in* split-lock washer over eye-bolt
xi Apply Loctite to threads of eye-bolt
xii Screw eye-bolt-washer pair into bulkhead so the eyelet is through the bottom face, opposing the orientation of the eye bolt.
xiii On the upper side where the eue-bolt threads are now showing, slide a 3/8 *in* washer
xiv Apply Loctite to threads of 3/8 *in* nut
xv Screw on 3/8 *in* nut and tighten until split-lock washers score the surface of the bulkheads
xvi Align ejection charge to upper bulkhead so mounting holes are concentric
xvii Insert thin-headed ¼-20 x 1 *in* bolt through ejection charge well
xviii Slide a washer over the bottom side of the ¼-20 bolt thread and fasten with a ¼-20 lock nut until charge well is fully secure
xix Repeat step 7.b.xvi to 7.b.xviii for other charge well
xx Connect female aviation connector of wiring of recovery electronic bay to male aviation connector end in bulkhead
xxi Screw in aviation connector to bulkhead
xxii Align holes of lower recovery bulkhead so gusset holes are concentric to bulkhead holes
xxiii Insert two thin-headed ¼-20 x 1 *in* bolts and secure bulkhead to spars
xxiv Slide recovery coupler over assembly until it is flush with the bulkhead
xxv Insert 4-40 x 3/8 *in* button head screws externally through airframe and coupler and tighten until pem nuts begin to deform the composite tubing

7.c. Post-Assembly

i Ensure spade connectors have continuity
ii Ensure U-Bolt is securely fastened
iii Ensure charge wells are securely fastened
iv Replace 4-40 bolts with 4-40 nylon shear pins once assembly is completed

A.8 Nosecone Bay Preparation

8.a. Pre-Assembly

i Gather one Tangent Ogive 4:1 nosecone

ii Gather one nosecone tip
iii Gather one nosecone adapter
iv Gather one nosecone bulkhead
v Gather one nosecone coupler
vi Gather four 0.75 *in* ¼-20 bolts
vii Gather four 0.75 *in* 4-40 bolts
viii Gather one 1 *in* ¼-20 bolt
ix Gather one ¼-20 washer with 1 *in* outer diameter
x Gather four 0.5 *in* 4-40 shear pins
xi Gather one 3/8 *in* eyebolt
xii Gather one 3/8 *in* split-lock washer
xiii Gather one 3/8 *in* hex lock nut
xiv Gather Loctite

8.b. Assembly

i Align tangent ogive 4:1 nosecone concentrically with nosecone tip
ii Attach 1 *in* ¼-20 bolt with ¼-20 washer
iii Screw in washer and bolt assembly into nosecone tip through the interior of the nosecone
iv Align holes in nosecone bulkhead concentrically with holes in nosecone adapter
v Screw in ¼-20 bolts into previously aligned holes to attach the nosecone bulkhead to insert
vi Align eyebolt with center hole in nosecone bulkhead facing downward
vii Insert washer-bolt assembly into bulkhead
viii Apply Loctite to eyebolt threads
ix Screw on hex locking nut onto eyebolt and tighten until split-lock washer scores the surface of the bulkhead
x Align nosecone coupler concentrically with nosecone bulkhead
xi Align radial holes in bulkhead with radial holes in nosecone coupler
xii Screw 1/4-20 bolts into nosecone bulkhead through the coupler

8.c. Post-Assembly

i Align completed nosecone assembly concentrically with parachute bay
ii Align radial holes on nosecone coupler with radial holes in parachute airframe
iii Use four 4-40 shear pins to attach nosecone bay to parachute bay

A.9 Main Parachute Bay Preparation

9.a. Pre-Assembly

i Gather three 3/8 *in* eye bolts
ii Gather three 3/8 *in* split-lock washers with 1 *in* outer diameter
iii Gather three 3/8 *in* hex lock nuts
iv Gather two thin-headed ¼-20 x 1*in* bolts
v Gather two ¼-20 hex lock nuts
vi Gather four 0.5 *in* 4-40 shear pins
vii Gather Loctite
viii Gather two charge wells
ix Gather upper recovery bulkhead
x Gather main parachute assembly
xi Gather parachute body tube
xii Gather one shock cord
xiii Ensure upper recovery bulkhead is rigidly epoxied into mid-point of parachute body tube

9.b. Assembly

i Align eyebolts with center hole in upper recovery bulkhead
ii Insert washer-bolt pair into center hole in the bulkhead
iii Apply Loctite to threads of eyebolt
iv Screw on 3/8 *in* nut and tighten until split-lock washers score the surface of the bulkhead
v Ensure single eyebolt is pointing down towards the ground
vi Repeat steps 9.b.i to 9.b.iv for all other eyebolts located in the outermost holes in the bulkhead
vii Ensure two outer eyebolts are pointing up towards the nosecone
viii Align ejection charge to upper bulkhead so mounting holes are concentric
ix Insert thin-headed ¼-20 x 1 *in* bolt through ejection charge well

x Slide a washer over the bottom side of the ¼-20 bolt thread and fasten with a ¼-20 lock nut until charge well is fully secure
xi Repeat step 9.b.viii to 9.b.x for other charge well
xii Attach shock cord to main parachute assembly via quick link
xiii Attach bottom quick link of the shock cord to the U-bolt
xiv Attach top quick link of the shock cord to the eye-bolt and tighten until it cannot be tightened further
xv Ensure parachute tip is facing upwards
xvi Ensure eye-bolts are secure
xvii Ensure parachute quick links are secured and tightened

9.c. Post-Assembly
i Slide parachute body tube over recovery coupler
ii Insert 4-40 shear pins through parachute bady tube and into recovery coupler
iii Ensure body tube is rigidly attached to the coupler
iv Ensure main recovery is connected according to description of C.7 Deployment Systems

A.10 Drogue Parachute Bay Preparation

10.a. Pre-Assembly
i Gather drogue parachute assembly
ii Gather two shock cord

10.b. Assembly
i Attach shock cord to drogue parachute assembly via quick link
ii Attach bottom two quick links to each of the eye-bolts on the upper recovery bulkhead
iii Attach top quick link to the eye-bolt on the nosecone bulkhead
iv Ensure tip of drogue parachute is pointing upwards
v Ensure quick links are secured by tightening them until they cannot be further tightened

10.c. Post-Assembly
i Align parachute body tube with nosecone coupler
ii Insert four 4-40 shear pins through parachute body tube and into nosecone coupler
iii Ensure connection between parachute body tube and nosecone coupler is rigid
iv Ensure drogue recovery is connected according to description of C.7 Deployment Systems

B. Preflight Checklist:

1B.1 Lower Rail to horizontal position ☐

1.a. Remove vehicle from transport truck and carry to pad ☐

1.b. Remove aluminum blanket wrap protection from vehicle ☐

1.c. Slide lower rail guide onto rail, ensuring no undue stress on the rail guide, until the upper rail guide slides onto rail ☐

1.d. Slide vehicle fully down rail ☐

1.e. Remove nose cone tip protection ☐

1.f. Turn on and connect to featherweight GPS trackers ☐ ☐

1.g. Turn on camera system ☐ ☐

1.h. Turn on SRAD electronics ☐ ☐

1.i. Turn on SAVA payload ☐

1B.2 Vehicle is vertical and locked in place on pad ☐

2.a. Arm COTS flight computers ☐

i Primary altimeter ☐
a. Remove pull pin switch to enable altimeter ☐
b. Listen for successful startup sequence of primary altimeter, AIM USB ☐
1) Observe beep pattern for main deployment of 1000 *ft* AGL ☐
c. Listen for beeps indicating continuity on both primary deployment lines ☐

ii Secondary altimeter ☐
a. Remove pull pin switch to enable altimeter ☐
b. Listen for successful sequence on secondary altimeter, StratoLogger ☐
1) Observe beep pattern for main deployment of 950 *ft* AGL ☐

c. Listen for a second set of beeps at a new tone, distinct from AIM, indicating continuity on both secondary deployment lines. ☐

iii Tertiary altimeter ☐

a. Remove pull pin switch to enable altimeter ☐

b. Listen for successful sequence on tertiary altimeter, RRC3+ ☐

1) Observe beep pattern for main deployment of 900 *ft* AGL ☐

c. Listen for a third set of beeps at a new tone, distinct from AIM and StratoLogger, indicating continuity on all RRC3+ deployment lines. ☐

iv Verify that all flight computers are on, in ready to launch mode, and have continuity across all charges ☐

2.b. Arm Motor ☐

i Insert e-match, which is wrapped around a wooden dowel for stability, up the motor ☐

ii Clip the ends of the e-match to the alligator clips supplied by the competition ☐

iii Using duct tape, tape down the ends of the e-match to ensure it does not become disconnected due to weather conditions ☐

iv Ensure continuity in the e-match ☐

C. Launch Checklist:

C.1 SRAD Avionics Green/Red ☐

1.a. Not applicable – SRAD avionics already running.

C.2 Payload Green/Red ☐

2.a. Not applicable – Payload electronics already running.

C.3 GPS Green/Red ☐

3.a. Both trackers have GPS lock and are tracking properly on the designated phones ☐ ☐

C.4 Visual Tracking Green/Red ☐

4.a. Team has a visual lock on the vehicle ☐

D. Recovery Checklist:

D.1 Flight completed:

1.a. Include off nominal checklist? **Yes** ☐ **No** ☐

i Off nominal points: _____

_____

1.b. Record vehicle GPS location from primary/secondary Featherweight GPS trackers

i Primary GPS location: _____

ii Secondary GPS location: _____

1.c. Record any flight anomalies:

i Unfired black powder charges ……..... ☐

ii Unexpected vehicle fragmentation ……... ☐

iii Ruptured batteries …… ☐

iv Miscellaneous: _____

1.d. Picked up GPS + radio pack from recovery tent & complete MCC check-in ..... ☐

1.e. Route to vehicle approved by team's Safety Officer ..... ☐

i Route to vehicle confirmed by MCC ..... ☐

1.f. Recovery team personnel deemed fit by team's Safety Officer ..... ☐

1.g. All clear to depart received from MCC ..... ☐

1.h. Misc. notes: _____

_____

D.2 Recovery team deployed:

2.a. Include off nominal checklist? **Yes** ☐ **No** ☐

i Off nominal points: _____

_____

2.b. Arrived at planned vehicle exit location ..... ☐

2.c. Confirm GPS locations are within same area as previously..... ☐ ☐

i Primary GPS location: _____

ii Secondary GPS location: _____

2.d. Exited recovery vehicle at planned location:

i Complete check-in with MCC ……...☐

2.e. Time of vehicle exit:_____

2.f. Begin on foot search for vehicle ……...☐

i MCC check-ins every 30 minutes: _____

ii Notable events during search: _____

2.g. Misc. notes: _____

_____

D.3 Vehicle Located:

3.a. Include off nominal checklist? **Yes** ☐ **No** ☐

i Off nominal points: _____

_____

3.b. Vehicle spotted ……☐

i Time of vehicle spotting: _____

ii Visual assessment of possible flight anomalies: _____

iii All parts of vehicle are present ……..☐

a. Parts not found with vehicle: _____

iv All battery systems are intact ……☐

a. Ruptured batteries: _____

v Confirmation by Safety Officer of depletion of all energetics ……..☐

a. Unspent energetics: _____

b. All hazards disarmed and removed from vehicle by Safety Officer

vi All clear to approach vehicle given by team's Safety Officer ……..☐

3.c. GPS location of vehicle: _____

3.d. Record apogee of primary/secondary recovery altimeters through beep readings …….☐ ☐

i Primary altimeter apogee [ft]: _____

ii Secondary altimeter apogee [ft]:_____

iii Recovery altimeters powered off …….☐ ☐

3.e. If applicable: Removal of vehicle sections from flora ……☐

3.f. SAVA payload system powered off ……☐

3.g. SRAD avionics powered off ……☐

i Record state indication of primary/secondary SRAD flight computers through LED blinks …..☐

a. Primary final state: _____

b. Secondary final state: _____

ii MARTHA boards powered off ……☐ ☐

3.h. Vehicle fully powered off ……..☐

3.i. MCC check-ins: _____

3.j. Misc. notes: _____

_____

D.4 Return to base camp:

4.a. Include off nominal checklist? **Yes** ☐ **No** ☐

i Off nominal points: _____

_____

4.b. All vehicle sections present at landing area collected **……..**☐

i Time of departure from vehicle landing area: _____

4.c. Arrived at recovery vehicle ……..☐

i Time of arrival to recovery vehicle: _____

ii All clear from Safety Officer to begin vehicular return to base camp ……..☐

4.d. Arrival at base camp

i Complete final MCC check-in & return GPS + radio pack ……..☐

ii Brought vehicle to post flight inspection ……..☐

4.e. Notable events during return: _____

4.f. Misc. notes: _____

_____

4.g. Completed recovery of vehicle ……☐

E. Off-Nominal Checklist

E.1 Assembly:

1.a. Battery punctured ☐

i Report to MCC battery rupture and possible fire ☐

ii If fire announce to people in the area ☐

a. If deemed safe, flight dynamics will quickly remove the motor from the area

b. If deemed safe, energetics team will quickly remove any energetics from the area

iii Retreat from the vehicle ☐

a. Maintain safe yet observable distance in case hazard increases ☐

iv Once fire is extinguished, assess damage and determine if the vehicle is still able to fly ☐

a. If so replace battery and continue ☐

b. If not abort launch ☐

1.b. GPS signal lost ☐

i Try and reconnect without disassembling ☐

ii Disassemble avionics airframe, remove bay and check battery voltage and restart trackers if necessary ☐

iii Consult manual for troubleshooting tips ☐

1.c. Coupler or airframe fractures ☐

i Assess damage ☐

a. If very minor, continue ☐

b. If repairable, use epoxy and carbon fiber to fix the area ☐

c. If not repairable, abort ☐

1.d. Flight computer does not power on ☐

i Check wiring and if all connectors are fully connected ☐

a. If necessary check continuity ☐

ii Check battery voltages ☐

iii Check switches to make sure they are functioning properly ☐

iv Tighten screw terminals ☐

v Consult manual of flight computer for further troubleshooting ☐

vi Replace flight computer if necessary ☐

1.e. Black powder charge tears ☐

i Clean up any spilled black powder ☐

ii Mix any contaminated black powder with water to dispose of it ☐

iii Make a new black powder charge ☐

E.2 Preflight:

2.a. Battery punctured ☐

i Report to MCC battery rupture and possible fire ☐

ii Retreat from the vehicle ☐

a. Maintain safe yet observable distance in case hazard increases ☐

iii Abort launch ☐

2.b. GPS signal lost ☐

i Hold launch ☐

ii Try and reconnect without disassembling ☐

iii Abort launch and return to setup area ☐

iv Disassemble and check battery voltage and restart trackers if necessary ☐

2.c. Coupler or airframe fractures ☐
- i Assess damage ☐
  - a. If very minor, continue ☐
  - b. If repairable abort and return to base camp, use epoxy and carbon fiber to fix the area ☐
  - c. If not repairable, abort ☐

2.d. Flight computer stops beeping or does not complete booting ☐
- i Check that power switch is in correct position ☐
- ii Turn the switch off for 30 seconds and back on ☐
- iii Abort launch and disassemble and troubleshoot ☐

E.3 Launch:

3.a. GPS signal loss ☐
- i Have two people quickly move to opposite ends of the launch site to get different vantage points and follow the vehicle's descent closely ☐
  - a. Use a phone's GPS to mark area where the vehicle was seen by the two members and focus search efforts on the area where each line of sight crosses ☐

3.b. Motor chuff ☐
- i Replace igniter ☐
  - a. If second failure, remove vehicle from rails and return to base camp ☐
    - 1) Replace motor ☐

E.4 Recovery:

4.a. Unspent energetics ☐
- i Safety Officer inspects vehicle ☐
  - a. Others remain at a safe distance ☐
  - b. Photograph unspent charge for failure analysis ☐
- ii Disconnect charges from wiring ☐
- iii Open unspent charge, pour unused black powder into designated water bottle to make inert ☐
- iv Repeat for all charges ☐

4.b. Unexpected vehicle fragmentation ☐
- i Identify debris field ☐
- ii Photograph sections of debris field ☐
- iii Analyze any missing sections of the vehicle ☐
- iv Collect fragments by hand or in bag depending on size and quantity of debris ☐

4.c. Ruptured battery(s) ☐
- i Report to MCC battery rupture and possible fire ☐
- ii Retreat from the vehicle ☐
  - a. Maintain safe yet observable distance in case hazard increases ☐
- iii Once the fire is extinguished, assess the damage and determine the vehicle's condition ☐
- iv If safe to do so, remove other batteries and energetics from vehicle immediately ☐

4.d. Loss of GPS signal ☐
- i Attempt to regain connection by changing location ☐
- ii Proceed to last known location as documented in checklist and begin search ☐
- iii If not found at the last known location/immediate area, contact MCC, giving description ☐

4.e. Heat stroke/medical situation ☐
   i Mitigate heat issues through proper attire and hydration ☐
   ii Contact MCC relaying situation and urgent need for medical assistance ☐
   iii If the situation has caused incapacitation, remain with the affected recovery team member ☐
   iv If movement is possible and travel feasible/not a risk to affected member or other recovery team members, return to recovery vehicle and relay as such to MCC ☐
      a. This is only in the extreme case that an immediate need to enter a climate-controlled environment is required, otherwise a shelter in place policy is enforced.

4.f. Radio pack failure ☐
   i Return to recovery vehicle/base camp immediately ☐
   ii Return radio pack and explain failure ☐
   iii Receive new pack and begin recovery again ☐

4.g. Vehicle is irretrievable ☐
   i Take photos of vehicle location and condition ☐
   ii Mark GPS location of vehicle ☐
   iii Return to base camp and assess proper tools for recovery ☐

Appendix G: Engineering Drawings

Appendix G: Engineering Drawings provides a comprehensive collection of detailed, revision-controlled technical drawings essential for defining the significant subsystems and components involved in the mission. This appendix is meticulously structured to include individual drawings for SRAD subsystems or components, each contributing to the overarching schematic of the top-level assembly. These engineering drawings are a crucial reference for the precise construction and assembly of the vehicle, ensuring all participants can visually understand and follow the technical specifications required for successful implementation. Drawings begin on the following page.

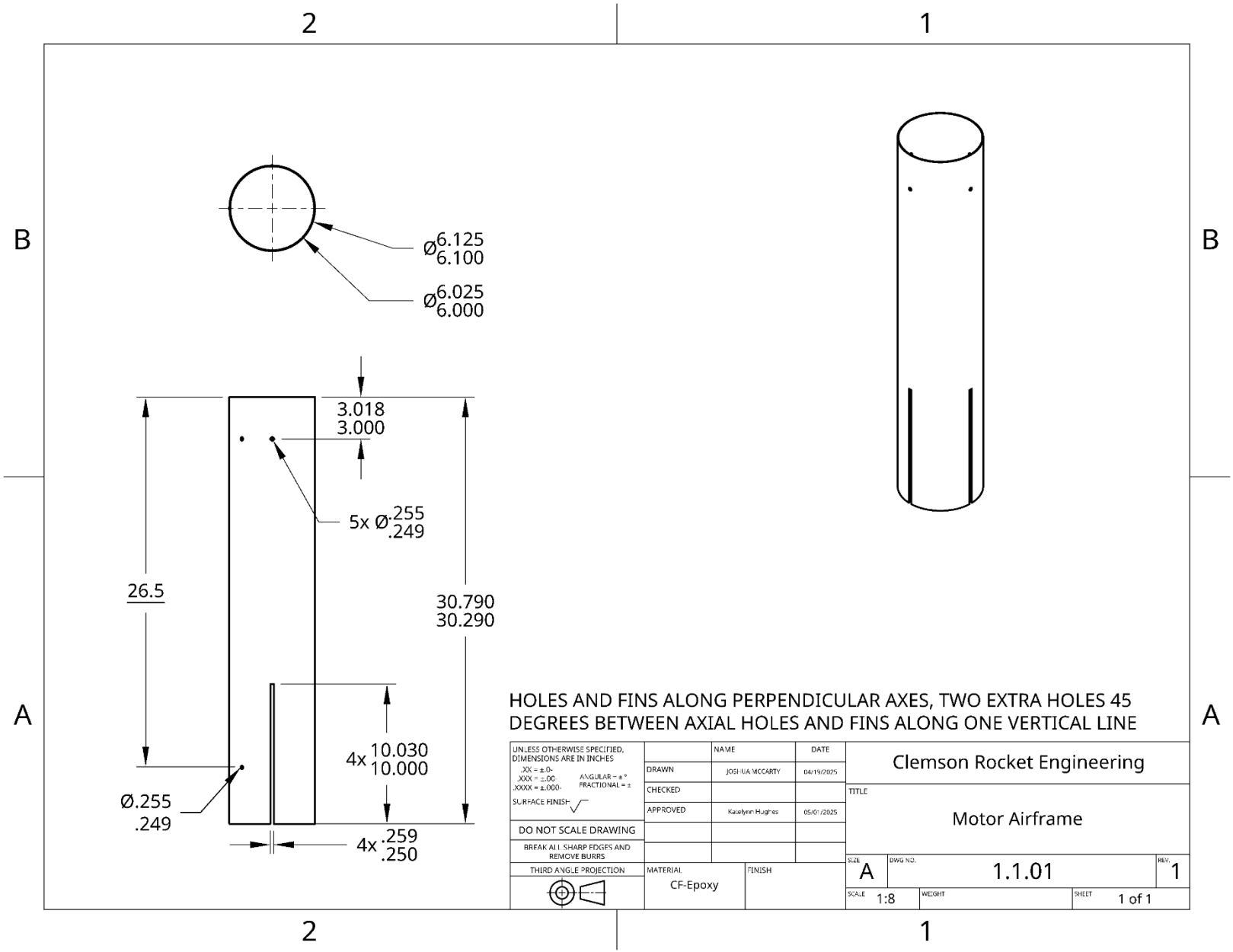
2
1
B
A
Ø6.125
6.100
Ø6.025
6.000
3.018
3.000
5x Ø.255
.249
26.5
30.790
30.290
4x 10.030
10.000
Ø.255
.249
4x .259
.250
HOLES AND FINS ALONG PERPENDICULAR AXES, TWO EXTRA HOLES 45 DEGREES BETWEEN AXIAL HOLES AND FINS ALONG ONE VERTICAL LINE
UNLESS OTHERWISE SPECIFIED, DIMENSIONS ARE IN INCHES
.XX = ±.0-
.XXX = ±.00
.XXXX = ±.000-
ANGULAR = ± °
FRACTIONAL = ±
SURFACE FINISH
DO NOT SCALE DRAWING
BREAK ALL SHARP EDGES AND REMOVE BURRS
THIRD ANGLE PROJECTION
NAME
DATE
DRAWN
JOSHUA MCCARTY
04/19/2025
CHECKED
APPROVED
Katelynn Hughes
05/01/2025
MATERIAL
CF-Epoxy
FINISH
Clemson Rocket Engineering
TITLE
Motor Airframe
SIZE
A
DWG NO.
1.1.01
REV.
1
SCALE
1:8
WEIGHT
SHEET
1 of 1

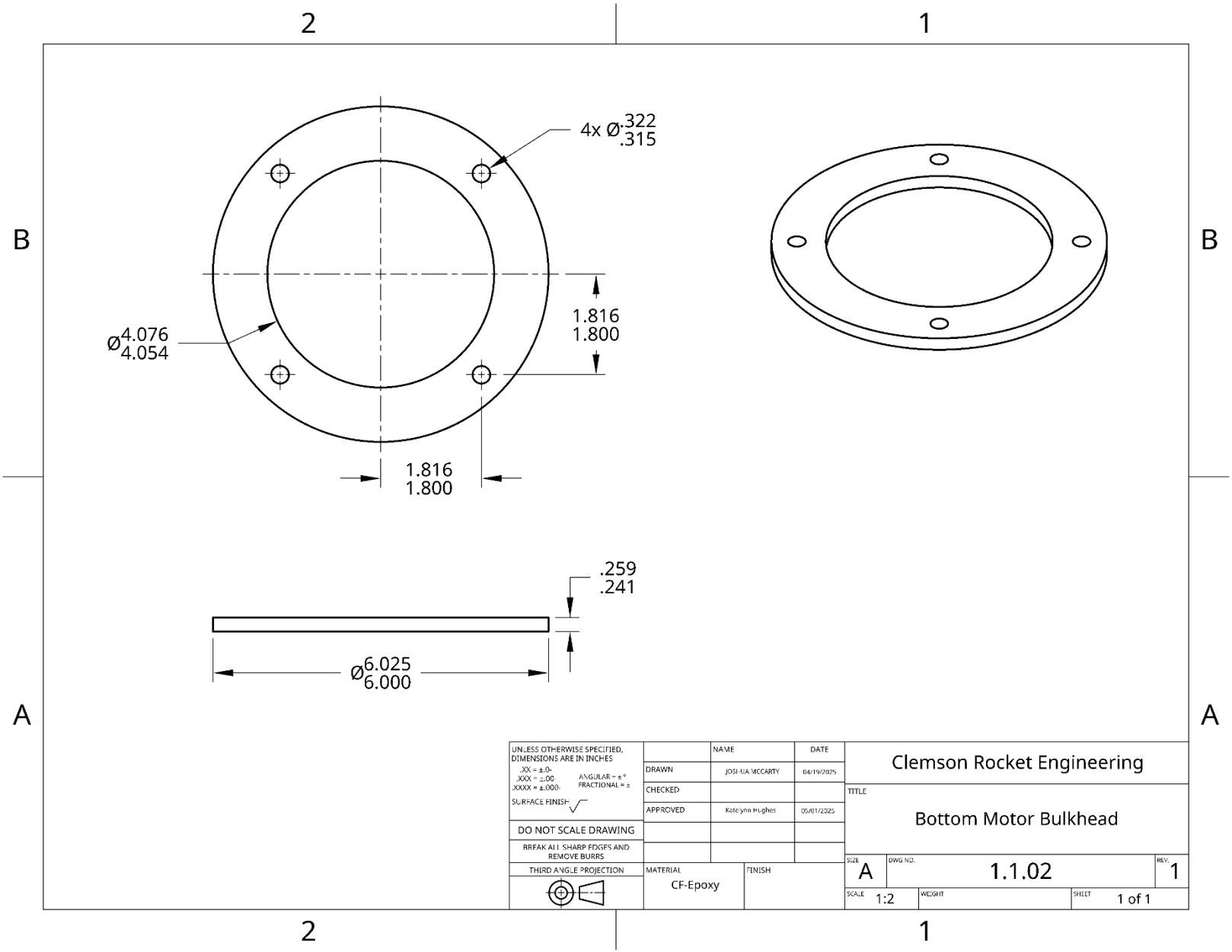
2
1
B
A
4x Ø.322 .315
Ø4.076 4.054
1.816 1.800
1.816 1.800
.259 .241
Ø6.025 6.000
UNLESS OTHERWISE SPECIFIED, DIMENSIONS ARE IN INCHES
.XX = ±.0-
.XXX = ±.00
.XXXX = ±.000-
ANGULAR = ± °
FRACTIONAL = ±
SURFACE FINISH
DO NOT SCALE DRAWING
BREAK ALL SHARP EDGES AND REMOVE BURRS
THIRD ANGLE PROJECTION
NAME
DATE
DRAWN
JOSHUA MCCARTY
04/19/2025
CHECKED
APPROVED
Katelynn Hughes
05/01/2025
MATERIAL
CF-Epoxy
FINISH
Clemson Rocket Engineering
TITLE
Bottom Motor Bulkhead
SIZE
A
DWG NO.
1.1.02
REV.
1
SCALE
1:2
WEIGHT
SHEET
1 of 1

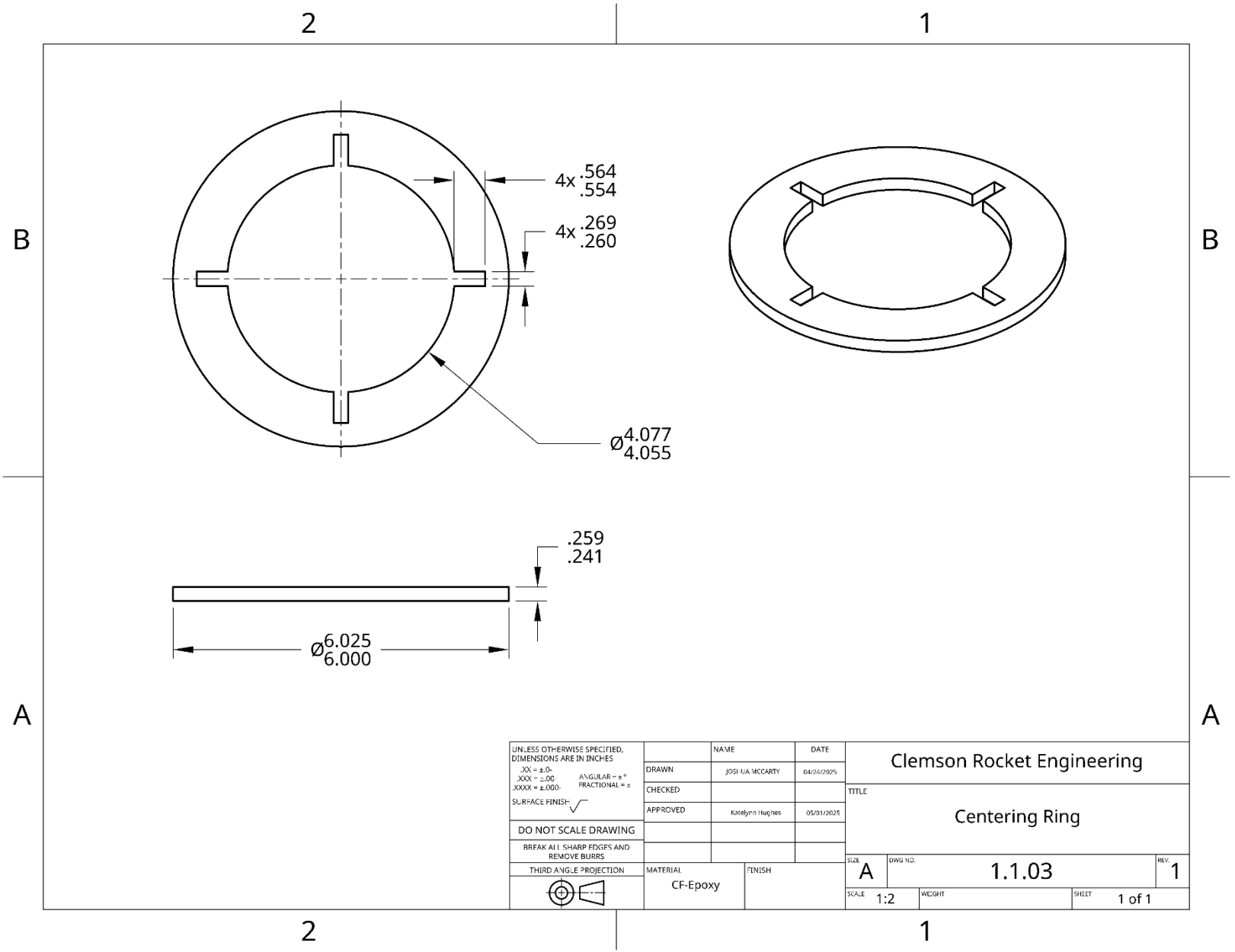
2
1
B
A
4x .564
.554
4x .269
.260
ø4.077
4.055
.259
.241
ø6.025
6.000
UNLESS OTHERWISE SPECIFIED, DIMENSIONS ARE IN INCHES
.XX = ±.0-
.XXX = ±.00
.XXXX = ±.000-
ANGULAR = ± °
FRACTIONAL = ±
SURFACE FINISH
DO NOT SCALE DRAWING
BREAK ALL SHARP EDGES AND REMOVE BURRS
THIRD ANGLE PROJECTION
NAME
DATE
DRAWN
JOSHUA MCCARTY
04/24/2025
CHECKED
APPROVED
Katelynn Hughes
05/01/2025
MATERIAL
CF-Epoxy
FINISH
Clemson Rocket Engineering
TITLE
Centering Ring
SIZE
A
DWG NO.
1.1.03
REV.
1
SCALE
1:2
WEIGHT
SHEET
1 of 1

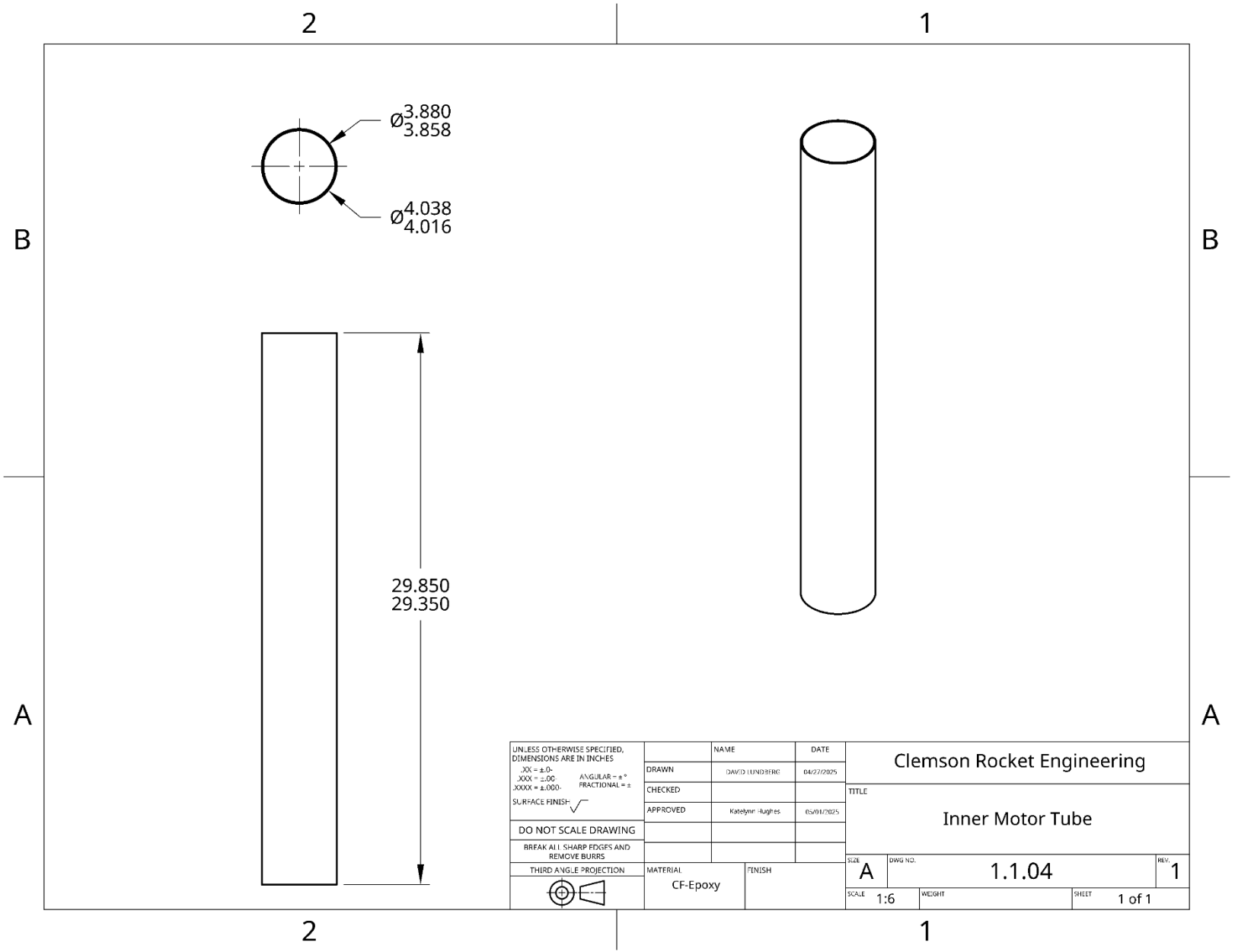
2
1
B
A
Ø3.880
3.858
Ø4.038
4.016
29.850
29.350
UNLESS OTHERWISE SPECIFIED, DIMENSIONS ARE IN INCHES
.XX = ±.0-
.XXX = ±.00
.XXXX = ±.000-
ANGULAR = ± °
FRACTIONAL = ±
SURFACE FINISH
DO NOT SCALE DRAWING
BREAK ALL SHARP EDGES AND REMOVE BURRS
THIRD ANGLE PROJECTION
NAME
DATE
DRAWN
DAVID LUNDBERG
04/27/2025
CHECKED
APPROVED
Katelynn Hughes
05/01/2025
MATERIAL
CF-Epoxy
FINISH
Clemson Rocket Engineering
TITLE
Inner Motor Tube
SIZE
A
DWG NO.
1.1.04
REV.
1
SCALE
1:6
WEIGHT
SHEET
1 of 1

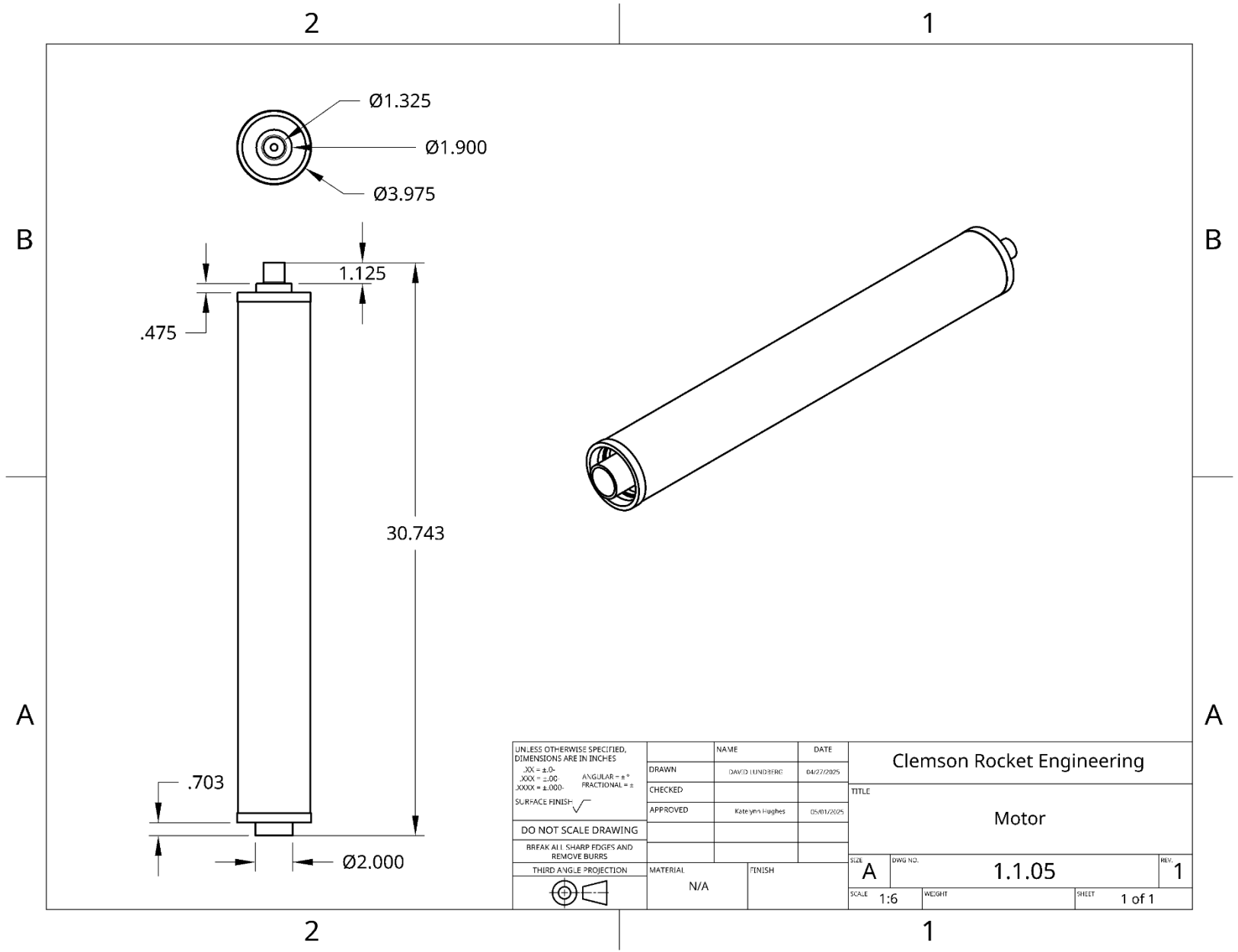
2
1
B
A
Ø1.325
Ø1.900
Ø3.975
1.125
.475
30.743
.703
Ø2.000
UNLESS OTHERWISE SPECIFIED, DIMENSIONS ARE IN INCHES
.XX = ±.0-
.XXX = ±.00
.XXXX = ±.000-
ANGULAR = ± °
FRACTIONAL = ±
SURFACE FINISH
DO NOT SCALE DRAWING
BREAK ALL SHARP EDGES AND REMOVE BURRS
THIRD ANGLE PROJECTION
NAME
DATE
DRAWN
DAVID LUNDBERG
04/27/2025
CHECKED
APPROVED
Katelynn Hughes
05/01/2025
MATERIAL
N/A
FINISH
Clemson Rocket Engineering
TITLE
Motor
SIZE
A
DWG NO.
1.1.05
REV.
1
SCALE
1:6
WEIGHT
SHEET
1 of 1

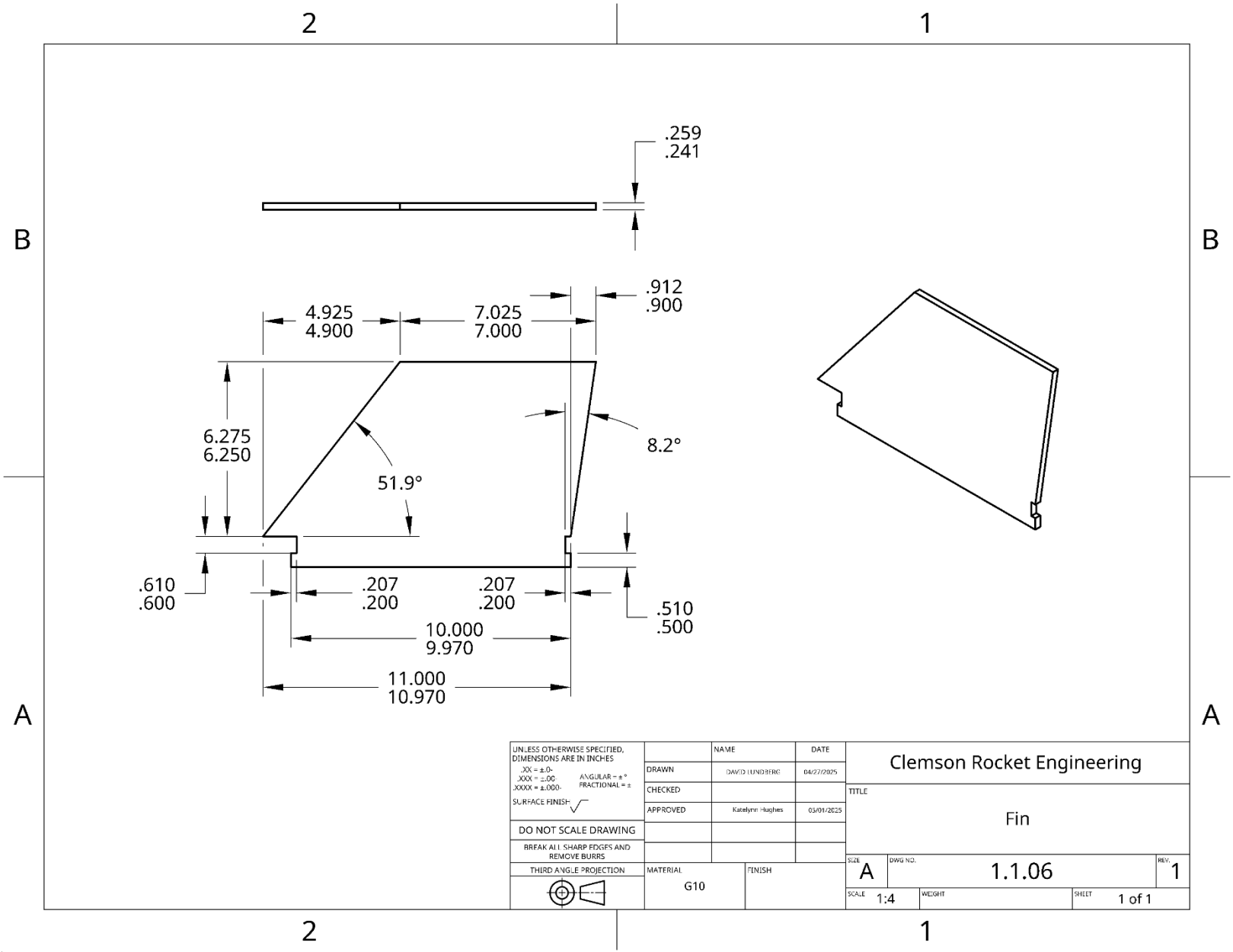
2
1
B
A
.259
.241
4.925
4.900
7.025
7.000
.912
.900
6.275
6.250
51.9°
8.2°
.610
.600
.207
.200
.207
.200
.510
.500
10.000
9.970
11.000
10.970
UNLESS OTHERWISE SPECIFIED, DIMENSIONS ARE IN INCHES
.XX = ±.0-
.XXX = ±.00
.XXXX = ±.000-
ANGULAR = ± °
FRACTIONAL = ±
SURFACE FINISH
DO NOT SCALE DRAWING
BREAK ALL SHARP EDGES AND REMOVE BURRS
THIRD ANGLE PROJECTION
NAME
DATE
DRAWN
DAVID LUNDBERG
04/27/2025
CHECKED
APPROVED
Katelynn Hughes
05/01/2025
MATERIAL
G10
FINISH
Clemson Rocket Engineering
TITLE
Fin
SIZE
A
DWG NO.
1.1.06
REV.
1
SCALE
1:4
WEIGHT
SHEET
1 of 1

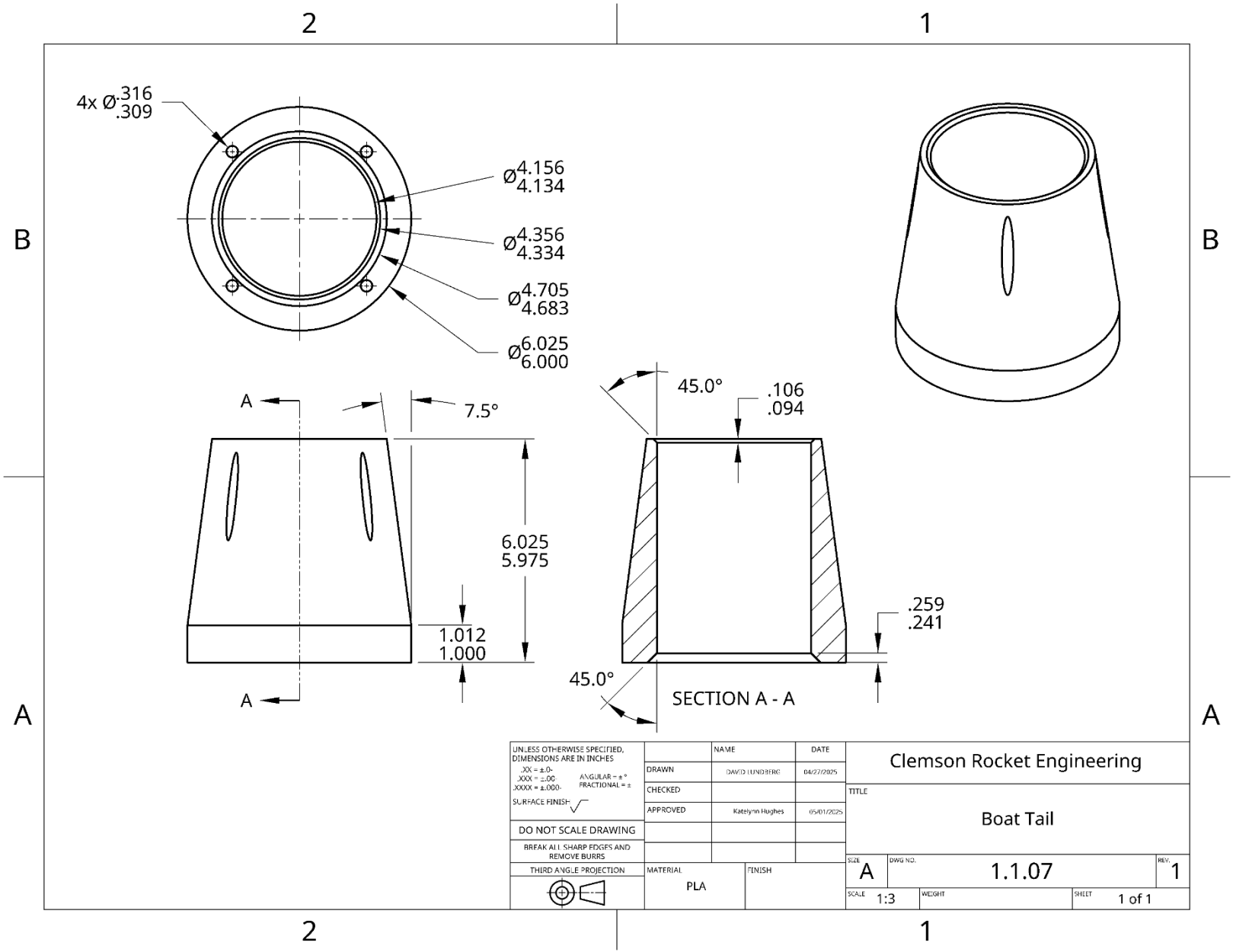
2
1
B
A
4x Ø.316 .309
Ø4.156 4.134
Ø4.356 4.334
Ø4.705 4.683
Ø6.025 6.000
A
7.5°
6.025 5.975
1.012 1.000
A
45.0°
.106 .094
.259 .241
45.0°
SECTION A - A
UNLESS OTHERWISE SPECIFIED, DIMENSIONS ARE IN INCHES
.XX = ±.0-
.XXX = ±.00
.XXXX = ±.000-
ANGULAR = ± °
FRACTIONAL = ±
SURFACE FINISH
DO NOT SCALE DRAWING
BREAK ALL SHARP EDGES AND REMOVE BURRS
THIRD ANGLE PROJECTION
NAME
DATE
DRAWN
DAVID LUNDBERG
04/27/2025
CHECKED
APPROVED
Katelynn Hughes
05/01/2025
MATERIAL
PLA
FINISH
Clemson Rocket Engineering
TITLE
Boat Tail
SIZE
A
DWG NO.
1.1.07
REV.
1
SCALE
1:3
WEIGHT
SHEET
1 of 1

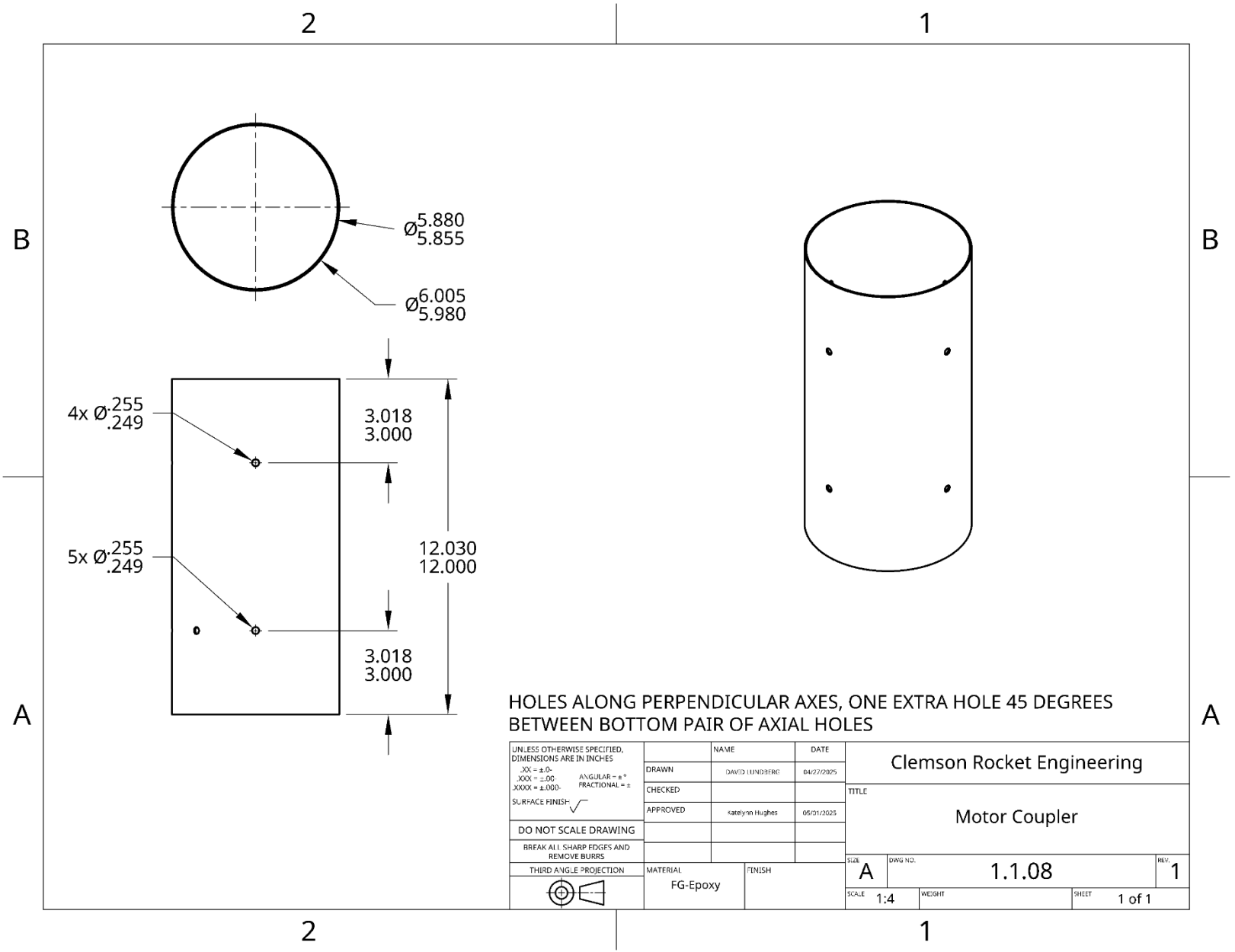
2
1
B
A
Ø5.880
5.855
Ø6.005
5.980
4x Ø.255
.249
3.018
3.000
5x Ø.255
.249
12.030
12.000
3.018
3.000
HOLES ALONG PERPENDICULAR AXES, ONE EXTRA HOLE 45 DEGREES BETWEEN BOTTOM PAIR OF AXIAL HOLES
UNLESS OTHERWISE SPECIFIED, DIMENSIONS ARE IN INCHES
.XX = ±.0-
.XXX = ±.00
.XXXX = ±.000-
ANGULAR = ± °
FRACTIONAL = ±
SURFACE FINISH
DO NOT SCALE DRAWING
BREAK ALL SHARP EDGES AND REMOVE BURRS
THIRD ANGLE PROJECTION
NAME
DATE
DRAWN
DAVID LUNDBERG
04/27/2025
CHECKED
APPROVED
Katelynn Hughes
05/01/2025
MATERIAL
FG-Epoxy
FINISH
Clemson Rocket Engineering
TITLE
Motor Coupler
SIZE
A
DWG NO.
1.1.08
REV.
1
SCALE
1:4
WEIGHT
SHEET
1 of 1

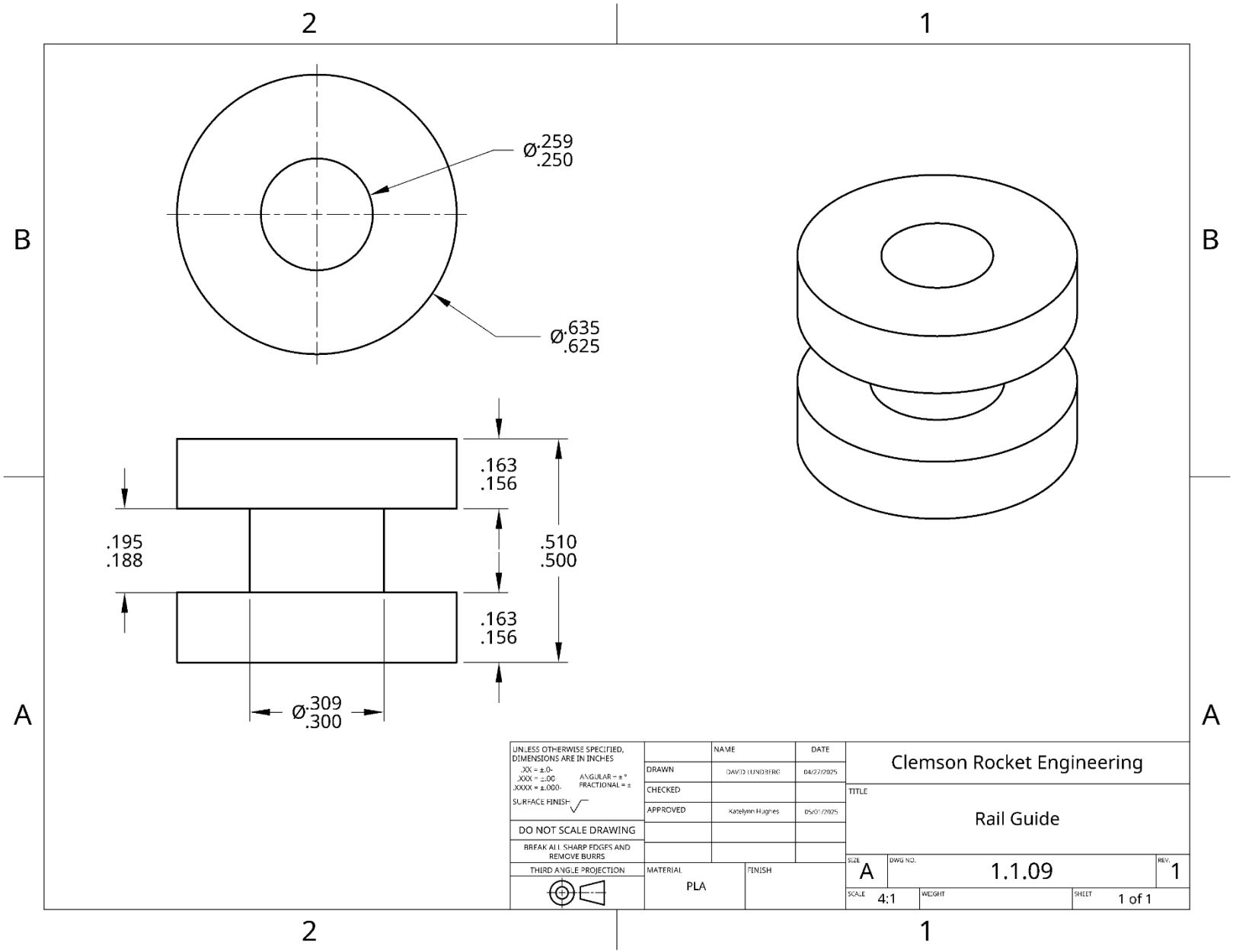
2
1
B
A
Ø.259
.250
Ø.635
.625
.163
.156
.195
.188
.510
.500
.163
.156
Ø.309
.300
UNLESS OTHERWISE SPECIFIED, DIMENSIONS ARE IN INCHES
.XX = ±.0-
.XXX = ±.00
.XXXX = ±.000-
ANGULAR = ± °
FRACTIONAL = ±
SURFACE FINISH
DO NOT SCALE DRAWING
BREAK ALL SHARP EDGES AND REMOVE BURRS
THIRD ANGLE PROJECTION
NAME
DATE
DRAWN
DAVID LUNDBERG
04/27/2025
CHECKED
APPROVED
Katelynn Hughes
05/01/2025
MATERIAL
PLA
FINISH
Clemson Rocket Engineering
TITLE
Rail Guide
SIZE
A
DWG NO.
1.1.09
REV.
1
SCALE
4:1
WEIGHT
SHEET
1 of 1

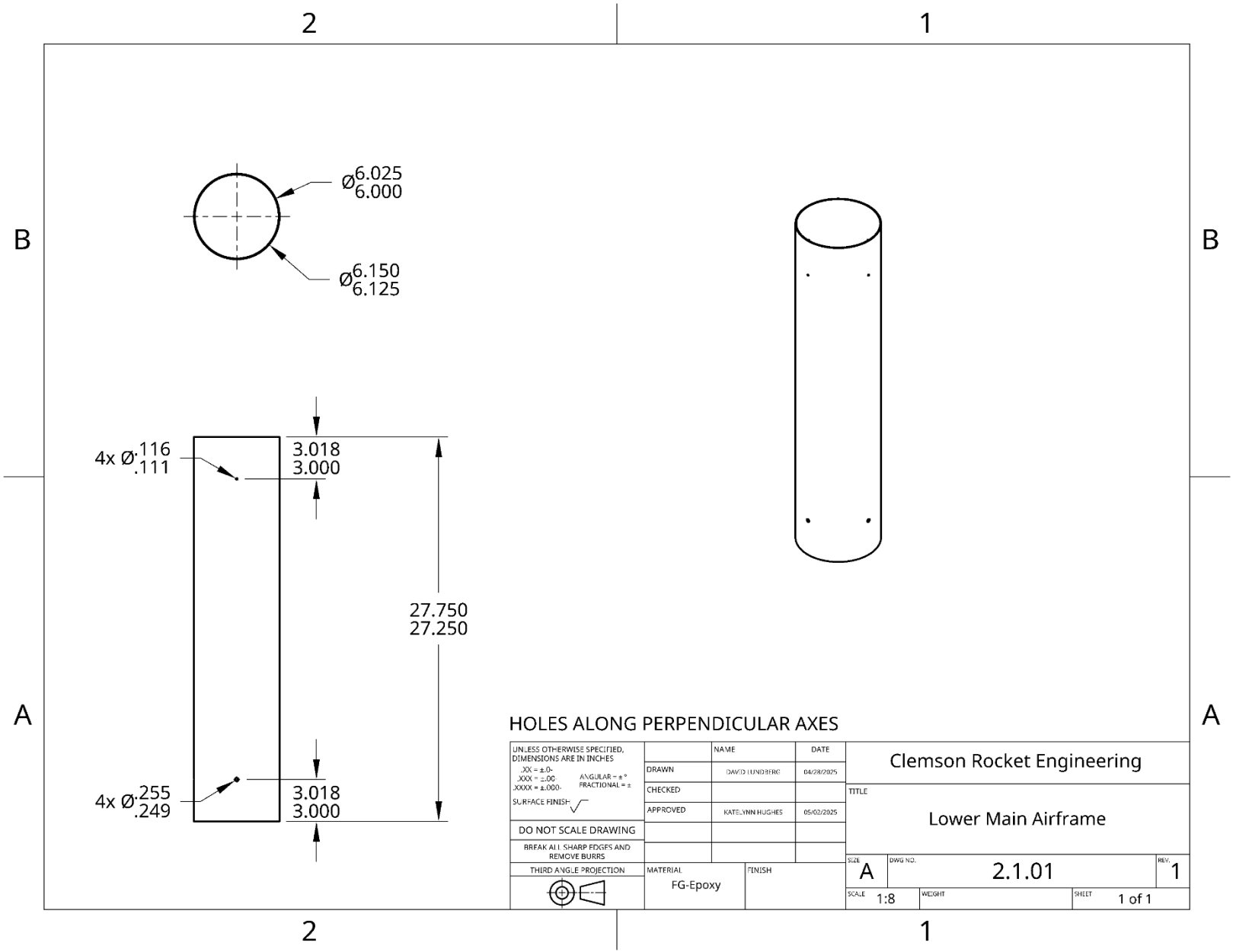
2
1
B
A
Ø6.025
6.000
Ø6.150
6.125
4x Ø.116
.111
3.018
3.000
27.750
27.250
4x Ø.255
.249
3.018
3.000
HOLES ALONG PERPENDICULAR AXES
UNLESS OTHERWISE SPECIFIED, DIMENSIONS ARE IN INCHES
.XX = ±.0-
.XXX = ±.00
.XXXX = ±.000-
ANGULAR = ± °
FRACTIONAL = ±
SURFACE FINISH
DO NOT SCALE DRAWING
BREAK ALL SHARP EDGES AND REMOVE BURRS
THIRD ANGLE PROJECTION
NAME
DATE
DRAWN
DAVID LUNDBERG
04/28/2025
CHECKED
APPROVED
KATELYNN HUGHES
05/02/2025
MATERIAL
FG-Epoxy
FINISH
Clemson Rocket Engineering
TITLE
Lower Main Airframe
SIZE
A
DWG NO.
2.1.01
REV.
1
SCALE
1:8
WEIGHT
SHEET
1 of 1

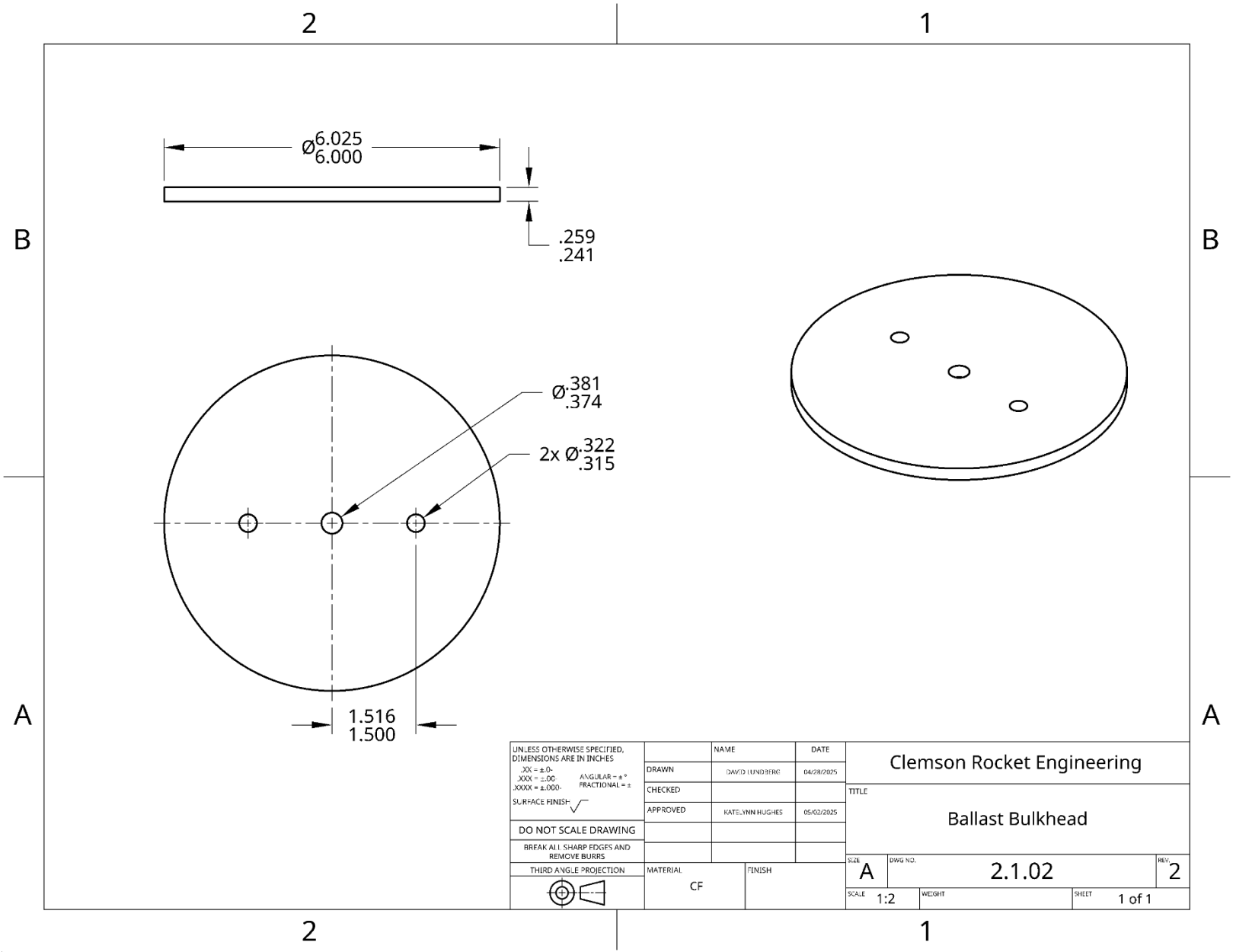
2
1
B
A
Ø6.025
6.000
.259
.241
Ø.381
.374
2x Ø.322
.315
1.516
1.500
UNLESS OTHERWISE SPECIFIED, DIMENSIONS ARE IN INCHES
.XX = ±.0-
.XXX = ±.00
.XXXX = ±.000-
ANGULAR = ± °
FRACTIONAL = ±
SURFACE FINISH
DO NOT SCALE DRAWING
BREAK ALL SHARP EDGES AND REMOVE BURRS
THIRD ANGLE PROJECTION
NAME
DATE
DRAWN
DAVID LUNDBERG
04/28/2025
CHECKED
APPROVED
KATELYNN HUGHES
05/02/2025
MATERIAL
CF
FINISH
Clemson Rocket Engineering
TITLE
Ballast Bulkhead
SIZE
A
DWG NO.
2.1.02
REV
2
SCALE
1:2
WEIGHT
SHEET
1 of 1

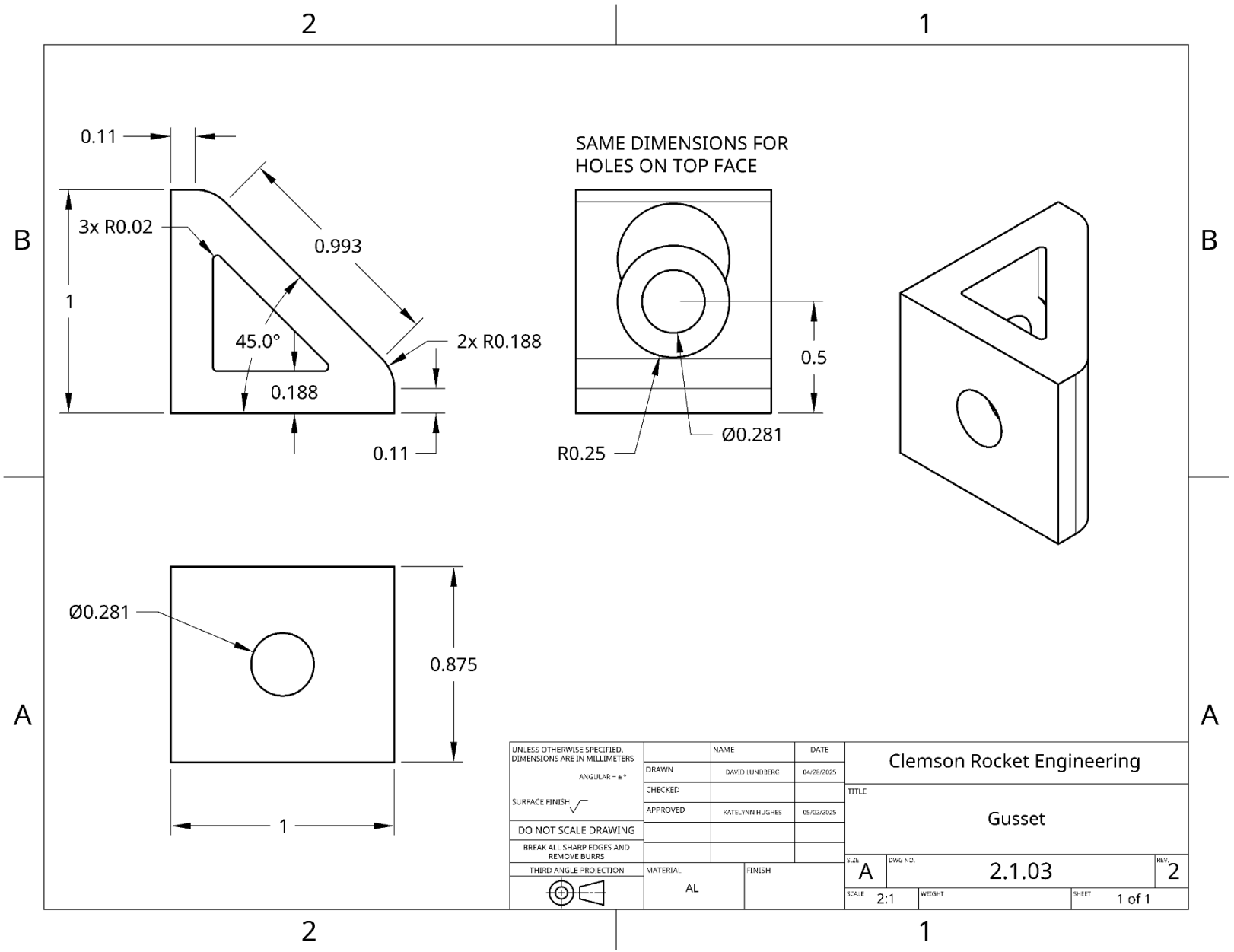
2
1
B
A
0.11
3x R0.02
0.993
1
45.0°
2x R0.188
0.188
0.11
SAME DIMENSIONS FOR
HOLES ON TOP FACE
0.5
R0.25
Ø0.281
Ø0.281
0.875
1
UNLESS OTHERWISE SPECIFIED, DIMENSIONS ARE IN MILLIMETERS
ANGULAR = ± °
SURFACE FINISH
DO NOT SCALE DRAWING
BREAK ALL SHARP EDGES AND REMOVE BURRS
THIRD ANGLE PROJECTION
NAME
DATE
DRAWN
DAVID LUNDBERG
04/28/2025
CHECKED
APPROVED
KATELYNN HUGHES
05/02/2025
MATERIAL
AL
FINISH
Clemson Rocket Engineering
TITLE
Gusset
SIZE
A
DWG NO.
2.1.03
REV
2
SCALE
2:1
WEIGHT
SHEET
1 of 1

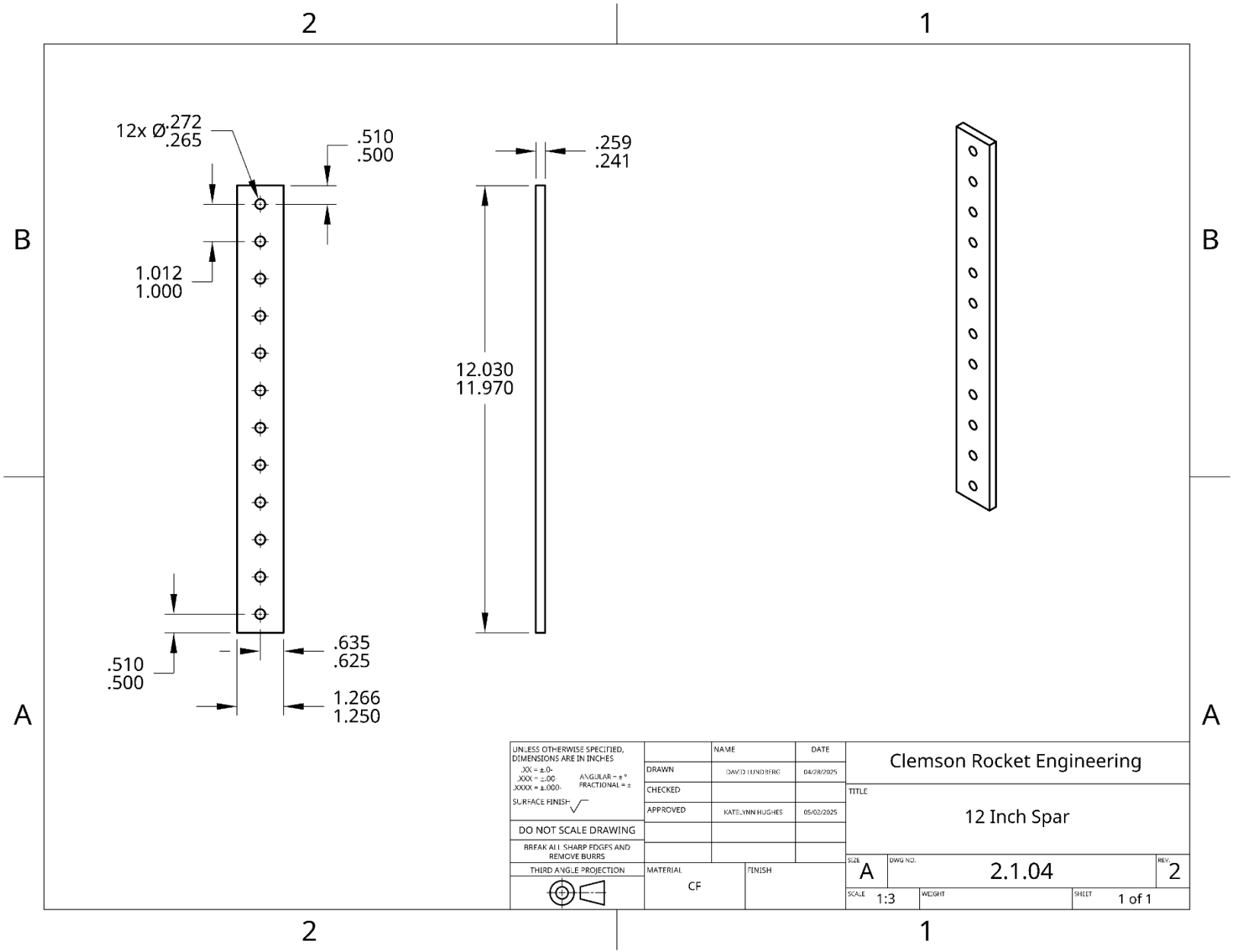
2
1
B
A
12x Ø.272
.265
.510
.500
1.012
1.000
.510
.500
.635
.625
1.266
1.250
.259
.241
12.030
11.970
UNLESS OTHERWISE SPECIFIED, DIMENSIONS ARE IN INCHES
.XX = ±.0-
.XXX = ±.00
.XXXX = ±.000-
ANGULAR = ± °
FRACTIONAL = ±
SURFACE FINISH
DO NOT SCALE DRAWING
BREAK ALL SHARP EDGES AND REMOVE BURRS
THIRD ANGLE PROJECTION
NAME
DATE
DRAWN
DAVID LUNDBERG
04/28/2025
CHECKED
APPROVED
KATELYNN HUGHES
05/02/2025
MATERIAL
CF
FINISH
Clemson Rocket Engineering
TITLE
12 Inch Spar
SIZE
A
DWG NO.
2.1.04
REV
2
SCALE
1:3
WEIGHT
SHEET
1 of 1

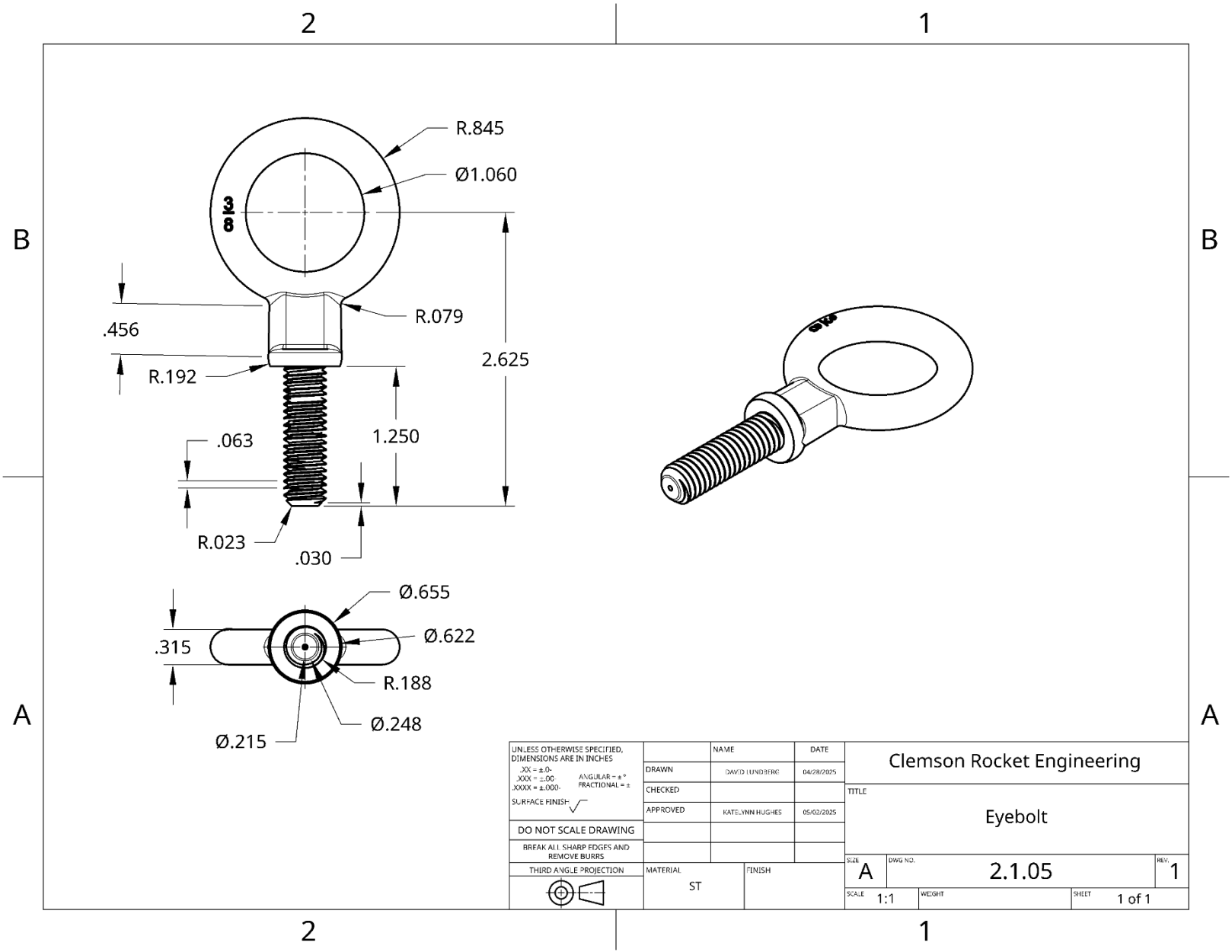
2
1
B
A
R.845
Ø1.060
3/8
.456
R.079
2.625
R.192
1.250
.063
R.023
.030
Ø.655
Ø.622
.315
R.188
Ø.248
Ø.215
UNLESS OTHERWISE SPECIFIED, DIMENSIONS ARE IN INCHES
.XX = ±.0-
.XXX = ±.00
.XXXX = ±.000-
ANGULAR = ± °
FRACTIONAL = ±
SURFACE FINISH
DO NOT SCALE DRAWING
BREAK ALL SHARP EDGES AND REMOVE BURRS
THIRD ANGLE PROJECTION
NAME
DATE
DRAWN
DAVID LUNDBERG
04/28/2025
CHECKED
APPROVED
KATELYNN HUGHES
05/02/2025
MATERIAL
ST
FINISH
Clemson Rocket Engineering
TITLE
Eyebolt
SIZE
A
DWG NO.
2.1.05
REV.
1
SCALE
1:1
WEIGHT
SHEET
1 of 1

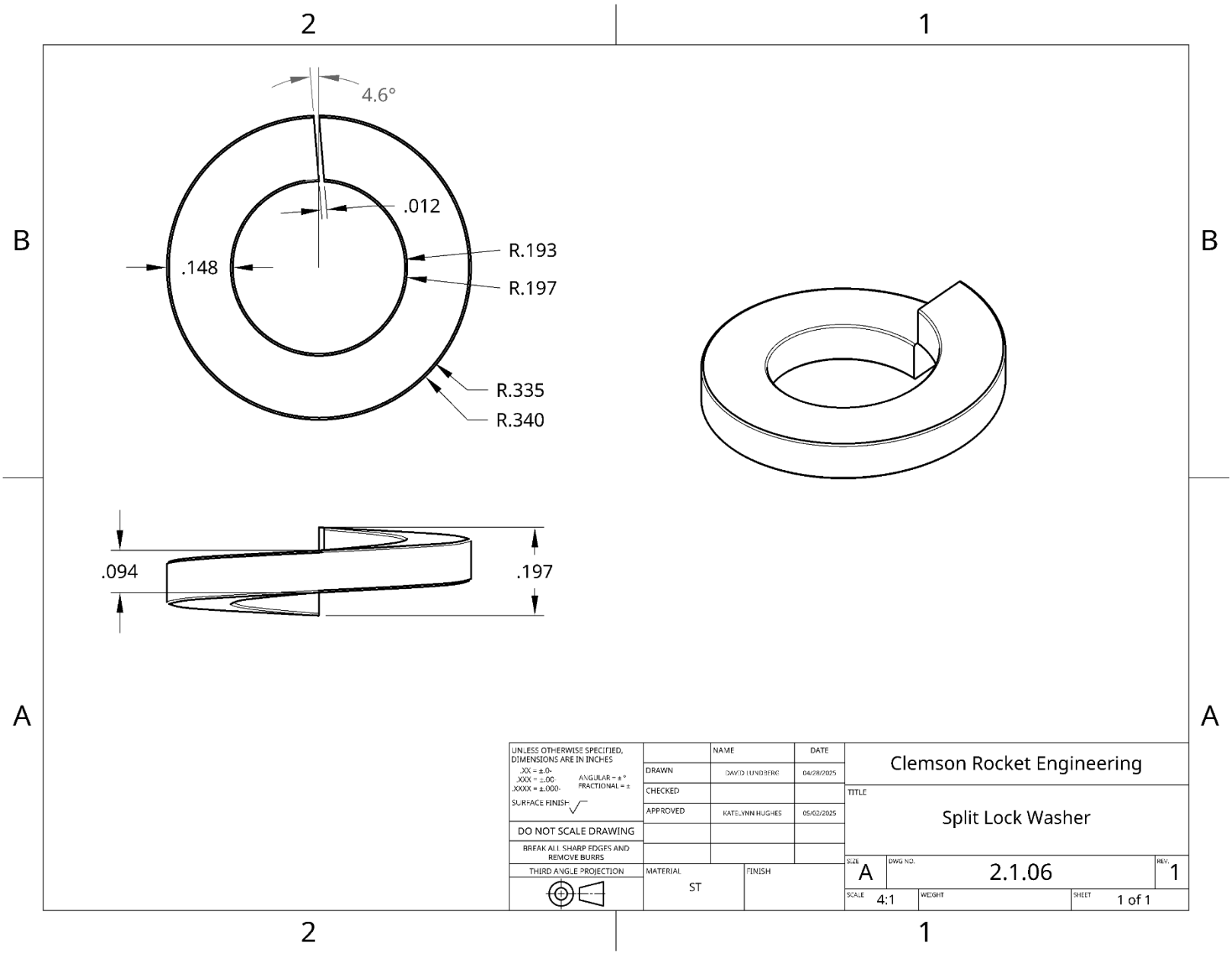
2
1
B
A
4.6°
.012
.148
R.193
R.197
R.335
R.340
.094
.197
UNLESS OTHERWISE SPECIFIED, DIMENSIONS ARE IN INCHES
.XX = ±.0-
.XXX = ±.00
.XXXX = ±.000-
ANGULAR = ± °
FRACTIONAL = ±
SURFACE FINISH
DO NOT SCALE DRAWING
BREAK ALL SHARP EDGES AND REMOVE BURRS
THIRD ANGLE PROJECTION
NAME
DATE
DRAWN
DAVID LUNDBERG
04/28/2025
CHECKED
APPROVED
KATELYNN HUGHES
05/02/2025
MATERIAL
ST
FINISH
Clemson Rocket Engineering
TITLE
Split Lock Washer
SIZE
A
DWG NO.
2.1.06
REV.
1
SCALE
4:1
WEIGHT
SHEET
1 of 1

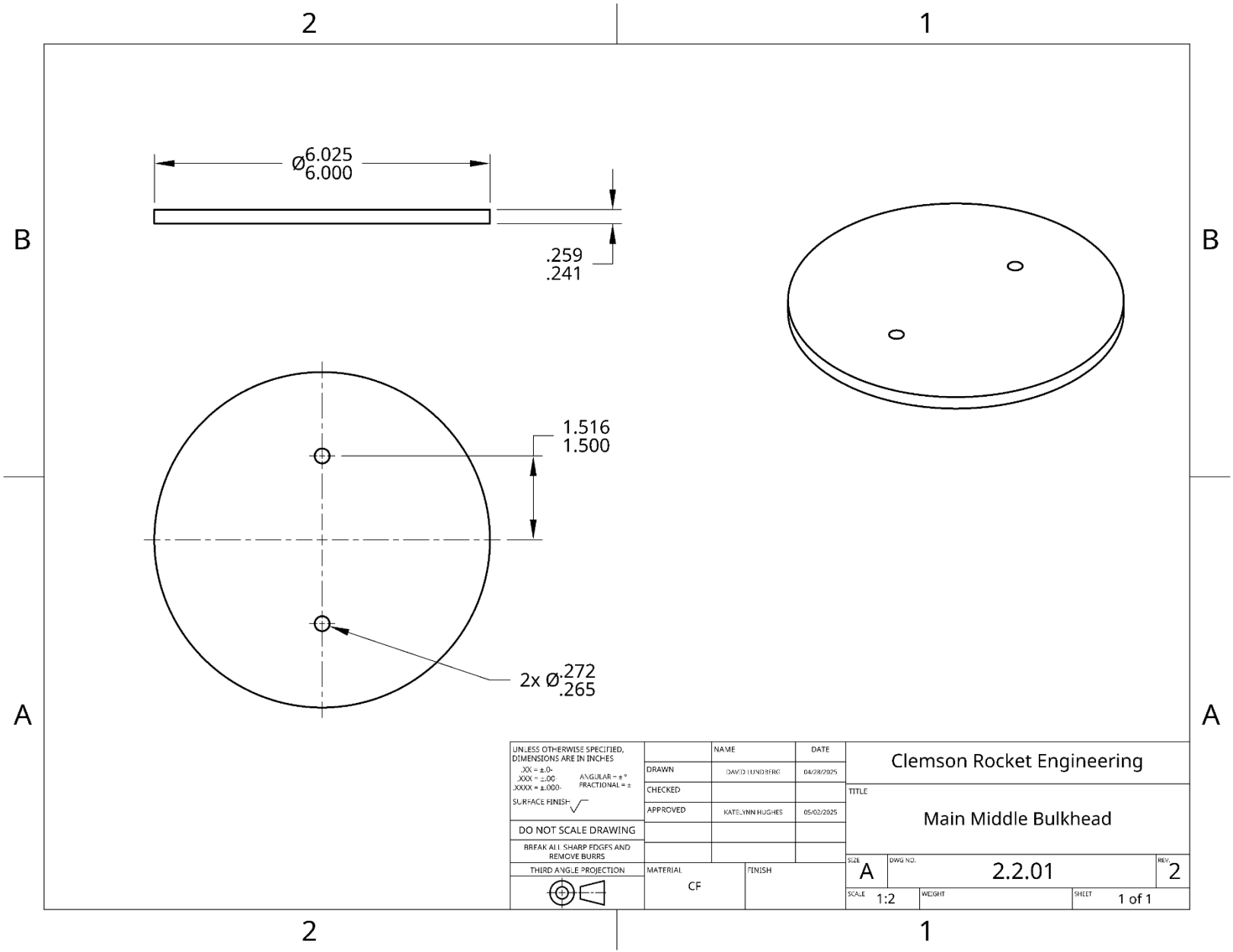
2
1
B
A
Ø6.025
6.000
.259
.241
1.516
1.500
2x Ø.272
.265
UNLESS OTHERWISE SPECIFIED, DIMENSIONS ARE IN INCHES
.XX = ±.0-
.XXX = ±.00
.XXXX = ±.000-
ANGULAR = ± °
FRACTIONAL = ±
SURFACE FINISH
DO NOT SCALE DRAWING
BREAK ALL SHARP EDGES AND REMOVE BURRS
THIRD ANGLE PROJECTION
NAME
DATE
DRAWN
DAVID LUNDBERG
04/28/2025
CHECKED
APPROVED
KATELYNN HUGHES
05/02/2025
MATERIAL
CF
FINISH
Clemson Rocket Engineering
TITLE
Main Middle Bulkhead
SIZE
A
DWG NO.
2.2.01
REV
2
SCALE
1:2
WEIGHT
SHEET
1 of 1

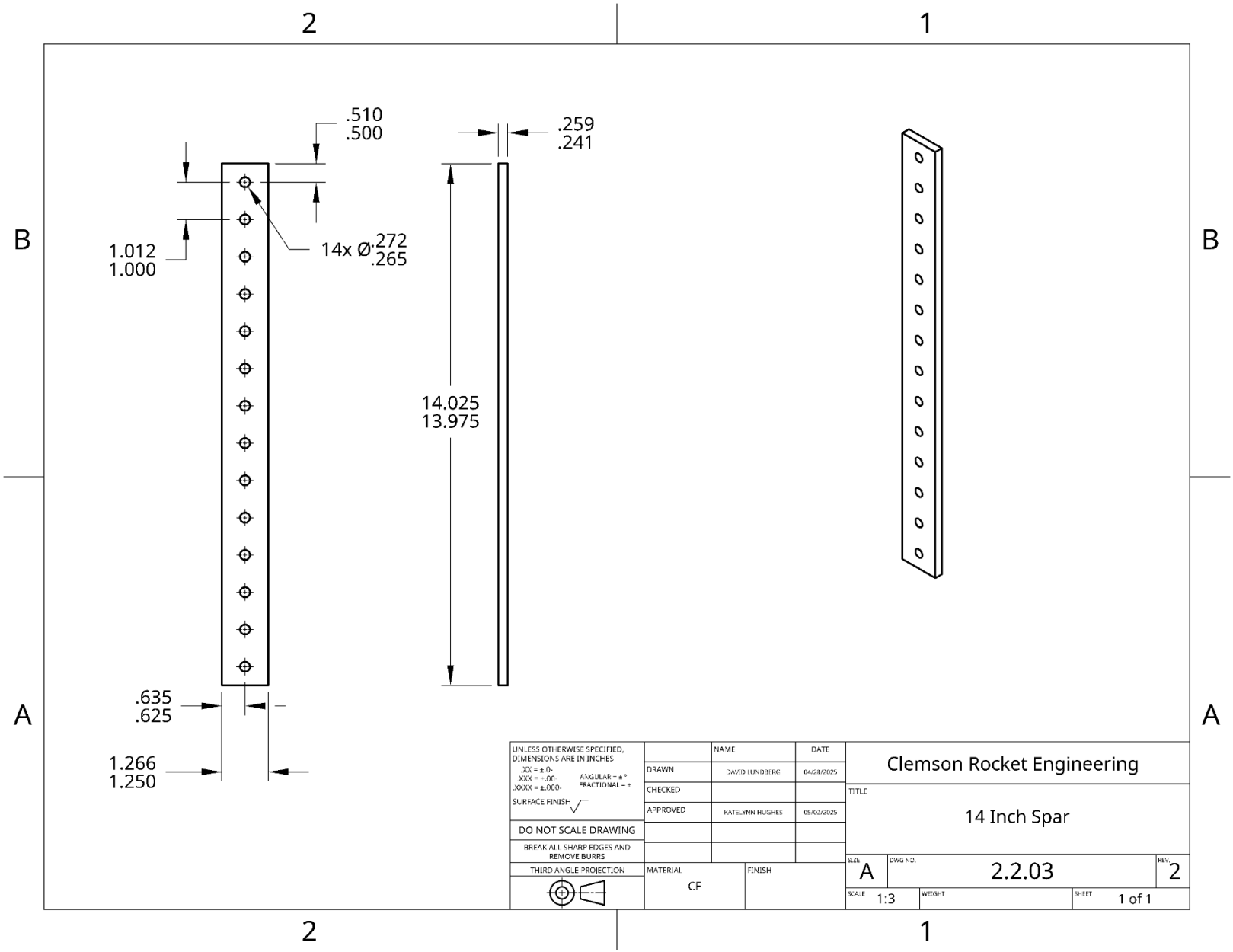
2
1
B
A
.510
.500
1.012
1.000
14x Ø.272
.265
.259
.241
14.025
13.975
.635
.625
1.266
1.250
UNLESS OTHERWISE SPECIFIED, DIMENSIONS ARE IN INCHES
.XX = ±.0-
.XXX = ±.00
.XXXX = ±.000-
ANGULAR = ± °
FRACTIONAL = ±
SURFACE FINISH
DO NOT SCALE DRAWING
BREAK ALL SHARP EDGES AND REMOVE BURRS
THIRD ANGLE PROJECTION
NAME
DATE
DRAWN
DAVID LUNDBERG
04/28/2025
CHECKED
APPROVED
KATELYNN HUGHES
05/02/2025
MATERIAL
CF
FINISH
Clemson Rocket Engineering
TITLE
14 Inch Spar
SIZE
A
DWG NO.
2.2.03
REV
2
SCALE
1:3
WEIGHT
SHEET
1 of 1

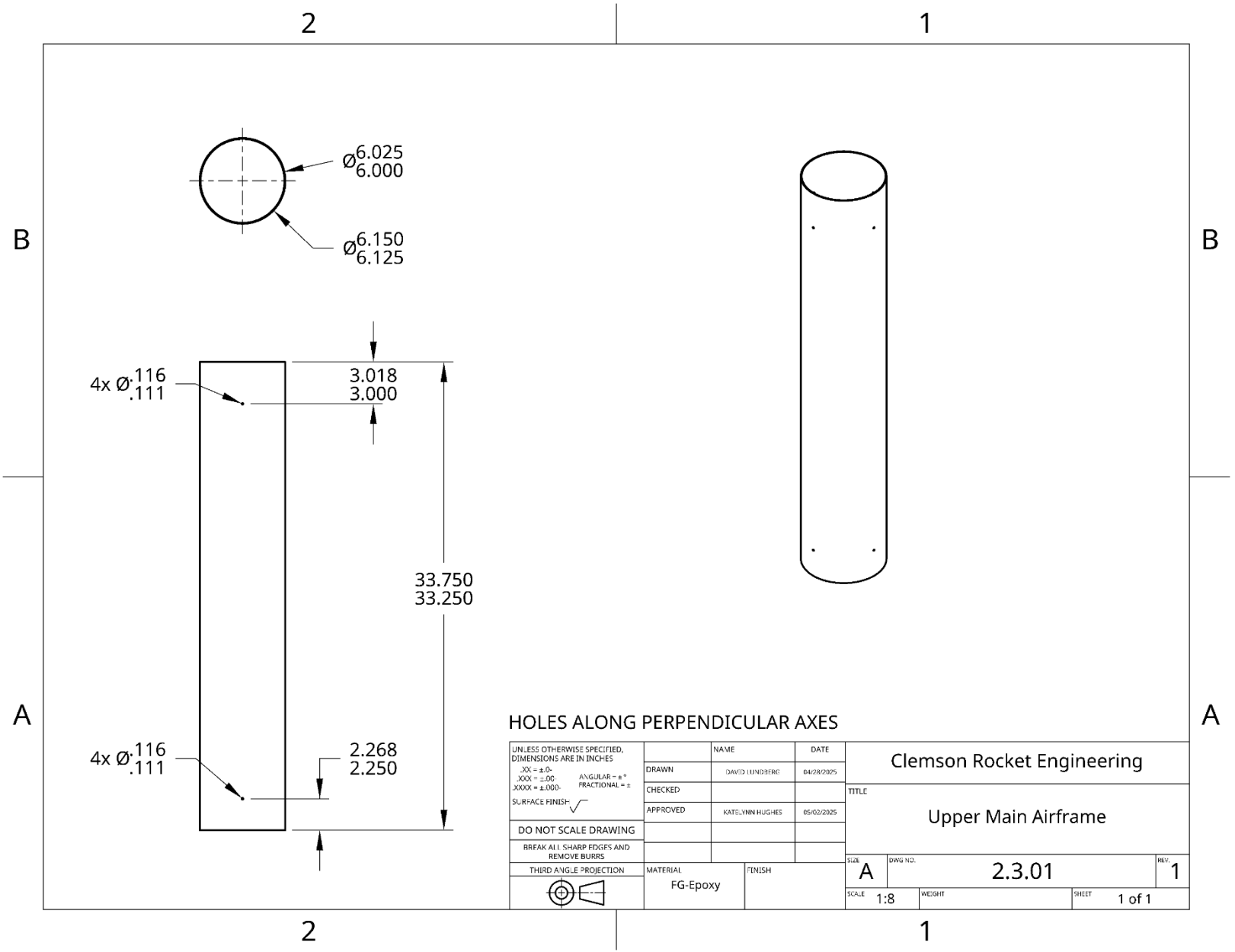
2
1
B
A
Ø6.025
6.000
Ø6.150
6.125
4x Ø.116
.111
3.018
3.000
33.750
33.250
4x Ø.116
.111
2.268
2.250
HOLES ALONG PERPENDICULAR AXES
UNLESS OTHERWISE SPECIFIED, DIMENSIONS ARE IN INCHES
.XX = ±.0-
.XXX = ±.00
.XXXX = ±.000-
ANGULAR = ± °
FRACTIONAL = ±
SURFACE FINISH
DO NOT SCALE DRAWING
BREAK ALL SHARP EDGES AND REMOVE BURRS
THIRD ANGLE PROJECTION
NAME
DATE
DRAWN
DAVID LUNDBERG
04/28/2025
CHECKED
APPROVED
KATELYNN HUGHES
05/02/2025
MATERIAL
FG-Epoxy
FINISH
Clemson Rocket Engineering
TITLE
Upper Main Airframe
SIZE
A
DWG NO.
2.3.01
REV.
1
SCALE
1:8
WEIGHT
SHEET
1 of 1

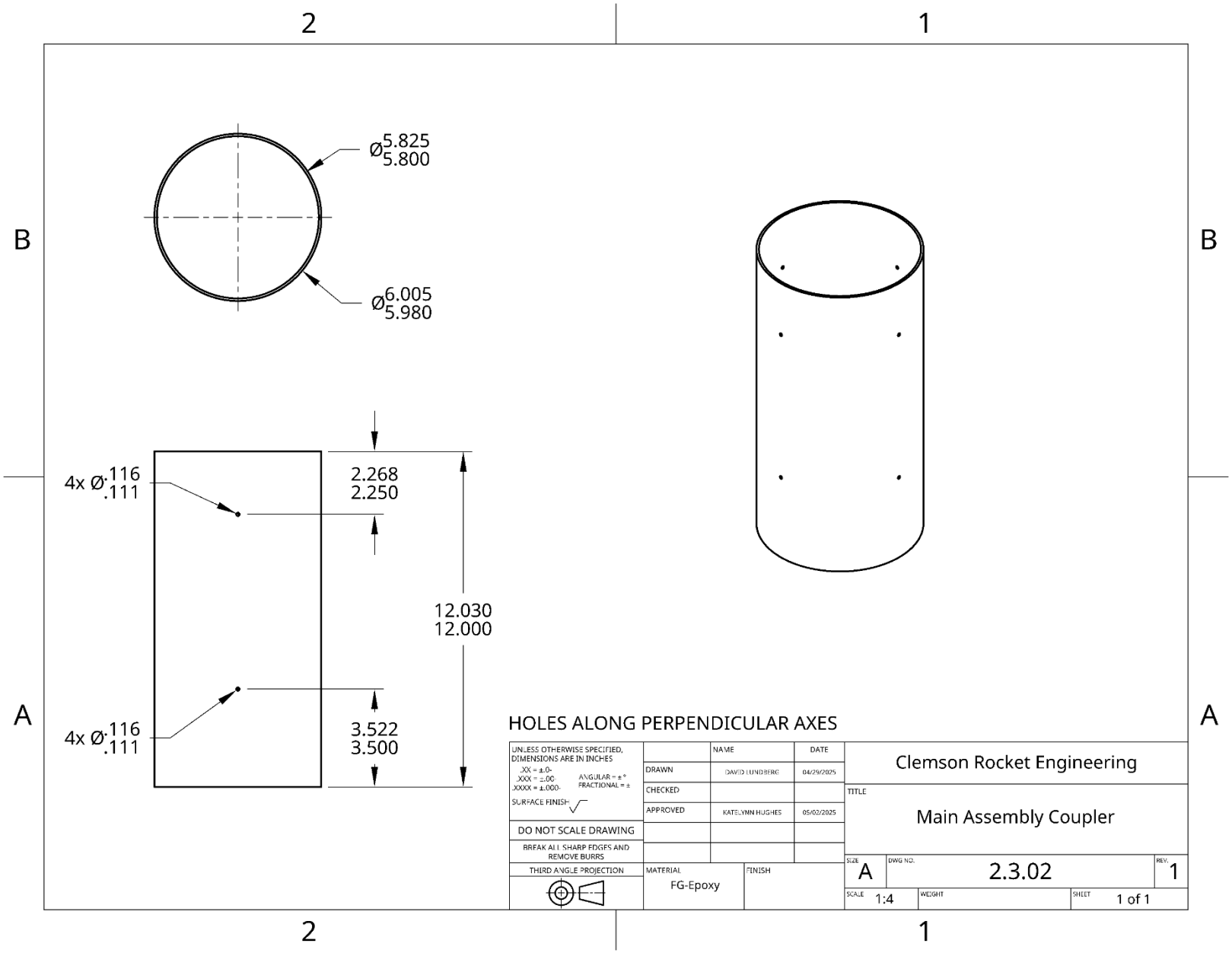
2
1
B
A
Ø5.825
5.800
Ø6.005
5.980
4x Ø.116
.111
2.268
2.250
12.030
12.000
4x Ø.116
.111
3.522
3.500
HOLES ALONG PERPENDICULAR AXES
UNLESS OTHERWISE SPECIFIED, DIMENSIONS ARE IN INCHES
.XX = ±.0-
.XXX = ±.00
.XXXX = ±.000-
ANGULAR = ± °
FRACTIONAL = ±
SURFACE FINISH
DO NOT SCALE DRAWING
BREAK ALL SHARP EDGES AND REMOVE BURRS
THIRD ANGLE PROJECTION
NAME
DATE
DRAWN
DAVID LUNDBERG
04/29/2025
CHECKED
APPROVED
KATELYNN HUGHES
05/02/2025
MATERIAL
FG-Epoxy
FINISH
Clemson Rocket Engineering
TITLE
Main Assembly Coupler
SIZE
A
DWG NO.
2.3.02
REV.
1
SCALE
1:4
WEIGHT
SHEET
1 of 1

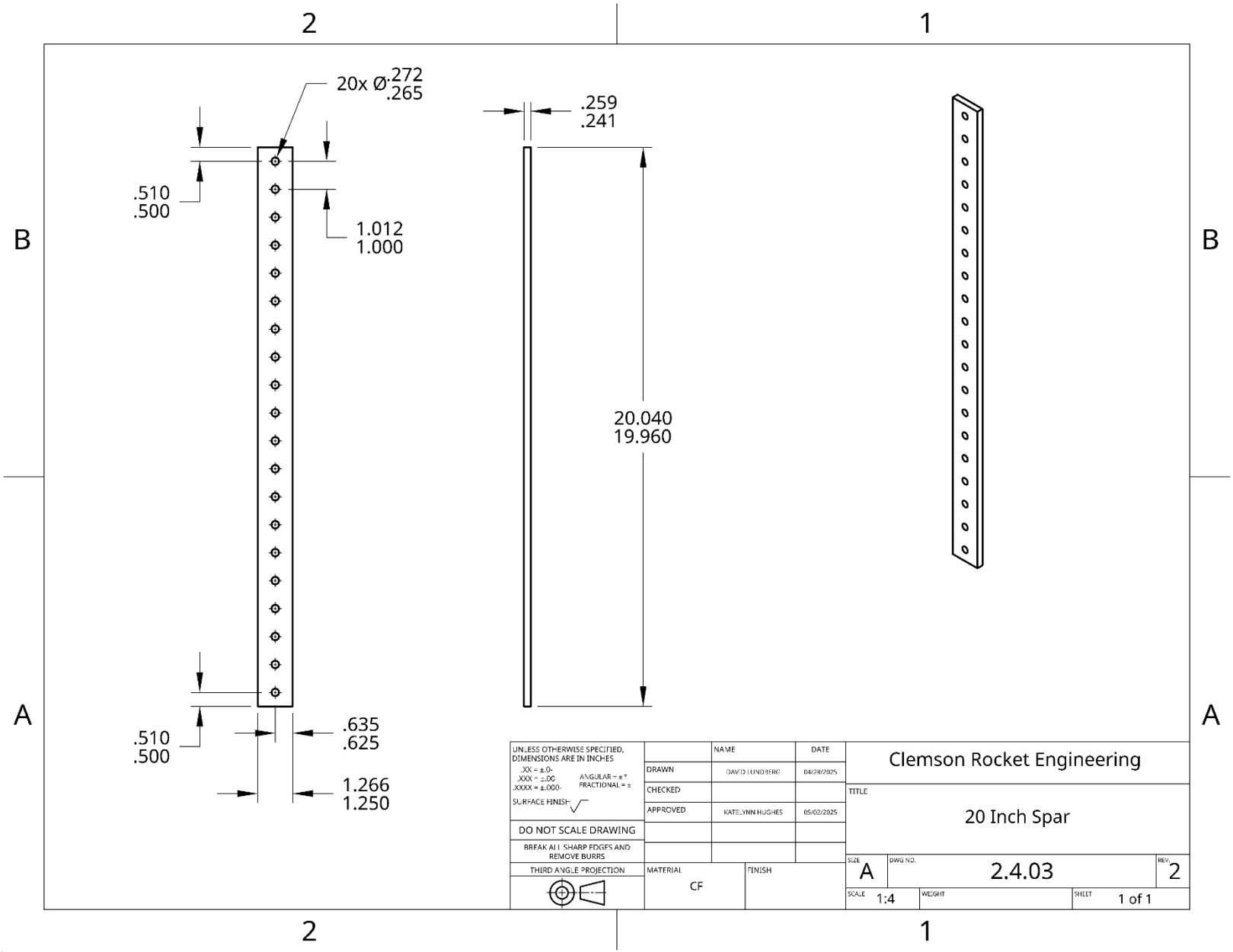
2
1
B
A
20x Ø.272
.265
.510
.500
1.012
1.000
.635
.625
.510
.500
1.266
1.250
.259
.241
20.040
19.960
UNLESS OTHERWISE SPECIFIED, DIMENSIONS ARE IN INCHES
.XX = ±.0-
.XXX = ±.00
.XXXX = ±.000-
ANGULAR = ± °
FRACTIONAL = ±
SURFACE FINISH
DO NOT SCALE DRAWING
BREAK ALL SHARP EDGES AND REMOVE BURRS
THIRD ANGLE PROJECTION
NAME
DATE
DRAWN
DAVID LUNDBERG
04/28/2025
CHECKED
APPROVED
KATELYNN HUGHES
05/02/2025
MATERIAL
CF
FINISH
Clemson Rocket Engineering
TITLE
20 Inch Spar
SIZE
A
DWG NO.
2.4.03
REV
2
SCALE
1:4
WEIGHT
SHEET
1 of 1

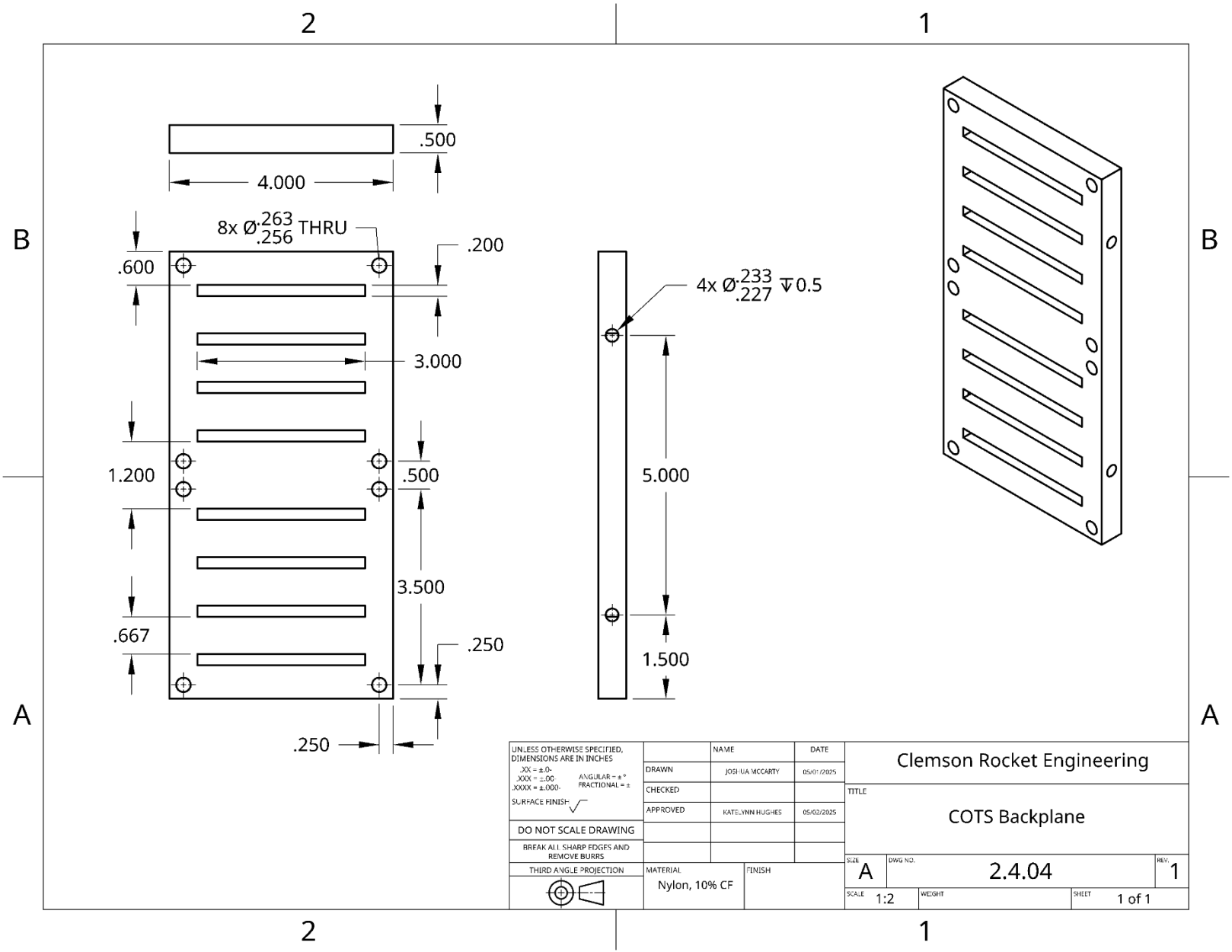
2
1
B
A
.500
4.000
8x Ø.263 .256 THRU
.200
.600
3.000
1.200
.500
3.500
.667
.250
.250
4x Ø.233 .227 ↧0.5
5.000
1.500
UNLESS OTHERWISE SPECIFIED, DIMENSIONS ARE IN INCHES
.XX = ±.0-
.XXX = ±.00
.XXXX = ±.000-
ANGULAR = ± °
FRACTIONAL = ±
SURFACE FINISH
DO NOT SCALE DRAWING
BREAK ALL SHARP EDGES AND REMOVE BURRS
THIRD ANGLE PROJECTION
NAME
DATE
DRAWN
JOSHUA MCCARTY
05/01/2025
CHECKED
APPROVED
KATELYNN HUGHES
05/02/2025
MATERIAL
Nylon, 10% CF
FINISH
Clemson Rocket Engineering
TITLE
COTS Backplane
SIZE
A
DWG NO.
2.4.04
REV.
1
SCALE
1:2
WEIGHT
SHEET
1 of 1

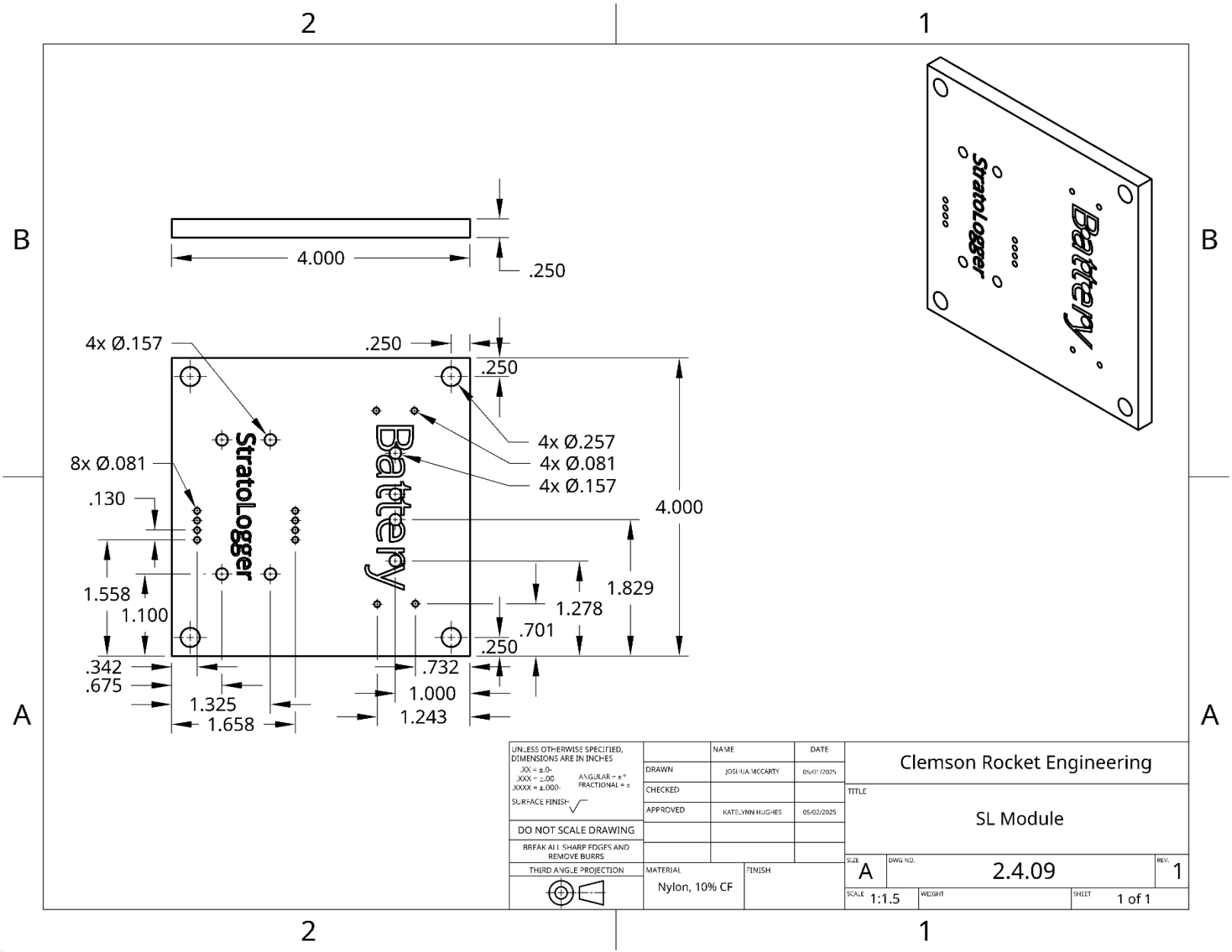
2
1
B
A
4.000
.250
4x Ø.157
.250
.250
4x Ø.257
4x Ø.081
4x Ø.157
8x Ø.081
.130
4.000
1.829
1.558
1.100
1.278
.701
.250
.342
.675
.732
1.000
1.243
1.325
1.658
StratoLogger
Battery
UNLESS OTHERWISE SPECIFIED, DIMENSIONS ARE IN INCHES
.XX = ±.0-
.XXX = ±.00
.XXXX = ±.000-
ANGULAR = ± °
FRACTIONAL = ±
SURFACE FINISH
DO NOT SCALE DRAWING
BREAK ALL SHARP EDGES AND REMOVE BURRS
THIRD ANGLE PROJECTION
NAME
DATE
DRAWN
JOSHUA MCCARTY
05/07/2025
CHECKED
APPROVED
KATELYNN HUGHES
05/02/2025
MATERIAL
Nylon, 10% CF
FINISH
Clemson Rocket Engineering
TITLE
SL Module
SIZE
A
DWG NO.
2.4.09
REV.
1
SCALE
1:1.5
WEIGHT
SHEET
1 of 1

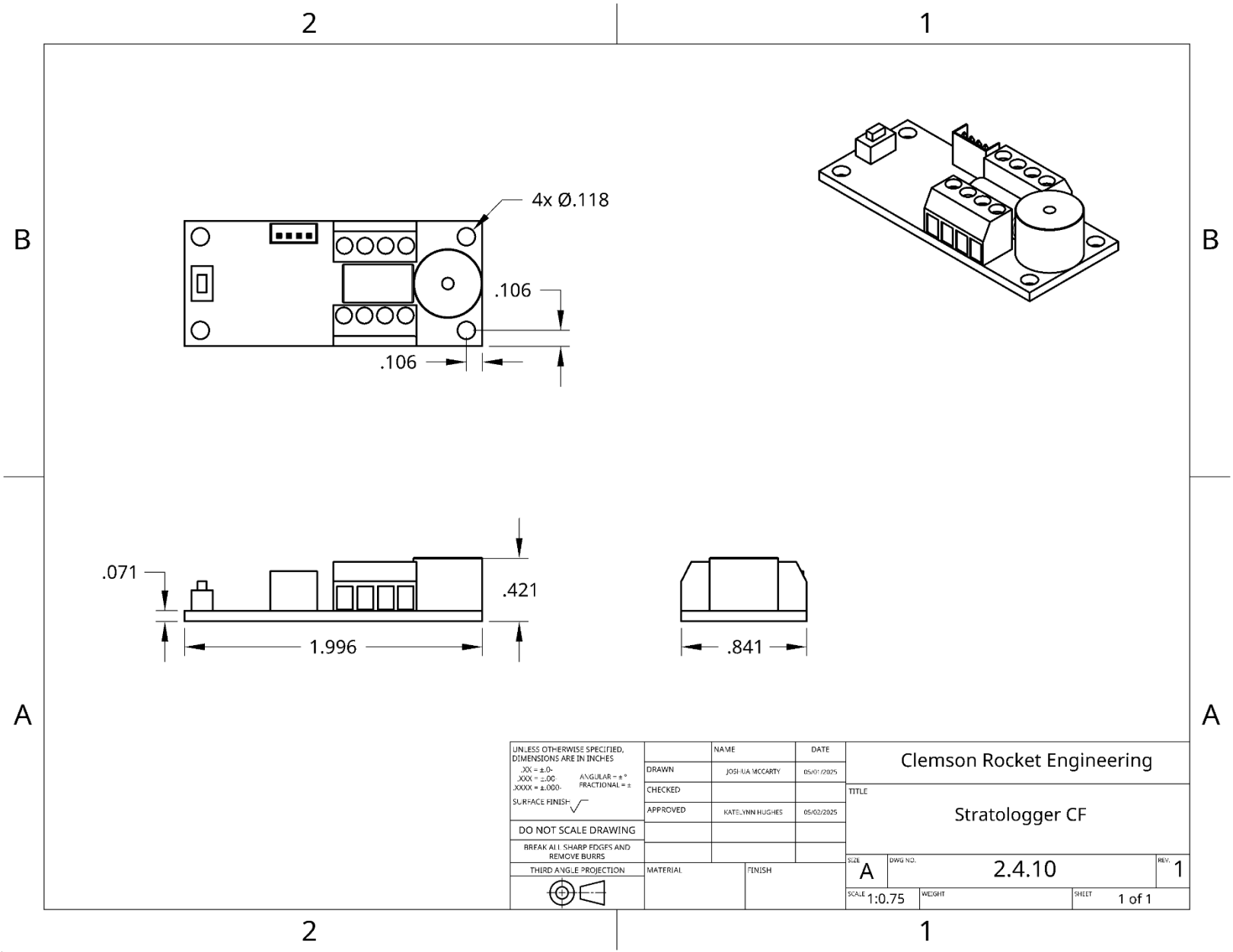
2
1
B
A
4x Ø.118
.106
.106
.071
.421
1.996
.841
UNLESS OTHERWISE SPECIFIED, DIMENSIONS ARE IN INCHES
.XX = ±.0-
.XXX = ±.00
.XXXX = ±.000-
ANGULAR = ± °
FRACTIONAL = ±
SURFACE FINISH
DO NOT SCALE DRAWING
BREAK ALL SHARP EDGES AND REMOVE BURRS
THIRD ANGLE PROJECTION
NAME
DATE
DRAWN
JOSHUA MCCARTY
05/07/2025
CHECKED
APPROVED
KATELYNN HUGHES
05/02/2025
MATERIAL
FINISH
Clemson Rocket Engineering
TITLE
Stratologger CF
SIZE
A
DWG NO.
2.4.10
REV.
1
SCALE
1:0.75
WEIGHT
SHEET
1 of 1

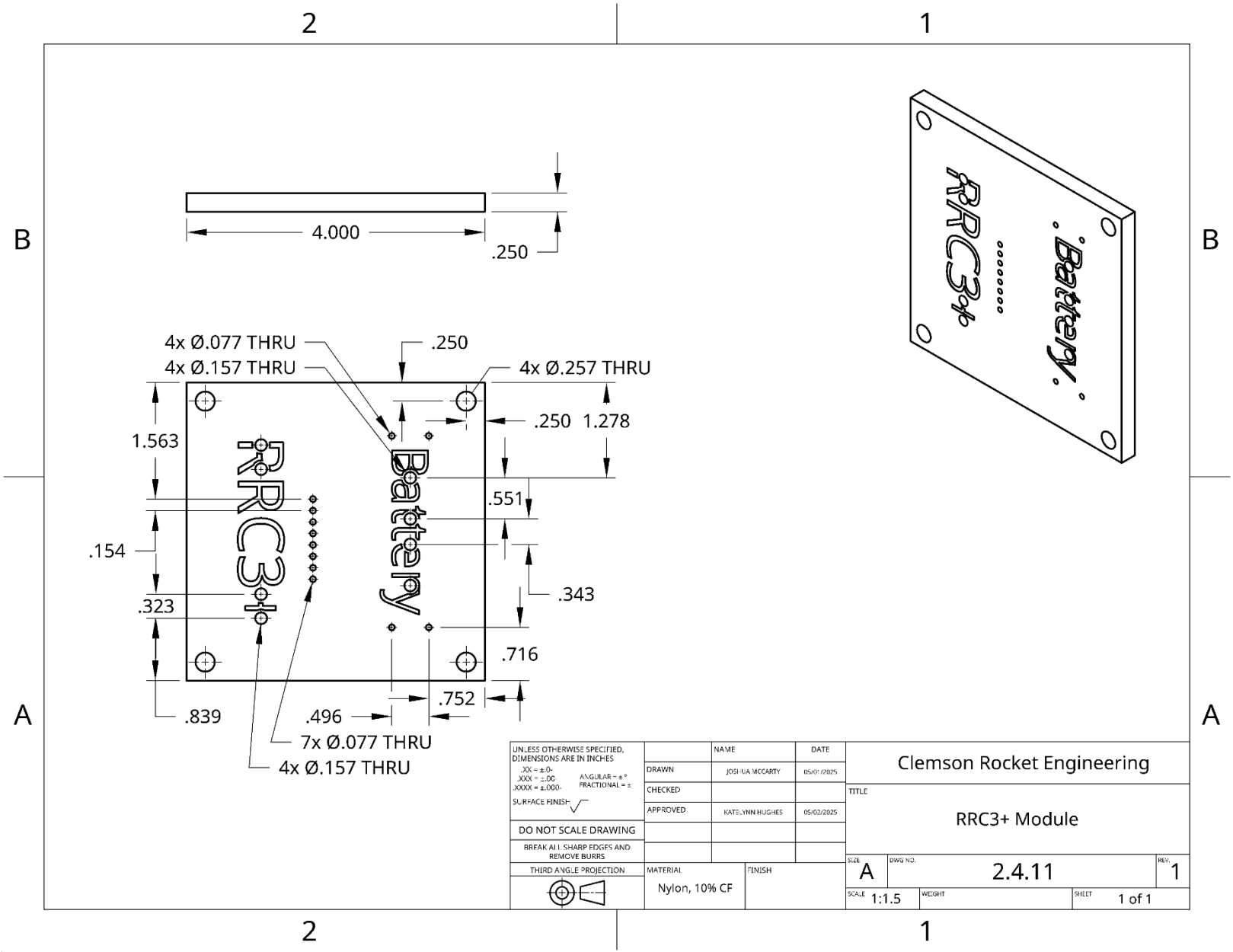
2
1
B
A
4.000
.250
4x Ø.077 THRU
4x Ø.157 THRU
.250
4x Ø.257 THRU
.250
1.278
1.563
.551
.154
.343
.323
.716
.839
.496
.752
7x Ø.077 THRU
4x Ø.157 THRU
RRC3+
Battery
UNLESS OTHERWISE SPECIFIED, DIMENSIONS ARE IN INCHES
.XX = ±.0-
.XXX = ±.00
.XXXX = ±.000-
ANGULAR = ± °
FRACTIONAL = ±
SURFACE FINISH
DO NOT SCALE DRAWING
BREAK ALL SHARP EDGES AND REMOVE BURRS
THIRD ANGLE PROJECTION
NAME
DATE
DRAWN
JOSHUA MCCARTY
05/07/2025
CHECKED
APPROVED
KATELYNN HUGHES
05/02/2025
MATERIAL
Nylon, 10% CF
FINISH
Clemson Rocket Engineering
TITLE
RRC3+ Module
SIZE
A
DWG NO.
2.4.11
REV.
1
SCALE
1:1.5
WEIGHT
SHEET
1 of 1

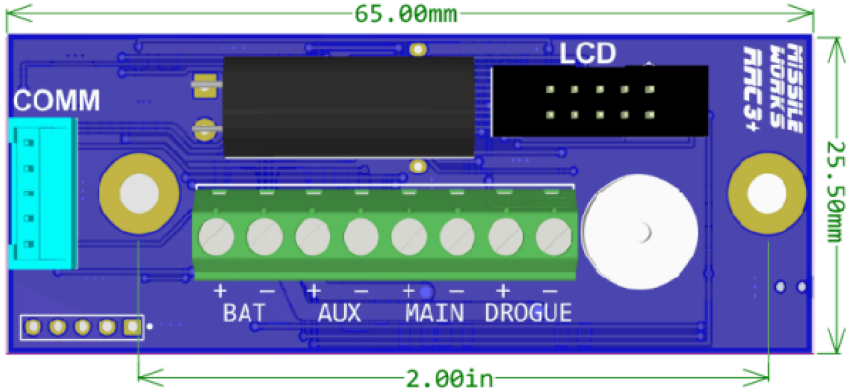

Clemson Rocket Engineering	
TITLE	RRC3+
SIZE A	DWG NO. 2.4.12
REV. 1	
SCALE	WEIGHT
SHEET 1 of 1	

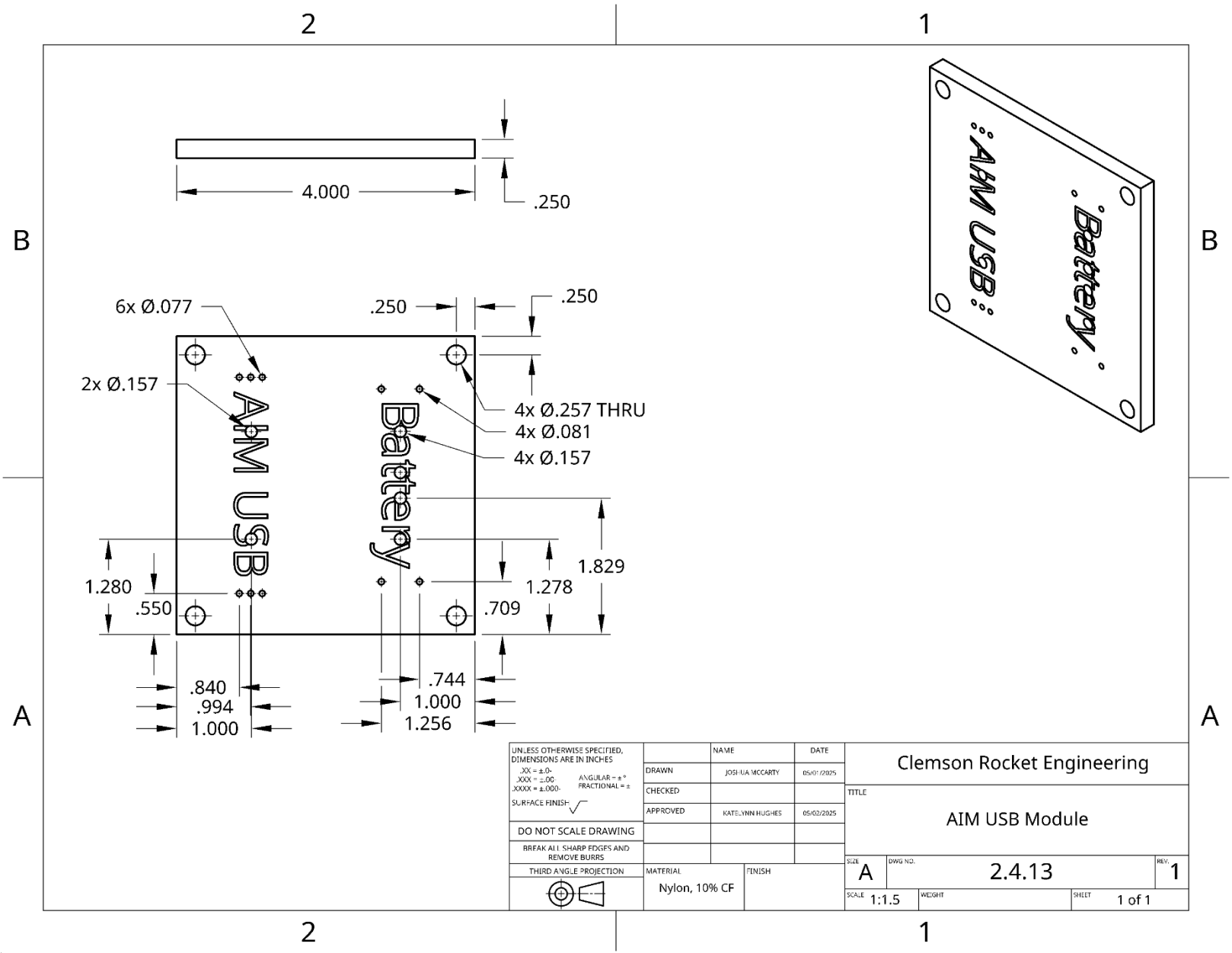
2
1
B
A
4.000
.250
6x Ø.077
.250
.250
2x Ø.157
4x Ø.257 THRU
4x Ø.081
4x Ø.157
AIM USB
Battery
1.280
.550
1.278
.709
1.829
.840
.994
1.000
.744
1.000
1.256
AIM USB
Battery
UNLESS OTHERWISE SPECIFIED, DIMENSIONS ARE IN INCHES
.XX = ±.0-
.XXX = ±.00
.XXXX = ±.000-
ANGULAR = ± °
FRACTIONAL = ±
SURFACE FINISH
DO NOT SCALE DRAWING
BREAK ALL SHARP EDGES AND REMOVE BURRS
THIRD ANGLE PROJECTION
NAME
DATE
DRAWN
JOSHUA MCCARTY
05/07/2025
CHECKED
APPROVED
KATELYNN HUGHES
05/02/2025
MATERIAL
Nylon, 10% CF
FINISH
Clemson Rocket Engineering
TITLE
AIM USB Module
SIZE
A
DWG NO.
2.4.13
REV
1
SCALE
1:1.5
WEIGHT
SHEET
1 of 1

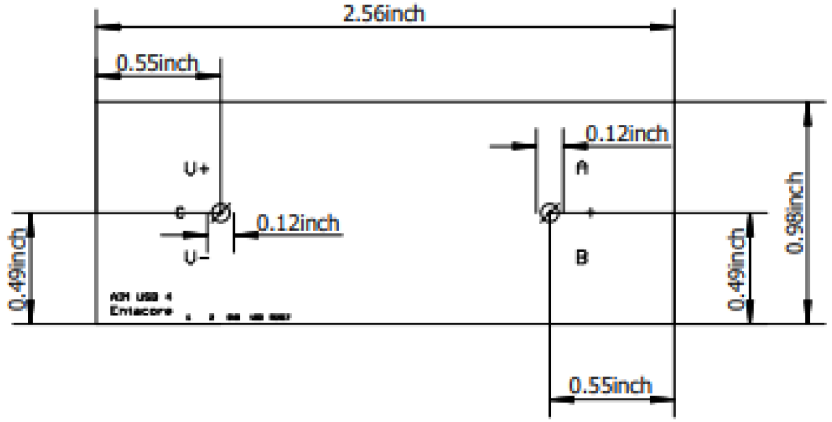

Clemson Rocket Engineering		
TITLE: AIM USB		
SIZE: A	DWG NO.: 2.4.14	REV: 1
SCALE:	WEIGHT:	SHEET: 1 of 1

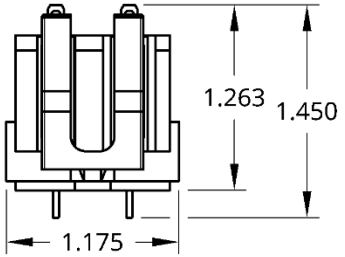

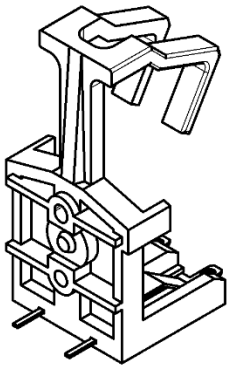

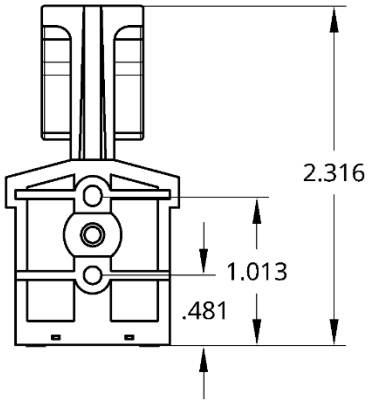

UNLESS OTHERWISE SPECIFIED, DIMENSIONS ARE IN INCHES .XX = ±.0- .XXX = ±.00 ANGULAR = ± ° .XXXX = ±.000- FRACTIONAL = ± SURFACE FINISH √		NAME	DATE
	DRAWN	JOSHUA MCCARTY	05/01/2025
	CHECKED		
	APPROVED	KATELYNN HUGHES	05/02/2025
DO NOT SCALE DRAWING			
BREAK ALL SHARP EDGES AND REMOVE BURRS			
THIRD ANGLE PROJECTION	MATERIAL	FINISH	
	Nylon		

Clemson Rocket Engineering		
TITLE: Battery Holder		
SIZE A	DWG NO. 2.4.15	REV 1
SCALE 1:1	WEIGHT	SHEET 1 of 1

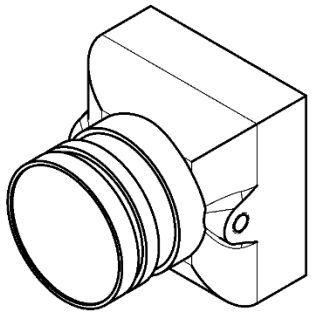

SCALE 2:1

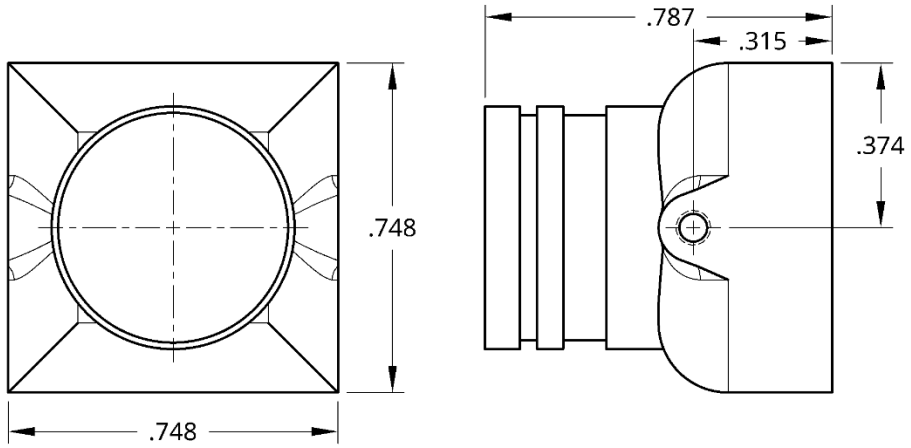

UNLESS OTHERWISE SPECIFIED, DIMENSIONS ARE IN INCHES .XX = ±.0- .XXX = ±.00 ANGULAR = ± ° .XXXX = ±.000- FRACTIONAL = ± SURFACE FINISH √		NAME	DATE
	DRAWN	JOSHUA MCCARTY	05/07/2025
	CHECKED		
	APPROVED	KATELYNN HUGHES	05/02/2025
DO NOT SCALE DRAWING			
BREAK ALL SHARP EDGES AND REMOVE BURRS			
THIRD ANGLE PROJECTION	MATERIAL	FINISH	

Clemson Rocket Engineering

TITLE: Runcam Split 3

SIZE	DWG NO.	REV
A	2.4.18	1
SCALE 3:1	WEIGHT	SHEET 1 of 1

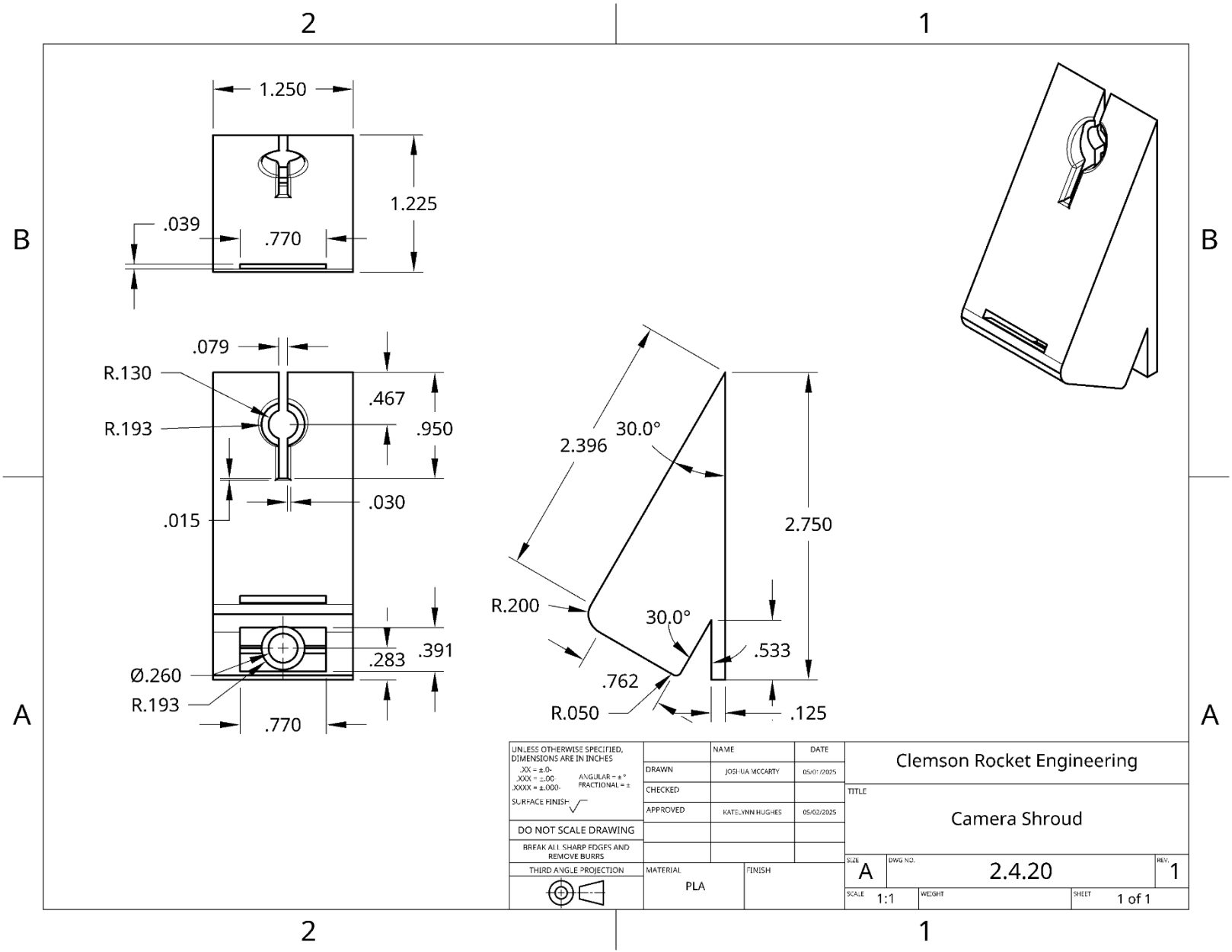
2
1
B
A
1.250
1.225
.039
.770
.079
R.130
R.193
.467
.950
.030
.015
.391
.283
Ø.260
R.193
.770
2.396
30.0°
2.750
R.200
30.0°
.533
.762
R.050
.125
UNLESS OTHERWISE SPECIFIED, DIMENSIONS ARE IN INCHES
.XX = ±.0-
.XXX = ±.00
.XXXX = ±.000-
ANGULAR = ± °
FRACTIONAL = ±
SURFACE FINISH
DO NOT SCALE DRAWING
BREAK ALL SHARP EDGES AND REMOVE BURRS
THIRD ANGLE PROJECTION
NAME
DATE
DRAWN
JOSHUA MCCARTY
05/07/2025
CHECKED
APPROVED
KATELYNN HUGHES
05/02/2025
MATERIAL
PLA
FINISH
Clemson Rocket Engineering
TITLE
Camera Shroud
SIZE
A
DWG NO.
2.4.20
REV.
1
SCALE
1:1
WEIGHT
SHEET
1 of 1

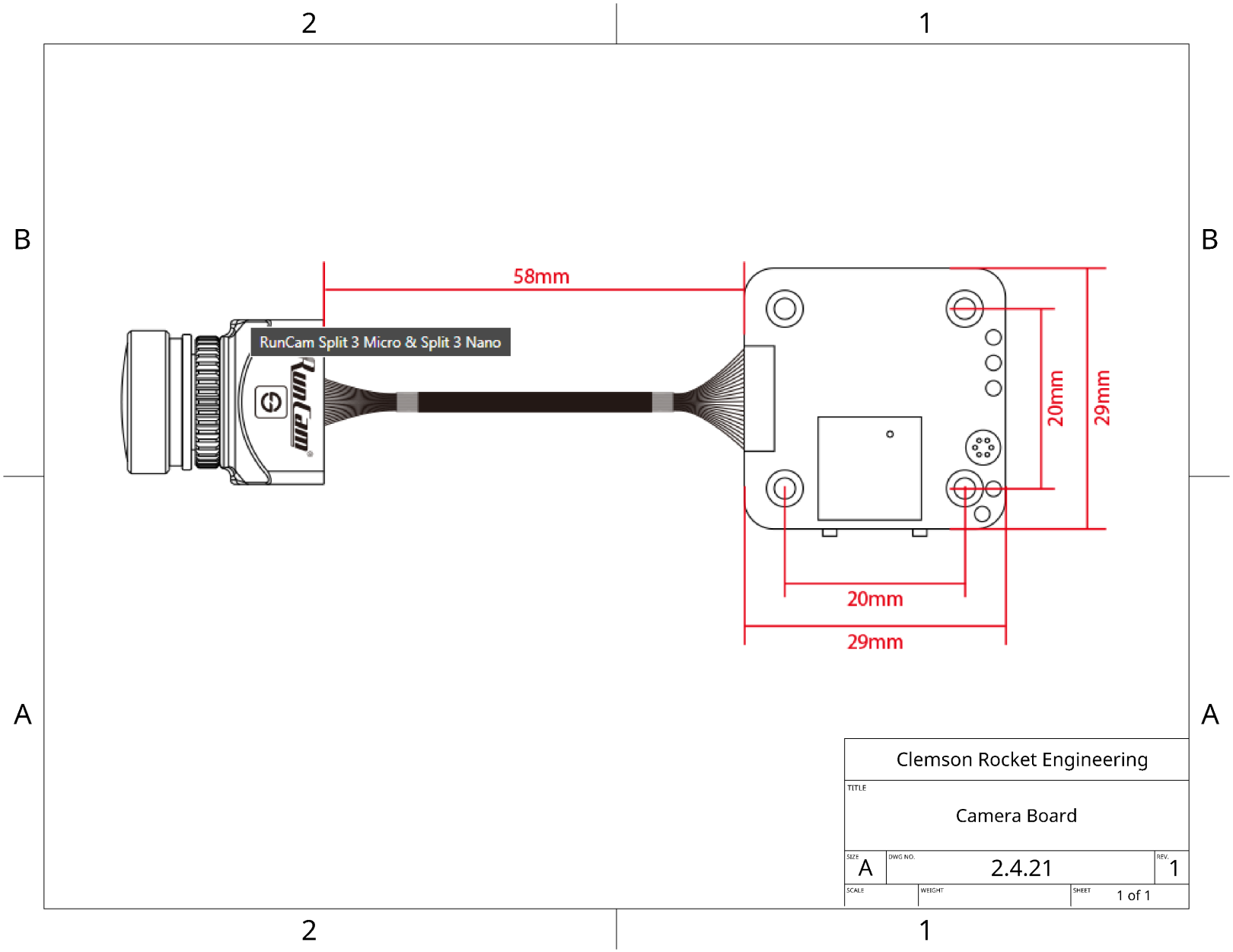
2
1
B
A
58mm
RunCam Split 3 Micro & Split 3 Nano
20mm
29mm
20mm
29mm
Clemson Rocket Engineering
TITLE
Camera Board
SIZE
A
DWG NO.
2.4.21
REV.
1
SCALE
WEIGHT
SHEET
1 of 1

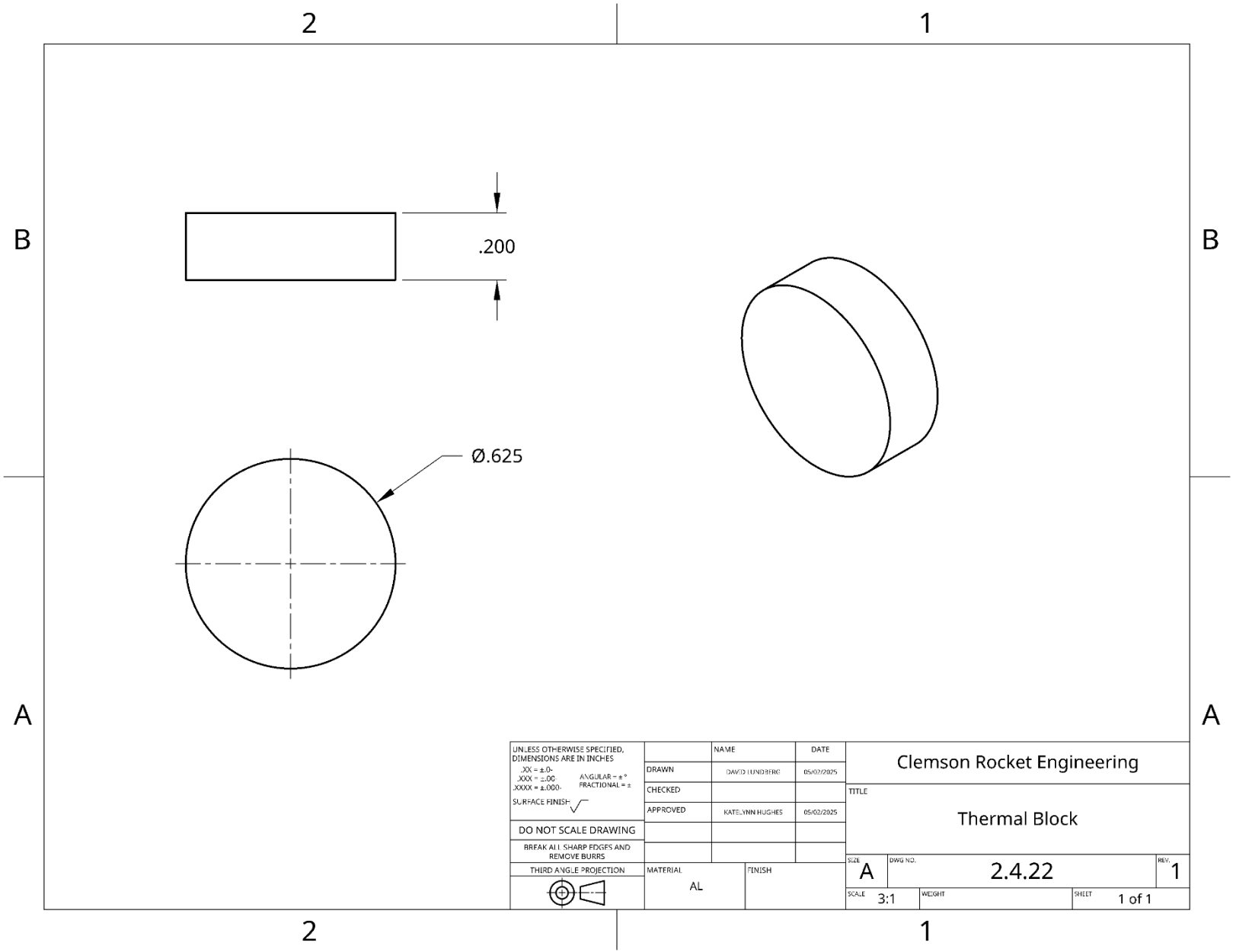
2
1
B
A
.200
Ø.625
UNLESS OTHERWISE SPECIFIED, DIMENSIONS ARE IN INCHES
.XX = ±.0-
.XXX = ±.00
.XXXX = ±.000-
ANGULAR = ± °
FRACTIONAL = ±
SURFACE FINISH
DO NOT SCALE DRAWING
BREAK ALL SHARP EDGES AND REMOVE BURRS
THIRD ANGLE PROJECTION
NAME
DATE
DRAWN
DAVID LUNDBERG
05/02/2025
CHECKED
APPROVED
KATELYNN HUGHES
05/02/2025
MATERIAL
AL
FINISH
Clemson Rocket Engineering
TITLE
Thermal Block
SIZE
A
DWG NO.
2.4.22
REV.
1
SCALE
3:1
WEIGHT
SHEET
1 of 1

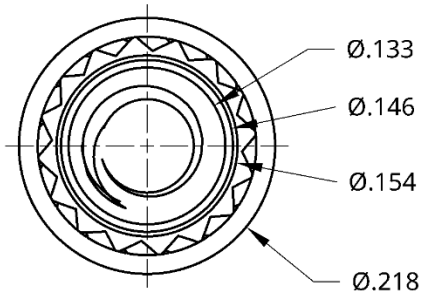

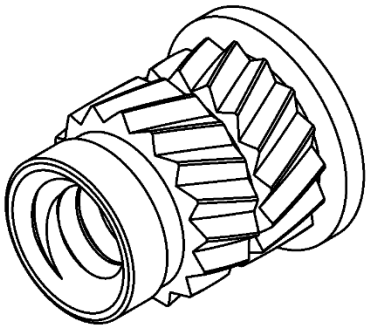

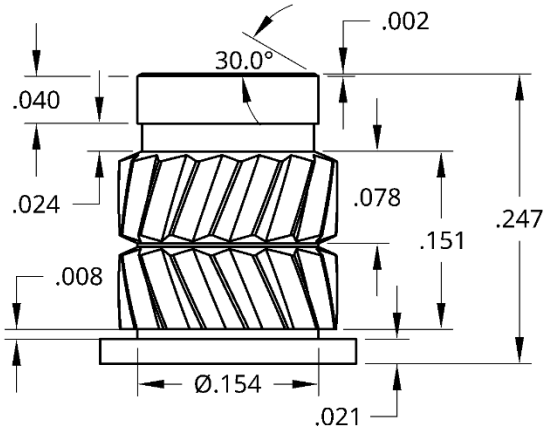

UNLESS OTHERWISE SPECIFIED, DIMENSIONS ARE IN INCHES .XX = ±.0- .XXX = ±.00 ANGULAR = ± ° .XXXX = ±.000- FRACTIONAL = ± SURFACE FINISH		NAME	DATE
	DRAWN	DAVID LUNDBERG	05/07/2025
	CHECKED		
	APPROVED	KATELYNN HUGHES	05/02/2025
DO NOT SCALE DRAWING			
BREAK ALL SHARP EDGES AND REMOVE BURRS			
THIRD ANGLE PROJECTION	MATERIAL: BR	FINISH	

Clemson Rocket Engineering

TITLE: Brass Heat-Set Insert

SIZE	DWG NO.	REV.
A	2.4.24	1
SCALE 8:1	WEIGHT	SHEET 1 of 1

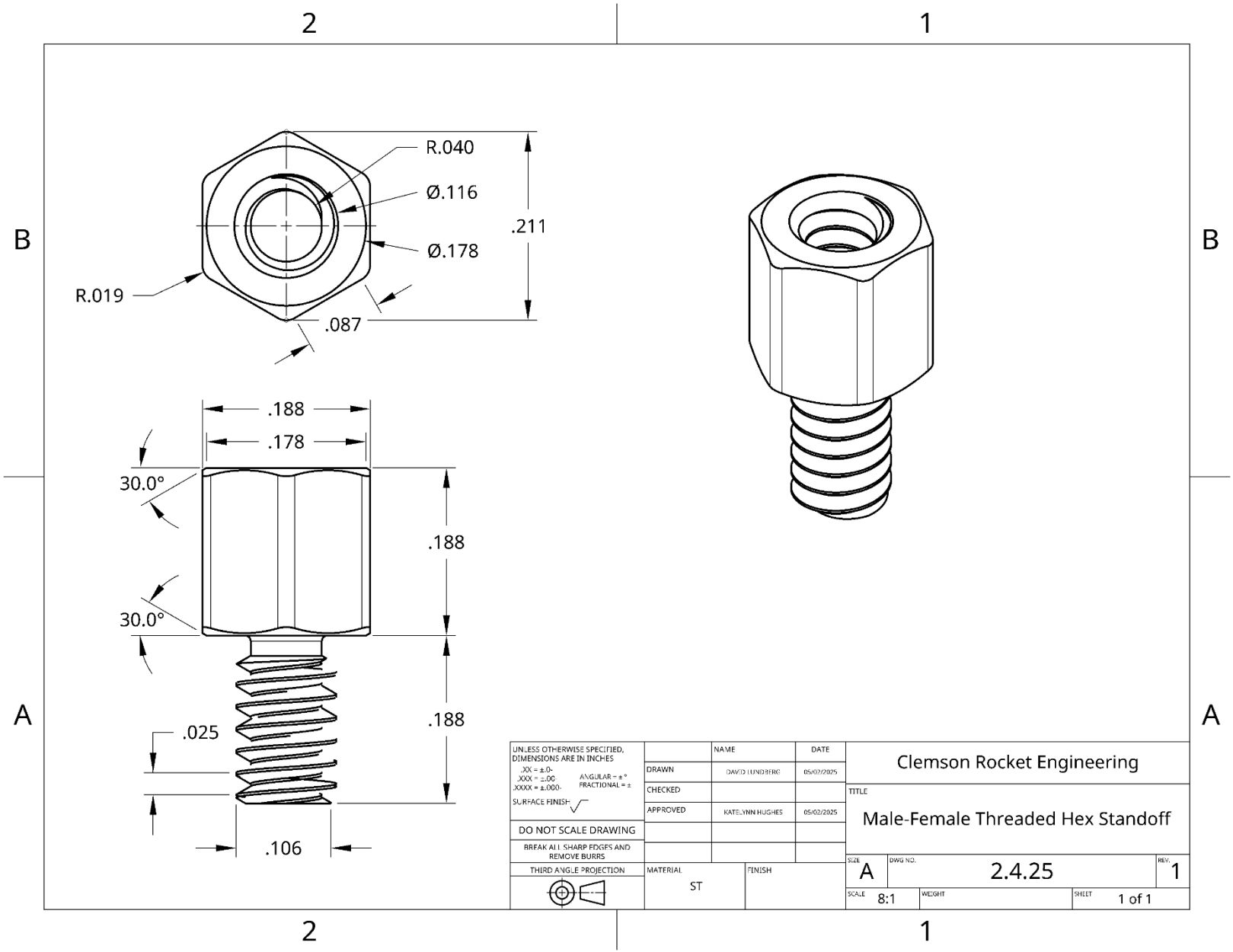
2
1
B
A
R.040
Ø.116
Ø.178
.211
R.019
.087
.188
.178
30.0°
.188
30.0°
.188
.025
.106
UNLESS OTHERWISE SPECIFIED, DIMENSIONS ARE IN INCHES
.XX = ±.0-
.XXX = ±.00
.XXXX = ±.000-
ANGULAR = ± °
FRACTIONAL = ±
SURFACE FINISH
DO NOT SCALE DRAWING
BREAK ALL SHARP EDGES AND REMOVE BURRS
THIRD ANGLE PROJECTION
NAME
DATE
DRAWN
DAVID LUNDBERG
05/02/2025
CHECKED
APPROVED
KATELYNN HUGHES
05/02/2025
MATERIAL
ST
FINISH
Clemson Rocket Engineering
TITLE
Male-Female Threaded Hex Standoff
SIZE
A
DWG NO.
2.4.25
REV.
1
SCALE
8:1
WEIGHT
SHEET
1 of 1

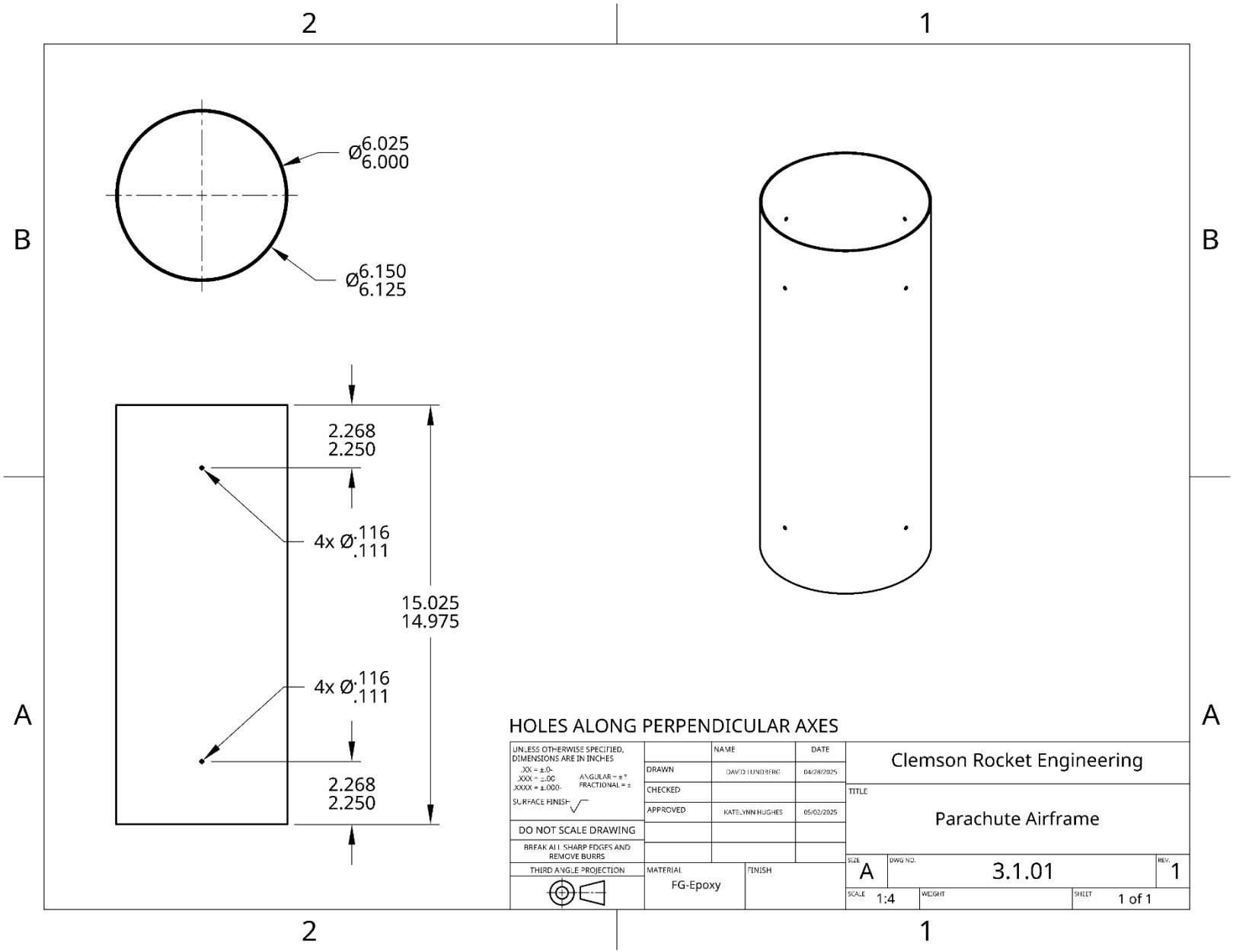
2
1
B
A
Ø6.025
6.000
Ø6.150
6.125
2.268
2.250
4x Ø.116
.111
15.025
14.975
4x Ø.116
.111
2.268
2.250
HOLES ALONG PERPENDICULAR AXES
UNLESS OTHERWISE SPECIFIED, DIMENSIONS ARE IN INCHES
.XX = ±.0-
.XXX = ±.00
.XXXX = ±.000-
ANGULAR = ± °
FRACTIONAL = ±
SURFACE FINISH
DO NOT SCALE DRAWING
BREAK ALL SHARP EDGES AND REMOVE BURRS
THIRD ANGLE PROJECTION
NAME
DATE
DRAWN
DAVID LUNDBERG
04/28/2025
CHECKED
APPROVED
KATELYNN HUGHES
05/02/2025
MATERIAL
FG-Epoxy
FINISH
Clemson Rocket Engineering
TITLE
Parachute Airframe
SIZE
A
DWG NO.
3.1.01
REV.
1
SCALE
1:4
WEIGHT
SHEET
1 of 1

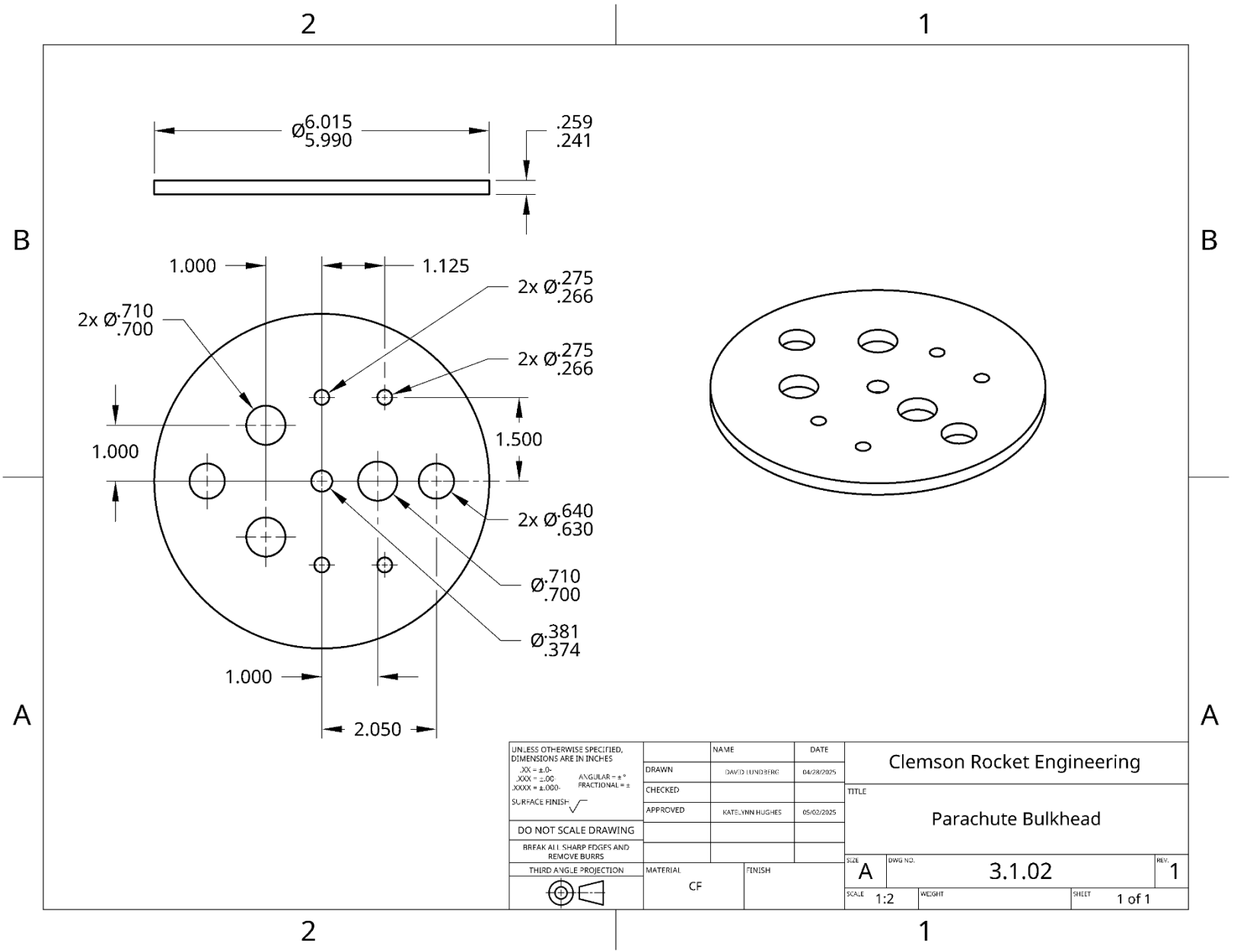
2
1
B
A
Ø6.015
5.990
.259
.241
1.000
1.125
2x Ø.275
.266
2x Ø.710
.700
2x Ø.275
.266
1.500
1.000
2x Ø.640
.630
Ø.710
.700
Ø.381
.374
1.000
2.050
UNLESS OTHERWISE SPECIFIED, DIMENSIONS ARE IN INCHES
.XX = ±.0-
.XXX = ±.00
.XXXX = ±.000-
ANGULAR = ± °
FRACTIONAL = ±
SURFACE FINISH
DO NOT SCALE DRAWING
BREAK ALL SHARP EDGES AND REMOVE BURRS
THIRD ANGLE PROJECTION
NAME
DATE
DRAWN
DAVID LUNDBERG
04/28/2025
CHECKED
APPROVED
KATELYNN HUGHES
05/02/2025
MATERIAL
CF
FINISH
Clemson Rocket Engineering
TITLE
Parachute Bulkhead
SIZE
A
DWG NO.
3.1.02
REV.
1
SCALE
1:2
WEIGHT
SHEET
1 of 1

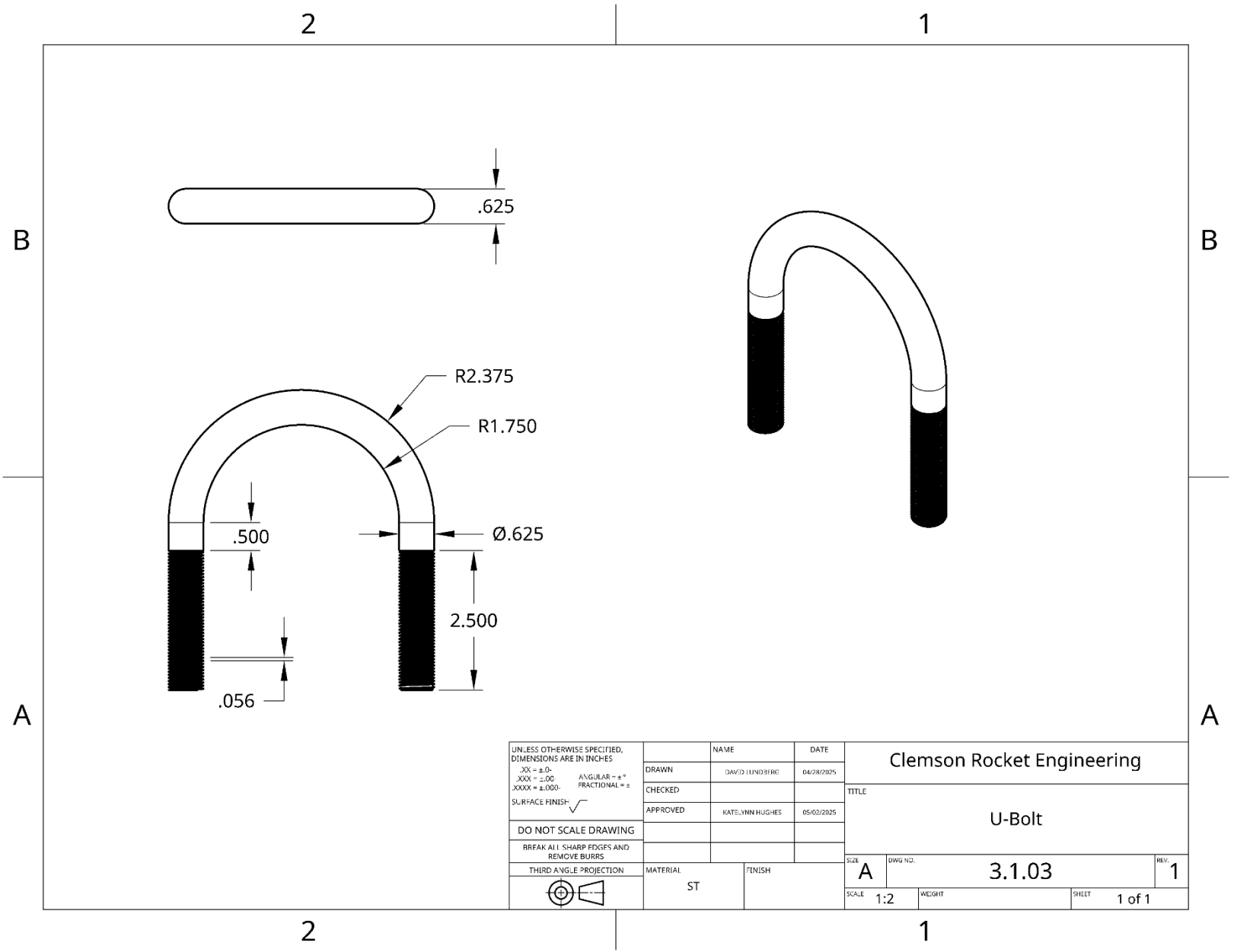
2
1
B
A
.625
R2.375
R1.750
.500
Ø.625
2.500
.056
UNLESS OTHERWISE SPECIFIED, DIMENSIONS ARE IN INCHES
.XX = ±.0-
.XXX = ±.00
.XXXX = ±.000-
ANGULAR = ± °
FRACTIONAL = ±
SURFACE FINISH
DO NOT SCALE DRAWING
BREAK ALL SHARP EDGES AND REMOVE BURRS
THIRD ANGLE PROJECTION
NAME
DATE
DRAWN
DAVID LUNDBERG
04/28/2025
CHECKED
APPROVED
KATELYNN HUGHES
05/02/2025
MATERIAL
ST
FINISH
Clemson Rocket Engineering
TITLE
U-Bolt
SIZE
A
DWG NO.
3.1.03
REV.
1
SCALE
1:2
WEIGHT
SHEET
1 of 1

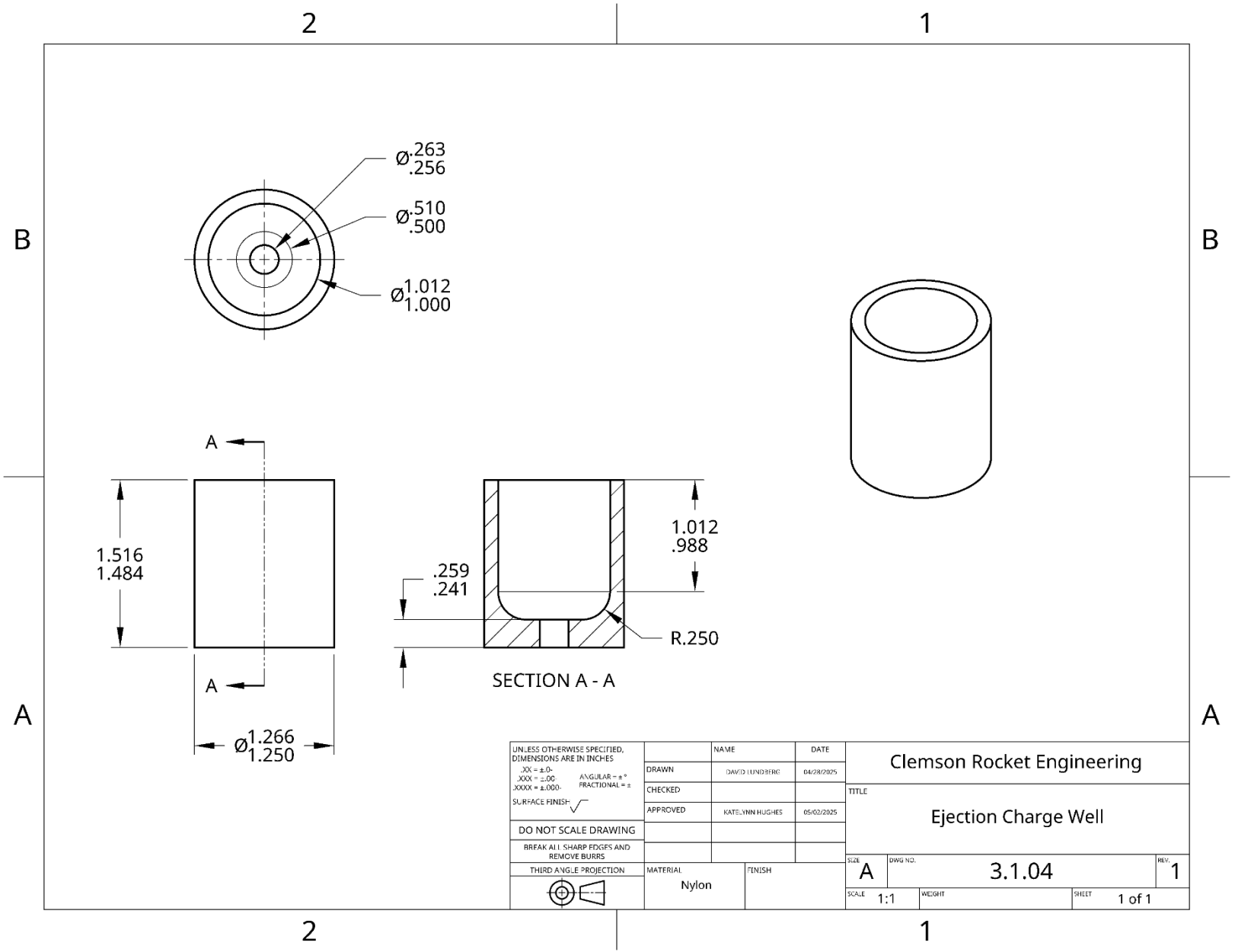
2
1
B
A
Ø.263
.256
Ø.510
.500
Ø1.012
1.000
A
1.516
1.484
A
Ø1.266
1.250
.259
.241
1.012
.988
R.250
SECTION A - A
UNLESS OTHERWISE SPECIFIED, DIMENSIONS ARE IN INCHES
.XX = ±.0-
.XXX = ±.00
.XXXX = ±.000-
ANGULAR = ± °
FRACTIONAL = ±
SURFACE FINISH
DO NOT SCALE DRAWING
BREAK ALL SHARP EDGES AND REMOVE BURRS
THIRD ANGLE PROJECTION
NAME
DATE
DRAWN
DAVID LUNDBERG
04/28/2025
CHECKED
APPROVED
KATELYNN HUGHES
05/02/2025
MATERIAL
Nylon
FINISH
Clemson Rocket Engineering
TITLE
Ejection Charge Well
SIZE
A
DWG NO.
3.1.04
REV.
1
SCALE
1:1
WEIGHT
SHEET
1 of 1

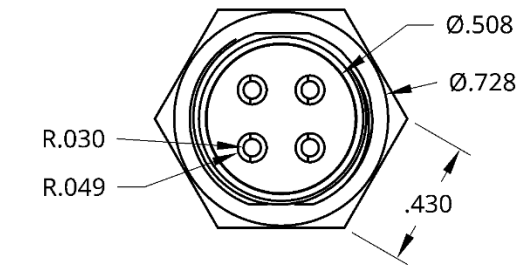

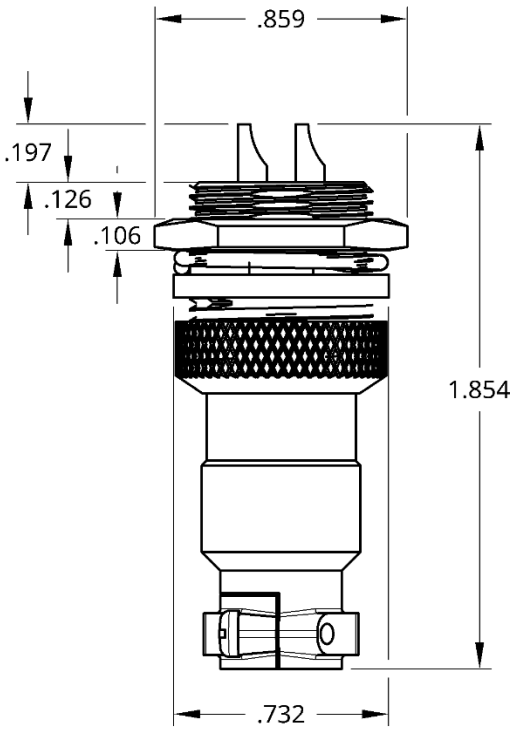

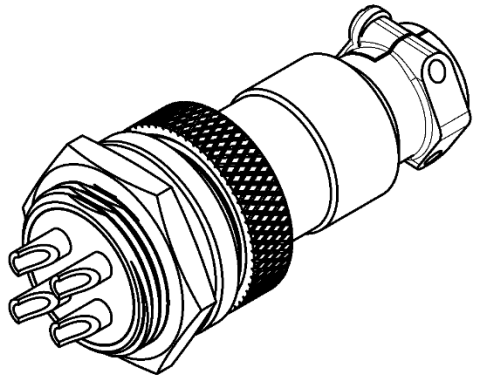

UNLESS OTHERWISE SPECIFIED, DIMENSIONS ARE IN INCHES .XX = ±.0- .XXX = ±.00 ANGULAR = ± ° .XXXX = ±.000- FRACTIONAL = ± SURFACE FINISH		NAME	DATE
	DRAWN	DAVID LUNDBERG	05/02/2025
	CHECKED		
	APPROVED	KATELYNN HUGHES	05/02/2025
DO NOT SCALE DRAWING			
BREAK ALL SHARP EDGES AND REMOVE BURRS			
THIRD ANGLE PROJECTION	MATERIAL: ST	FINISH	

Clemson Rocket Engineering		
TITLE: Aviation Connector		
SIZE: A	DWG NO.: 3.1.05	REV: 1
SCALE: 2:1	WEIGHT	SHEET: 1 of 1

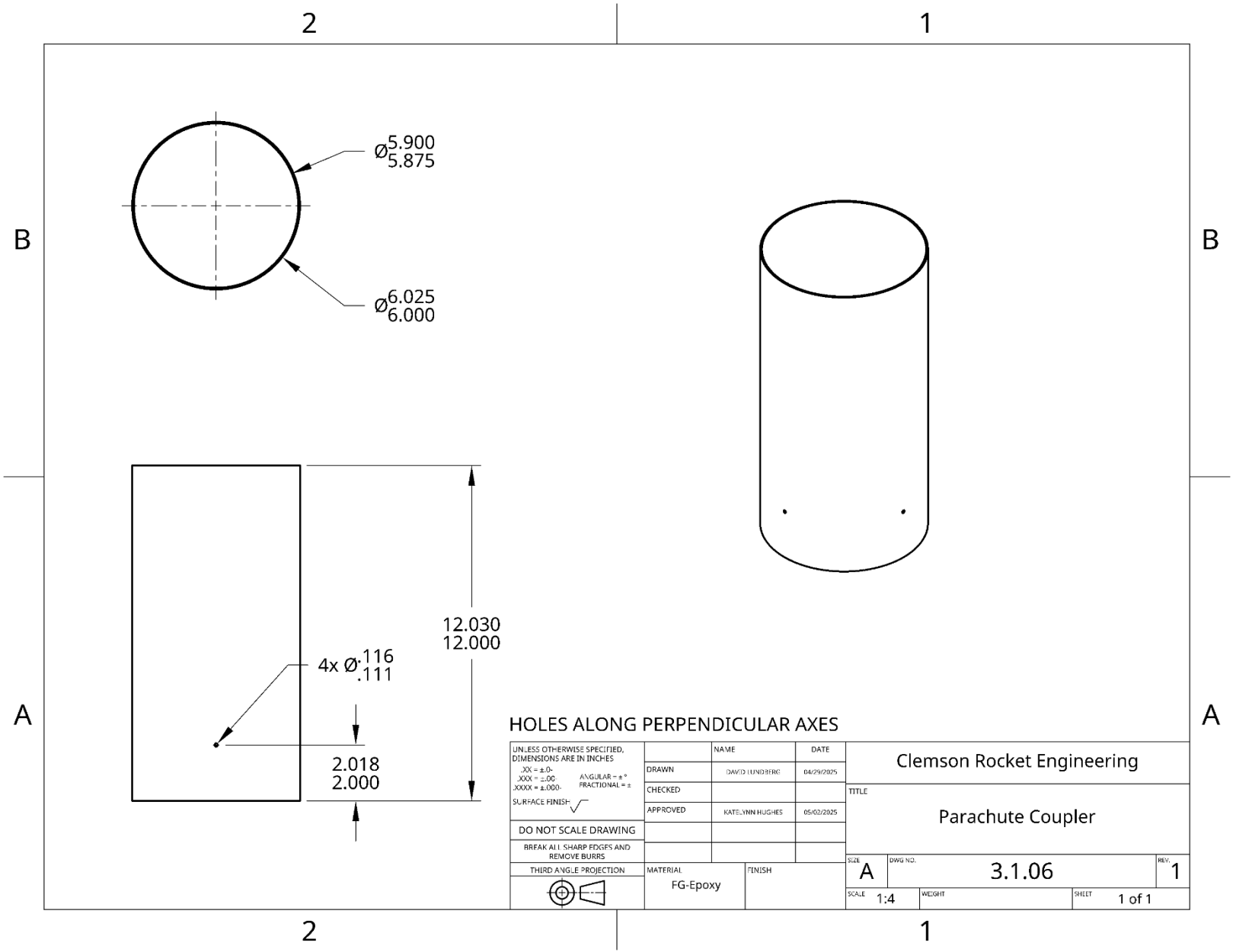
2
1
B
A
Ø5.900
5.875
Ø6.025
6.000
12.030
12.000
4x Ø.116
.111
2.018
2.000
HOLES ALONG PERPENDICULAR AXES
UNLESS OTHERWISE SPECIFIED, DIMENSIONS ARE IN INCHES
.XX = ±.0-
.XXX = ±.00
.XXXX = ±.000-
ANGULAR = ± °
FRACTIONAL = ±
SURFACE FINISH
DO NOT SCALE DRAWING
BREAK ALL SHARP EDGES AND REMOVE BURRS
THIRD ANGLE PROJECTION
NAME
DATE
DRAWN
DAVID LUNDBERG
04/29/2025
CHECKED
APPROVED
KATELYNN HUGHES
05/02/2025
MATERIAL
FG-Epoxy
FINISH
Clemson Rocket Engineering
TITLE
Parachute Coupler
SIZE
A
DWG NO.
3.1.06
REV.
1
SCALE
1:4
WEIGHT
SHEET
1 of 1

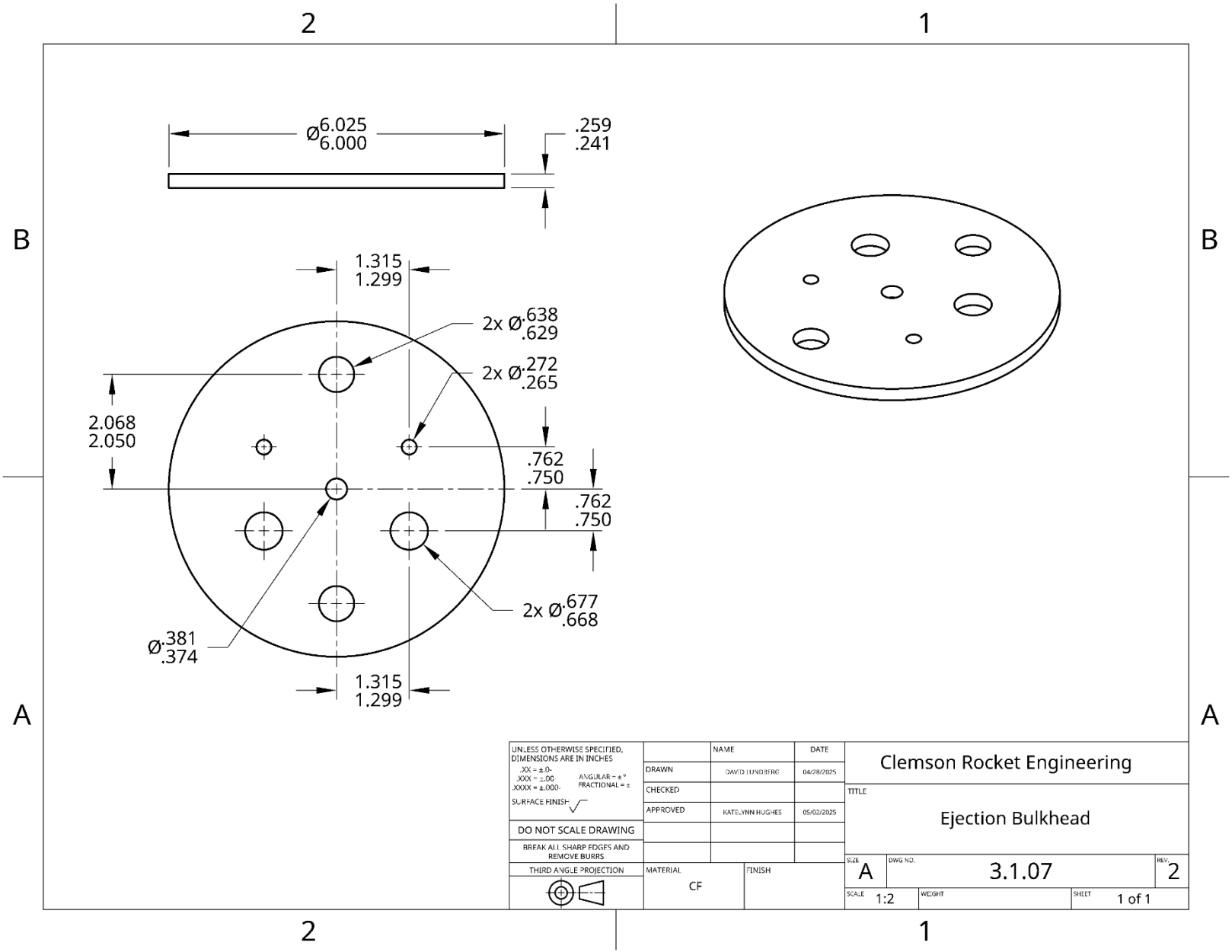
2
1
B
A
Ø6.025
6.000
.259
.241
1.315
1.299
2x Ø.638
.629
2x Ø.272
.265
2.068
2.050
.762
.750
.762
.750
2x Ø.677
.668
Ø.381
.374
1.315
1.299
UNLESS OTHERWISE SPECIFIED, DIMENSIONS ARE IN INCHES
.XX = ±.0-
.XXX = ±.00
.XXXX = ±.000-
ANGULAR = ± °
FRACTIONAL = ±
SURFACE FINISH
DO NOT SCALE DRAWING
BREAK ALL SHARP EDGES AND REMOVE BURRS
THIRD ANGLE PROJECTION
NAME
DATE
DRAWN
DAVID LUNDBERG
04/28/2025
CHECKED
APPROVED
KATELYNN HUGHES
05/02/2025
MATERIAL
CF
FINISH
Clemson Rocket Engineering
TITLE
Ejection Bulkhead
SIZE
A
DWG NO.
3.1.07
REV
2
SCALE
1:2
WEIGHT
SHEET
1 of 1

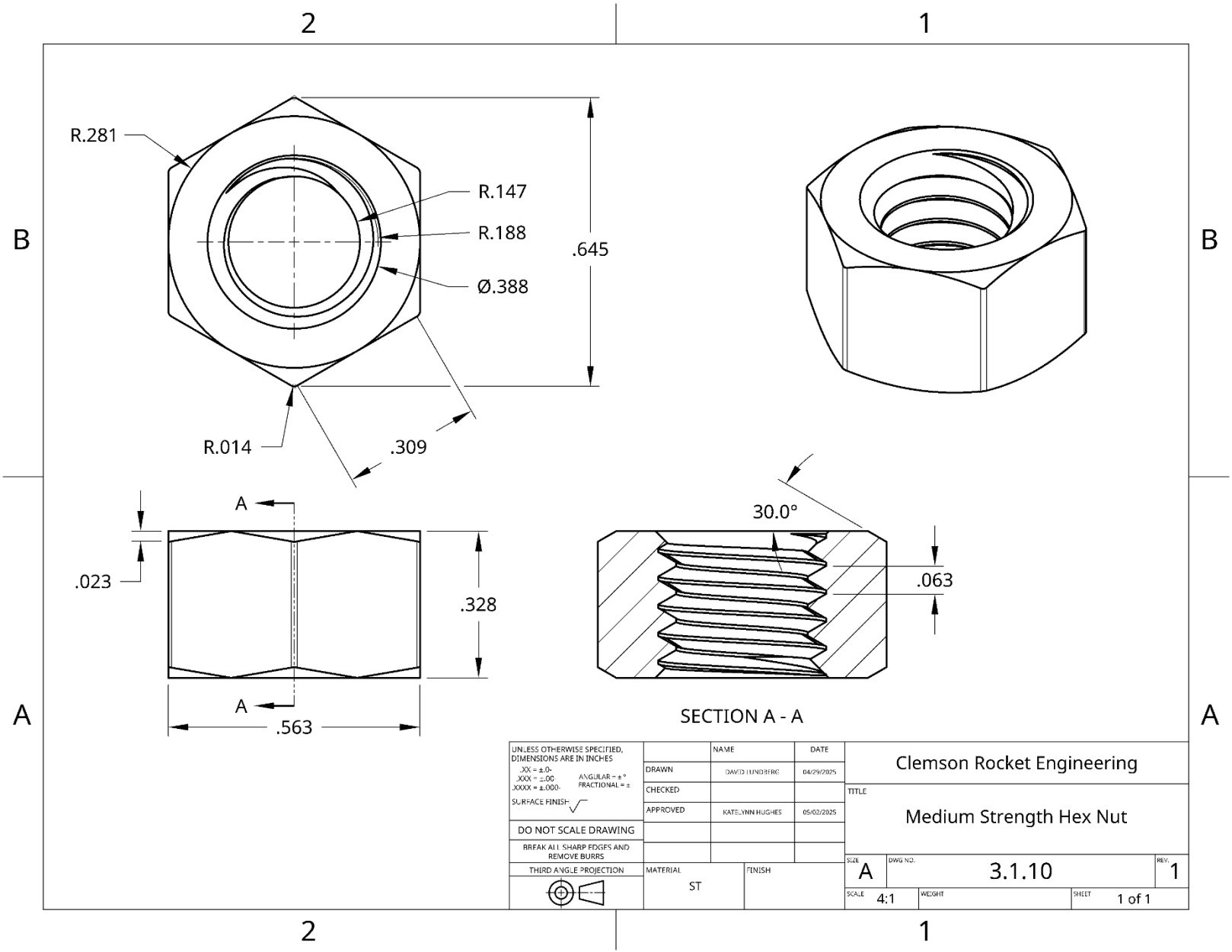
2
1
B
A
R.281
R.147
R.188
Ø.388
.645
R.014
.309
A
.023
.328
A
.563
30.0°
.063
SECTION A - A
UNLESS OTHERWISE SPECIFIED, DIMENSIONS ARE IN INCHES
.XX = ±.0-
.XXX = ±.00
.XXXX = ±.000-
ANGULAR = ± °
FRACTIONAL = ±
SURFACE FINISH
DO NOT SCALE DRAWING
BREAK ALL SHARP EDGES AND REMOVE BURRS
THIRD ANGLE PROJECTION
NAME
DATE
DRAWN
DAVID LUNDBERG
04/29/2025
CHECKED
APPROVED
KATELYNN HUGHES
05/02/2025
MATERIAL
ST
FINISH
Clemson Rocket Engineering
TITLE
Medium Strength Hex Nut
SIZE
A
DWG NO.
3.1.10
REV.
1
SCALE
4:1
WEIGHT
SHEET
1 of 1

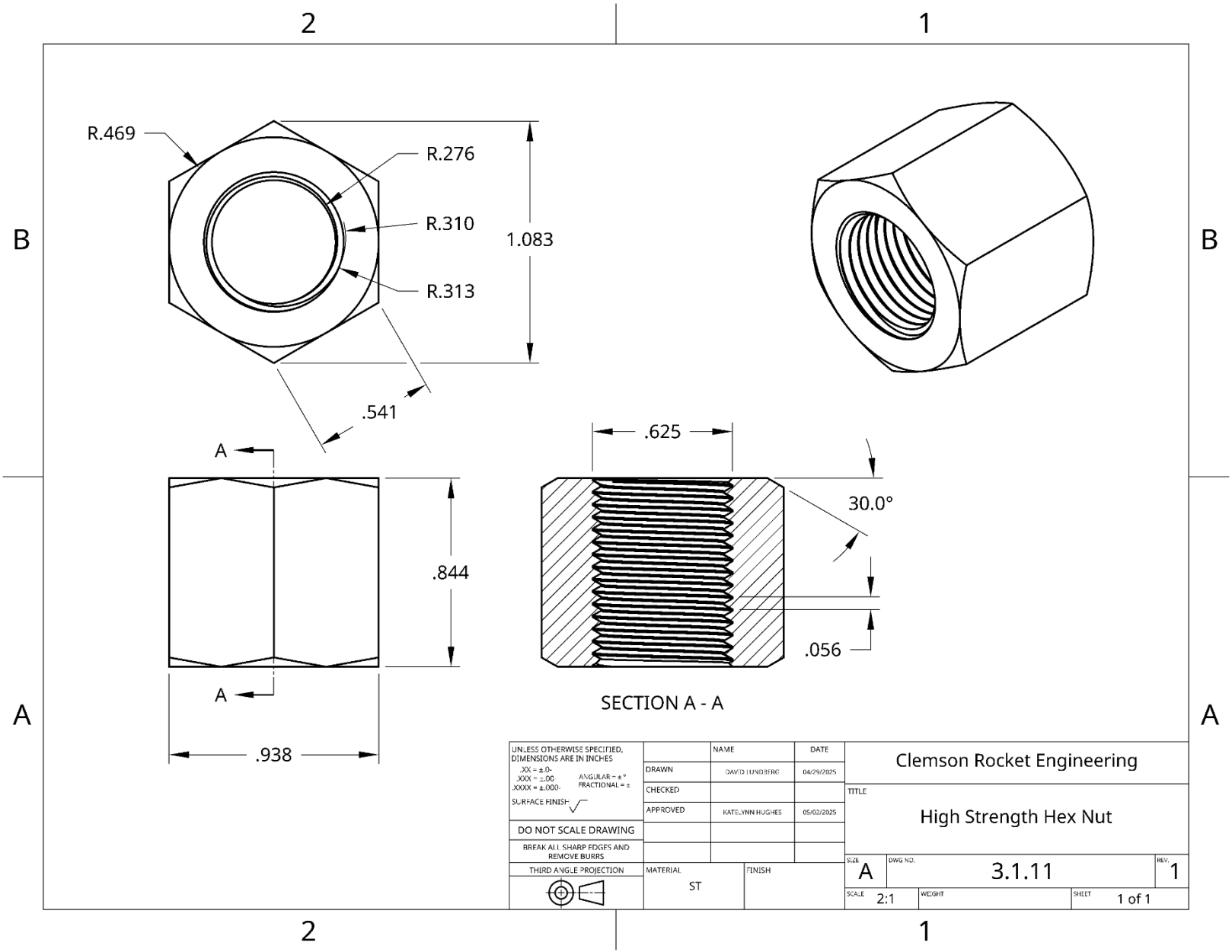
2
1
B
A
R.469
R.276
R.310
R.313
1.083
.541
A
.844
A
.938
.625
30.0°
.056
SECTION A - A
UNLESS OTHERWISE SPECIFIED, DIMENSIONS ARE IN INCHES
.XX = ±.0-
.XXX = ±.00
.XXXX = ±.000-
ANGULAR = ± °
FRACTIONAL = ±
SURFACE FINISH
DO NOT SCALE DRAWING
BREAK ALL SHARP EDGES AND REMOVE BURRS
THIRD ANGLE PROJECTION
NAME
DATE
DRAWN
DAVID LUNDBERG
04/29/2025
CHECKED
APPROVED
KATELYNN HUGHES
05/02/2025
MATERIAL
ST
FINISH
Clemson Rocket Engineering
TITLE
High Strength Hex Nut
SIZE
A
DWG NO.
3.1.11
REV.
1
SCALE
2:1
WEIGHT
SHEET
1 of 1

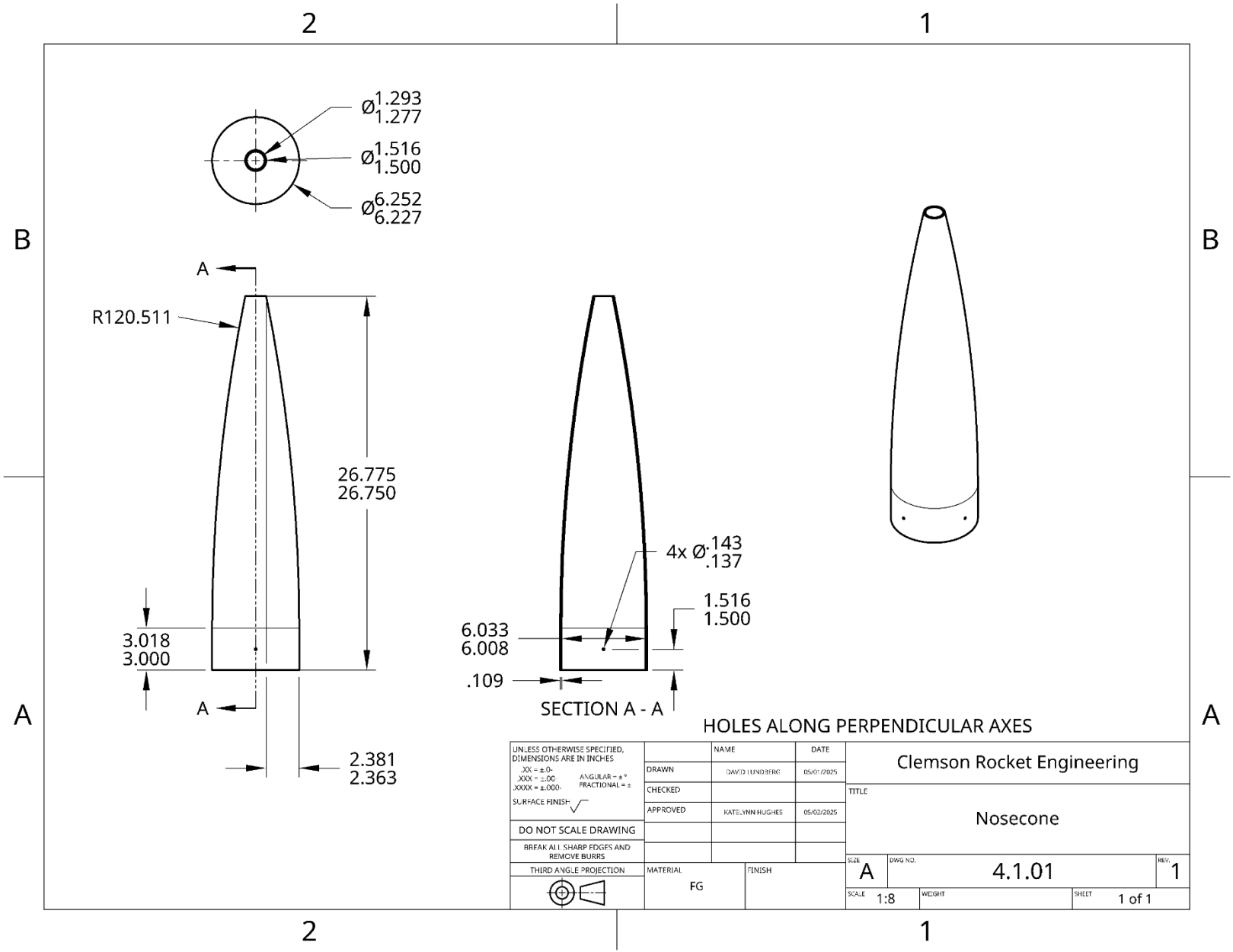
2
1
B
A
Ø1.293
1.277
Ø1.516
1.500
Ø6.252
6.227
A
R120.511
26.775
26.750
3.018
3.000
A
2.381
2.363
4x Ø.143
.137
1.516
1.500
6.033
6.008
.109
SECTION A - A
HOLES ALONG PERPENDICULAR AXES
UNLESS OTHERWISE SPECIFIED, DIMENSIONS ARE IN INCHES
.XX = ±.0-
.XXX = ±.00
.XXXX = ±.000-
ANGULAR = ± °
FRACTIONAL = ±
SURFACE FINISH
DO NOT SCALE DRAWING
BREAK ALL SHARP EDGES AND REMOVE BURRS
THIRD ANGLE PROJECTION
NAME
DATE
DRAWN
DAVID LUNDBERG
05/01/2025
CHECKED
APPROVED
KATELYNN HUGHES
05/02/2025
MATERIAL
FG
FINISH
Clemson Rocket Engineering
TITLE
Nosecone
SIZE
A
DWG NO.
4.1.01
REV.
1
SCALE
1:8
WEIGHT
SHEET
1 of 1

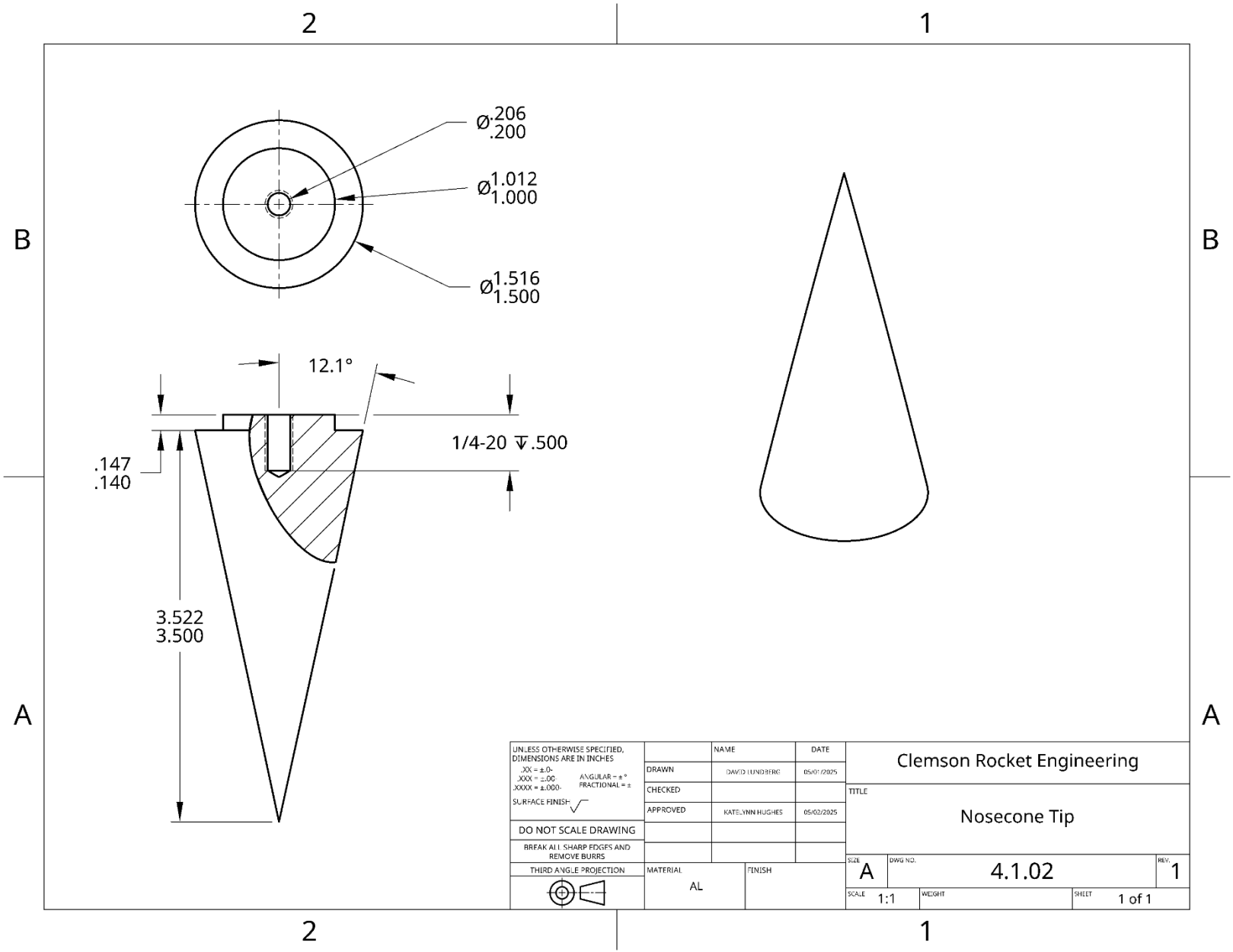
2
1
B
A
Ø.206
.200
Ø1.012
1.000
Ø1.516
1.500
12.1°
1/4-20 ↧.500
.147
.140
3.522
3.500
UNLESS OTHERWISE SPECIFIED, DIMENSIONS ARE IN INCHES
.XX = ±.0-
.XXX = ±.00
.XXXX = ±.000-
ANGULAR = ± °
FRACTIONAL = ±
SURFACE FINISH
DO NOT SCALE DRAWING
BREAK ALL SHARP EDGES AND REMOVE BURRS
THIRD ANGLE PROJECTION
NAME
DATE
DRAWN
DAVID LUNDBERG
05/01/2025
CHECKED
APPROVED
KATELYNN HUGHES
05/02/2025
MATERIAL
AL
FINISH
Clemson Rocket Engineering
TITLE
Nosecone Tip
SIZE
A
DWG NO.
4.1.02
REV.
1
SCALE
1:1
WEIGHT
SHEET
1 of 1

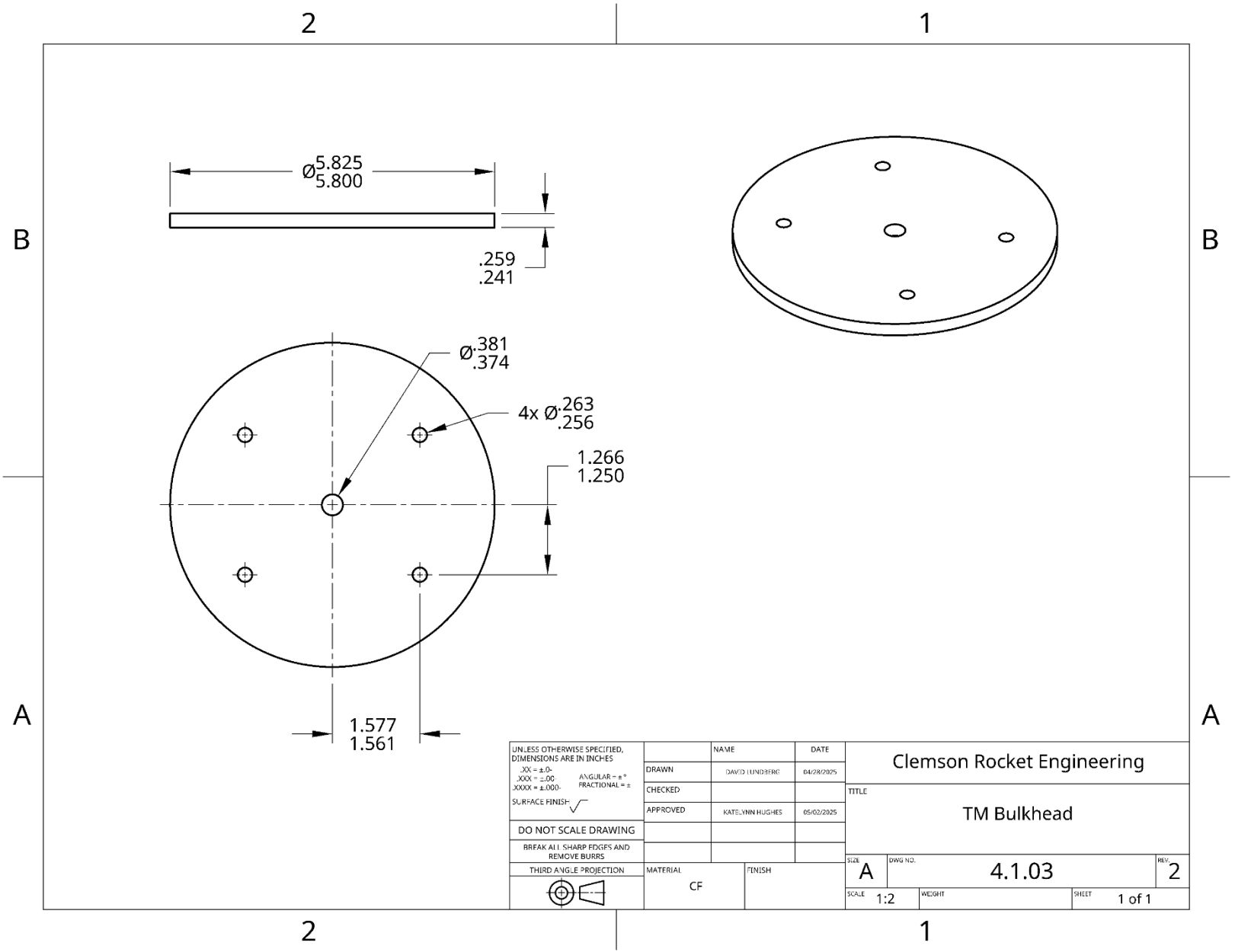
2
1
B
A
Ø5.825
5.800
.259
.241
Ø.381
.374
4x Ø.263
.256
1.266
1.250
1.577
1.561
UNLESS OTHERWISE SPECIFIED, DIMENSIONS ARE IN INCHES
.XX = ±.0-
.XXX = ±.00
.XXXX = ±.000-
ANGULAR = ± °
FRACTIONAL = ±
SURFACE FINISH
DO NOT SCALE DRAWING
BREAK ALL SHARP EDGES AND REMOVE BURRS
THIRD ANGLE PROJECTION
NAME
DATE
DRAWN
DAVID LUNDBERG
04/28/2025
CHECKED
APPROVED
KATELYNN HUGHES
05/02/2025
MATERIAL
CF
FINISH
Clemson Rocket Engineering
TITLE
TM Bulkhead
SIZE
A
DWG NO.
4.1.03
REV
2
SCALE
1:2
WEIGHT
SHEET
1 of 1

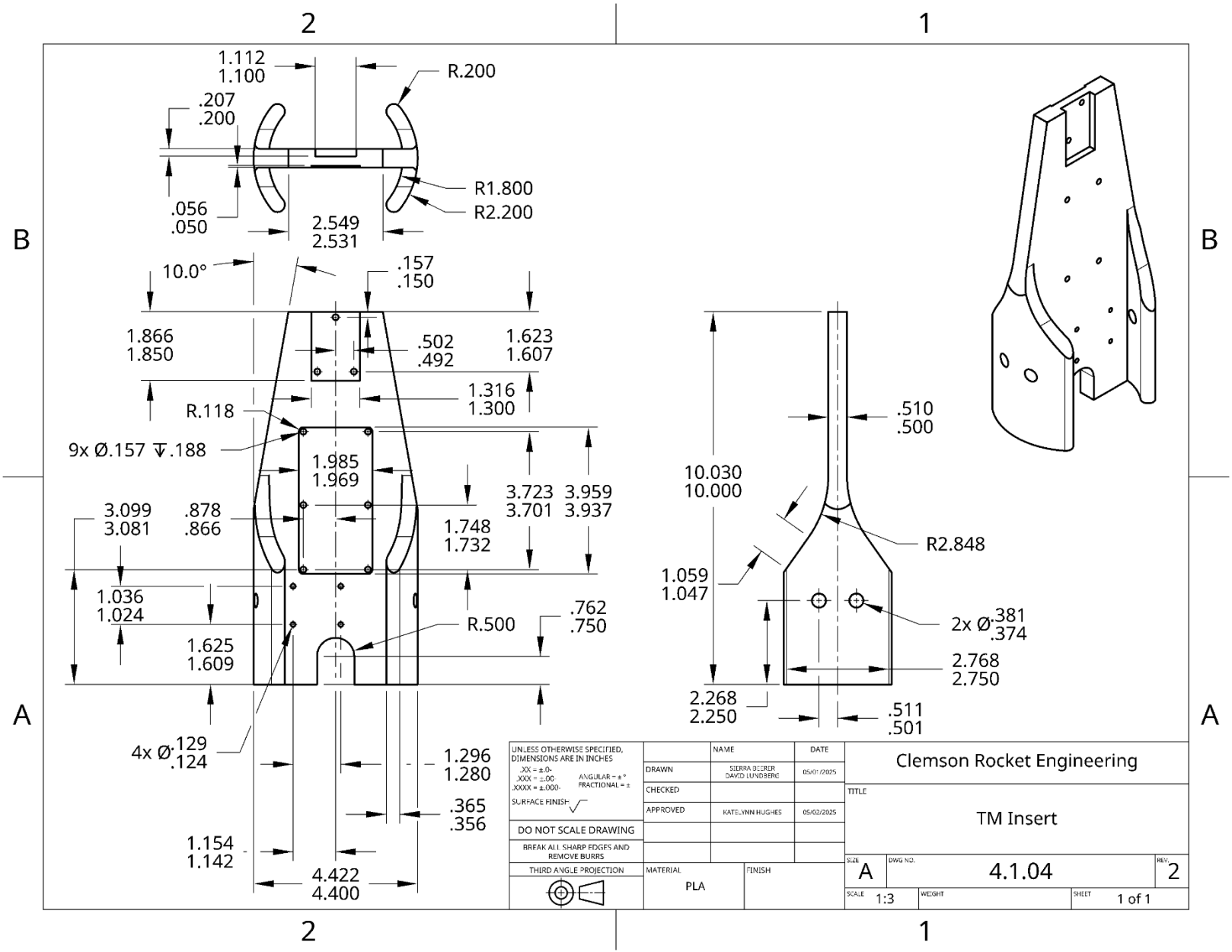
2
1
B
A
1.112
1.100
R.200
.207
.200
R1.800
R2.200
.056
.050
2.549
2.531
10.0°
.157
.150
1.866
1.850
.502
.492
1.623
1.607
1.316
1.300
R.118
9x Ø.157 ↧.188
1.985
1.969
3.723
3.701
3.959
3.937
3.099
3.081
.878
.866
1.748
1.732
1.036
1.024
R.500
.762
.750
1.625
1.609
4x Ø.129
.124
1.296
1.280
.365
.356
1.154
1.142
4.422
4.400
.510
.500
10.030
10.000
R2.848
1.059
1.047
2x Ø.381
.374
2.768
2.750
2.268
2.250
.511
.501
UNLESS OTHERWISE SPECIFIED, DIMENSIONS ARE IN INCHES
.XX = ±.0-
.XXX = ±.00
.XXXX = ±.000-
ANGULAR = ± °
FRACTIONAL = ±
SURFACE FINISH
DO NOT SCALE DRAWING
BREAK ALL SHARP EDGES AND REMOVE BURRS
THIRD ANGLE PROJECTION
NAME
DATE
DRAWN
SIERRA BEERER
DAVID LUNDBERG
05/07/2025
CHECKED
APPROVED
KATELYNN HUGHES
05/02/2025
MATERIAL
PLA
FINISH
Clemson Rocket Engineering
TITLE
TM Insert
SIZE
A
DWG NO.
4.1.04
REV
2
SCALE
1:3
WEIGHT
SHEET
1 of 1

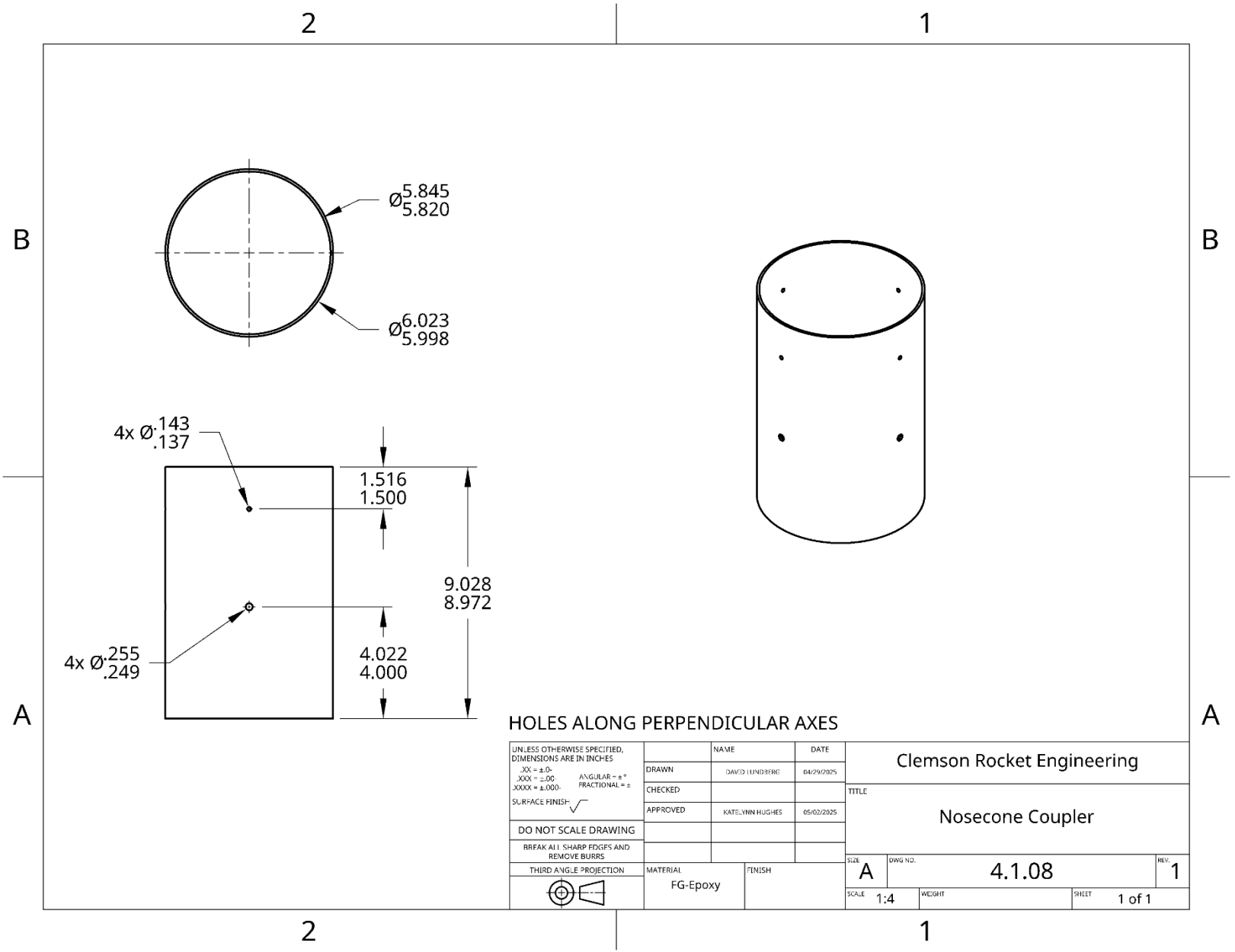
2
1
B
A
Ø5.845
5.820
Ø6.023
5.998
4x Ø.143
.137
1.516
1.500
9.028
8.972
4x Ø.255
.249
4.022
4.000
HOLES ALONG PERPENDICULAR AXES
UNLESS OTHERWISE SPECIFIED, DIMENSIONS ARE IN INCHES
.XX = ±.0-
.XXX = ±.00
.XXXX = ±.000-
ANGULAR = ± °
FRACTIONAL = ±
SURFACE FINISH
DO NOT SCALE DRAWING
BREAK ALL SHARP EDGES AND REMOVE BURRS
THIRD ANGLE PROJECTION
NAME
DATE
DRAWN
DAVID LUNDBERG
04/29/2025
CHECKED
APPROVED
KATELYNN HUGHES
05/02/2025
MATERIAL
FG-Epoxy
FINISH
Clemson Rocket Engineering
TITLE
Nosecone Coupler
SIZE
A
DWG NO.
4.1.08
REV.
1
SCALE
1:4
WEIGHT
SHEET
1 of 1

COTS AV Bay

Simplified Power Diagram

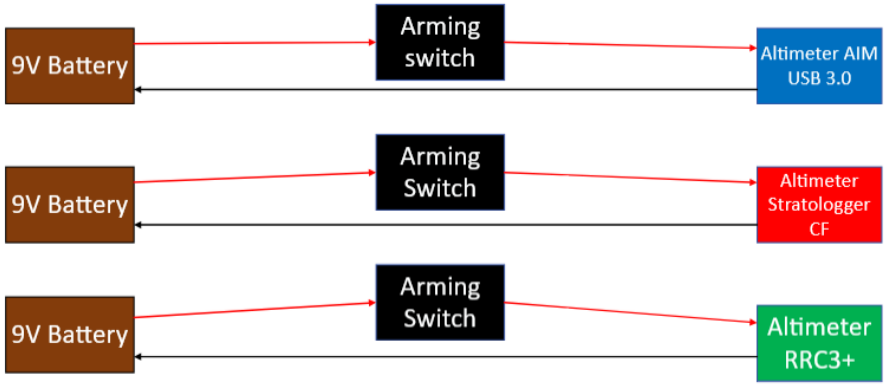

Simplified Ejection Charge Diagram

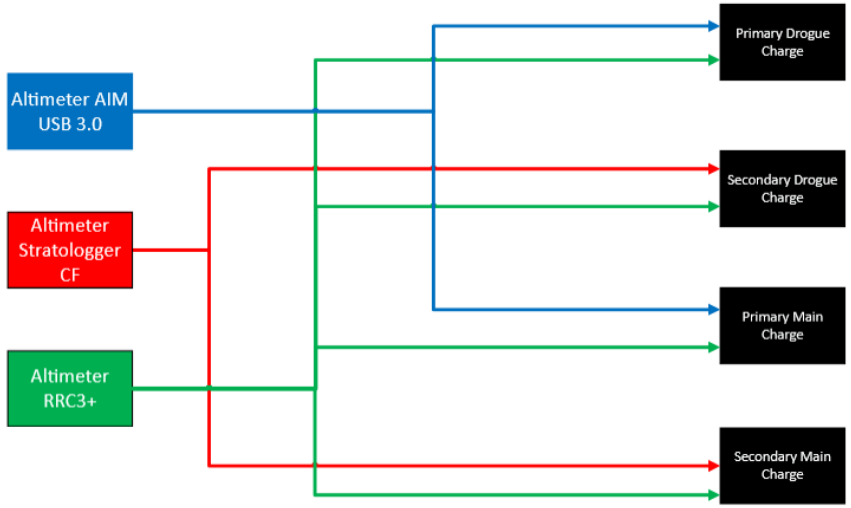

Full Diagram:

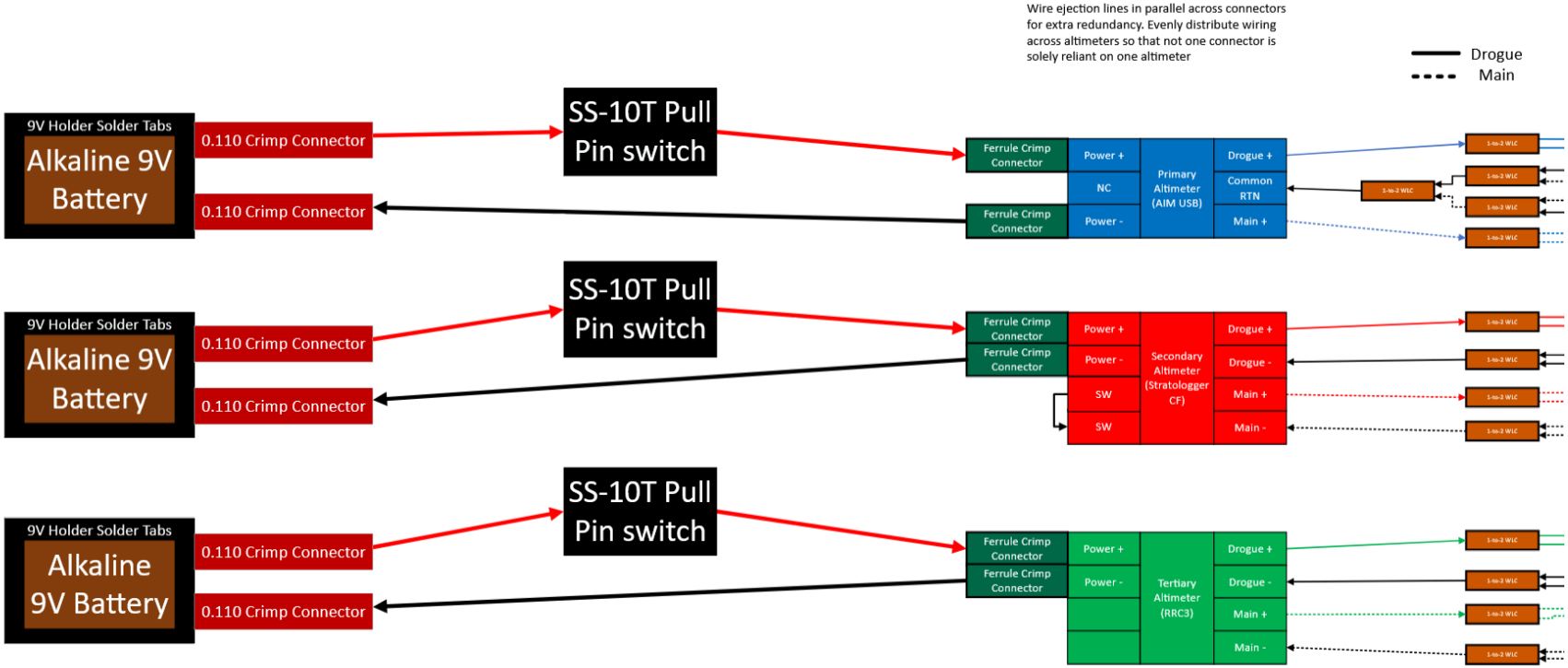

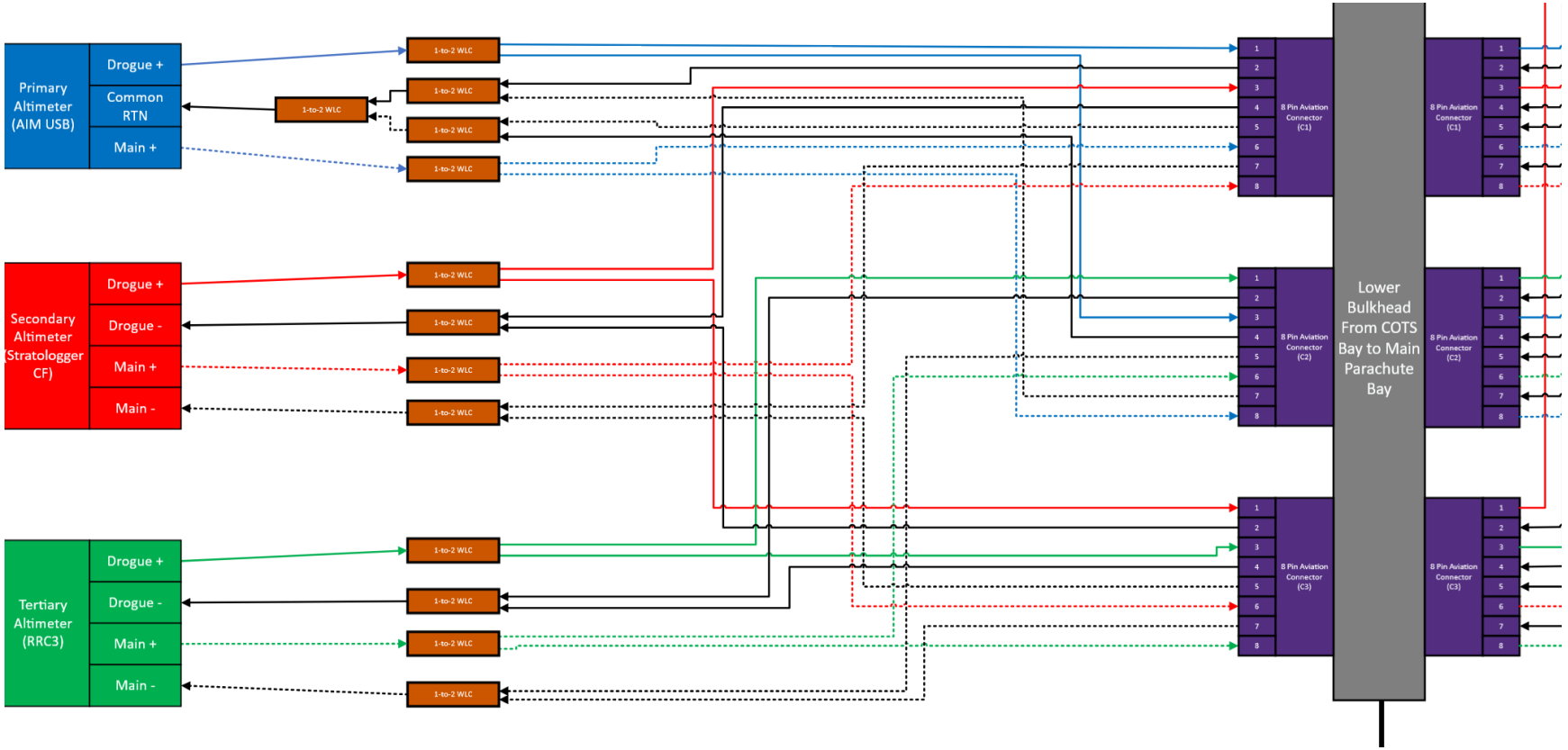
Primary Altimeter (AIM USB)
Drogue +
Common RTN
Main +
Secondary Altimeter (Stratologger CF)
Drogue +
Drogue -
Main +
Main -
Tertiary Altimeter (RRC3)
Drogue +
Drogue -
Main +
Main -
1-to-2 WLC
8 Pin Aviation Connector (C1)
8 Pin Aviation Connector (C2)
8 Pin Aviation Connector (C3)
Lower Bulkhead From COTS Bay to Main Parachute Bay

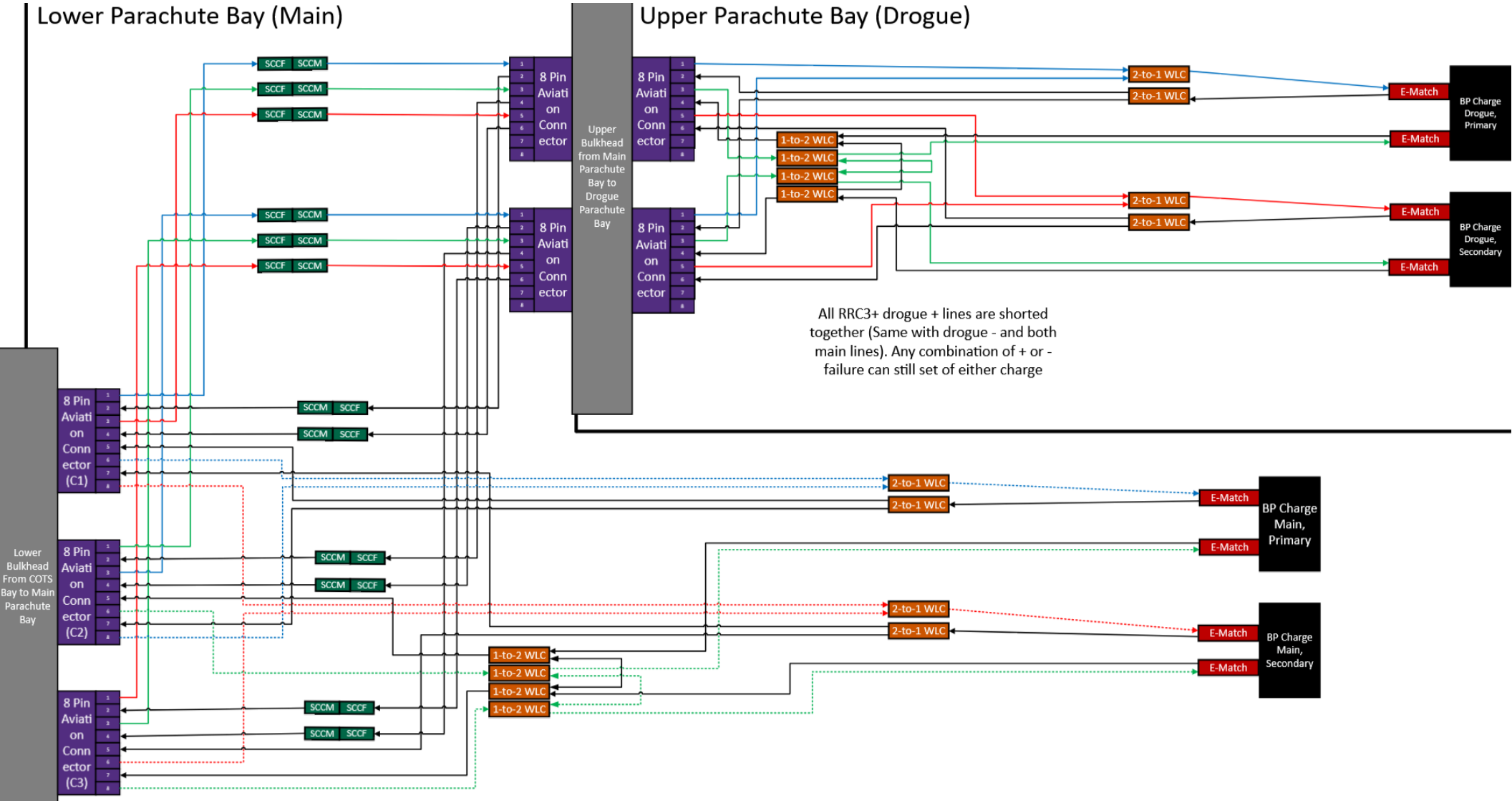
Lower Parachute Bay (Main)
Upper Parachute Bay (Drogue)
Upper Bulkhead from Main Parachute Bay to Drogue Parachute Bay
Lower Bulkhead From COTS Bay to Main Parachute Bay
8 Pin Aviation Connector (C1)
8 Pin Aviation Connector (C2)
8 Pin Aviation Connector (C3)
8 Pin Aviation Connector
SCCF
SCCM
1-to-2 WLC
2-to-1 WLC
E-Match
BP Charge Drogue, Primary
BP Charge Drogue, Secondary
BP Charge Main, Primary
BP Charge Main, Secondary
All RRC3+ drogue + lines are shorted together (Same with drogue - and both main lines). Any combination of + or - failure can still set of either charge

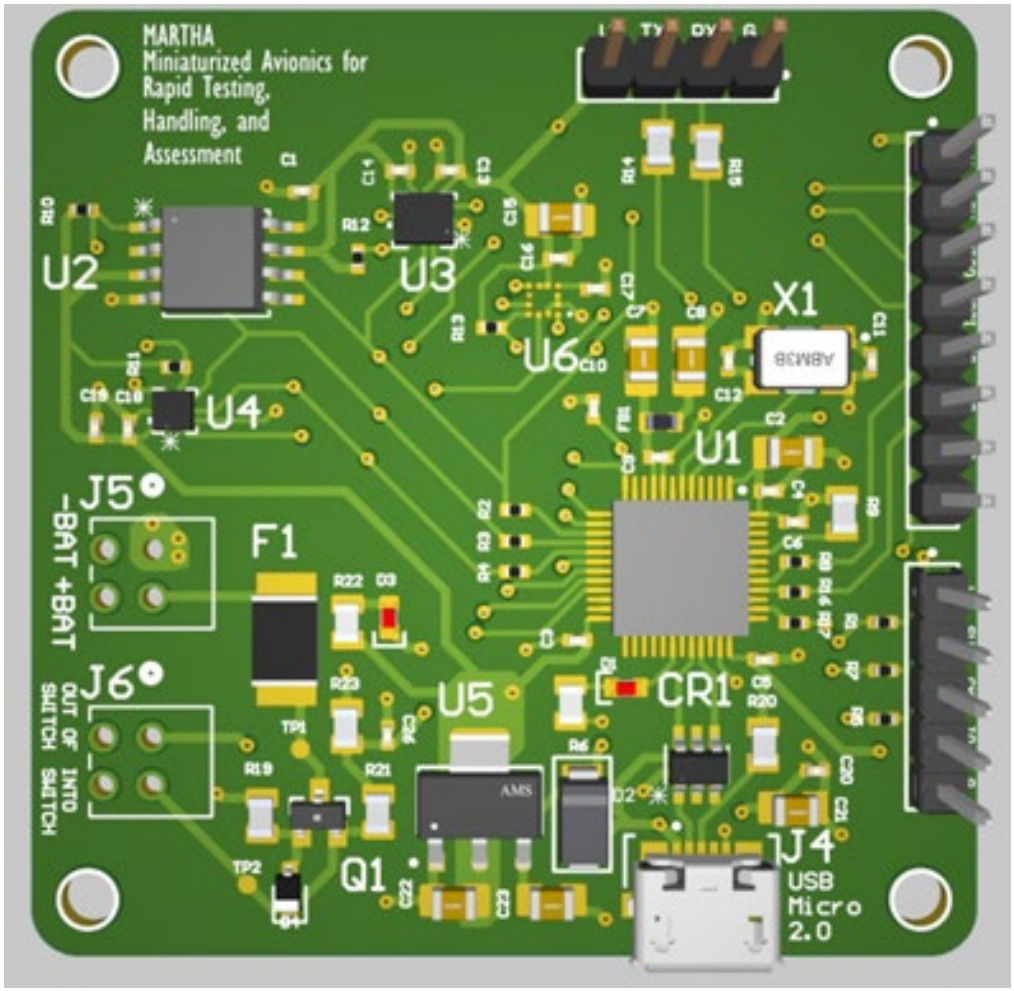
MARTHA
Miniaturized Avionics for
Rapid Testing,
Handling, and
Assessment
U2
U3
U6
X1
U4
U1
J5
-BAT +BAT
F1
J6
OUT OF SWITCH
INTO SWITCH
U5
CR1
Q1
J4
USB
Micro
2.0


MARTHA v1.3
10/11/24
Designer: Trevor Miller
Co-Designer: Kyle Jones
Clemson Rocket
Engineering

CURE MARTHA

A reduced form factor avionics platform

Power and Digital Flow Charts

DIGITAL SIGNALS

SPI
- Used to quickly communicate with: W25Q128JVSIQ, LIS3MDL, BMP390, LSM6DSOX
- Switching from I2C to increase speed of communication and processing power
- Will need Chip Select pins for each "Slave" respectively on MCU

UART
- UART will be used as backup communication

USB B 2.0
- Used to communicate from computer to controller
- Runs through ESD protection

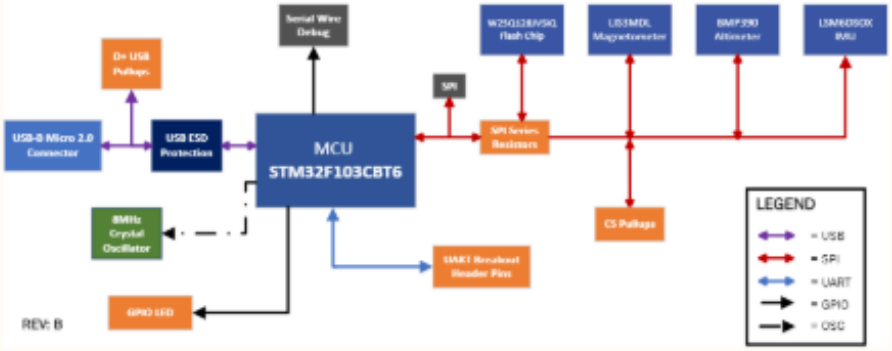

POWER ANALYSIS

Power Flow (BAT)
- Power originates from battery (+9V)
- Flows into locking switch to turn on board
- Flows into Fuse 1, Zener diode, and Reverse Polarity Protection to protect from back-flow power
- Converted into +3V3 by AMS1117-3.3 LDO
- Power on indicated by buzzer and Power LED
- Power flows into sensors, flash memory, and breakouts

USB-B 2.0 Micro
- Power flows from Laptop or other connection with +3V3.
- Flows into Shottky Diode
- Flows into ESD Protection
- Into AMS1117-3.3 and Power LED
- Into sensors, flash memory, and breakouts

Battery Life
- Uses about 100mA for the board
- Average +9V battery is 500mAh
- 5hr battery life for 1 +9V battery
- 4s Li-Ion battery is around 2500mAh
- 25hr battery life for 1 4s Li-Ion battery

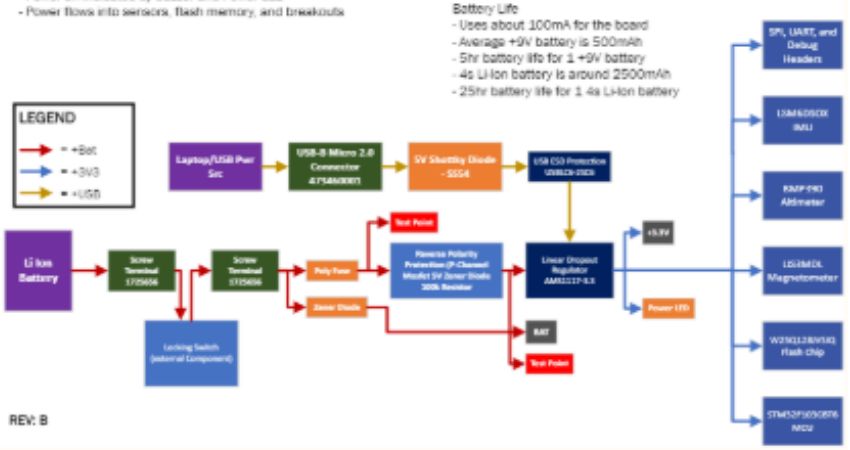

Title		
Size: A	Number:	Revision:
Date: 4/06/2025		Sheet of
File: Flow Chart SchDoc		Drawn By:

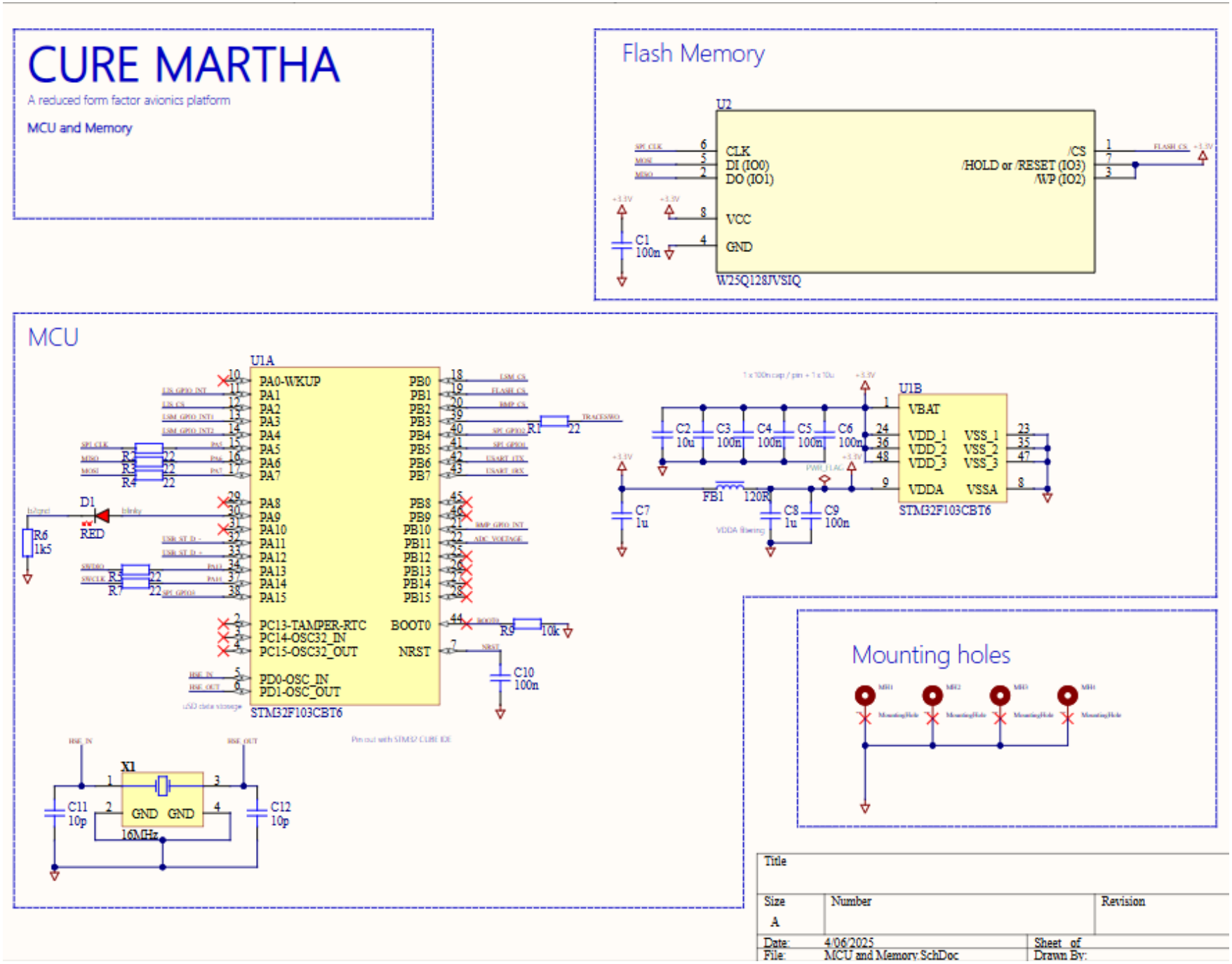
CURE MARTHA
A reduced form factor avionics platform
MCU and Memory
Flash Memory
U2
CLK
DI (IO0)
DO (IO1)
VCC
GND
/CS
/HOLD or /RESET (IO3)
/WP (IO2)
C1
100n
W25Q128JVSIQ
MCU
U1A
PA0-WKUP
PA1
PA2
PA3
PA4
PA5
PA6
PA7
PA8
PA9
PA10
PA11
PA12
PA13
PA14
PA15
PB0
PB1
PB2
PB3
PB4
PB5
PB6
PB7
PB8
PB9
PB10
PB11
PB12
PB13
PB14
PB15
PC13-TAMPER-RTC
PC14-OSC32_IN
PC15-OSC32_OUT
PD0-OSC_IN
PD1-OSC_OUT
BOOT0
NRST
STM32F103CBT6
U1B
VBAT
VDD_1
VDD_2
VDD_3
VSS_1
VSS_2
VSS_3
VDDA
VSSA
STM32F103CBT6
C2 10u
C3 100n
C4 100n
C5 100n
C6 100n
C7 1u
C8 1u
C9 100n
C10 100n
C11 10p
C12 10p
FB1 120R
R1 22
R2 22
R3 22
R4 22
R5 22
R6 1k5
R7 22
R9 10k
D1
RED
X1
16MHz
Mounting holes
Title
Size
A
Number
Revision
Date: 4/06/2025
Sheet of
File: MCU and Memory.SchDoc
Drawn By:

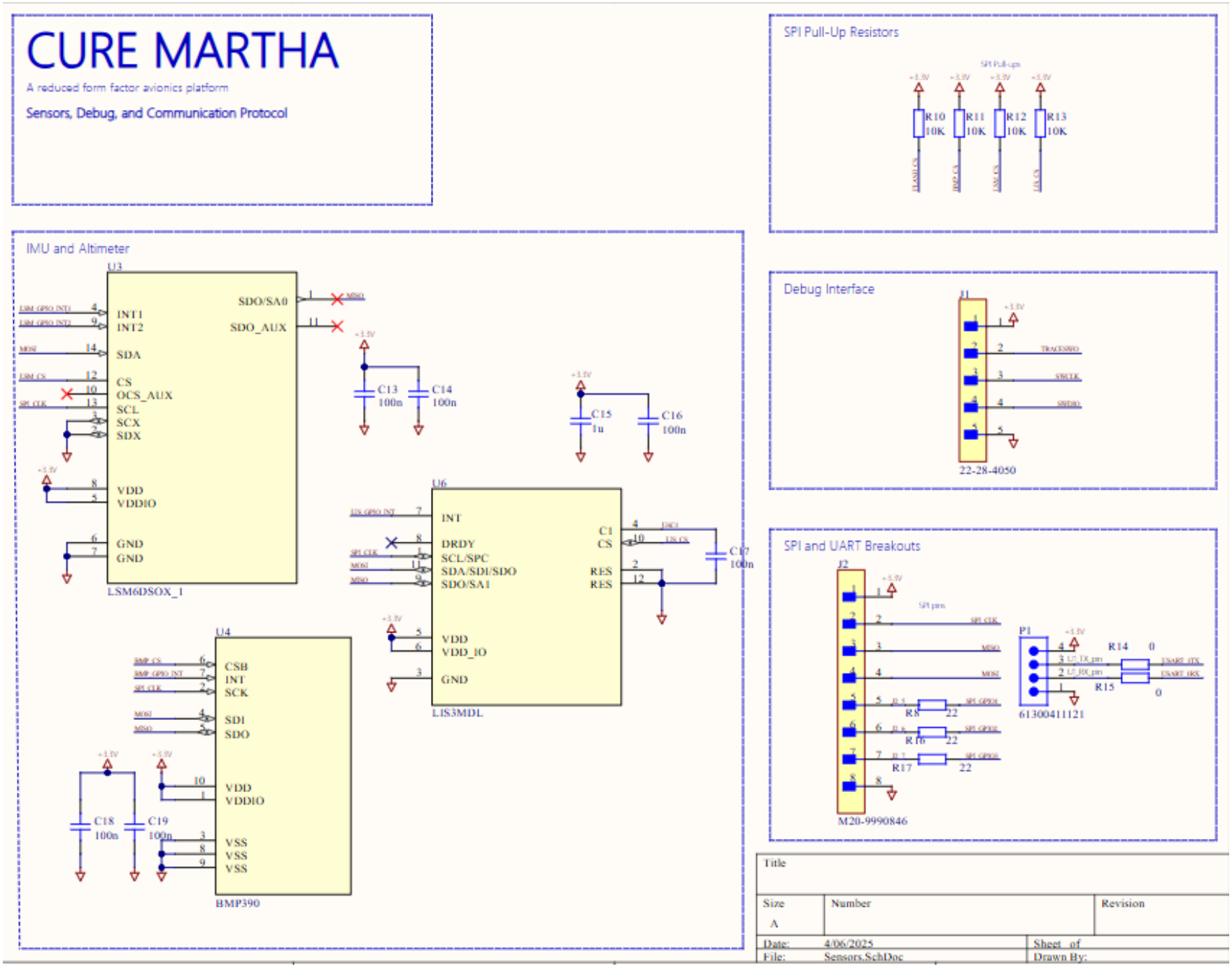
CURE MARTHA
A reduced form factor avionics platform
Sensors, Debug, and Communication Protocol
SPI Pull-Up Resistors
R10 10K
R11 10K
R12 10K
R13 10K
IMU and Altimeter
U3
INT1
INT2
SDO/SA0
SDO_AUX
SDA
CS
OCS_AUX
SCL
SCX
SDX
VDD
VDDIO
GND
GND
LSM6DSOX_1
C13 100n
C14 100n
C15 1u
C16 100n
U6
INT
DRDY
SCL/SPC
SDA/SDI/SDO
SDO/SA1
C1
CS
RES
RES
VDD
VDD_IO
GND
C17 100n
LIS3MDL
U4
CSB
INT
SCK
SDI
SDO
VDD
VDDIO
VSS
VSS
VSS
C18 100n
C19 100n
BMP390
Debug Interface
J1
22-28-4050
SPI and UART Breakouts
J2
M20-9990846
P1
61300411121
R8 22
R16 22
R17 22
R14 0
R15 0
Title
Size
A
Number
Revision
Date: 4/06/2025
File: Sensors.SchDoc
Sheet of
Drawn By:

CURE MARTHA

A reduced form factor avionics platform

Power Regulation and USB

Battery and ESD protection

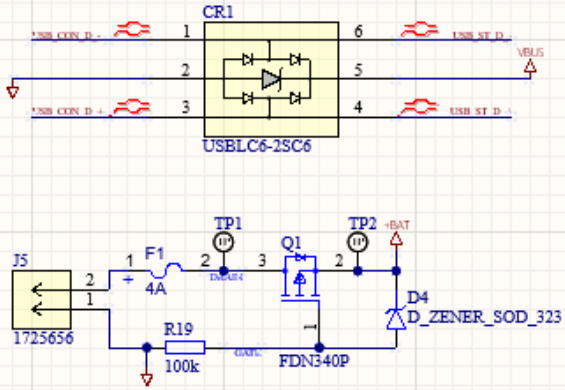

LDO

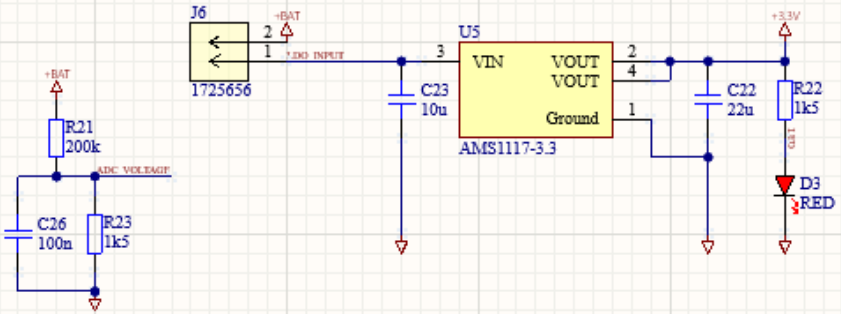

USB Micro 2.0 Connector

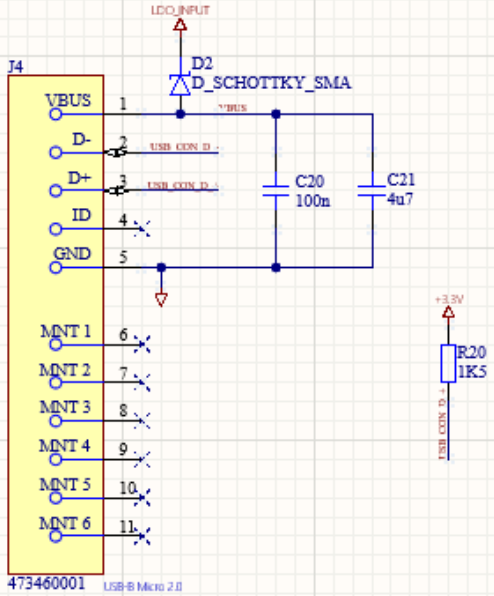

Title		
Size: A	Number	Revision
Date: 4/30/2025		Sheet of
File: C:\Users\...\Power and USB.SchDoc		Drawn By:

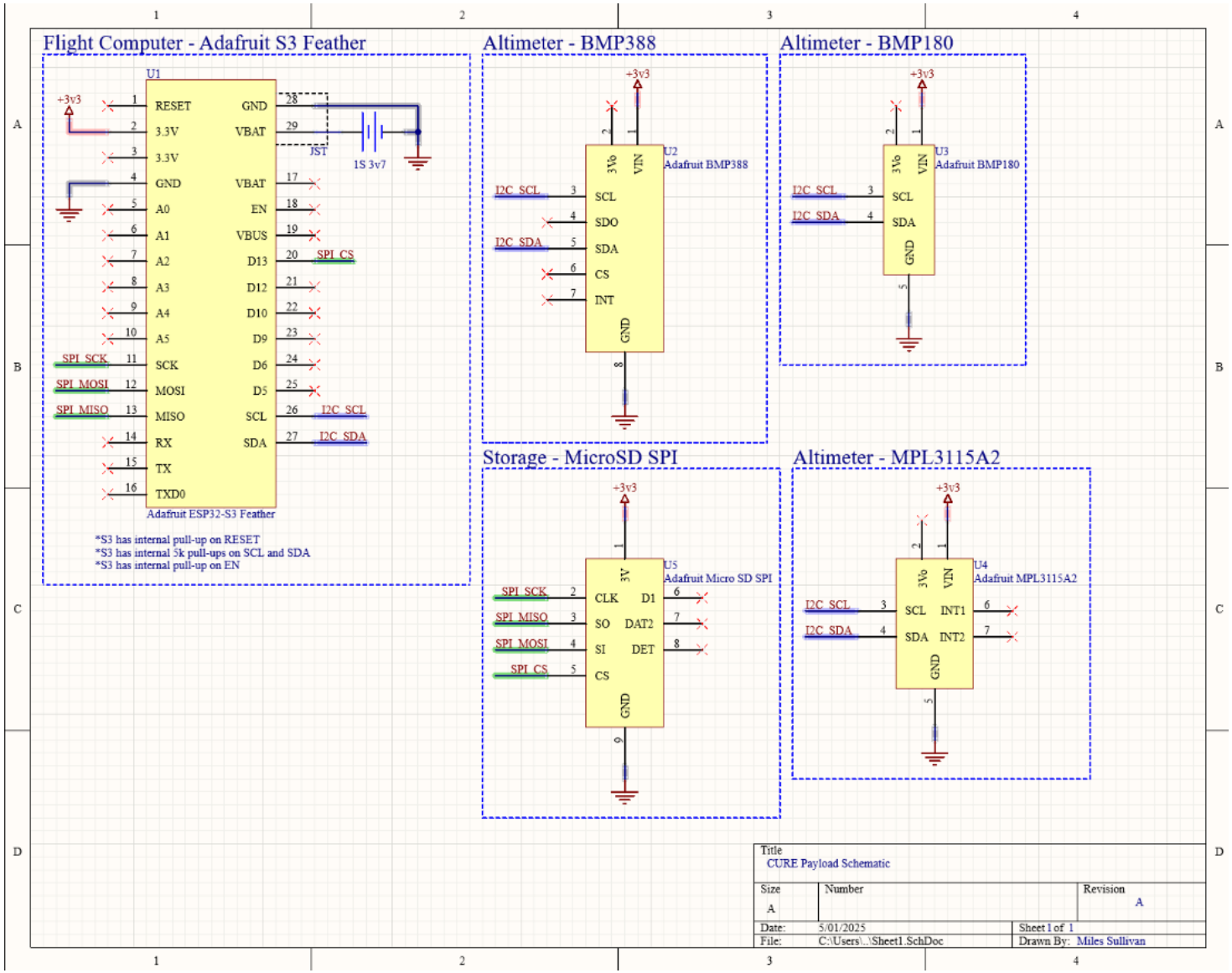
Flight Computer - Adafruit S3 Feather
U1
+3v3
RESET
3.3V
3.3V
GND
A0
A1
A2
A3
A4
A5
SCK
MOSI
MISO
RX
TX
TXD0
GND
VBAT
VBAT
EN
VBUS
D13
D12
D10
D9
D6
D5
SCL
SDA
JST
1S 3v7
SPI_CS
I2C_SCL
I2C_SDA
SPI_SCK
SPI_MOSI
SPI_MISO
Adafruit ESP32-S3 Feather
*S3 has internal pull-up on RESET
*S3 has internal 5k pull-ups on SCL and SDA
*S3 has internal pull-up on EN
Altimeter - BMP388
U2
Adafruit BMP388
3Vo
VIN
SCL
SDO
SDA
CS
INT
GND
Altimeter - BMP180
U3
Adafruit BMP180
Storage - MicroSD SPI
U5
Adafruit Micro SD SPI
3V
CLK
SO
SI
CS
D1
DAT2
DET
Altimeter - MPL3115A2
U4
Adafruit MPL3115A2
INT1
INT2
Title
CURE Payload Schematic
Size
A
Number
Revision
A
Date: 5/01/2025
Sheet 1 of 1
File: C:\Users\...\Sheet1.SchDoc
Drawn By: Miles Sullivan

Appendix H: Component Inventory and Product Specifications

This appendix is a comprehensive inventory of the various parts and products used to construct our vehicle. It includes detailed specifications and sourcing information for each component, from structural elements to electronic systems. This appendix provides an apparent reference for the materials and technologies implemented, ensuring transparency and facilitating future replication or modification of the vehicle design. Vendor details and relevant technical parameters, such as dimensions, materials, and performance characteristics, accompany each item. This resource is intended to support the understanding and evaluating of our vehicle's design and functionality by providing essential data at a glance.

[1]ADXL345, 3-Axis Accelerometer Breakout Board | Adafruit Industries LLC, MPN: 1231

[2]AIM, Dual Deployment Altimeter | Entracore, Model: 09139

[3]AMS1117-3.3, IC LDO REG 3.3V 1 A SOT223 | EVVO, MPN: AMS1117-3.3

[4]AutomationDirect Selector Switch, Two positions - 22 mm size | AutomationDirect, MPN: GCX1350

[5]BMP388, Precision Barometric Pressure and Altimeter | Adafruit Industries LLC, MPN: 3966

[6]CESS Aviation Connectors, 0.63 *in* Diameter Plug and Socket | CESS, MPN: JCX

[7]DB9 Male Breakout Board, Screw terminals - Right angle - Ultra thin| MDFLY, ASIN: B07ZT56BJF

[8]DragonPlate, EconomyPlate ~ 1/4 in×24 in×24 in | Allred & Associates Inc., SKU: FEPL08T902424

[9]Eyebolt, 3/8-in 3-9/32-in Plain Coarse Thread | Hillman, Model: 320604

[10]FEATHERS3, 2.4GHz ESP32-S3 Transceiver | Adafruit Industries LLC, MPN: 5399

[11]Featherweight GPS Ground Station, Base Station Enclosure Unit | Featherweight Altimeters, Model: Ground Station

[12]Featherweight GPS Tracker, Antenna Unit | Featherweight Altimeters, Model: Tracker

[13]LIS3MDLTR, Ultralow-power 3-axis Magnetic Sensor | STMicroelectronics, Model: LIS3MDLTR

[14]LSM6DSOX, 3D Digital Accelerometer and 3D Digital Gyroscope | STMicroelectronics, Model: LSM6DSOXTR

[15]M2500T-P, AeroTech High Powered Motor | Balsa Machining Service, Catalog #: 13250P

[18]MPL3115A2, I2C Barometric Pressure/Altitude/Temperature Sensor | Adafruit Industries LLC, MPN: 1893

[16]PMSA003I, STEMMA QT Air Quality Sensor | Adafruit Industries LLC, MPN: 4632

[17]RunCam Split 3, 165° DC 5-20 V M12 Lens | RunCam, SKU: SPLIT-HD-3DM

[18]Shock Cord, Large, 9/16 in – 3000 lbf Rating | Fruity Chutes, SKU: SCN-688-10

[19]Siemens Selector Switch, Non-Illuminated - two positions - 30 mm size | Siemens, MPN: 52SA2AABK1

[20]STM32F103C8T6, Arm® Cortex®-M3 32-bit RISC Core MCU | STMicroelectronics, Model: STM32F103C8T6

[21]StratoLogger CF, Compact Footprint StratoLogger Altimeter | PerfectFlight Direct, SKU: SLCFA

[22]Swivel, Stainless Steel Barrel Swivel – 3000 lbf Rating | Rocketman Parachutes, Model: 3000-Barrel-Swivel

[23]Wago Lever Connector, 12-24 AWG Splicing Connector | WAGO, SKU: 1006737809

[24]XT-30 Connectors, Gold Plated Pins | DFRobot, MPN: FIT0586

[25]Silver Gusset Bracket, 1" Long for 1" High Rail T-Slotted Framing | McMaster-Carr, MPN: 47065T663.

[26]Alloy Steel Low-Profile Socket Head Screw, Hex Drive, Zinc Plated, 1/4"-20 Thread Size, 1" Long | McMaster-Carr, MPN: 90665A161.

[27]Zinc-Plated Steel Threaded Rod, 1/4"-20 Thread Size, 6" Long | Hillman Group (via Amazon), MPN: 44826.

[28]Zinc-Plated Steel Hex Coupling Nut, 1/4"-20 Thread Size, 1.18" Long | Wensilon (via Amazon), MPN: B0D4DH7K2B.

[29]Medium-Strength Steel Hex Nut, Grade 5, Zinc-Plated, 1/4"-20 Thread Size | McMaster-Carr, MPN: 95462A029.

[30]High-Strength Steel Nylon-Insert Locknut, Black-Oxide, 1/4"-20 Thread Size | McMaster-Carr, MPN: 97135A414.

[31]Brass Heat-Set Insert for Plastic, Flanged, 4-40 Thread Size, 0.226" Installed Length | McMaster-Carr, MPN: 97171A120.

[32]Male-Female Threaded Hex Standoff, 18-8 Stainless Steel, 3/16" Hex, 3/16" Long, 4-40 to 4-40 Thread | McMaster-Carr, MPN: 91075A460.

[33]Nylon Pan Head Screw, Phillips Drive, 4-40 Thread, 1/4" Long | McMaster-Carr, MPN: 94735A717.

[34]4F Black Powder, Granulated for Ejection Charge Use | CS Rocketry, MPN: BP-FFG.

[35]StratoLoggerCF Altimeter, Dual-Deployment Flight Computer with Data Logging | PerfectFlite, MPN: STRATOLOGGERCF

[36]AIM USB Altimeter Interface Module, USB Data Transfer Device for AIM Series Altimeters | Entacore, MPN: AIMUSB.

[37]RRC3 Altimeter, Triple-Deployment Flight Computer with Data Logging | Missile Works, MPN: RRC3.
[38]Snap Action Switch, SPDT, 10.1gf Operating Force, Straight Lever Actuator | Omron, MPN: SS-10T.
[39]Gorilla Super Glue Gel, 0.5 oz, General Purpose Adhesive | ULINE, MPN: S-22520.
[40]Battery Holder, AA x 2, Wire Leads, Plastic Enclosure | Bulgin, MPN: BX0033.
[41]WAGO 221 Lever Nuts Kit, 90pc Compact Splicing Wire Connector Assortment with Case (Includes 221-2401, 221-412, 221-413, 221-415) | Amazon, MPN: B0BN6MBR7X.
[42]Haisstronica Heat Shrink Spade Connectors, 460pcs Quick Disconnect Terminals, AWG 22–10, Male and Female Set | Amazon, MPN: B0BZNHX532.
[43]Solder Seal Wire Connectors, 350pcs Heat Shrink Butt Splice Terminals, Waterproof and Insulated for Marine, Automotive, and Electrical Use | Amazon, MPN: B0CD77KTB6.
[44]Sopoby Ferrule Crimping Tool Kit, Self-Adjustable Ratchet Crimper with 2000pcs Insulated Wire Ferrule Terminals | Amazon, MPN: B0C2HGQ4N2.
[45]Brother PTE110 Industrial Handheld Labeling Tool Kit, Prints Labels up to 12 mm, Orange | Amazon, MPN: B074B4112Q.
[46]Alpha Wire Heat Shrink Tubing, 1/4" ID, 2:1 Shrink Ratio, Clear, 100 ft Spool | DigiKey, MPN: F221B1/4-CL100.
[47]Loctite Threadlocker Blue 242, Medium Strength Adhesive for Fasteners, 0.2 oz Tube | Loctite, MPN: 242.

Acknowledgments

The Clemson University Rocket Engineering team thanks our academic supporters and sponsors. We acknowledge Clemson University, the College of Engineering, Computing and Applied Sciences, and the Department of Mechanical Engineering for their academic support—special thanks to Dr. Garrett Pataky for his invaluable guidance.

Our project was also made possible by the generous contributions of the Clemson Student Funding Board, the Clemson University Rocket Alumni Association, AirTable, Slack, Ansys, OnShape, and SAIC. We appreciate their support and resources, which have been crucial in achieving our project goals.

This mission could not be complete without the extensive guidance and help from our mentor, Peter Tarlé. Without his effort, this organization could not run as it does.

References

[1] Adafruit, *Adafruit Unified Sensor, Reference Library*, Ver. 1.1.14. [Online]. Available: https://github.com/adafruit/Adafruit_Sensor/blob/master/README.md
[2] AirTable, *Project Management Software*, Ver. Free. [Online]. Available: https://airtable.com/
[3] CURocketEngineering, *Avionics, Github Software Repository*, Ver. 1.0.0. [Online]. Available: https://github.com/CURocketEngineering/Avionics
[4] Featherweight Altimeters, *Featherweight UI*, Ver. 1.0. [Online]. Available: https://www.featherweightaltimeters.com/blue-raven-altimeter.html
[5] Clemson University Board of Trustees and SC Commission on Higher Education, "Mission and Vision," *Clemson University*. [Online]. Available: https://www.clemson.edu/brand/positioning/mission-vision.html
[6] Featherweight Altimeters, *Featherweight GPS Tracker User's Manual*. [Online]. Available: https://www.featherweightaltimeters.com/uploads/1/0/9/5/109510427/gps_tracker_manual_2021oct25.pdf
[7] Slack Technologies, *Slack: Team Communication Platform*. [Online]. Available: https://slack.com/
[8] Lenovo, *What is a Cat 5 Cable?* [Online]. Available: https://www.lenovo.com/us/en/glossary/what-is-a-cat-5/?orgRef=https%253A%252F%252Fwww.google.com%252F&srsltid=AfmBOopg3KDxzJdkK-M852bDMkcLqH5JMneMdddo4GCzqbRqweFUBo_d
[9] Onshape, *Collaborative CAD Software*, Ver. 1.175. [Online]. Available: https://www.onshape.com/en/
[10] OpenRocket, *Simulation Software*, Ver. 23.09. [Online]. Available: https://openrocket.info/
[11] HeroX, *IREC 2025: Intercollegiate Rocket Engineering Competition*. [Online]. Available: https://www.herox.com/IREC2025
[12] Experimental Sounding Rocket Association, *SoundingRocket.org*. [Online]. Available: https://www.soundingrocket.org/
[13] PlatformIO, *PlatformIO Core 6, Software IDE*, Ver. 6.1.15. [Online]. Available: https://platformio.org/
[14] RASAero, *RASAero II Simulation Software*, Ver. 1.0.2.0. [Online]. Available: https://www.rasaero.com/dl_software_ii.htm
[15] SolidWorks, *CAD Software*, Ver. 2023. [Online]. Available: https://www.solidworks.com/
[16] STMicroelectronics, *STM32CubeIDE-Win*, Ver. 1.15.1. [Online]. Available: https://www.st.com/content/st_com/en/stm32cubeide.html
[17] McMaster-Carr, "Carr." *McMaster*. [Accessed: May 9, 2025].
[18] Experimental Sounding Rocket Association, *2025 IREC Design, Test, & Evaluation Guide*, Rev. 1.1.6, Feb. 14, 2025. [Online]. Available: *2025-irec_dteg_v1.1.6_02-14-25.pdf*
[19] MatWeb, *Overview of Materials for Epoxy/Carbon Fiber Composite*. [Online]. Available: https://www.matweb.com/search/datasheet_print.aspx?matguid=39e40851fc164b6c9bda29d798bf3726
[20] ANSYS, *CAD Software*, Ver. 2022 R1. [Online]. Available: https://www.ansys.com/
[21] MatWeb, *Overview of Materials for Nylon 66, 10% Carbon Fiber Filled*. [Online]. Available: https://www.matweb.com/search/datasheet_print.aspx?matguid=74fc8373189d42ebb0c35442433a4d16
[22] Apogee Rockets, *AIM USB 4 Manual*. [Online]. Available: 09139-AIM-Manual.pdf
[23] Apogee Rockets, *RRC3 – Rocket Recovery Controller 3 User Manual*. [Online]. Available: Microsoft Word - RRC3 User Manual v1.60.doc
[24] PerfectFlite, *StratoLoggerCF Users Manual*. [Online]. Available: SLCF manual for pdf
[25] Aerotech, *Aerotech Rocket Motor Product Page*. [Online]. Available: https://aerotech-rocketry.com/products/product_8b286cf9-67c9-cda8-2c15-10c1b91c1026?_pos=1&_sid=e3dacac3b&_ss=r
[26] PCBWay, "3D Printing in PA12 | Manufacturing Materials." [Online]. Available: https://www.pcbway.com/rapid-prototyping/3d-printing/pa12.html
[27] FOW Mould, "PA 12 (Nylon 12) Material Explained." [Online]. Available: https://www.fowmould.com/blog/pa-12-nylon-12-material.html
[28] Formlabs, Inc., *Nylon 12 Powder – SLS Powder for Strong, Functional Prototypes and End-Use Parts*, Rev. 01, Aug. 19, 2020. [Online]. Available: 2001447-TDS-ENUS-0.pdf
[29] Altium, *Altium Designer: PCB Design Software*, Ver. 2.3.0. [Online]. Available: https://www.altium.com/
[30] STMicroelectronics, *LSM6DSOX Datasheet*, REV 4. [Online]. Available: https://www.st.com/resource/en/datasheet/lsm6dsox.pdf
[31] STMicroelectronics, *LIS3MDL Datasheet*, REV 7. [Online]. Available: https://www.st.com/resource/en/datasheet/lis3mdl.pdf
[32] Bosch Sensortec, *BMP390 Datasheet*, REV 1.7. [Online]. Available: https://www.bosch-sensortec.com/media/boschsensortec/downloads/datasheets/bst-bmp390-ds002.pdf
[33] STMicroelectronics, *STM32F103CBT6 Datasheet*, REV 19. [Online]. Available: https://www.st.com/resource/en/datasheet/cd00161566.pdf
[34] Winbond, *W25Q128JV Datasheet*, REV E. [Online]. Available: https://www.winbond.com/resource-files/w25q128jv%20revf%2003272018%20plus.pdf
[35] Unexpected Maker, *Introducing the FeatherS3*. [Online]. Available: https://esp32s3.com/feathers3.html
[36] CURocketEngineering, *Native Software Repository*. GitHub. [Online]. Available: https://github.com/CURocketEngineering/Native [Accessed: May 2, 2025].
[37] E. Dougal, J. Kwok, and E. Luckett, *Digital Detection of Rocket Apogee*, Rice University, Houston, TX, USA, Dec. 2013. [Online]. Available: https://cnx.org/content/col11599/1.1/ [Accessed: May 2, 2025].
[38] CURocketEngineering, *GitHub Organization Repositories*. GitHub. [Online]. Available: https://github.com/CURocketEngineering [Accessed: May 2, 2025].
[39] Experimental Sounding Rocket Association, *IREC 2025: Intercollegiate Rocket Engineering Competition Rules & Requirements*, ver. 1.6, Mar. 4, 2025. [Online]. Available: *irec_rules_and_requirements_document_v_1.6_.pdf*